ENGINEERING GEOLOGY ASSESSMENT OF SLOPE INSTABILITY ON FOREST LANDS IN SOUTH WESTLAND

A thesis
submitted in partial fulfilment
of the requirements for the Degree
of
Master of Science in Engineering Geology
in the
University of Canterbury
by

MARK J EGGERS

University of Canterbury
1987

Frontispiece The Grave Earthflow (rotational slide-earthflow complex slope movement type) situated in Cretaceous-Tertiary Hill Country on State Highway 6 between the Whakapohai River and Ship Creek, South Westland. Oblique view looking south-southeast. (N.Z. Geological Survey photo CN 5892b, Photographer: D.L. Homer)

ABSTRACT

Assessment of slope instability on forest lands in South Westland was limited to the resource allocation level of evaluating slope movements on forest lands with the prime objective of providing an overview of slope movement potential adequate for forestry development planning. Three sites were selected for detailed investigation on the three most unstable landform units which were identified by previous studies, viz:-

1. Greenland Group Hill Country: Boulder Creek;
2. Alpine Fault Zone slopes: Havelock Creek, and;
3. Cretaceous-Tertiary Hill Country: Grave Creek.

Investigations were divided into three stages, engineering geology field and laboratory studies, assessment of slope movement processes and instability controls, and implications of slope instability for forest management.

The dominant type of slope failure at Boulder Creek is debris slump/slide-avalanche in crushed hornfelsed sandstone and puggy tectonic breccia bedrock materials with failures typically initiated during high intensity rainstorm events and seismic events. The Boulder creek catchment is presently undergoing a period of increased slope activity which is generating a substantial quantity of sediment and is overloading the stream channel with rock debris. Boulder Creek provides an exceptional example of slope instability problems in Greenland Group Hill Country, this being explained by the oversteepened sides of the glaciated Moeraki River valley in fault-crushed bedrock.

Alpine Fault Zone slopes fail most commonly by debris slide-avalanche in crushed mylonite schist and crushed garnet schist bedrock triggered by high intensity rainstorm events. Investigations at Havelock Creek also identified large-scale rock (block) slide failures in the same crushed bedrock materials which are initiated by infrequent seismic events.

The Grave Earthflow, located in Cretaceous-Tertiary Hill Country, was triggered by construction of State Highway 6 in 1963-65. Failure is taking place by a complex rotational slide-earthflow type of movement along a zone of basal shear in grey mud material derived from faulting in lower Otumotu Formation bedrock. Surface movement monitoring investigations measured a high rate of movement of up to 419cm/year. Unloading of toe support in December 1984 caused an instantaneous acceleration in movement rates which subsequently declined during the monitoring period of March 1985 to June 1986. This deceleration process obscured any climatic influences on movement.

Slope failure potential in South Westland slopes is governed by the fundamental causes of slope instability: the distribution of weak fault zone materials and crushed bedrock, and the steep topography (20-65^{o}). Aerial photograph evidence suggests that slope instability features develop very rapidly (within one rainstorm event) and active instability periods occur in short-lived episodes (less than 50 years) which are coincident with the occurrence of heavy precipitation periods.

Recommendations for future management of South Westland forest lands are:-

1. Alpine Fault Zone slopes should be limited to protection forestry management practices.
2. Greenland Group Hill Country and Cretaceous-Tertiary Hill Country should be assessed by more detailed phases of evaluation for small-scale bush-mill harvesting methods only.
3. Engineering geology methods of investigation and data presentation have been demonstrated to make a valuable contribution to forest resource allocation studies and it is recommended that these methods be applied to all levels of evaluation of slope movement potential on forest lands.

TABLE OF CONTENTS

	Page
CHAPTER ONE : INTRODUCTION	1
1.1 PROJECT BACKGROUND	1
1.2 PHYSICAL CHARACTERISTICS OF THE PROJECT AREA	4
1.2.1 Location	4
1.2.2 Geological Setting	4
1.2.3 Geomorphology	6
1.2.4 Hydrology	6
1.2.5 Vegetation	11
1.2.6 Climate	11
1.2.7 Landuse	13
1.3 SCOPE OF THE PROJECT AND THESIS LAYOUT	16
1.3.1 Conceptual Approach to Evaluating Slope Movements on Forest Lands	16
1.3.2 Thesis Objectives	17
1.3.3 Project Organisation and Thesis Layout	17
1.4 INVESTIGATION METHODS	18
1.4.1 Fieldwork	18
1.4.2 Base Maps	18
1.4.3 Laboratory Work	19
1.4.4 Note on Terminology	19
CHAPTER TWO : GEOLOGICAL SETTING OF SOUTH WESTLAND	20
2.1 PREVIOUS AND PRESENT WORK	20
2.2 PRE-CRETACEOUS ROCKS	21
2.2.1 Greenland Group	21
(i) Distribution	21
(ii) Description	21
(iii) Structure	23
(iv) Age	25
2.2.2 Tuhua Group	25
(i) Distribution	25
(ii) Description	26
(iii) Age	26
2.2.3 Haast Schist	26
(i) Distribution	26
(ii) Description	26
(iii) Structure	27
(iv) Age	27

Page

2.3 CRETACEOUS AND TERTIARY ROCKS 29
2.3.1 Stratigraphy 29
2.3.2 Structure 30
2.4 QUATERNARY ROCKS 33
2.4.1 Glacial Deposits 33
(i) Background 33
(ii) Older Glacial Unit 1 33
(iii) Older Glacial Unit 2 33
(iv) Moana Formation 35
(v) Interglacial Terraces 35
2.4.2 Postglacial Deposits 35
2.4.3 Late Quaternary Paleogeography 36
2.5 GEOLOGY OF THE ALPINE FAULT ZONE 36
2.5.1 Distribution of Fault Zone Rocks 36
2.5.2 Fault Zone Rock Description 38
(i) Fault Gouge, Tectonic Breccia and Cataclasite 38
(ii) Mylonite Schist 40
(iii) Amphibolite 40
(iv) Wispy Schist 40
2.5.3 Dip of the Fault Zone 42
2.5.4 Age of Fault Zone Rocks 42

CHAPTER THREE : SLOPE MOVEMENT TERMINOLOGY AND SITE SELECTION 44
3.1 OBJECTIVES 44
3.2 SLOPE MOVEMENT TYPES AND PROCESSES 44
3.2.1 Slope Movement Classification 44
3.2.2 Types of Movement 45
3.2.3 Types of Material 47
3.2.4 State of Slope Activity 47
3.2.5 Sequence or Repetition of Movement, Nomenclature and Rates of Movement 47
3.2.6 Causes of Slope Movements 50
3.3 IMPACTS OF FOREST MANAGEMENT ACTIVITIES ON SLOPE PROCESSES 50
3.4 RECENT SLOPE STABILITY HISTORY OF SOUTH WESTLAND 55
3.5 SELECTION OF LANDFORM UNITS FOR INVESTIGATION 56

Page

3.5.1 Landform Unit Identification and Description 56
3.5.2 Relative Slope Stability 56
3.5.3 Site Selection 63
3.6 APPROACH TO ENGINEERING GEOLOGICAL INVESTIGATIONS 63

CHAPTER FOUR : GREENLAND GROUP HILL COUNTRY: BOULDER CREEK 65
4.1 OUTLINE OF APPROACH 65
4.2 GEOMORPHIC SETTING AND RECENT HISTORY OF SLOPE ACTIVITY 67
4.3 ENGINEERING GEOLOGICAL INVESTIGATIONS 71
4.3.1 Investigation Programme 71
4.3.2 Bedrock Geology 72
(i) Hornfelsed Sandstone Basement Rock 72
(ii) Fault Gouge and Tectonic Breccia 74
(iii) Structure 78
4.3.3 Surficial Geology 80
(i) Slope Storage Debris 81
(ii) Debris Accumulations 81
(iii) Rock Debris Alluvium 84
(iv) Stream Gravels 84
4.3.4 Slope Morphology 84
4.3.5 Geohydrology 87
4.3.6 Laboratory Investigations 89
(i) Laboratory Programme 89
(ii) Grain-size Distribution 92
(iii) In-situ Moisture Content and Atterberg Limits 92
(iv) Clay Mineralogy 94
4.4 SLOPE MOVEMENT PROCESSES 96
4.4.1 Objectives 96
4.4.2 Slopes in Intact Hornfelsed Sandstone 96
(i) Rock Falls 96
(ii) Rock Slide 97
4.4.3 Slopes in Crushed Hornfelsed Sandstone 97
(i) Rock Creep 98
(ii) Debris Falls 100
(iii) Debris Slump/Slide-Avalanches 102
4.4.4 Slopes in Tectonic Breccia 104

Page

4.4.5 Ancient Slope Movement Features 105
4.4.6 Assessment of Slope Instability 106
(i) Scope 106
(ii) Rock Slide in Intact Bedrock Slopes 106
(iii) Failures in Crushed Bedrock and Tectonic Breccia 107
4.5 HYDROLOGIC PROCESSES 108
4.5.1 Objectives 108
4.5.2 Development of Debris Lobes and Sediment "Waves" 108
4.5.3 Description of Transported Material 111
4.5.4 Rock Debris Lobe Movement and Sieve Deposition 111
4.5.5 Rheologic Motion 113
4.5.6 State Highway 6 Bridge Crossing 117
4.6 SLOPE INSTABILITY ON GREENLAND GROUP HILL COUNTRY 120
4.6.1 Objectives 120
4.6.2 Slope Evolution of Boulder Creek 121
4.6.3 Slope Movements on Greenland Group Hill Country 121
4.6.4 Implications for Forest Management 127
4.7 SYNTHESIS 130

CHAPTER FIVE : ALPINE FAULT ZONE SLOPES: HAVELOCK CREEK 132
5.1 OUTLINE OF APPROACH 132
5.2 GEOMORPHIC AND GEOLOGIC SETTING 132
5.2.1 Topography and Vegetation 132
5.2.2 Fault Movement 135
5.2.3 Recent History of Slope Activity 137
5.3 ENGINEERING GEOLOGY INVESTIGATIONS 137
5.3.1 Investigation Programme 137
5.3.2 Bedrock Geology 138
(i) Garnet Schist 138
(ii) Mylonite Schist 140
(iii) Fault Gouge and Tectonic Breccia 141
(iv) Glacial Gravels 142
5.3.3 Surficial Geology 142
(i) Slope Storage Debris and Debris Accumulation 142

Page

(ii) Stream Gravels 143
5.3.4 Slope Morphology 143
5.3.5 Geohydrology 144
5.3.6 Laboratory Investigations 147
(i) Laboratory Programme 147
(ii) Grain-size Distribution 147
(iii) In-situ Moisture Content and Atterberg Limits 150
(iv) Clay Mineralogy 152
5.4 SLOPE MOVEMENT PROCESSES 152
5.4.1 Objectives 152
5.4.2 Slopes in Intact Schist 152
5.4.3 Slopes in Crushed Schist 154
(i) Rock Block Slide 155
(ii) Debris Slide-Avalanches 159
5.4.4 Slopes in crushed Mylonite Schist 161
(i) Debris Slide and Debris Falls 161
(ii) Rock Slide 161
5.4.5 Slopes in Tectonic Breccia and Fault Gouge 162
(i) Debris Slides 162
(ii) Debris Flows 165
5.4.6 Assessment of Slope Instability 165
5.5 SLOPE INSTABILITY ON ALPINE FAULT ZONE SLOPES 167
5.5.1 Objectives 167
5.5.2 Slope Evolution of Havelock Creek 167
5.5.3 Slope Movements on Alpine Fault Zone Slopes 169
(i) Catchment Slopes 169
(ii) Fault-bounded Mountain Front Slopes 174
5.5.4 Implications for Forest Management 174
5.6 SYNTHESIS 176

CHAPTER SIX : CRETACEOUS-TERTIARY HILL COUNTRY: GRAVE CREEK 178
6.1 OUTLINE OF APPROACH 178
6.2 SITE GEOLOGY AND GEOMORPHOLOGY 179
6.2.1 Location and Objectives 179
6.2.2 Bedrock Geology 179
6.2.3 Surficial Deposits 182

		Page
6.2.4	Geomorphology	184
(i)	Slope Morphology	184
(ii)	Slope Movement	184
6.3	EARTHFLOW DESCRIPTION	185
6.3.1	Objectives	185
6.3.2	History of Movement	187
6.3.3	Earthflow Materials	190
6.3.4	Slope Morphology	193
(i)	Topographic Surveys	193
(ii)	Slope Morphology Features	193
6.3.5	Subsurface Investigations	198
(i)	Objectives and Methods	198
(ii)	Shallow Trial Pit Excavations	198
6.3.6	Laboratory Investigations	207
(i)	Laboratory Programme	207
(ii)	Grain-size Distribution	207
(iii)	In-situ Moisture Content and Atterberg Limits	209
(iv)	Clay Mineralogy	209
6.4	EARTHFLOW STABILITY AND REMEDIAL OPTIONS	210
6.4.1	Objectives	210
6.4.2	Grave Creek Survey Network	210
6.4.3	Surface Movement Monitoring Investigations	212
(i)	Movement Data	212
(ii)	Total Displacement	214
(iii)	Correlation of Movement with Rainfall	218
(iv)	Hodographs of Movement	220
(v)	Synthesis	222
6.4.4	Stability Assessment	223
(i)	Quantitative Analysis	223
(ii)	Failure Model	223
6.4.5	Remedial Options	224
(i)	Potential Remedial Measures	224
(ii)	Dewatering	226
(iii)	Planting	226
(iv)	Buttressing	227
(v)	Relocation of Highway	227
(vi)	Maintaining the Present Situation	227
(vii)	Recommendations	228

Page

6.5 SLOPE MOVEMENT ON CRETACEOUS-TERTIARY HILL COUNTRY 229
6.5.1 Objectives 229
6.5.2 Slope Evolution of Grave Creek 229
6.5.3 Slope Movement on Coastal Slopes 231
(i) Rock Fall and Shallow Debris Slide 231
(ii) Flaggy Point Rock Slide 231
6.5.4 Implications for Forest Management 236
6.6 SYNTHESIS 238

CHAPTER SEVEN : SUMMARY AND CONCLUSIONS 240
7.1 ENGINEERING GEOLOGY INVESTIGATIONS AND METHODOLOGY 240
7.2 SLOPE FAILURE MECHANISMS 241
7.2.1 Greenland Group Hill Country: Boulder Creek 241
(i) Slopes in Intact Hornfelsed Sandstone 241
(ii) Slopes in Crushed Hornfelsed Sanstone 241
(iii) Slopes in Tectonic Breccia 242
7.2.2 Alpine Fault Zone Slopes: Havelock Creek 242
(i) Slopes in Intact Schist 242
(ii) Slopes in Crushed Schist and Mylonite Schist 242
(iii) Slopes in Tectonic Breccia and Fault Gouge 243
7.2.3 Cretaceous-Tertiary Hill Country: Grave Creek 243
7.3 CAUSES OF SLOPE FAILURE 244
7.3.1 Fundamental Causes 244
7.3.2 Triggering Mechanisms 244
7.4 CONCLUSIONS 245
7.4.1 Current Slope Instability 245
7.4.2 Implications for Forest Management 245
(i) Resource Allocation Evaluation 245
(ii) Recommendations 247
7.4.3 Engineering Geological Approach to Evaluating Slope Instability on Forest Lands 248

Page

ACKNOWLEDGEMENTS 250

REFERENCES 252

APPENDICES

1 Technical Liaison Committee Terms of Reference 259
2 Rock and Soil Description Terminology 261
3 Geological Time Scale 265
4 Vertical Aerial Photographs 266
5 Laboratory Tests 267
6 Stereographic Assessment of Slopes in Intact Hornfelsed Sandstone at Boulder Creek 276
7 Geotechnical Assessment of Slope Instability on Crushed Hornfelsed Sandstone and Tectonic Breccia Slopes at Boulder Creek 299
8 Grave Creek Survey Network 306
9 Grave Earthflow Surface Movement Monitoring Results 313

LIST OF FIGURES

Figure		Page
1.1	Locality map showing position of sites	5
1.2	Glaciated Paringa River valley	7
1.3	Hunts Beach State Forest on an extensive alluvial outwash surface	8
1.4	Greenland Group Hill Country between the Paringa and Haast Rivers	9
1.5	Haast alluvial outwash plain	10
1.6	Mean annual rainfall map	14
2.1	Simplified geological map of South Westland	22
2.2	Crystalline siliceous sandstone and mudstone of the Greenland Group at Boulder Creek	24
2.3	Stratigraphic sequence between Buttress Point and Ship Creek	31
2.4	Lower member of the Otumotu Formation at Tokakoriri Creek	32
2.5	Tauperikaka Coal Measures at Breccia Creek	32
2.6	Paleogeographic maps of South Westland at 14 000 and 5000 years B.P.	37
2.7	Composite section of the Alpine Fault Zone	39
2.8	Idealised section of the Alpine Fault Zone	39
2.9	Fault gouge overthrusting post-glacial gravels at Havelock Creek	41
2.10	Mylonite schist at Havelock Creek	41
2.11	Models of the dip of the Alpine Fault Zone	43
3.1	Varnes (1978) slope movement classification scheme	46
3.2	Nomenclature of slope movement features	49
3.3	Rates of slope movement scale	51
3.4	Factor of safety variation due to deforestation of a slope	51
3.5	Distribution of landforms between the Cook and Paringa Rivers	58

Figure		Page
3.6	Distribution of landforms between the Paringa and Haast Rivers	59
4.1	Sketch map of Boulder Creek showing the position of localities	66
4.2	Aerial oblique view of the Boulder Creek study catchment	68
4.3	Boulder Creek alluvial fan	69
4.4	Long profile of Boulder Creek	70
4.5	Sketch diagram of the crushed rock mass	76
4.6	Fault gouge zones at BE 1 and BE 4	77
4.7	Puggy tectonic breccia at BE 1	79
4.8	Debris accumulation at the base of the escarpment slope at BE 6	82
4.9	Panorama of the escarpment slope at BE 2	83
4.10	Rock debris alluvium overloading the streambed above a log jam waterfall	85
4.11	Face log of stream gravels on alluvial fan	86
4.12	Gully erosion in crushed bedrock at the top of the escarpment gully complex at BE 11	88
4.13	Sketch diagram of water springs above fault gouge zones	90
4.14	Fault gouge and tectonic breccia samples plotted on the plasticity chart	93
4.15	Large scale deformation features of a valley which has been unloaded by erosion or deglaciation	99
4.16	Gravitational deformation by release jointing	99
4.17	Face log of crushed rock mass at BE 2	101
4.18	Debris slide-avalanche in crushed bedrock at BE 6	103
4.19	Shallow debris sliding of the forested regolith/ colluvium cover at BE 2	103
4.20	Front of debris lobe No. 3 near BE 2	109
4.21	Cross-section of á debris lobe on the alluvial fan surface	112
4.22	Rock debris lobe No. 2 at BE 4	114

Figure Page

4.23 Rock debris lobe No. 1 above BE 7 during high flow 115

4.24 Boulder Creek during high flow on the alluvial fan surface adjacent to the State Highway 6 bridge crossing 118

4.25 Encroachment of alluvial fan onto adjacent forest lands 119

4.26 Deposition of stream gravels immediately adjacent to the southeastern bridge road approach 119

4.27 Slope evolution model of Boulder Creek 122

4.28 Sediment movement process model of Boulder Creek 123

4.29 Shallow debris slide-avalanche failures at Mistake Creek 124

4.30 Shallow debris slide-avalanche failures at Power Creek 126

5.1 Aerial oblique view of the Havelock Creek study catchment 133

5.2 Sketch map of Havelock Creek showing the position localities 134

5.3 Sketch map of overthrust napplet at Havelock Creek 136

5.4 "Rafts" of vegetation sliding over saturated gouge material 145

5.5 Gully erosion on escarpment slope in crushed mylonite schist at HE 5 145

5.6 Cold water H_2S spring 146

5.7 State Highway 6 bridge crossing of Havelock Creek minutes after flood waters passed over the bridge decking 148

5.8 Bulldozers clearing and realigning the stream channel 148

5.9 Fault gouge and tectonic breccia samples plotted on the plasticity chart 151

5.10 Eroding western flank of the rock slide at HE 6 156

5.11 Headscarp of rock slide at HE 6 156

5.12 "Pinnacles" of crushed bedrock and sag deposits in rock slide at HE 6 157

Figure		Page
5.13	Stereo-diagram of the rock slide at HE 6	158
5.14	Sketch diagram of the evolution of the rock slide at HE 6	160
5.15	Sketch diagram of the rock slide at HE 9	163
5.16	Degraded shallow debris slide failure scar in puggy tectonic breccia at HE 2	164
5.17	Remnant initial failure surface of slide at HE 2	166
5.18	Sketch diagram of debris slide scar at HE 2	166
5.19	Slope evolution model of Havelock Creek	170
5.20	Debris slide-avalanche in crushed mylonite schist at Bullock Creek	172
5.21	Debris torrent at Saltwater Creek	172
5.22	Debris slide-flow in puggy tectonic breccia at Saltwater Creek	173
5.23	Slope failure scarp at Slippery Face, Robinson Creek	173
5.24	Debris slide-avalanche on fault-bounded mountain front slope	175
6.1	Geological map of the coastal area between Ship Creek and Otumotu Point	181
6.2	Sandstone colluvium overlying raised beach deposits	183
6.3	Debris slide above the road culvert at Grave Creek during construction of State Highway 6 in 1963-65	186
6.4	Grave Earthflow in August 1984	188
6.5	Grave Earthflow in January 1985	189
6.6	Grave Earthflow in February 1986	191
6.7	Saturated grey mud in the eastern lateral shear zone	192
6.8	Sketch map of the surface morphology around the Grave Earthflow	195
6.9	Debris flow on the eastern flank of the road batter	197
6.10	GEP 1 trial excavation log	200
6.11	GEP 2 trial excavation log	201

Figure Page

6.12 Trial pit GEP 2 202

6.13 GEP 3 trial excavation log 203

6.14 Trial pit GEP 3 204

6.15 GEP 4 trial excavation log 205

6.16 Trial pit GEP 4 206

6.17 Map of the Grave Creek survey network 211

6.18 Map of the Grave Earthflow monitoring network 213

6.19 Map of displacement vectors 216

6.20 Graphs of the change in the rate of total displacement 217

6.21 Correlation of rainfall with movement 219

6.22 Hodographs of the average rate of total movement 221

6.23 Model of interrelationships between the causes of the Grave Earthflow 225

6.24 Slope evolution model of Grave Creek 230

6.25 Rock fall in lower Otumotu Formation bedrock at Otumotu Point 232

6.26 Sketch diagrams of the three coastal slope settings in Tokakoriri Formation bedrock 233

6.27 Rock slide on coastal slopes at Flaggy Point 234

6.28 Sketch map of the Flaggy Point rockslide 235

LIST OF TABLES

Table		Page
1.1	SWMEP studies and agencies responsible	2
1.2	Mean sediment yields and erosion rates for selected rivers in the study area	12
1.3	Monthly and annual distribution of rainfall	15
2.1	Summary of structure of the Alpine Schists	28
2.2	Quaternary Mapping units	34
3.1	Terminology describing a sequence or repetition of slope movement	48
3.2	Summary of the causes of slope movements	52
3.3	Specific action of the various components of a forest cover favourable to sloe stability	54
3.4	List of landform units in South Westland	57
3.5	Summary of the characteristics of representative landform units in South Westland	60
3.6	Relative slope stability ranking between the Cook and Paringa Rivers	61
3.7	Relative slope stability ranking between the Paringa and Haast Rivers	62
4.1	Summary of rock material properties for bedrock map units at Boulder Creek	73
4.2	Summary of rock mass properties for hornfelsed sandstone bedrock map units at Boulder Creek	75
4.3	Summary of laboratory test results for Boulder Creek samples	91
4.4	d-spacings of peaks obtained from Boulder Creek samples	95
4.5	Correlation of sediment pulses with slope source area	110
4.6	Critical slope angles for Greenland Group Hill Country slope failure mechanisms	129

Table		Page
5.1	Summary of rock material properties for bedrock map units at Havelock Creek	139
5.2	Summary of laboratory test results for Havelock Creek samples	149
5.3	d-spacings of peaks obtained from Havelock Creek samples	153
5.4	Summary of slope angle data for major slope movements at Havelock Creek	168
6.1	Engineering geological descriptions of bedrock map units at Grave Creek	180
6.2	Summary of laboratory test results for samples from the Grave Earthflow	208
6.3	Rate of total cumulative displacement for each monitoring station on the Grave Earthflow	215
6.4	Summary of geomorphic settings and slope movement types in Cretaceous-Tertiary Hill Country	237

CONTENTS OF MAP POCKET

Figure

1 1:2000 Engineering Geology Plan of Boulder Creek

2 1:2500 Engineering Geology Assessment of Slope and Hydrologic Processes at Boulder Creek

3 1:2000 Engineering Geology Plan of Havelock Creek

4 1:2500 Engineering Geology Assessment of Slope Movement Processes at Havelock Creek

5 Engineering Geology Data Summary of Grave Creek

6 1:250 Engineering Geology Plan of the Grave Creek Slump-Earthflow

CHAPTER ONE

INTRODUCTION

1.1 PROJECT BACKGROUND

In September 1981, the Minister of Forests and the Minister for the Environment jointly announced the following decisions:-

1. addition of South Okarito and Waikukupa State Forests to Westland National Park;
2. imposition of a moratorium on the production of timber from State forests south of the Cook River until 1990;
3. undertaking of an interdisciplinary study to ensure that decisions on future management of the moratorium area are based on comprehensive, sound information.

As a result the South Westland Management Evaluation Programme (SWMEP) was established in 1983 to carry out the third of these decisions. The objectives of the programme are set out in the Terms of Reference for the Technical Liaison Committee (TLC), which is the steering committee for the programme, and are reproduced in Appendix 1.

The SWMEP is jointly controlled and co-ordinated by the N.Z. Forest Service and Department of Lands and Survey. Other government agencies involved in the programme include the DSIR, Wildlife Service, Ministry of Agriculture and Fisheries, and Forest Research Institute (FRI). Table 1.1 lists the various studies conducted and agencies responsible with research beginning in 1983 on the lowland forests between the Cook and Paringa Rivers. Subsequent years were to see study of high country east of the Alpine Fault, lowland forests between the Paringa and Haast Rivers, and the Cascade area south of Jackson Bay. Premature cessation of funding for the programme in 1985 resulted in only lowland forests between the Cook and Haast Rivers being studied in any detail. A final report will be collated by the TLC from interim reports prepared from research completed before cessation of funding and will cover those matters listed under section 6 of the TLC

STUDY	ORGANISATION RESPONSIBLE
Geology	N.Z. Geological Survey
Soils	Soil Bureau DSIR
Vegetation Mapping	N.Z. Forest Service
Wildlife (Birds)	Wildlife Service
Fisheries	Ministry of Agr. & Fish.
Invertebrates	Zoology Dept. Uni. of Canty
Kahikatea Ecology	Ecology Division DSIR
Landform Types	Forest Research Institute
Forest Volumetric Inventory	N.Z. Forest Service
Chainsaw Mill Development	Forest Research Institute
Helicopter Timber Extraction	N.Z. Forest Service
Recreation Strategy	N.Z. Forest Service
Historic Research	N.Z. Forest Service
Landscape Studies	Forest Research Institute
Botanical Surveys	Botany Division DSIR
Agricultural Development	Dept. of Lands and Survey
Minerals	NZGS/Ministry of Energy
Wild Animals	Forest Research Institute
Recreational Fisheries	Wildlife Service
Population/Employment Statistics	MWD/NZFS/West Coast United Council

Table 1.1 SWMEP studies and agencies responsible.

Terms of Reference (see Appendix 1). It is considered that the final report should be a strategic planning document (Halkett 1985).

The purpose of FRI's involvement was to obtain information about the physical characteristics of South Westland's forested landforms to assist future forest management decisions. Such information would enable delineation of boundaries of forests located on various landforms which could be managed for production of wood without serious adverse consequences to soil and water values, and likewise determine the limits of forests occupying fragile or sensitive terrain where protection of slope stability and water and soil values must be regarded as the dominant aim of management (Fitzsimons et al. 1985).

The landform study commenced in December 1983 covering the area between the Cook and Paringa Rivers (Fitzsimons and O'Loughlin 1984) and was extended in late 1984 and 1985 to include the area between the Paringa and Haast Rivers (Fitzsimons et al. 1985). The investigation identified specific landforms as having major slope instability problems which could influence or limit future forest operations, and this thesis study arose from the need for more detailed information on the origin and nature of these problems (Section 1.3.2 details the thesis objectives).

The author's involvement in the SWMEP commenced in December 1983 while working for the N.Z. Geological Survey assisting mapping the geology between the Cook and Paringa Rivers. This involvement continued in December 1984 both assisting mapping the geology between the Paringa and Haast Rivers and assisting fieldwork for the FRI landform study which allowed site selection and reconnaissance for the thesis project. Detailed work on the thesis commenced in March 1985 in conjunction with the FRI for the SWMEP.

1.2 PHYSICAL CHARACTERISTICS OF THE PROJECT AREA

1.2.1 Location

South Westland is situated on the West Coast of the South Island, New Zealand, approximately between latitudes 43° 30'S and 44° 30'S. The project covers an area of approximately 1000km^2 extending from the Cook River in the north to the Haast River in the south and is bound to the west by the coastline and to the east by the Alpine Fault (Fig. 1.1).

The project area is covered by the following NZMS 1 (1:63 360 scale) maps:-

1. S70 Gillespie;
2. S77 Paringa;
3. S78 Bruce Bay;
4. S87 Haast.

Grid references to specific localities mentioned in the text are given on the NZMS 1 1000-yard grid as no metric NZMS 260 series maps are available.

1.2.2 Geological Setting

The Alpine Fault forms a marked topographic and geological boundary in South Westland. On the eastern side the mountains are formed of laminated schist (Haast Schist) with glaciated valleys containing extensive postglacial deposits. On the western lowlands and hill country the oldest rocks are interbedded greywacke and argillite (Greenland Group) intruded by granite (Tuhua Group). These basement rocks are unconformably overlain by a late Cretaceous and early Tertiary succession consisting of basal breccia and conglomerate (Otumotu Formation), coal measures (Tauperikaka Coal Measures), marine sandstone (Whakapohai Sandstone), basaltic flows and breccia (Arnott Basalt), volcanogenic conglomerate (Buttress Conglomerate), calcareous sandstone and mudstone (Tokakoriri Formation), muddy limestone and calcareous mudstone (Abbey Formation), and basaltic flows and agglomerate (Otitia Basalt). During the late Quaternary glaciations much of the area was covered in ice leaving extensive glacial features and deposits covering older rocks in many places.

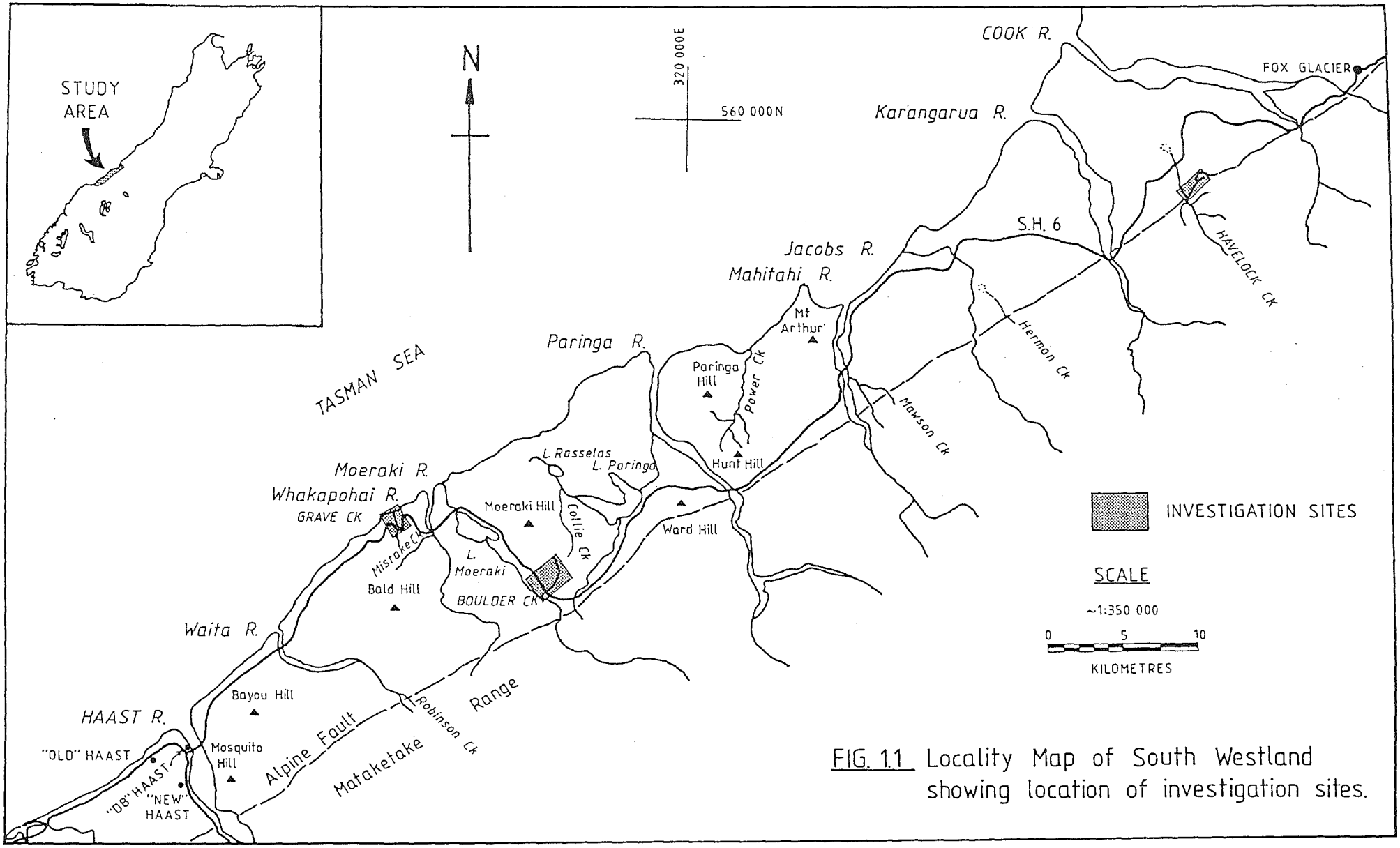

FIG. 1.1 Locality Map of South Westland showing location of investigation sites.

1.2.3 Geomorphology

The broad physiography of the project area consists of a narrow coastal plain interrupted by steep, low altitude hill country and glaciated valleys (Fig. 1.2). The eastern margin of the region is formed by the western slopes of the Southern Alps which can be regarded as a giant fault scarp consequent on uplift on the Alpine Fault (Adams 1984).

The coastal plain in the study area can be divided into two geomorphological regions, the first being north of the Paringa River where the dominant landforms are large, upstanding Pleistocene moraines which are separated by alluvial plains and rivers. During Pleistocene glaciations the Mahitahi, Jacobs, Karangarua, Copland, Cook and Fox Valleys (see Fig. 1.1) all contained large glaciers which coalesced west of the mountain front forming a piedmont ice sheet. This ice sheet eroded remaining hill country leaving residual hills and large morainic landforms and during deglaciation, areas between moraines were infilled by outwash gravels forming the now extensive alluvial plains (Fitzsimons et al. 1985) (Fig. 1.3).

In contrast, the area south of the Paringa River, being the second geomorphological region, supported relatively small valley glaciers which were confined out to and beyond the present day coastline. This resulted in much of the hill country escaping erosion by ice and prevented any large accumulations of outwash and morainic deposits (Fig. 1.4). A major exception is the Haast Valley which contained a large glacier which expanded west of the mountain front to form a small ice sheet. This ice sheet shaped the area in which the Haast Plain was later deposited and residual hills such as Mosquito and Bayou Hills are remnants of a formerly more extensive tract of hill country (Fitzsimons et al. 1985) (Fig. 1.5).

1.2.4 Hydrology

South Westland rivers and streams have high specific discharges and are powerful sediment transporters. Estimates of sediment yield and derived erosion rates for various rivers in the project area (Table 1.2) support the contention that regional erosion rates are as much as ten times the world

Fig. 1.2 The glaciated Paringa River valley which flows from schist mountain country, across the Alpine Fault, and through Cretaceous-Tertiary Hill Country before joining the Tasman Sea. Oblique view looking southeast. (N.Z. Geological Survey photo CN 5020b, photographer: D.L. Homer)

Fig. 1.3 Hunts Beach State Forest situated on an extensive alluvial outwash surface bounded by large lateral moraines of the last (Moana) glacial advance.

Fig. 1.4 Greenland Group Hill Country between the Paringa and Haast Rivers, as seen from the top of the Mataketake Range, looking north. Top escarpment slopes of Boulder Creek (arrowed) are clearly visible.

Fig. 1.5 The Haast alluvial outwash plain and Mosquito Hill, as seen from Bald Hill, looking southwest.

average specific yields for mountainous areas (Griffiths 1979). As a result many of the rivers and streams have unstable channels and may rapidly aggrade their beds or suddenly change course, causing damage to farmland, roads and bridges.

A number of large post-glacial lakes (Lakes Paringa, Rasselas and Moeraki) have formed in the hill country south of the Paringa River and extensive swamps have developed on large low lying alluvial outwash surfaces throughout the region due to high rainfall and poor drainage.

1.2.5 Vegetation

The distribution of vegetation species within the project area is dependent on a number of factors including geology, soils, landform type and climate. Generally the region is covered in some combination of mixed podocarp-beech-hardwood forest of rimu, kahikatea, kamahi, rata and silver beech. Coastal vegetation consists of kiekie and cabbage trees while swampland is covered in herbaceous vegetation. Hill country forest commonly regenerates to wineberry, swamp forest to manuka treeland and alluvial surfaces to treefern. Limited alluvial plain and terrace forest areas have been cleared to grasslands for rural use (Dept. of Lands & Survey 1984).

1.2.6 Climate

The climate of Westland is considerably influenced by its location and orography in relation to the general weather systems of all New Zealand regions and is an important factor to consider when dealing with slope movement processes on the West Coast. New Zealand lies within the hemispheric temperate zone where weather systems usually move eastward and the frequently changing synoptic patterns cause considerable variability in the weather. The Southern Alps create a barrier to the prevailing westerly airstream which is both deflected by them and forced to ascend; this causes rain which is often heavy and prolonged (Hessell 1982).

Surface winds on the West Coast tend to be light and variable, being influenced both by the meteorological situation and by large frictional effects caused by the mountain

RIVER	SITE	ANNUAL SEDIMENT YIELD 10^6 kg yr^{-1}	EROSION RATE tonnes km^{-2} yr^{-1}
Cook	Coast	337	1265
Cook	Alpine Fault	550	3176
Karangarua	Alpine Fault	288	793
Jacobs	Coast	62	521
Mahitahi	Coast	111	720
Paringa	Alpine Fault	140	600

Table 1.2 Mean sediment yields and erosion rates for selected rivers in study area (after Adams 1980).

barrier to the east. However, the weather is strongly influenced by the wind flow in the free atmosphere above the friction layer. Disturbed westerly flows, which occur more frequently in spring, bring heavy orographic rainfall to Westland. Extensive northerly airflows between anticyclone and depression are usually accompanied by prolonged rainfall which can reach torrential intensities in the mountains. Nearly all of Westland's rain occurs in winds having a northerly component and the temperature during the rain maybe relatively mild. Southeasterly gradients bring foehn winds and clear skies to the West Coast as the air has lost moisture in the uplift on the eastern side of the Alps (Hessell 1982).

The most important meteorological element in determining the climate of the region is rainfall. Dry spells (no rain for at least 15 days) are rare averaging about one every four years at Haast (Hessell 1982). The pattern of mean annual rainfall (Fig. 1.6) shows a gradual increase from north to south and a rapid increase from west to east. However in the project area, Paringa has a higher mean annual rainfall (5441mm) than Bruce Bay to the north (3943mm) and Haast to the south (3470mm) (N.Z. Meteorological Service 1973) which is probably due to the block of higher altitude hill country around Paringa compared to the lower country to the north and south. Table 1.3 gives monthly and annual totals of rainfall for a number of stations in the project area. This shows a fairly even seasonal distribution of rainfall but with notable minima in winter contrasting with the higher spring rainfalls.

Surface winds at low levels are dominated by southwesterly sea breezes near the coast, cold easterly katabatic down-valley winds at night and warm gusty foehn-type southeasterlies. The mean temperature range is small with Haast having an annual mean temperature of 11.0^{o}C, an annual mean daily range of 7.8^{o}C and an extreme range of 32.4^{o}C (Hassell 1982).

1.2.7 Landuse

The majority of South Westland is designated as State Forest with some farming on the larger river flats. Between the Cook and Haast Rivers there are seven State Forests:-

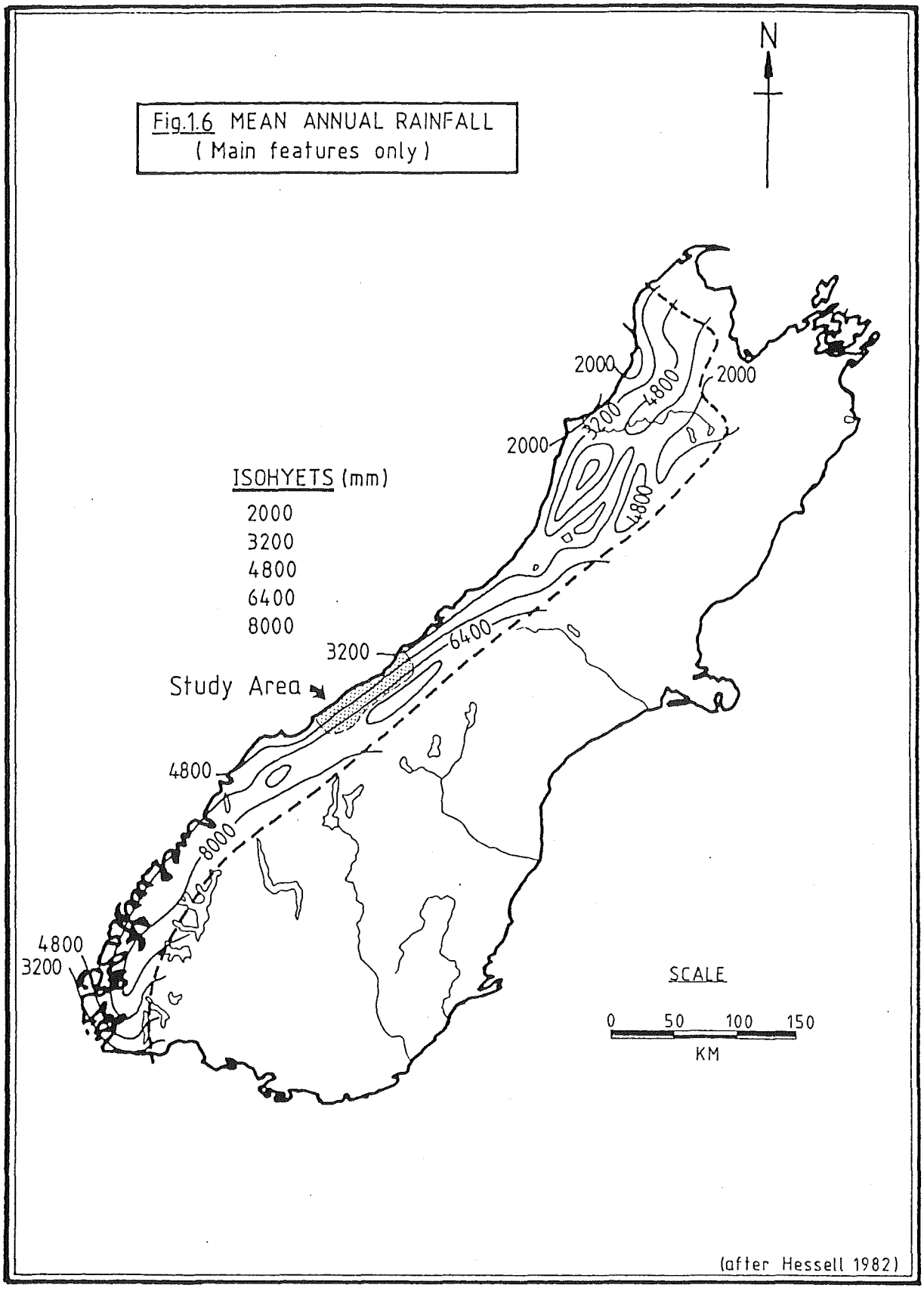
Fig.1.6 MEAN ANNUAL RAINFALL
(Main features only)
N
ISOHYETS (mm)
2000
3200
4800
6400
8000
Study Area
2000
2000
4800
3200
2000
4800
6400
3200
4800
8000
4800
3200
SCALE
0 50 100 150
KM
(after Hessell 1982)

STATION	Fox Glacier	Haast
PERIOD	1942-1978	1941-1976
JANUARY	363	282
FEBRUARY	396	314
MARCH	379	329
APRIL	384	279
MAY	405	294
JUNE	294	230
JULY	338	235
AUGUST	376	247
SEPTEMBER	421	300
OCTOBER	463	309
NOVEMBER	453	350
DECEMBER	393	272
ANNUAL	4680	3458
MINIMUM	3380	2725
MAXIMUM	6969	4564

Table 1.3 Monthly and annual distribution of rainfall (in mm) for two South Westland stations (after Hessell 1982).

1. Karangarua State Forest;
2. Hunts Beach State Forest;
3. Makawhio State Forest;
4. Bruce Bay State Forest;
5. Ohinemaka State Forest;
6. Paringa State Forest;
7. Mataketake State Forest.

The two largest settlements in the area, Fox Glacier and Haast, serve as service centres for forestry, farming, fishing and tourism activities. The smaller settlements of Karangarua, Jacobs River, Mahitahi and Paringa are farming communities which consist of several farmhouses with a school at Jacobs River. Seasonal fishing communities exist at the mouths of the Mahitahi (Bruce Bay), Paringa, Moeraki and Whakapohai Rivers.

Apart from rock for river protection work, there are currently no mining activities in the project area. Mineral resources known to exist include coal, gold (quartz veins, alluvial and blacksand leads), ilmenite (and associated minerals), sheet mica, limestone and possibly galena (Mortimer et al. 1984). Small parties or individuals have profitably worked blacksands concentrated on beaches for gold in the past whilst sheet mica was mined from 1944 to 1945 on the northern end of the Mataketake Range for the construction of electrical condensers during World War 2 (Wellman 1955).

1.3 SCOPE OF THE PROJECT AND THESIS LAYOUT

1.3.1 Conceptual Approach to Evaluating Slope Movements on Forest Lands

Prellitz et al. (1983) and Prellitz (1985) proposed a forest land management analysis system for dealing with landslide potential on forested slopes. This system provides information at three levels of land management activities:-

Level 1 - Resource Allocation: provides land managers with an overview of landslide potential adequate for development planning;

Level 2 - Project Planning: predicts response of slide-prone areas to various harvesting systems and transportation routes;

Level 3 - Critical Site Stabilisation: evaluates stabilisation techniques at critical sites before and after construction.

The scope of this study is limited to the resource allocation phase of land management activity, in accordance with clauses 2(b) and 6(d) of the TLC Terms of Reference where the purpose of scientific investigations is, "...to understand and evaluate physical and biological features and processes on a regional basis", and to recognise, "...the constraints on productive development imposed by topography, climate, soils and geology" (see Appendix 1).

1.3.2 Thesis Objectives

The main objectives of this thesis are:

1. To investigate the geological nature and origin of slope instability on a number of selected landform types, specifically to:-
   a) describe the features, mechanisms and causes of slope movements;
   b) determine the geomorphic evolution of slope instability, and;
   c) qualitatively assess slope instability

   at each site;
2. To apply engineering geological methods of investigation and data presentation to the SWMEP with the aim that these methods could be applied to future forestry resource planning studies.

1.3.3 Project Organisation and Thesis Layout

The major part of this study consists of three site investigations each located on one of the three most unstable landform types identified by FRI's landform studies for the SWMEP. The three sites are (location shown in Fig. 1.1):-

1. Greenland Group Hill Country - Boulder Creek;
2. Alpine Fault Zone Slopes - Havelock Creek;
3. Cretaceous-Tertiary Hill Country - Grave Creek.

This thesis is organised into seven chapters, the first introducing the SWMEP and thesis involvement in the programme, describing the physical character of the area, and outlining the scope of the project. Chapter two summarises the geological setting of South Westland whilst chapter three discusses the region's landform types and presents the slope movement classification adopted and possible impacts of timber harvesting systems on slope processes. The following three chapters are essentially self-contained engineering geological reports on each of the three investigation sites and the associated landform type. The final chapter presents the thesis summary and conclusions and proposes recommendations for further work and for future forestry resource planning projects.

1.4 INVESTIGATION METHODS

1.4.1 Fieldwork

Most of the fieldwork was carried out during March to May 1985 and again in February 1986. In addition, the Grave Earthflow was visited every 2-3 months between the period March 1985 to June 1986 to resurvey the surface movement monitoring network.

Each of the three sites were mapped in terms of engineering geology at a scale of 1:2000, with information recorded on bedrock geology, surficial deposits, slope morphology and slope movement features. A surface movement monitoring network was installed on the Grave Earthflow and EDM survey methods were used to map the earthflow and to monitor surface movements. Other fieldwork included logging trial pits on the earthflow and conducting three rock defect surveys at Boulder Creek. Disturbed bag samples were collected at all three sites to allow a preliminary assessment of selected bedrock and surficial materials engineering properties.

1.4.2 Base Maps

Uncontrolled aerial photograph enlargements were used as field maps, these being enlarged from a scale of approximately 1:27 000 to the field scale of 1:2000 by N.Z. Aerial

Mapping Ltd. The aerial survey and run numbers used were:-

1. Boulder Creek: 5941/C42 (8/1/82);
2. Havelock Creek: 5941/D44 (11/3/83);
3. Grave Creek: 5941/A20 (19/10/81).

Photogrammetric contour plans of Boulder and Havelock Creeks were produced by the Photogrammetric Branch, Department of Lands and Survey at a scale of 1:4000 to be used as base maps for this project; these were enlarged photographically to the mapping scale of 1:2000. The 1:250 plan of the Grave Creek earthflow was surveyed by the author using a Nikon NTD-3 uniaxial theodolite-distancemeter.

1.4.3 Laboratory Work

The following laboratory tests were performed on samples collected during engineering geological mapping:-

1. In-situ moisture content;
2. Atterberg limits;
3. Grainsize distribution by dry sieve and hydrometer analysis;
4. Clay fraction mineralogy by X-ray diffraction.

The primary objective of this laboratory programme was to characterise the materials according to the above standard geotechnical tests to allow a preliminary assessment of their engineering properties.

1.4.4 Note on Terminology

Appendix 2 lists the terminology adopted in this thesis according to the following recommended guidelines:

1. Rock and Soil Descriptions - Bell and Pettinga (1984), Presentation of Geological Data;
2. Preparation of Maps and Sections - Geological Society (1972), The preparation of maps and plans in terms of engineering geology; and, IAEG (1981), Recommended symbols for engineering geological mapping.

CHAPTER TWO

GEOLOGICAL SETTING OF SOUTH WESTLAND

2.1 PREVIOUS AND PRESENT WORK

The Cretaceous and Tertiary rocks of South Westland were first recorded by Cox (1877) who described the lithographic limestone workings and underlying coal measures at Abbey Rocks, and by Haast (1879) who presented a geological map of Canterbury and Westland that showed a strip of Tertiary beds extending along the South Westland coast from Bruce Bay almost to Milford Sound. Haast also mapped the boundaries of moraine and recent sediment.

During the early 1900's Charlie E. Douglas compiled a topographic and geological map based on his explorations of South Westland over the previous 30 years (Pascoe 1957). A number of Douglas' mineral localities were investigated by a prospecting party in the 1930's (Bolitho 1937). Wellman and Willett (1942a, b) gave a brief account of South Westland geology in which the Alpine Fault was identified for the first time. Wellman (1955) was the first to consider the stratigraphy of the area between Bruce Bay and Haast, and presented a geological map at the scale of 1:63 360.

The study area is covered in the 1:250 000 geological map series by parts of Sheet 17, Hokitika (Warren 1967), Sheet 18, Mt Cook (Gair 1967) and Sheet 19, Haast (Mutch and McKellar 1965). During construction of the last section of State Highway 6 between Paringa and Haast, Gair and Gregg (1962) carried out an initial geological survey to assess the various routes under consideration, and Young (1968) considered some engineering geological factors affecting the choice of route along the coast in terms of road and culvert design and construction.

Suggate (1968) described postglacial sediments immediately upstream from the Paringa bridge and Nathan & Moar (1975) described late Quaternary terraces between the Whakapo-

hai River and Ship Creek. Nathan (1977) mapped the upper Cretaceous and lower Tertiary rocks between Buttress Point and Ship Creek, revising the stratigraphy of Wellman (1955). Waters (1983) mapped and described schists around the Paringa-Otoko Rivers junction.

The most recent geological work has been in connection with the SWMEP, and Mortimer et al. (1984) presents an interim report for the SWMEP covering the area between the Cook and Paringa Rivers. The interim report for the Paringa to Haast area is presently in preparation, and in addition a number of separate NZGS reports are being prepared to present more detail than that given in the SWMEP interim reports, including reports on the Greenland Group, Cretaceous and Tertiary rocks, and the Alpine Fault. Two theses are also being undertaken in the area: Adams (in prep.) on the Cretaceous and Eocene geology of South Westland, and Aliprantis (in prep.) on the Tertiary geology of the Paringa area, South Westland, with emphasis on structure.

2.2 PRE-CRETACEOUS ROCKS

2.2.1 Greenland Group

(i) Distribution

The Greenland Group constitutes the oldest rocks in the area and probably forms the majority of the pre-Cretaceous basement beneath the Cretaceous and Tertiary rocks. It outcrops on Paringa Hill in the headwaters of Power Creek, Moeraki Hill in the headwaters of Collie Creek and in the Whakapohai River catchment, as shown on a regional geological map presented in Figure 2.1. It is also inferred to form the core of a moraine ridge on the east side of the Karangarua River, between State Highway 6 and the coast (Mortimer et al. 1984).

(ii) Description

The Greenland Group as exposed in South Westland is similar to that in North Westland and Buller (as described by Laird 1972; Laird & Shelley 1974). It consists of alternating

LEGEND

- Post-glacial Deposits — QUATERNARY
- Moana Formation — Late Pleistocene — QUATERNARY
- Older Glacial Units 1 & 2 — Late Pleistocene — QUATERNARY

REGIONAL UNCONFORMITY

- Upper Tertiary Rocks — LATE CRETACEOUS & TERTIARY
- Upper Cretaceous & Lower Tertiary Rocks — LATE CRETACEOUS & TERTIARY

REGIONAL UNCONFORMITY

- Haast Schist Group — MESOZOIC
- Tuhua Group (Granite) — PALEOZOIC
- Greenland Group — PALEOZOIC

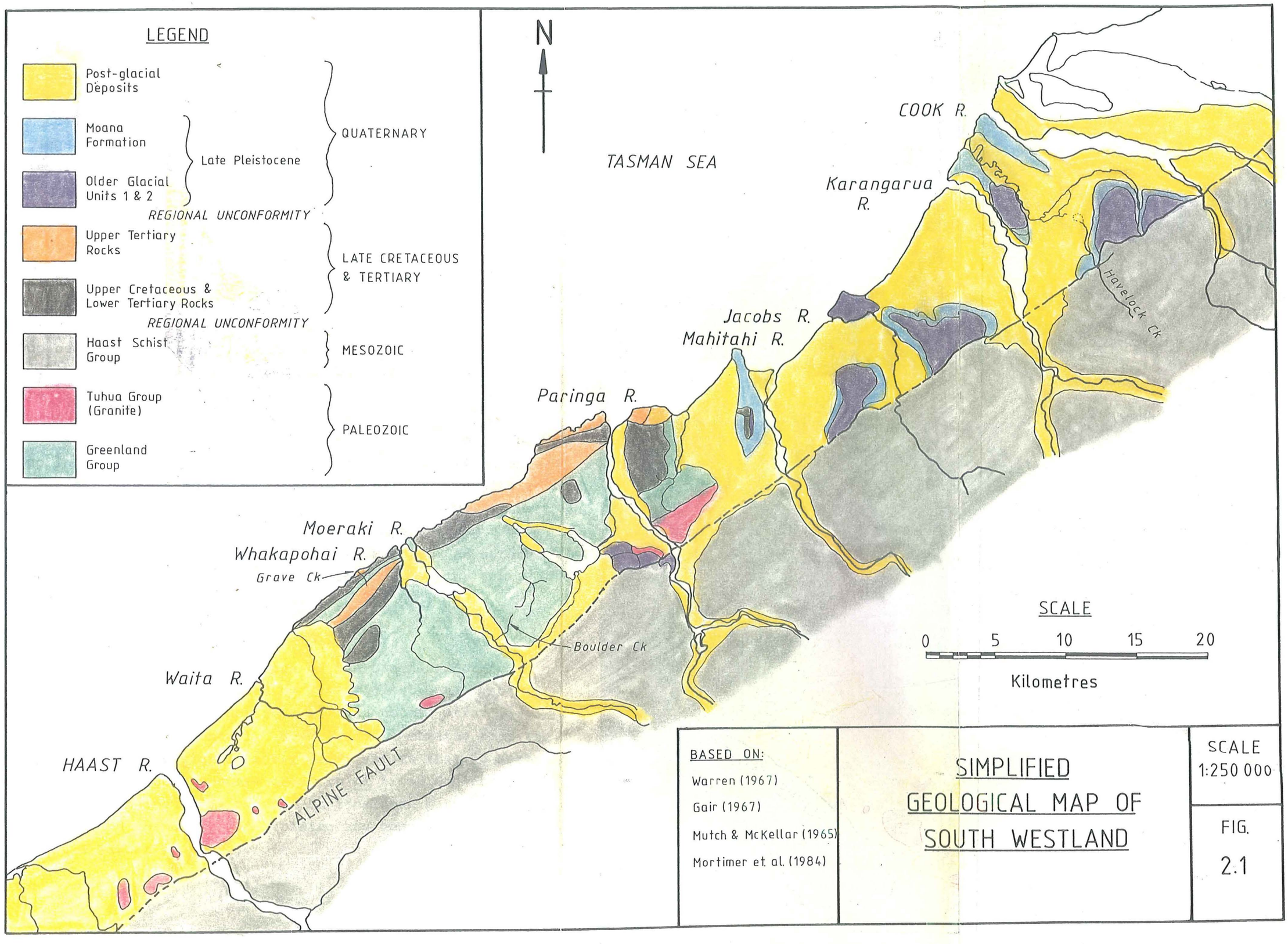

BASED ON:

Warren (1967)

Gair (1967)

Mutch & McKellar (1965)

Mortimer et. al. (1984)

SIMPLIFIED GEOLOGICAL MAP OF SOUTH WESTLAND

SCALE 1:250 000

FIG. 2.1

beds of indurated greenish-grey sandstone (greywacke) and mudstone (argillite), with sandstone predominant (Fig. 2.2). A metamorphic overprint covering much of the Greenland Group has obscured small-scale sedimentary structures. Bedding can be identified in most exposures but face directions are difficult to determine. Sandstone beds vary in thickness from thin partings to massive beds more than 2.0m thick. Grain size varies from very fine to coarse sand (dominantly fine to medium sand) with rare granule to pebble conglomerate (Stewart & Nathan in prep.).

Close to the margins of granite plutons Greenland Group rocks have been recrystallised to dark grey biotite hornfels and schist. Since most of the plutons are confined to a zone 2-3km west of the Alpine Fault (Nathan 1977) the Greenland Group becomes progressively more metamorphosed from the coast, where it is relatively unaltered, towards the Alpine Fault, where it is dominantly biotite hornfels.

Available sedimentological information on the Greenland Group in South Westland is inadequate for paleo-environmental interpretation, although the alternating greywacke-argillite succession is similar to that seen in North Westland (Stewart & Nathan in prep.). Laird (1972) and Laird & Shelley (1974) interpreted the Greenland Group in North Westland as a turbidite sequence forming proximal deposits on submarine fans, probably fed by submarine canyons.

(iii) Structure

Structural interpretations of the Greenland Group in South Westland are constrained by insufficient data, lack of exposure, lack of marker horizons or distinctive stratigraphy, and lack of younging control. However it is obvious that the structural style is significantly different to that in North Westland, where the structure consists of broad sub-horizontal to shallow plunging folds of open to isoclinal nature. In South Westland no macroscopic folding has been identified (Stewart & Nathan in prep.).

Fig. 2.2 Greenish grey, well indurated, highly contorted, interbedded crystalline siliceous sandstone and mudstone of the Greenland Group, as exposed at Boulder Creek.

The structural style in South Westland appears to be different north and south of the Moeraki River. To the north in the Power and Collie Creek areas bedding strikes dominantly ENE/WSW (070-090°) and dips steeply north and south, with all identified face directions younging north. Cleavage in Power Creek is poorly developed, being largely overprinted by metamorphism from a granitic pluton immediately to the south. In Collie Creek cleavage is uniform dipping at a low to moderate angle to the east or southeast. To the south in the Whakapohai River catchment bedding is more variable but in general dips gently to moderately (10-40°) to the east and Cleavage dips gently to the northeast (Stewart & Nathan in prep.).

The most important structural style appears to be faulting. The overlying Cretaceous and Tertiary cover is preserved as a series of fault bounded slivers which presumably penetrate into the basement Greenland Group rocks which are commonly sheared with associated silification and quartz veining (Stewart & Nathan in prep.). Drainage is strongly controlled by faulting, mostly sub-parallel to the Alpine Fault, especially in the Whakapohai River catchment.

(iv) Age

The age of the Greenland Group was first determined by Cooper (1974) from a single graptolite locality near Reefton. This indicated an age of early Ordovician (Tremadocian - see Appendix 3), which is supported by Adams (1975) from Rb-Sr whole rock analyses yielding an age of 495 ± 11Ma (late Cambrian to early Ordovician). Samples for these latter analyses were collected from various sites on the West Coast including one from State Highway 6 near Moeraki (S77/012303) (Adams 1975).

2.2.2 Tuhua Group

(i) Distribution

A number of granite plutons have intruded the Greenland Group and these have been mapped as Tuhua Group on the 1:250 000 maps and by Mortimer et al (1984). North of the Paringa River granites have been mapped on the south side of Hunt Hill (S78/240340), in a slip on moraine east of the

Karangarua River (S78/488577), and on a low hill 1500m northeast of Paringa Bridge (S78/256340). South of Paringa River granites occur on the lower northern slopes of Ward Hill (S78/200320), on the south side of Moeraki Hill, around Lake Law (S87/038202) and on Mosquito Hill and other isolated hills on the Haast outwash plains (see Fig. 2.1).

(ii) Description

Mason (1961) described a granite sample from an old quarry in the Paringa pluton (S78/243339) as consisting of quartz, microcline, plagioclase, biotite and hornblende with accessory sphene, apatite and zircon. From a nearby quarry (S78/246338) similar coarse-grained light grey granite contains numerous xenoliths of dark grey fine to medium-grained biotite hornfels which is probably metamorphosed Greenland Group (Mortimer et al. 1984).

(iii) Age

The date of granite emplacement is uncertain, but a biotite concentrate from granite in the old quarry in the Paringa pluton gave a K-Ar age of 286Ma (Mason 1961). This may represent the time of emplacement or a later thermal or uplift event. The age of the Greenland Group (c.495Ma) gives a maximum age so the granite is between 495-286Ma.

2.2.3 Haast Schist

(i) Distribution

The Haast Schist Group forms a thick sequence of steeply dipping regional schists east of the Alpine Fault (see Fig. 2.1). The schists decrease in metamorphic grade towards the east passing from high rank oligoclase-zone rocks at the Alpine Fault through garnet, biotite, and chlorite subzones 4, 3 and 2 into the non-schistose greywacke and argillite (Torlesse Supergroup) of chlorite subzone 1 in the east (Gair 1967).

(ii) Description

The dominant rock type is grey to dark brown, thinly laminated quartzo-feldspathic schist. Locally, bands of greenish-grey to black amphibolite are interlayered within

quartzo-feldspathic schist, which probably represent volcanic rocks (mainly tuffs) interbedded within the Torlesse sediments (Mortimer et al. 1984). Mortimer et al. (1984) noted that interlayered amphibolite bands were common close to the Alpine Fault between the Cook and Paringa Rivers. Waters (1983) mapped an approximately 1km wide amphibolite belt near junction of the Paringa-Otoko Rivers. All these outcrops probably form part of the semi-continuous Pounamu Ultramafic Belt described by Cooper and Reay (1983) (see also Mortimer et al. 1984).

(iii) Structure

Findlay (1979) summarised the structural geology of the Haast Schist in the Central Southern Alps. Five episodes of folding were identified and are summarised in Table 2.1. Grindley (1963) identified "early" F_2 large recumbent folds (including the Karangarua Syncline) and mapped several regionally extensive "late" F_3 south plunging structures in South Westland. In the Haast River area Cooper (1974) described post-metamorphic regional southwest plunging open folds and kink folds as F_3 folds. The geometry and style of these folds implies that they are coeval with the late folds in the Central Southern Alps (Findlay 1979).

(iv) Age

Potassium-argon studies of the Haast Schist Group, as reviewed by Adams (1979), indicate that during the Rangitata orogenic phase the Haast schists were metamorphosed in the early Jurassic at depths of 25-30km and then uplifted to within 5-10km of the surface during the interval mid-Jurassic to mid-Cretaceous. Late Cenozoic uplift (about 5km) which formed the present Southern Alps, began in the late Miocene and still continues. A band of very young K-Ar mineral isochron ages (5 $\pm$ 2Ma) occurs within 10km of the Alpine Fault which correspond to the time of Kaikoura uplift, during which rapid differential movement of the Alpine Schists close to the Alpine Fault caused a separate thermal event, probably induced by shearing and/or frictional heating during fault movements (Adams 1979).

EPISODE OF FOLDING	STRUCTURAL EVENTS
F_1	Fold bedding and are small, complex mesoscopic folds, possibly indicative of "soft- sediment" deformation. F_1 folds do not develop an axial plane fabric and are recognisable only in the Chlorite Zone.
F_2	Fold S_0 and are mesoscopic to 0.5km scale isoclines. Develop an axial plane fabric S_2.
F_3	Fold S_0 and S_2 and are associated with the steeply west- to northwest-dipping "Alpine schistosity" S_3. S_3 lies parallel to subparallel to the axial planes of mesoscopic F_3 folds. Structure is often dominated by kilometre-scale F_3 folds plunging southwest. Parasitic folds on all scales, including microscopic, occur on the limbs of the regional folds.
F_4	F_4 folds are small upright mesoscopic folds sporadically evident only in rocks of the oligoclase isograd and refold coaxially F_3 structures.
F_5	F_5 folds are minor steeply-plunging kinks developed across the dominant east-trending set of joints.

Table 2.1 Summary of structure of the Alpine Schists, Central Southern Alps. (after Findlay 1979)

2.3 CRETACEOUS AND TERTIARY ROCKS

2.3.1 Stratigraphy

The distribution of Cretaceous and Tertiary rocks in the study area is shown in Figure 2.1 with the stratigraphy, as described by Nathan (1977), summarised in Figure 2.3. The stratigraphic sequence outlined below covers that part of the succession which is encountered at the Grave Creek site.

OTUMOTU FORMATION

Age: ? early Haumurian or Piripauan

Description: Lower member consists of maroon, poorly sorted, angular to sub-rounded cobble clasts of unweathered Greenland Group and minor quartz set in a matrix of maroon muddy sandstone (Fig. 2.4). Mostly massive but locally beds of conglomerate are separated by thin layers of maroon sandy mudstone similar to the matrix. Lower member grades up into the upper member which consists of interbedded grey sandstone, greywacke conglomerate, and carboneous mudstone with scattered thin lenses of coal and carbonised plant fragments.

TAUPERIKAKA COAL MEASURES

Age: Haumurian

Description: White or light grey quartz sandstone containing scattered bands of rounded quartz pebbles interbedded with thin bands of dark brown carbonaceous mudstone and rare lensiod coal seams (Fig. 2.5). It is characteristically dominated by thick massive beds of white to yellowish-brown quartz sandstone.

WHAKAPOHAI SANDSTONE

Age: Haumurian

Description: Light greenish-grey, massive, highly bioturbated, slightly glauconitic, medium to fine-grained sandstone, with interbedded sequences of hard, calcite-cemented fine-grained sandstone and non-calcareous brown mudstone. Commonly stained yellowish-brown by weathering.

ARNOTT BASALT

Age: ? late Haumurian or early Teurian

Description: Underlying Whakapohai Sandstone contains brown tuffaceous material in the uppermost 5m and grades upwards into 5-20m of weathered, reddish-brown, basaltic tuff which forms a distinctive band at the base of the Arnott Basalt. The tuff is overlain by thick flows of black, columnar-jointed basalt interbedded with volcanic breccia and tuff.

2.3.2 Structure

The Cretaceous and Tertiary rocks exposed along the coast (Fig. 2.1) are steeply dipping and strike subparallel to the northeast trending coastline. Cotton (1956) interpreted these steeply dipping beds to be the complex vertical limb of a giant monoclinal fold (the Coastal Monocline) trending parallel to the coast from Milford Sound to Buttress Point. Geophysical evidence has enabled the fold to be traced northwards for over 100km (McNaughton & Gibson 1970). The gently dipping upper limb of the monocline has mostly been eroded away except for a number of places such as Bald Hill (S87/985245) where flat-lying breccia and sandstone is interpreted as a remnant of the upper limb (Nathan 1977). The lower limb of the monocline lies entirely offshore.

Nathan (1977) interpreted the Coastal Monocline as reflecting a major basement fault zone active in late Cenozoic time, and possibly as a southern extension of the offshore Cape Foulwind Fault mapped north of Hokitika. The relatively soft Cretaceous and Tertiary sediments have been internally deformed, probably by being draped over the basement fault zone (Nathan 1977).

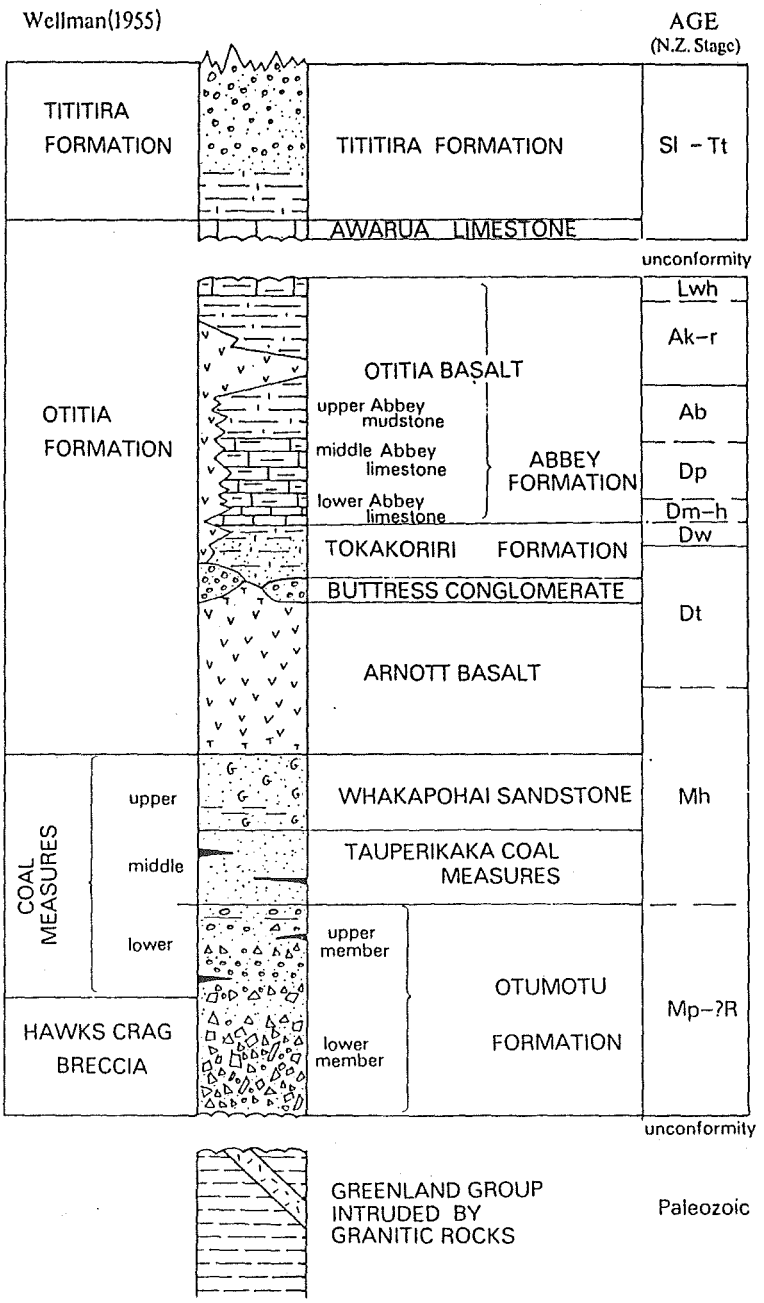

Fig. 2.3 Stratigraphic sequence in the area between Buttress Point and Ship Creek (from Nathan 1977).

Fig. 2.4 Lower member of the Otumotu Formation (as exposed in Tokakoriri Creek) consisting of angular to sub-rounded cobble clasts of unweathered Greenland Group and minor quartz set in a matrix of maroon muddy sandstone.

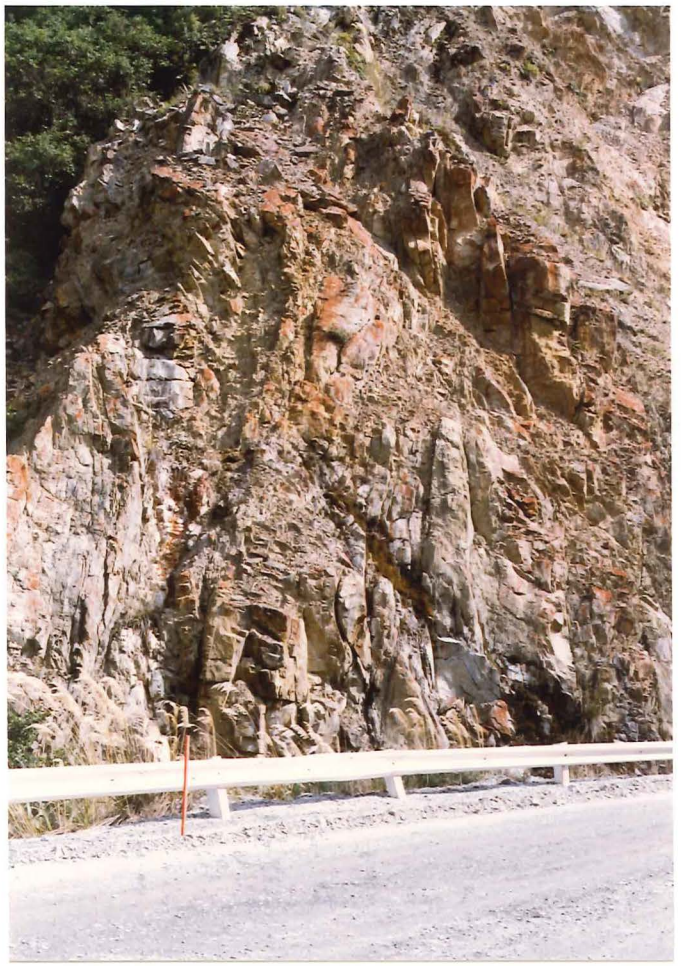

Fig. 2.5 Weathered yellowish brown quartz sandstone of the Tauperikaka Coal Measures at Breccia Creek.

2.4 QUATERNARY DEPOSITS

2.4.1 Glacial Deposits

(i) Background

Detailed stratigraphy of the glacial deposits in South Westland is poorly understood, Warren (1967) and Gair (1967) mapping only two Lower Quaternary units on the 1:250 000 maps. The Moana Formation was defined as being deposited during the last major ice advance, and the Okarito Formation as being deposited during the Otira Glaciation and possibly remnants of pre-Otira (Waimea or Waimaunga) Glaciations.

Mortimer et al. (1984) reinterpreted the glacial stratigraphy recognising three sets of surfaces which were thought to represent three distinct ice advances. The Moana Formation (mn_1, mn_2) was retained for deposits of the last ice advance and older glacial deposits, previously mapped as Okarito Formation, were divided into two units informally named Older Glacial Unit 1 (og_1) and Older Glacial Unit 2 (og_2). The relationship of these units with the type Okarito Formation is uncertain and they are not correlated in any way. Table 2.2 summarises the Quaternary mapping units used on the 1:250 000 maps and in Mortimer et al. (1984).

(ii) Older Glacial Unit 1 (og_1)

This unit represents remnant deposits of an old glacial event which has largely been obliterated by subsequent ice advances. Og_1 surfaces lie at a height of 400-500m above sea level and are dominantly elongate ridges subparallel to the Alpine Fault (see Fig. 2.1) (Mortimer et al. 1984).

(iii) Older Glacial Unit 2 (og_2)

Og_2 surfaces range from 300-375m above sea level. It is the most extensive glacial unit between the Cook and Paringa Rivers being preserved in the high plateau areas between the Alpine Fault and State Highway 6 and in areas of a number of the large lateral moraine ridges extending from State Highway 6 to the coastline (see Fig. 2.1) (Mortimer et al. 1984).

UNITS USED ON 1:250 000 MAPS	UNITS USED BY MORTIMER et al. (1984)	INFERRED AGE
un-named (f)	Postglacial deposits	Present-day to 13 500 years B.P.
Moana Formation (mn)	Moana Formation (mn_1) (mn_2)	13 500 to 15 000 years B.P.
Okarito Formation (oa)	Older Glacial Unit 2 (og_2)	15 000 to ? 17 000 years B.P.
	Older Glacial Unit 1 (og_1)	? 17 000 to ? 19 000 years B.P. or older

Table 2.2 Quaternary mapping units used on the 1:250 000 maps and by Mortimer et al. (1984). (after Mortimer et al. 1984)

(iv) Moana Formation (mn_1, mn_2)

Surfaces from the last glaciation lie 250-300m above sea level near the Alpine Fault and the large, gently sloping ridges between State Highway 6 and the present coastline are interpreted as lateral moraines deposited by Moana glaciers (see Fig. 2.1). Moana morainic material and associated outwash gravels (mn_1), deposited during the peak of the ice advance, are distinguished from moraine thought to be deposited as the glaciers retreated (mn_2 - Moana recessional deposits) (Mortimer et al. 1984).

(v) Interglacial Terraces

In the narrow coastal strip between Ship Creek and the Whakapohai River three terraces are preserved (Nathan & Moar 1975):-

Sardine-2 Terrace	(24-32m a.s.l);
Sardine-1 Terrace	(56-60m a.s.l);
Knights Point Terrace	(140-147m a.s.l).

Both the Knights Point and Sardine-2 Terraces are underlain by marine sediments deposited during interglacial high stands of sea level. The Sardine-1 Terrace is underlain by river gravel resting on lake silts and it is uncertain whether it was formed in a glacial or interglacial period (Nathan & Moar 1975). All the terraces are older than 40,000 years and are correlated (Nathan & Moar 1975) as follows:-

Sardine-2 Terrace	Oturian Stage;
Sardine-1 Terrace	Waimean or Terangian Stage;
Knights Point Terrace	pre-Terangian.

2.4.2 Postglacial Deposits

Postglacial sediments cover over half the study area between the Cook and Paringa River, and also the Haast Plain between the Haast and Waita Rivers (see Fig. 2.1), and includes river gravels and swamp deposits with beach sands on the coast. Along the Alpine Fault bounded mountain front material from post-glacial rapidly eroding valleys is being deposited in alluvial fans on the adjacent outwash plains while narrow glaciated valleys extending east of the Alpine Fault are covered with river gravel and alluvial fan material.

2.4.3 Late Quaternary Paleogeography

During the og_2 and older major ice advances the main valleys of South Westland were filled with glaciers which extended beyond the Alpine Fault to probably form a piedmont ice sheet on the lowland area north of the Hunt Hill-Paringa Hill block and on the Haast Plain, while intervening hill country supported valley glaciers to beyond the present coastline. Sea level was approximately 100-110m lower than present during glacial periods and consequently the coastline was 15-20km west of its present position (as indicated by the present 100m isobath) (Mortimer et al. 1984).

During the Moana advance (15 000-13 500 years B.P.) individual glacier tongues where separated close to the Alpine Fault by og_2 moraine north of the Paringa River and the Haast Plain supported a relatively large ice tongue (Fig. 2.6a). The western extent of these glaciers is uncertain as no terminal moraines have been recognised onshore. Hill country between the Paringa and Waita Rivers carried relatively small valley glaciers which probably did not extend beyond the present coastline.

Retreat of the glaciers started about 13 500 years B.P. and sea level rose gradually until it stabilised at its present height about 6000 years ago which caused the coastline to retreat eastwards flooding parts of the coastal lowland (Fig 2.6b). Since then, the large sediment load carried by the rivers has caused the coastline to prograde westward to the present day position (Mortimer et al. 1984).

2.5 GEOLOGY OF THE ALPINE FAULT ZONE

2.5.1 Distribution of Fault Zone Rocks

Movement along the Alpine Fault has generated a zone of altered and crushed rock locally within a complex of at least two fault traces, although in most places in South Westland the Alpine Fault Zone has been obscured by river gravels and alluvial fans accumulating along the fault-bounded mountain front. However, between the Cook and Mahitahi Rivers and the Moeraki and Waita Rivers Alpine Fault Zone rocks outcrop at a

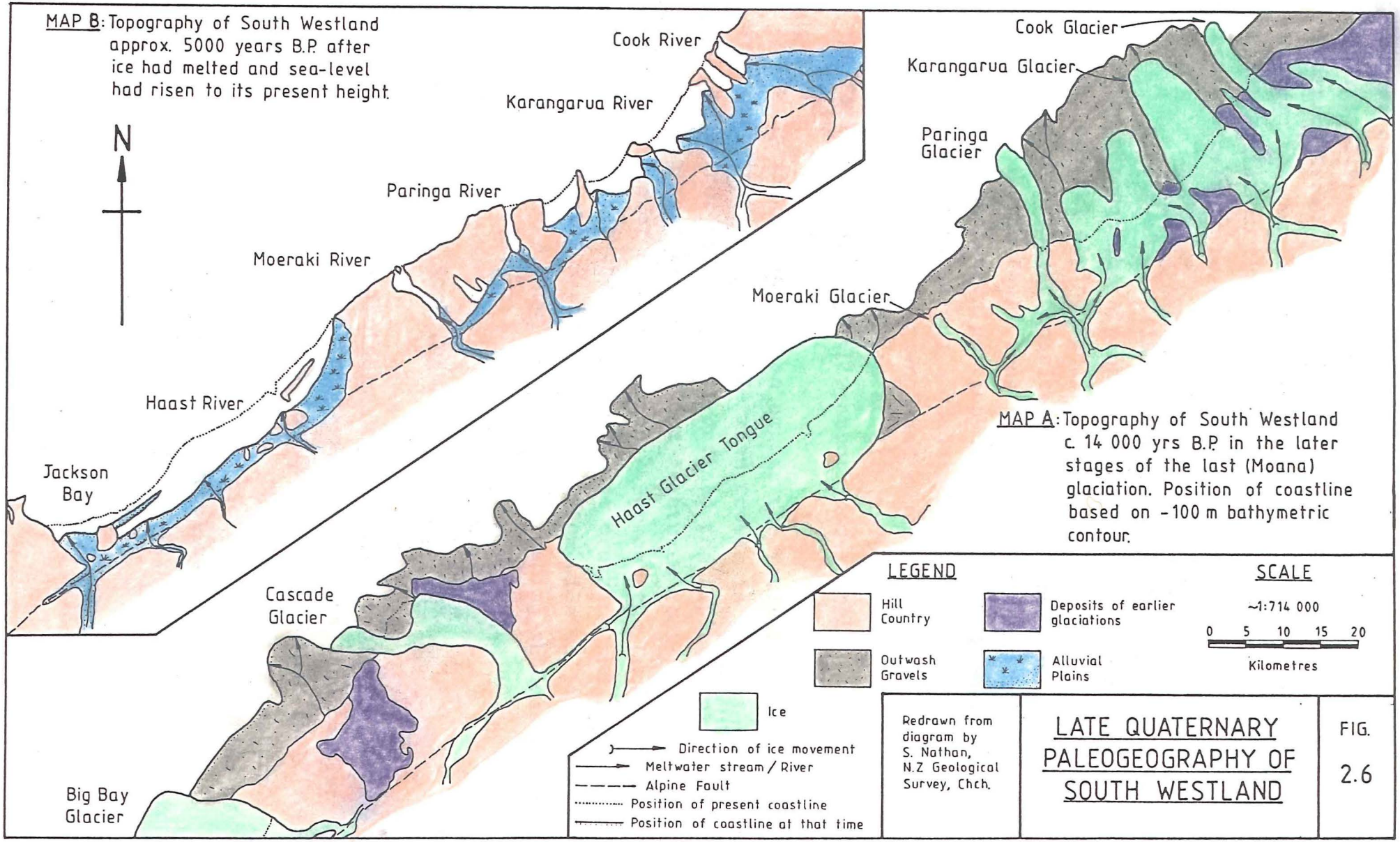
MAP B: Topography of South Westland approx. 5000 years B.P. after ice had melted and sea-level had risen to its present height.
N
Cook River
Karangarua River
Paringa River
Moeraki River
Haast River
Jackson Bay
Cascade Glacier
Big Bay Glacier
Haast Glacier Tongue
Moeraki Glacier
Paringa Glacier
Karangarua Glacier
Cook Glacier
MAP A: Topography of South Westland c. 14 000 yrs B.P. in the later stages of the last (Moana) glaciation. Position of coastline based on -100 m bathymetric contour.
LEGEND
Hill Country
Deposits of earlier glaciations
Outwash Gravels
Alluvial Plains
Ice
Direction of ice movement
Meltwater stream / River
Alpine Fault
Position of present coastline
Position of coastline at that time
SCALE
~1:714 000
0 5 10 15 20
Kilometres
Redrawn from diagram by S. Nathan, N.Z Geological Survey, Chch.
LATE QUATERNARY PALEOGEOGRAPHY OF SOUTH WESTLAND
FIG. 2.6

number of localities, the best exposures being Havelock Creek (S78/565549), Hermann Creek (S78/428456) and Slippery Face, Robinson Creek (S87/993170). No continuous sections between western basement rocks (Greenland Group and Tuhua Granite) and Haast Schist to the east have been found, and all fault zone rocks appear to be derived from Haast Schist.

Sibson et al. (1979) presented an idealised composite section through the Alpine Fault Zone broadly characteristic of the central Alpine Fault region (Fig. 2.7). In any particular exposure this composite section may be truncated at any place within the fault zone by the most recent fault break, with the southeastern portion of the section thrust over Quaternary gravels along a gouge zone. Other gouge zones may locally disrupt the sequence and cause repetition of lithologies. According to Sibson et al. (1979) the total width of the fault zone is typically about 1000-1500m.

An idealised section across the fault zone based on the exposures in Havelock and Hermann Creeks is given in Figure 2.8. Mortimer et al. (1984) defined the Alpine Fault Zone to include the zone of crushed and fractured rock which is wider than the zone of mylonitisation. Between the Cook and Mahitahi Rivers area the zone of intense crushing and fracturing extends up to 1000m wide averaging 750m wide while further south at Slippery Face this zone of crushing reduces to less than 500m wide (Eggers 1984).

2.5.2 Fault Zone Rock Description

(i) Fault Gouge, Tectonic Breccia and Cataclasite

Fault gouge zones range from 2-10m wide and consist mainly of green clay containing fragments of other fault zone rocks (Fig. 2.9). Immediately to the east of the western gouge exposures is a belt of tectonic breccia consisting of intensely crushed mylonite or amphibolite in a puggy matrix. This breccia varies between 10-100m wide and passes eastwards into less strongly crushed rocks.

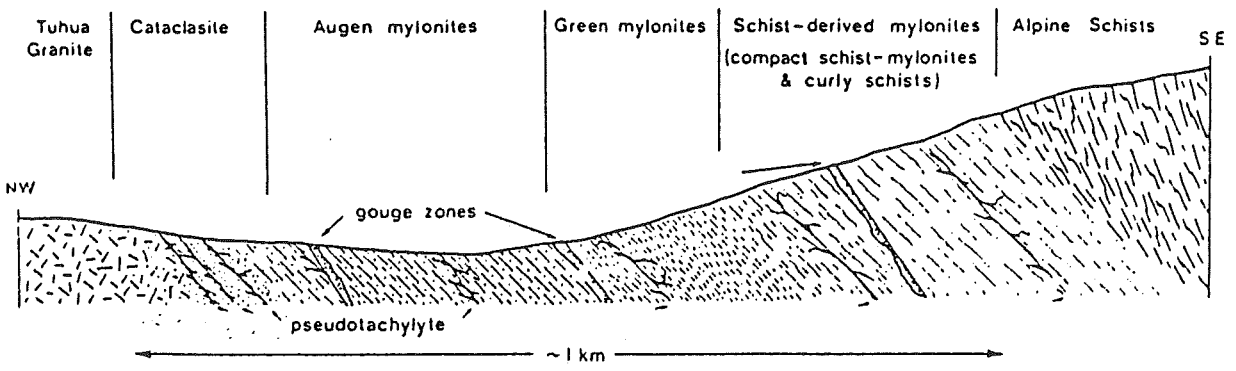

Fig. 2.7 Schematic composite section through the Alpine Fault Zone proposed by Sibson et al. (1979).

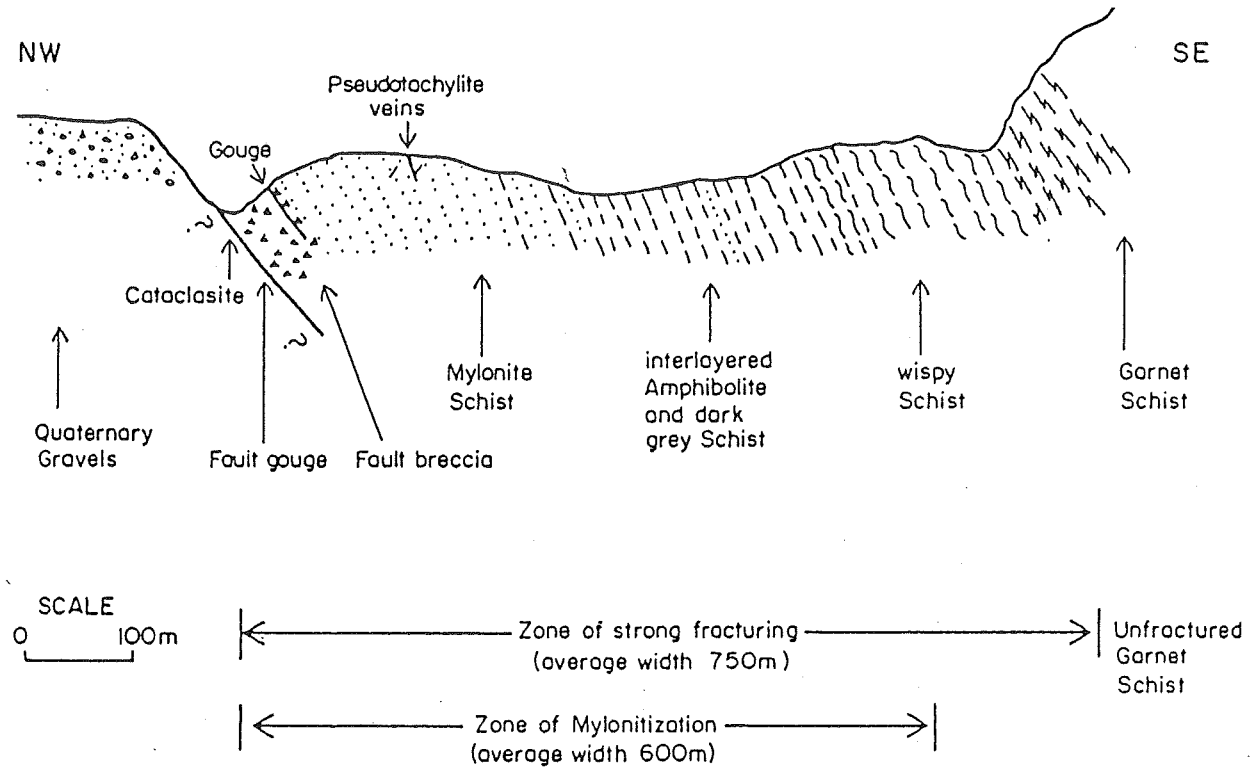

Fig. 2.8 Diagrammatic cross-section across the Alpine Fault Zone based on exposures in Havelock and Hermann Creeks (from Mortimer et al. 1984).

At Hermann Creek there is a 2-3m wide band of grey-brown to light green cataclasite about 20m east of the western gouge zone. Mortimer et al. (1984) interpreted this as a band of brecciated rock formed close to the fault at depth and which had been subsequently compacted and uplifted to the surface.

(ii) Mylonite Schist

East of the tectonic breccia is a zone of grey-brown to black mylonite schist ranging in width from 50-350m (Fig. 2.10). The rocks have undergone intense deformation at metamorphic depths (25-30km), and are schistose and of the same metamorphic grade as the nearby oligoclase-garnet schists (Mortimer et al. 1984).

Pseudotachylite veins have been found cross-cutting mylonite schists in Havelock Creek (Nathan 1984) and in Thomson Creek (S87/066216) (Seward & Sibson 1985). Pseudotachylite vein complexes are regarded as the product of frictional fusion during discrete seismic slip events in dry crystalline rock (Seward & Sibson 1985).

(iii) Amphibolite

Dark green, medium to coarse grained amphibolite interlayered with grey-brown mylonite forms a belt immediately east of the zone of mylonite. This is apparently equivalent to the belt of "green mylonites" figured by Sibson et al. (1979) (see Fig. 2.7). Despite being interlayered with and more crushed and fractured than the mylonite schists, the amphibolites generally do not show cataclastic deformation textures (Mortimer et al. 1984).

(iv) Wispy Schist

"Wispy" or "curly" schists is a field term used to describe schists which contain alternating light and dark laminae reduced to very thin (<1mm) lensoidal streaks which represents the first stage of mylonitisation. The belt of wispy schists (50-200m wide) grades eastwards into normal, unaltered oligoclase-garnet schist.

Fig. 2.9 Light greyish green fault gouge overthrusting post-glacial slope materials in the Alpine Fault Zone at Havelock Creek.

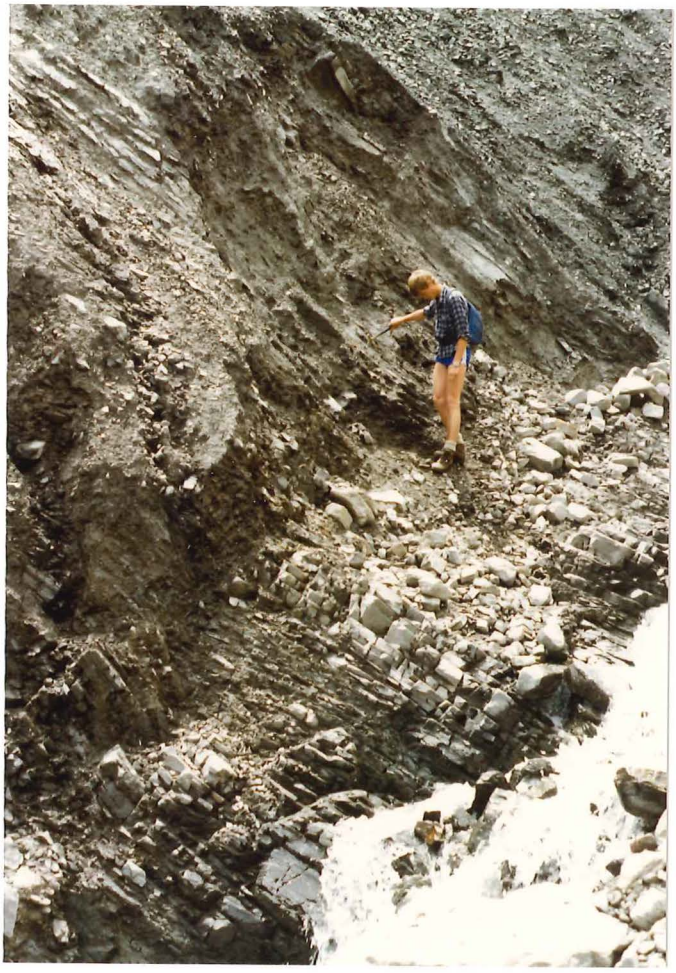

Fig. 2.10 Dark grey to black mylonite schist in the Alpine Fault Zone at Havelock Creek.

2.5.3 Dip of the Fault Zone

Wellman (1955) and Suggate (1963) demonstrated the widespread occurrence of gravity collapse "napplets" along the steeper parts of the Alpine front and suggested that the dip of the fault steepens to near-vertical values at depth (Fig. 2.11a). However, Sibson et al. (1979), who observed that these napplets are well developed only in intensely crushed rock whose behaviour resembles that of a cohesionless aggregate, suggest a value of 40-50° for the dip of the fault zone at depth (Fig. 2.11b) based on the attitude of mylonitic foliation.

2.5.4 Age of Fault Zone Rocks

According to Sibson et al. (1979) structural data indicates that the fabrics of the Alpine Fault mylonites developed during the Late Cenozoic phase of oblique compression, and that they could not have arisen from purely transcurrent movements. As the gouge zones, cataclasites and pseudotachylites are of similar age to, or postdate the mylonites, it appears that all fabrics within the fault zone developed during this Late Cenozoic period of movement.

Carter & Norris (1976) suggested on stratigraphic grounds that the reverse slip on the Alpine Fault began in the Late Miocene (c.10Ma ago) continuing spasmodically through the Plio-Pleistocene to the present-day. By late Pliocene to early Pleistocene (c.2-3Ma ago) the Alpine Schists were exposed to erosion.

A single pseudotachylite sample from Thomson Creek on the Mataketake Range, South Westland (S87/066216) was fission-track dated yielding an age of 0.43 ± 0.17Ma. (Seward & Sibson 1985) which possibly represents a discrete seismic event at that time. Taking an average late Quaternary uplift rate of 5mm/yr, crude estimates suggest that the material was generated by slip at a depth of at least 2.2 ± 1.0km (Seward & Sibson 1985).

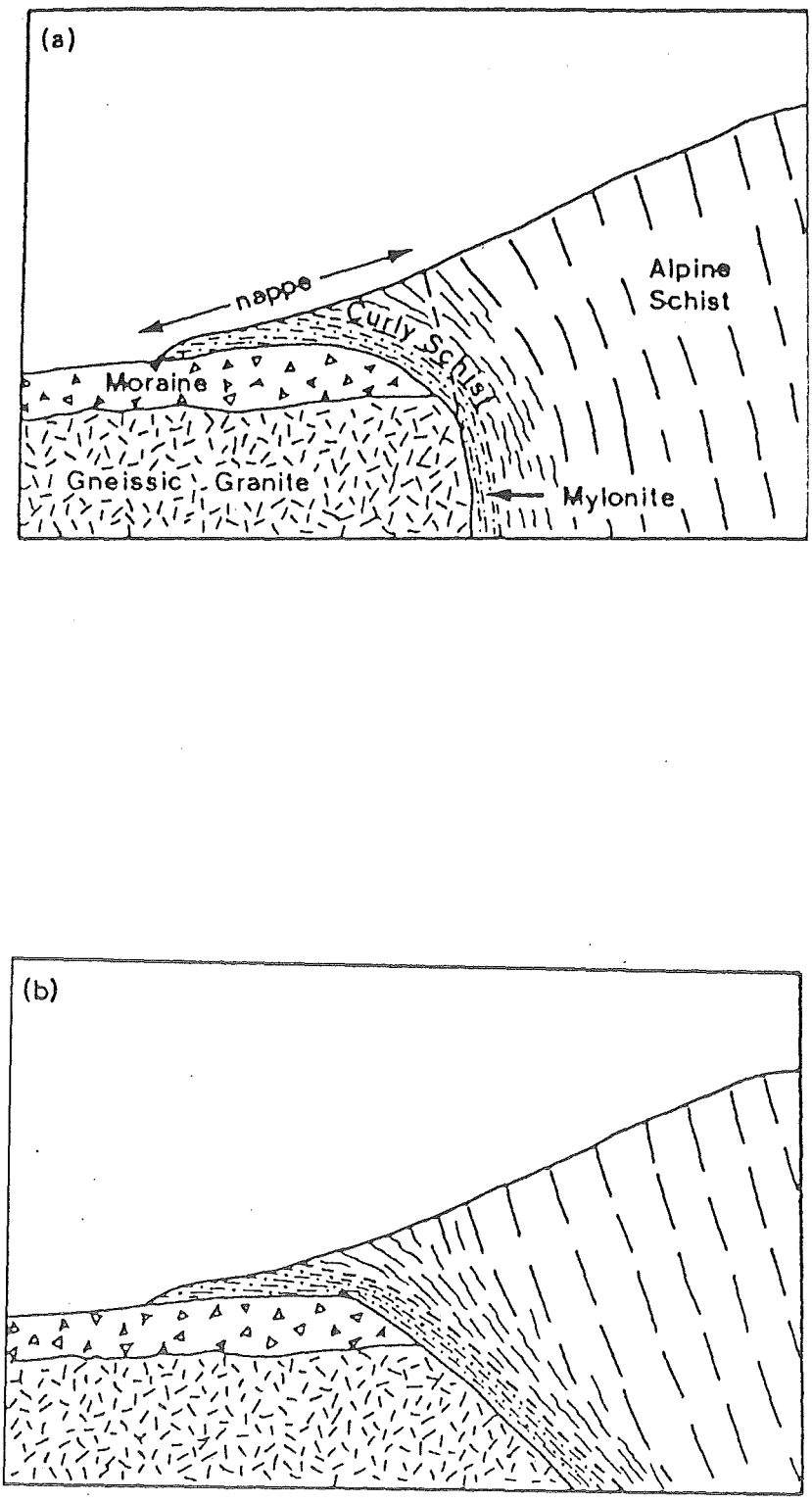

Fig. 2.11 Alternative models for the dip of the Alpine Fault Zone at depth;
a) after Wellman (1955),
b) after Sibson et al. (1979).

CHAPTER THREE

SLOPE MOVEMENT TERMINOLOGY AND SITE SELECTION

3.1 OBJECTIVES

The objectives of this chapter are to:-

1. Give background information on:-
   a) classification and terminology of slope movement types and processes;
   b) impacts of forest management activities on slope processes;
2. Outline the methodology used to select the investigation sites, which involves:-
   a) identification and description of landform units;
   b) evaluation of the relative slope stability of landform units;
   c) selection of landform units and investigation sites for study based on this information;
3. Outline the approach to engineering geological investigations.

3.2 SLOPE MOVEMENT TYPES AND PROCESSES

3.2.1 Slope Movement Classification

Numerous classification schemes have been proposed to describe the gravitational downslope movement of geologic materials. The most important and widely accepted of these include:-

1. Sharpe (1938) - uses type of movement and its relative rate as the primary criterion together with type of material involved and relative water or ice content of the moving mass to describe slope movements;
2. Varnes (1958; 1978) - presents an alternative scheme (developed in 1958, revised and extended in 1978) based largely on Sharpe (1938), using as chief criteria type of movement primarily and type of material secondarily;

3. Hutchinson (1968) - devised a scheme dividing slope movement processes into creep, frozen ground phenomena and landslides. Northey et al. (1974) modified this scheme to suit New Zealand conditions.

The Varnes (1978) classification scheme has been adopted for describing slope movement processes and features in this study, being the most detailed and complete scheme available. Figure 3.1 presents the scheme together with examples of some of the combinations of movements and materials. The classification develops a vocabulary of terms by which slope processes and their deposits may be described. Terminology relevant to this study is outlined below.

3.2.2 Types of Movement

Types of slope movement are divided into five main groups: falls, topples, slides, lateral spreads and flows. A sixth group, complex slope movements, includes combinations of two or more of the other five types. Important movement types in this study are falls, slides and flows:-

1. Falls - a mass of any size is detached from a steep slope or cliff, along a surface on which little or no shear displacement takes place, and descends mostly through the air by free fall, leaping, bouncing, or rolling.
2. Slides - movement consists of shear strain and displacement along one or several surfaces or within a relatively narrow zone. Slides can be classed into rotational (rotational movement about an axis parallel to the slope) and translational (movement out or down and along a planar surface).
3. Flows - flow involves distribution of displacement throughout the moving mass and its behaviour resembles that of a viscous fluid. Slip surfaces within the moving mass are usually not visible or are short-lived. The boundary between moving mass and material in place may be a sharp surface of differential movement or a zone of distributed shear.

(DOMINANT) TYPE OF MOVEMENT	TYPE OF MATERIAL (BEFORE MOVEMENT)*			
	BEDROCK	ENGINEERING SOILS		
		PREDOMINANTLY COARSE	DEBRIS	EARTH / PREDOMINANTLY FINE
I. FALLS Mass in motion travels most of the distance through the air. Includes free fall, movement by leaps and bounds, and rolling of fragments of bedrock or soil.	(2.1a1) ROCK FALL, extremely rapid a		DEBRIS FALL b	EARTH FALL c
II. TOPPLES Movement due to forces that cause an overturning moment about a pivot point below the center of gravity of the unit. If unchecked, will result in a fall or slide.	(2.1a1) ROCK TOPPLE (see Hoek and Watson, 2.37). (2.1a2) d	(2.1a1) DEBRIS TOPPLE e		EARTH TOPPLE f
III. SLIDES Movements involving shear displacement along one or several surfaces, or within a relatively narrow zone, which are visible or may reasonably be inferred.	A. ROTATIONAL Movement due to forces that cause a turning moment about a point above the center of gravity of the unit. Surface of rupture concaves upward. (2.1g) ROCK SLUMP, extremely slow to moderate g		DEBRIS SLUMP h	(2.1i1) EARTH SLUMP i
	B. TRANSLATIONAL Movement predominantly along more or less planar or gently undulatory surfaces. Movement frequently is structurally controlled by surfaces of weakness, such as faults, joints, bedding planes, and variations in shear strength between layers of bedded deposits, or by the contact between firm bedrock and overlying detritus. (2.1j1) (Hamblin, 2.15; after Sharp, 2.5) (2.1j2) ROCK BLOCK SLIDE j	(2.1k1) DEBRIS SLIDE, very slow to rapid k		(2.1l1) EARTH BLOCK SLIDE (Hansen, 2.5) l
IV. LATERAL SPREADS Distributed lateral extension movements in a fractured mass. A. Attributed to wedging failure controlling basal shear surface or zone of plastic flow (predominantly in bedrock). B. In which extension of rock or soil results from liquefaction or plastic flow of subjacent material.	(2.1m2) (Zaruba and Mencl, 2.19)21) (2.1m1) (Sharp, 2.7) (2.1m3) (Varnes, 2.118) m		n	(2.1o) EARTH LATERAL SPREAD, very rapid o
V. FLOWS A. IN BEDROCK Involves distinctly continuous deformation and surficial or small gross, involves extremely slow and generally nonaccelerating differential movements among relatively intact units. Movements may 1. Be along many shear surfaces that are apparently not connected; 2. Result in folding, bending, or bulging; or 3. Roughly simulate those of viscous fluids in distribution of velocities. B. IN SOIL Movement within displaced mass such that the form taken by moving material or the apparent distribution of velocities and displacements resemble those of viscous fluids. Slip surfaces within moving material are usually not visible or are short-lived. Boundary between moving mass and material in place may be a shear surface of differential movement or a zone of distributed shear. Movement ranges from extremely rapid to extremely slow.	A (2.1a1) (Newmark, Peale, and Rysdal, 2.116) (2.1a3) (Zischinsky, 2.154) (2.1a4) (Rysdal and Door, 2.127) p (2.1a2) (Zischinsky, 2.154) Gravity downslope movement of uneven rocks and soil on the margin of a sedimentary basin Note: Sacking or gravitational sagging is illustrated by p1, p2, and p3.	B (2.1q1) DEBRIS FLOW, very rapid (2.1q3) DEBRIS AVALANCHE, very rapid to extremely rapid (2.1q5) BLOCK STREAM q	(2.1q2) SOLIFLUCTION (2.1q4) SOIL CREEP, extremely slow Note: Drawings in q2, q4, and q5 courtesy of G. M. Richmond, from Colluvium, an unpublished chart.	WET FLOWS (2.1r1) WET SAND OR SILT FLOW, rapid to very rapid (2.1r2) RAPID EARTH FLOW (QUICK CLAY FLOW), very rapid (Sharpe, 2.145) MUD FLOW (2.1r3) EARTH FLOW, very slow to rapid (Zaruba and Mencl, 2.182) (2.1r5) LOESS FLOW (dry, caused by earthquake), extremely rapid and short in unit (2.1r4) DRY SAND FLOW, rapid to very rapid DRY FLOWS r
VI. COMPLEX Movement is by a combination of one or more of the five principal types of movement described above. Many landslides are complex, although one type of movement generally dominates over the others in certain areas within a slide or at a particular time.	EXAMPLES (2.1s1) ROCK FALL–DEBRIS FLOW (ROCK-FALL AVALANCHE), Extremely rapid (After Heim, 2.58, Elm, Switzerland, 1881) (2.1s2) SLUMP AND TOPPLE (Zaruba, 2.182) (2.1s3) ROCK SLIDE–ROCK FALL (Hamblin, Peale, Rysdal, 2.116)	(2.1u1) CAMBERING AND VALLEY BULGING	(2.1s5) SLUMP–EARTH FLOW	Note: Most, if not all slow earth flows in cohesive materials are complex in that finite shear occurs along the flanks and basal surface, although the distribution of velocities within the displaced material may indicate plastic flow. s

Fig. 3.1 Varnes (1978) classification of slope movement types

3.2.3 Types of Material

Four terms are used to describe the types of material involved in slope movements:-

1. Bedrock - hard or firm rock that was intact and in its natural place before the initiation of movement;
2. Engineering Soil - any loose, unconsolidated, or poorly cemented aggregate of solid particles together with any interstitial gas or liquid. Engineering soil is divided into debris and earth material:-
   a) Debris - material in which 20 to 80% of the fragments are greater than 2mm in size and the remainder of the fragments less than 2mm;
   b) Earth - material in which about 80% or more of the fragments are smaller than 2mm.

3.2.4 State of Slope Activity

Slopes are defined as either active or inactive in terms of state of slope activity. Active slopes are those currently moving or those which may have moved during the last cycle of seasons. Slopes are inactive if there is no evidence of movement within the last cycle of seasons. They may be dormant in which case the causes of failure remain and movement maybe renewed, or they may be stabilised in which case factors essential to movement have been removed naturally or by human activity. Long-inactive slopes are often referred to as ancient slope movements and may be modified by erosion or be covered with vegetation.

3.2.5 Sequence or Repetition of Movement, Nomenclature and Rates of Movement

Table 3.1 list terms that describe special kinds of slope failure that involve a sequence or repetition of movement. Terminology used to describe the main features of slope movements are illustrated in Figure 3.2 in relation to a rotational slide-earthflow example. A rate of movement scale and associated descriptive terms are presented in Figure 3.3.

TERM	DEFINITION
ADVANCING	Failures that enlarge in the direction of movement.
RETRORESSIVE	Failures that are retreating.
PROGRESSIVE	Failures that are both advancing and retreating simultaneously.
COMPLEX	Failures that display more than one of the major modes of movement.
COMPOUND	Movements in which the failure surface is a combination of curved and planar elements giving the slide movement a part-rotational, part-translational character.
MULTIPLE	The manifold development of the same mode of movement.
SUCCESSIVE	Any type of multiple movements that develop successively on time.
MULTISTORIED	The development of movements one on top of another.

Table 3.1 Terminology describing a sequence or repetition of slope movement (after Varnes 1978).

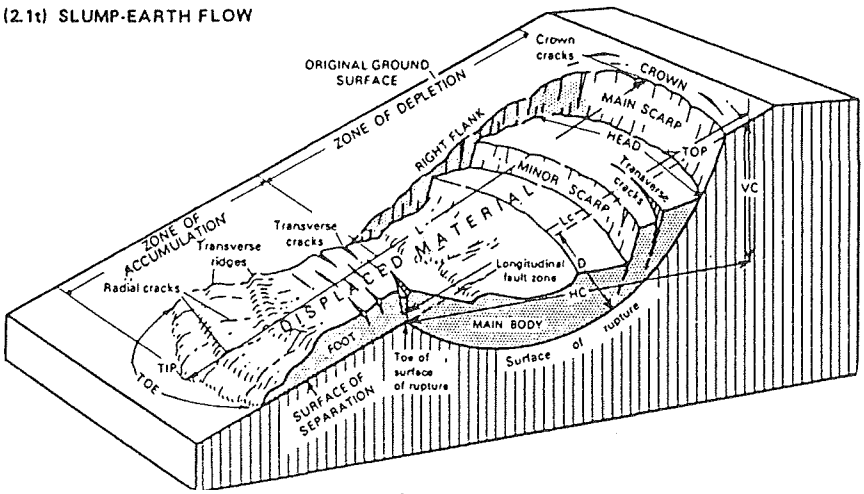

NOMENCLATURE

MAIN SCARP—A steep surface on the undisturbed ground around the periphery of the slide, caused by the movement of slide material away from undisturbed ground. The projection of the scarp surface under the displaced material becomes the surface of rupture.

MINOR SCARP—A steep surface on the displaced material produced by differential movements within the sliding mass.

HEAD—The upper parts of the slide material along the contact between the displaced material and the main scarp.

TOP—The highest point of contact between the displaced material and the main scarp.

TOE OF SURFACE OF RUPTURE—The intersection (sometimes buried) between the lower part of the surface of rupture and the original ground surface.

TOE—The margin of displaced material most distant from the main scarp.

TIP—The point on the toe most distant from the top of the slide.

FOOT—That portion of the displaced material that lies downslope from the toe of the surface of rupture.

MAIN BODY—That part of the displaced material that overlies the surface of rupture between the main scarp and toe of the surface of rupture.

FLANK—The side of the landslide.

CROWN—The material that is still in place, practically undisplaced and adjacent to the highest parts of the main scarp.

ORIGINAL GROUND SURFACE—The slope that existed before the movement which is being considered took place. If this is the surface of an older landslide, that fact should be stated.

LEFT AND RIGHT—Compass directions are preferable in describing a slide, but if right and left are used they refer to the slide as viewed from the crown.

SURFACE OF SEPARATION—The surface separating displaced material from stable material but not known to have been a surface on which failure occurred.

DISPLACED MATERIAL—The material that has moved away from its original position on the slope. It may be in a deformed or undeformed state.

ZONE OF DEPLETION—The area within which the displaced material lies below the original ground surface.

ZONE OF ACCUMULATION—The area within which the displaced material lies above the original ground surface.

Fig. 3.2 Nomenclature of slope movement features (from Varnes 1978).

3.2.6 Causes of Slope Movements

For failure to occur on a slope the total shear stress must exceed the total shear strength of a particular surface in the slope material. Terzaghi (1950) divides the causes of slope movements into two types:-

1. External Causes - those which produce an increase of total shear stress at unaltered shear resistance of material beneath a slope to the point of failure;
2. Internal Causes - those which produce a decrease in total shear strength of the slope material without changing the total shear stress.

In most cases a number of causes exist simultaneously and the final factor may only be a triggering event. If this is the case then it is possible to separate the triggering phenomenon from the fundamental cause(s) (Palmquist & Bible 1980). The principal factors contributing to slope instability in slope-forming materials are outlined in Table 3.2.

3.3 IMPACTS OF FOREST MANAGEMENT ACTIVITIES ON SLOPE PROCESSES

It is generally well accepted that forest vegetation plays an important role in stabilising slopes and reducing the movement rate and occurrence of slope movement processes. Specific action of the various components of a forest cover are summarised in Table 3.3.

There are basically three types of timber harvesting systems: clearfelling, selective logging, and bush-mill logging, with clearfelling potentially having the greatest impact on slope stability. Immediate termination of the stabilising effects of a forest cover brings about a series of conditions which lowers the factor of safety of a slope. Initially relief of the load, cessation of the mechanical action of wind in tree tops, and cessation of root wedging causes an immediate increase in slope stability (Fig. 3.4). However, after a certain amount of time stability decreases due to discontinuance of the interception, retention and evapotranspiration of rainwater increasing the amount that reaches the ground and

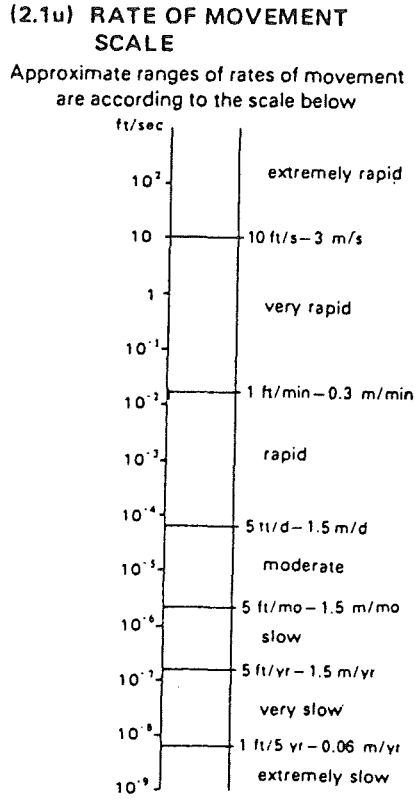

Fig. 3.3 Rate of movement scale and descriptive terms (from Varnes 1978).

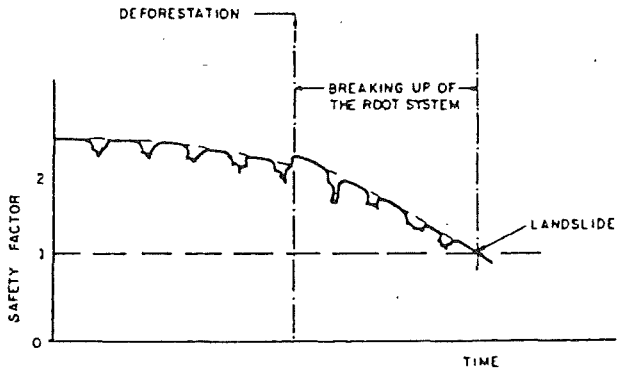

Fig. 3.4 Factor of safety variation due to deforestation of a slope (from Prandini et al. 1977).

A.	Factors contributing to increased shear stress		
	1. Removal of lateral support	i	Erosion by water
		ii	Weathering, wetting, drying, thermal stresses, and frost action
		iii	Slope steepness increased by mass movement
		iv	Man-made excavations
		v	Sudden drawdown
	2. Overloading by	i	Weight of water, snow, talus, or other mass movement from above
		ii	Fills, wastepiles, structures, vehicles
		iii	Growth of vegetation
		iv	Stress concentrations caused by fissures
	3. Transitory stress	i	Earthquakes
		ii	Man-made vibrations
		iii	Wind action on trees
	4. Removal of underlying support	i	Undercutting by running water
		ii	Subaerial weathering, wetting, drying, thermal stresses, and frost action
		iii	Subterranean erosion (eluviation of fines or solution of salts)
		iv	Mining activities
	5. Lateral pressure	i	Water in fissures
		ii	Freezing of water
		iii	Swelling by hydration of clays
		iv	Seepage forces (viscous drag of moving water on soil grains)
		v	Wedging action of roots
	6. Tectonic movement	i	General steepening of slope
B.	Factors contributing to reduced shear strength		
	1. Composition and texture	i	Presence or development of planes of weaker material
		ii	Unfavourable pattern of jointing in rocks
		iii	Loosely packed materials - spontaneous liquefaction, sensitive soils
		iv	Overconsolidated clays - long-term stability
	2. Physico-chemical reactions	i	Cation exchange
		ii	Chemical weathering, decomposition, oxidation-reduction, leaching
		iii	Physical weathering, breaking of particles by frost, capillary and thermal stresses
	3. Effects of porewater	i	Excess porewater pressure
		ii	Reduction of capillary tension

Table 3.2 Summary of factors which contribute to slope instability (from Pettinga 1981: Mass Movement handout, based on Varnes 1978)

infiltrates the soil, loss of effects of the superficial debris layer with the consequent increase in erosion and infiltration, and a rise in ground water-table level as a consequence of the increase of rainwater entering the soil with the possible effects of saturating the soil and surcharging the slope. Also, the loss, within a certain amount of time, of mechanical effects of the root system eventually reduces the induced apparent cohesion and consequently lowers the shear strength of the natural mass (Prandini et al. 1977).

Clearfelling and selective logging both involve road construction for transportation of timber from the site. Principal impacts of road construction are to interrupt the natural balance between shear strength and shear stress of a marginally stable slope material and alteration of subsurface and surface water movement. Instability can result from poor design and construction of cut and fill slopes on steep ground and improper design of drainage systems. Roads alter the routing of water by interception of surface water and carrying this excess water through ditches. Instability commonly occurs where natural and artificial drainage systems are inadequate to handle this excess water (Swanston & Swanson 1976).

The relationship between forest removal and increased slope instability is well documentated. O'Loughlin & Pearce (1976) studied effects of clearfelling of beech-podocarp-hardwood forests and their replacement with Pinus radiata plantations on steep, dissected hill country underlain by late Tertiary sandstone and siltstone in North Westland. They reported an increase in slope movement density from $1km^{-2}$ to $20km^{-2}$ upon clearfelling. Most slope movements were triggered by high intensity rainstorm events and failed on an allophane-rich sliding surface at the regolith-bedrock interface. Slope stability analysis indicated slopes greater than 25^{o}, when saturated, were unstable unless additional shear strength is provided by a network of tree roots. The critical slope angle (FS = 1) for moist, unsaturated regolith is 44^{o}. Root decay time on clearfelling was about 5 years with a subsequent 10 year period of potential erosion before the Pinus radiata forest root network re-establishes. Their principal conclu-

COMPONENT OF FOREST COVER	INFLUENCE ON SLOPE STABILITY
A. ASSEMBLAGE OF TREES & OTHER VEGETATION ABOVE GROUND.	(a) Intercepts & protects slope from action of sunshine, wind & rain. (b) Retains rainwater by wetting of leaves, branches, trunks & associated epiphytes. Elimination of this water as vapour equivalent to a decrease of rainfall in area in terms of water that reaches the ground. (c) Eliminates water by evapotranspiration; lowers effective infiltration into slope.
B. VEGETAL DEBRIS ON FOREST GROUND.	(a) Immobilises large amount of water that reaches ground due to it's high retention capacity. (b) Helps establish, in association with superficial root system, the underflow. (c) Cuts down runoff under conditions of heavy rainfall allowing this water to join the underflow.
C. ROOT SYSTEM	(a) Increases shear strength of soil by mechanical binding effects, and root network helps distribute point shear stresses throughout the slope. (b) Establishes the underflow with the consequent reduction of the effective infiltration into the slope. (c) Creates negative pore pressures by biological suction increasing soil cohesion using water that would otherwise be part of the effective infiltration into the slope.

Table 3.3 Specific action of the various components of a forest cover favourable to slope stability (after Prandini et al. 1977).

sion is to restrict future clearfelling of similar areas to slopes less than 25°.

Little or no information is known on the impacts of bush-mill harvesting systems. This involves removal of single trees or small groups of trees using chainsaw mills processing timber at the site of felling and using helicopters to transport the mill to and from the site and to extract the timber. This is one system being investigated by the N.Z. Forest Service for possible harvesting of timber from South Westland forests.

3.4 RECENT SLOPE STABILITY HISTORY OF SOUTH WESTLAND

FRI landform studies analysed historical aerial photograph records extending back to 1947 in an attempt to outline the recent erosion history of South Westland. In general the investigation concluded that both individual and groups of slope instability features develop very rapidly, and active instability periods occur in short-lived episodes (less than 50 years). Revegetation of slope movement scars is rapid with a good cover of scar surfaces within 5 years after an event (Fitzsimons & O'Loughlin 1984). Rainfall data indicates an approximate correlation of instability and the incidence of heavy precipitation periods therefore rainfall data may provide evidence for the recent instability history of South Westland's slopes.

During the period 1947 to 1965, aerial photograph records show an increase in the number of slope movement scars indicating a period of active instability and between 1965 and 1981, instability remained relatively constant. After 1981 South Westland slopes generally stabilised apart from Alpine Fault Zone slopes which are currently experiencing an episode of increased instability, beginning in the late 1970's.

3.5 SELECTION OF LANDFORM UNITS FOR INVESTIGATION

3.5.1 Landform Unit Identification and Description

Identification of landform units during the FRI study was based on a number of geomorphological criteria, the principal criteria being (Fitzsimons et al. 1985):-

1. geology of parent materials;
2. slope gradient;
3. frequency and type of "mass wasting";
4. drainage;
5. susceptibility to flooding, and;
6. degree of dissection by streams.

Nine landform units were identified between the Cook and Paringa Rivers (Fitzsimons & O'Loughlin 1984) and eight units between the Paringa and Haast Rivers (Fitzsimons et al. 1985) as listed in Table 3.4. Their distribution is shown in Figures 3.5 and 3.6 with characteristics of representative landform units summarised in Table 3.5 under the six criteria listed above.

3.5.2 Relative Slope Stability

To investigate relative slope stability of the different landform types, slope failure densities for each landform type were calculated by FRI studies, based on slope failures identified on aerial photographs with surface areas over approximately 200m^2. A summary of this data is presented in Tables 3.6 and 3.7.

Stability ranking according to this data shows greywacke hill country to be the least stable landform type in both the Cook to Paringa and the Paringa to Haast areas (3.1 and 14.8 slope failures per km^2 respectively). This is followed by deformed schist slopes, steep moraine faces and schist mountain slopes in the Cook to Paringa area (2.5, 1.2 and 1.0 slope failures per km^2 respectively) and by Cretaceous-Tertiary hill country, deformed schist slopes and schist mountain slopes in the Paringa to Haast area (2.8, 2.5 and 1.0 slope failures per km^2 respectively).

COOK TO PARINGA RIVERS AREA	PARINGA TO HAAST RIVERS AREA
Moraine Tops	Moraine Slopes
Gentle Moraine Faces	Greywacke Hill Country
Steep Moraine Faces	Cretaceous-Tertiary Hill Country
Composite Hill Country	Deformed Schist Slopes
Schist Mountain Slopes in proximity to the Alpine Fault	Schist Mountain Slopes
Schist Mountain Slopes	Alluvial Outwash Surfaces
Alluvial Outwash Surfaces	Terraces
Valley Bottom Terraces	Alluvial Fans
Alluvial Fans	

Table 3.4 List of landform units identified between the Cook to Paringa Rivers and Paringa to Haast Rivers areas, South Westland, by FRI SWMEP studies (after Fitzsimons & O'Loughlin 1984 and Fitzsimons et al. 1985).

SCALE

0 5 10

Kilometres

N

COOK R.

Karangarua R.

TASMAN SEA

Jacobs R.

Mahitahi R.

Powers Ck

PARINGA R.

HAVELOCK CK

LEGEND

- Moraine Top
- Steep Moraine Face
- Gentle Moraine Face
- Alluvial Outwash Surface
- Alluvial Fan
- Alluvial Terrace
- Glaciofluvial Terrace
- Tertiary Hill Country
- Granite Hill Country
- Greywacke Hill Country
- Alpine Fault Zone Slopes
- Schist Mountain Slopes

LANDFORM TYPES BETWEEN THE COOK & PARINGA RIVERS, SOUTH WESTLAND

(Redrawn from Fitzsimons & O'Loughlin 1984)

SCALE 1:150 000

FIG. 3.5

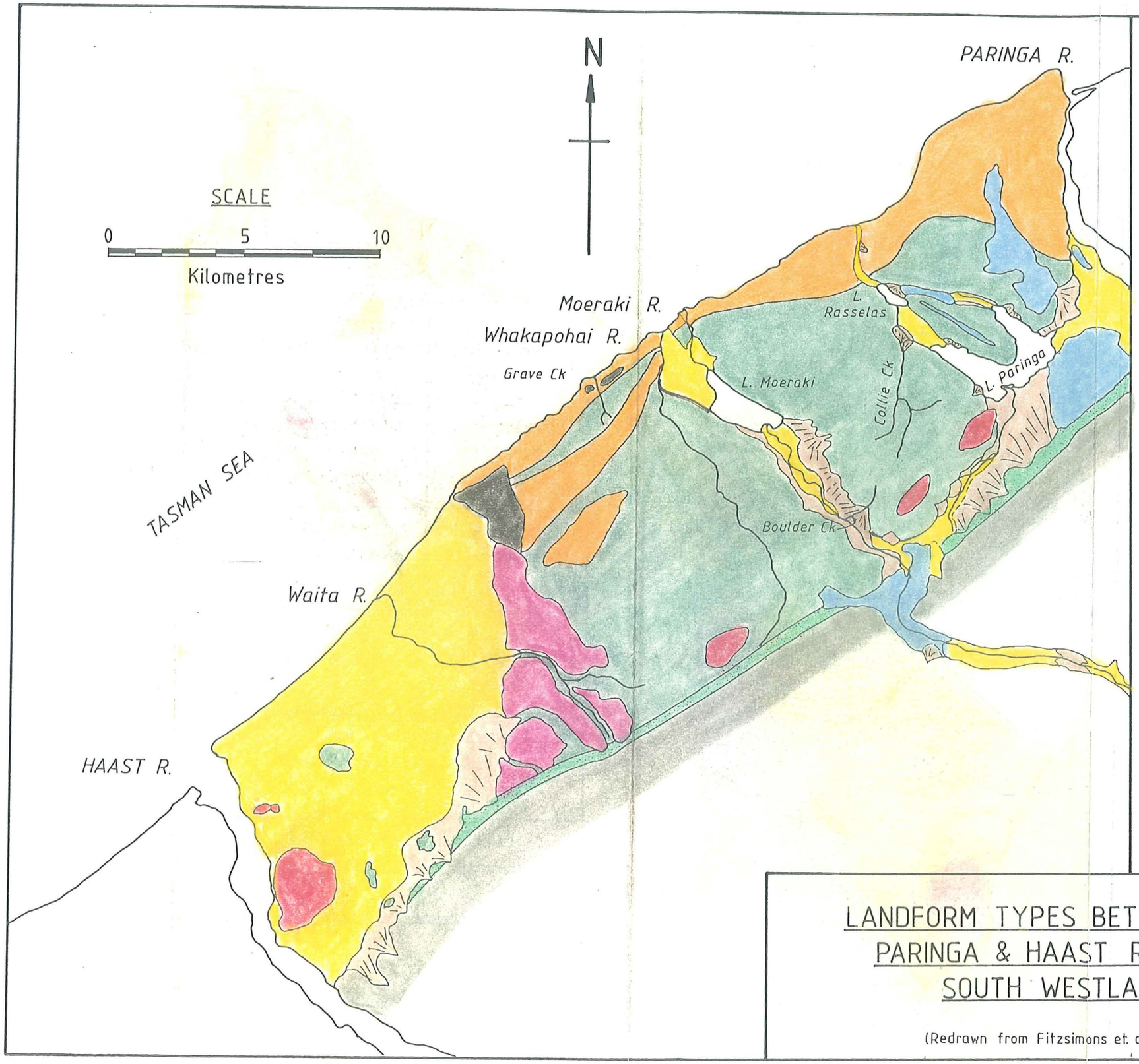

LEGEND

- Alluvial Outwash Surface
- "Active" Alluvial Fan
- "Stable" Alluvial Fan
- Terrace
- Moraine Slope
- Cretaceous-Tertiary Hill Country
- Greywacke Hill Country
- Granite Hill Country
- Alpine Fault Zone Slopes
- Schist Mountain Slopes

LANDFORM TYPES BETWEEN THE PARINGA & HAAST RIVERS, SOUTH WESTLAND

(Redrawn from Fitzsimons et. al. 1985)

SCALE ~1:150 000

FIG. 3.6

LANDFORM UNIT	GEOLOGY OF PARENT MATERIAL	SLOPE GRADIENT	SLOPE STABILITY	DRAINAGE	FLOOD SUSCEPTIBILITY	STREAM DISSECTION
MORAINE SLOPES	Glacial deposits ranging from thick beds of silts and sands to unsorted till.	Dominantly >25°	Generally stable slopes with few landslides.	Well Drained	Not Susceptible	Poorly Dissected
GREYWACKE & GRANITE HILL COUNTRY	Greenland Group greywacke, argillite and biotite hornfels; Tuhua Group granite.	Dominantly >30°	Slopes unstable with numerous landslides. Granite slopes stable.	Well Drained	Not Susceptible	Well Dissected
CRET.-TERT. HILL COUNTRY	Predominantly breccias, coal measures, sandstone, mudstone, limestone and basaltic flows.	Dominantly >25°	Moderately unstable with most of the instability within major fault zones.	Well Drained	Not Susceptible	Moderately Dissected
ALLUVIAL FANS	Unsorted, loose, subangular to subrounded boulders, cobbles and pebbles in a sandy matrix.	5-25°	Unstable stream channels with some debris flow in steep fan channels.	Well Drained	Susceptible causing aggradation.	Poorly to well dissected.
ALLUVIAL OUTWASH SURFACES	Alluvial gravels overlain in poorly drained areas by a thick peaty surface.	<5°	Stable	Poorly drained and swampy.	Highly Susceptible	Poorly Dissected
TERRACES	Well rounded schistose and quartz pebbles and quartzose micaceous sands.	c.5°	Stable	Moderately to poorly drained.	Not Susceptible	Poorly Dissected
DEFORMED SCHIST SLOPES	Fault zone materials consisting of gouge, tectonic breccia and mylonite schist.	Dominantly >35°	Highly unstable slopes.	Poorly to well drained.	Not Susceptible	Well Dissected
SCHIST MOUNTAIN SLOPES	Oligoclase-garnet schist of the Haast Schist Group.	>35°	Slopes unstable with dominantly rock defect controlled failure.	Well Drained	Not Susceptible	Well Dissected

Table 3.5 Summary of the characteristics of representative landform units between the Cook and Haast Rivers, South Westland. (Based on Fitzsimons & O'Loughlin 1984 and Fitzsimons et al. 1985)

LANDFORM UNIT	SLOPE MOVEMENT DENSITY (no. km^{-2})
Greywacke Hill Country	3.1
Deformed Schist Slopes	2.5
Steep Moraine Faces	1.2
Schist Mountain Slopes	1.0
Tertiary Hill Country	0.6
Granite Hill Country	0.3
Gentle Moraine Faces	0.1
Moraine Tops	0
Alluvial Outwash Surfaces	0
Valley Bottom Terraces	0
Alluvial Fans	0

Table 3.6 Relative slope stability ranking based on slope movement densities on landform units between the Cook and Paringa Rivers area (after Fitzsimons & O'Loughlin 1984).

LANDFORM UNIT	SLOPE MOVEMENT DENSITY (no. km^{-2})
Greywacke Hill Country	14.8
Cretaceous-Tertiary Hill Country	2.8
Deformed Schist Slopes	2.5
Schist Mountain Slopes	1.0
Moraine Slopes	0.8
Alluvial Outwash Surfaces	0
Terraces	0
Alluvial Fans	0

Table 3.7 Relative slope stability ranking based on slope movement densities on landform units between the Paringa and Haast Rivers area (after Fitzsimons et al. 1985).

Field observations generally support this stability ranking. However, if failure volume is taken into account the relative slope stability changes. Large slope failures are more frequent on deformed schist slopes which would subjectively rank it the least stable landform unit.

3.5.3 Site Selection

The three most unstable landform types were chosen for detailed investigation as they were recognised during the period of preliminary field investigations to have the most severe slope stability problems which could limit or influence future forest operations in the region. These three landform types are greywacke hill country (referred to in this thesis as Greenland Group Hill Country), deformed schist slopes (referred to in this thesis as Alpine Fault Zone slopes) and Cretaceous-Tertiary Hill Country.

Field reconnaissance was carried out to investigate each of these three landform units regionally, and types and causes of slope movements were studied in relation to geomorphic setting. On the basis of this preliminary field work one site on each of these three landform types was selected for detailed investigation. As well as geomorphic setting, selection was influenced by severity of the slope instability problems, bedrock exposure and accessibility. The three sites chosen are (location shown in Fig. 1.1):-

1. Greenland Group Hill Country - Boulder Creek;
2. Alpine Fault Zone Slopes - Havelock Creek;
3. Cretaceous-Tertiary Hill Country - Grave Creek.

3.6 APPROACH TO ENGINEERING GEOLOGICAL INVESTIGATIONS

Philosophy of the method of investigation at the three study sites can be divided into three stages:-

1. Engineering Geology Field and Laboratory Studies: collection of data on bedrock geology and basic geotechnical properties, surficial geology, slope morphology, slope movement features, and hydrogeology. The main purpose of this stage of the investigation was to identify the slope settings within which slope failure

is taking place.

2. Slope Movement Processes: assessment of slope movement processes operating within each slope setting identified, incorporating interpretative information on slope movement types and mechanisms, and factors contributing to failure.
3. Assessment of Slope Instability: qualitative assessment of slope failure.

The objective of this approach was to separate factual data from interpretative information, and two maps for each site have therefore been compiled as follows:-

1. 1:2000 engineering geology plan containing factual data;
2. 1:2500 engineering geology assessment of slope processes containing interpretative information.

Investigations at each site identified a number of features which required further field investigation within the scope of the study. These additional studies and variations to the basic investigation methodology for each study site are outlined at the beginning of each chapter.

CHAPTER FOUR

GREENLAND GROUP HILL COUNTRY: BOULDER CREEK

4.1 OUTLINE OF APPROACH

Boulder Creek was selected as the main investigation site based on preliminary field studies of slope instability in South Westland. This reconnaissance fieldwork identified a variety of slope movement types operating within a number of slope settings in the Boulder Creek catchment which were considered typical of Greenland Group Hill Country throughout the study area. The stream catchment is also presently undergoing a period of increased slope activity, and this is generating a large amount of sediment which is being transported from the stream catchment and deposited on an alluvial fan at the base of the hillfront in the Moeraki River valley. This current period of activity provided an opportunity to study the processes of slope movement within the context of the complete system of sediment generation, transportation, and deposition.

The method of approach to investigations was based on the scheme outlined in Section 3.6 and includes an assessment of hydrologic processes operating in the stream, removing sediment generated by slope failures. Investigations at Boulder Creek are reported under the following main headings:-

1. Engineering geology investigations;
2. Slope movement processes;
3. Hydrologic processes.

Following the main discussion of Boulder creek investigations, a summary of observations made during reconnaissance fieldwork of Greenland Group Hill Country in South Westland is made and possible implications for future forest management are reviewed by way of conclusion. The position of localities mentioned in the text are shown in Figure 4.1. Any distance measurement given to localities are ground distances measured from the State Highway 6 bridge crossing.

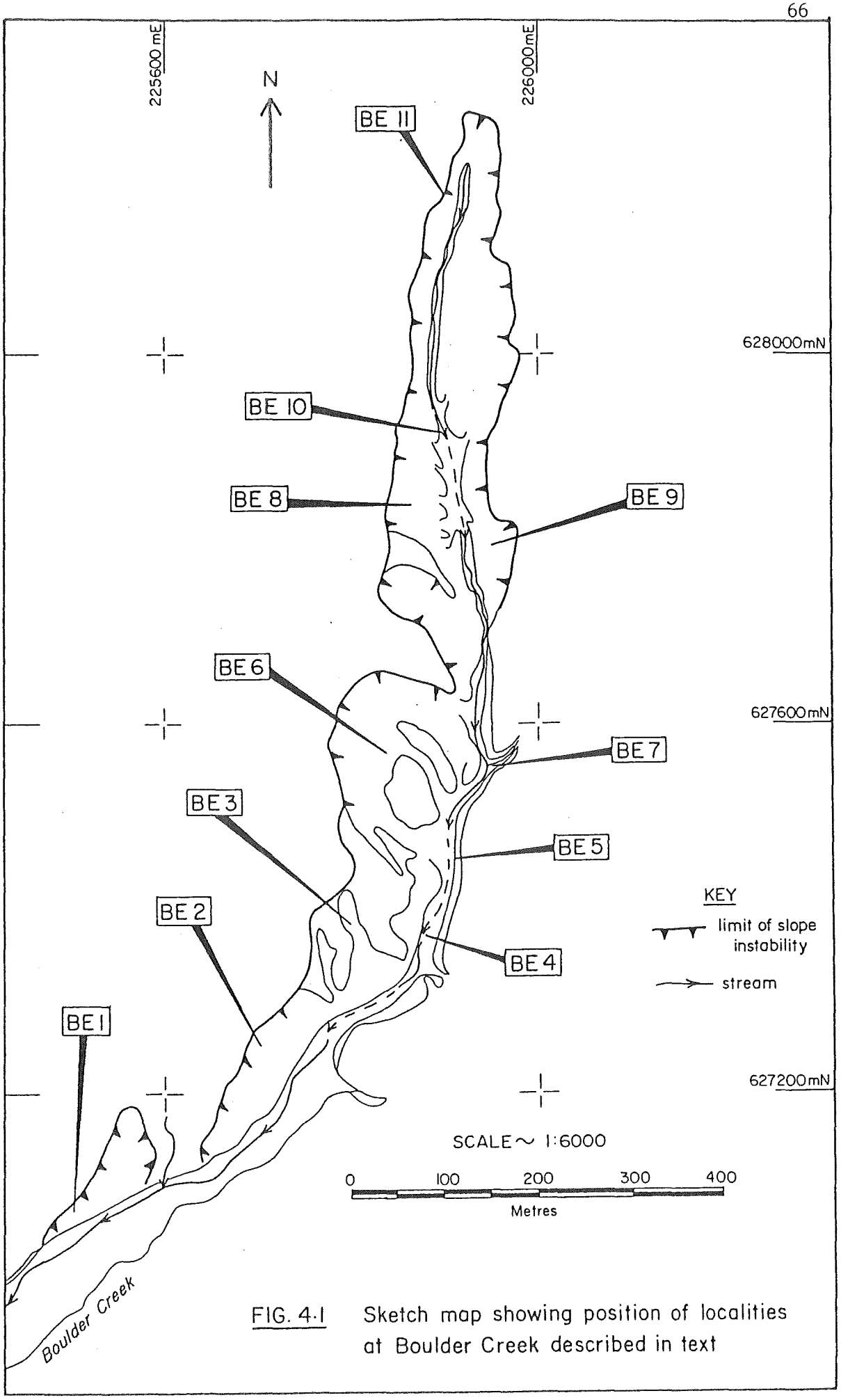

FIG. 4·1 Sketch map showing position of localities at Boulder Creek described in text

4.2 GEOMORPHIC SETTING AND RECENT HISTORY OF SLOPE ACTIVITY

Boulder Creek (Fig. 4.2 and 4.3) is situated on the northeastern side of the Moeraki River valley (S87/095264) approximately 12km southwest of Lake Paringa and 5km southeast of Lake Moeraki along State Highway 6. Total catchment area is 997 000m^2 incorporating 126 000m^2 (12.6%) of bare ground and 871 000m^2 (87.4%) of forested slopes. Relative relief of the catchment is 896m from the drainage divide to the local baselevel provided by the Moeraki River, with a stream length of 2320m and an average stream gradient of 21^o (see Fig. 4.4). Forested upper slopes support mainly Rimu/Kamahi-Freycinetia forest, and the lower slopes and alluvial fan Kahikatea/Kamahi forest (J.Pfaflert NZFS pers. comm.).

The glacial origin of the Moeraki River Valley is an important factor in the geomorphic setting of Boulder Creek, in that ice erosion oversteepened the valley sides and perhaps provided the initial trigger to slope instability. Since the last glaciation (Moana advance 13 500 years B.P.) the valley has been infilled by post-glacial sediments, which include river gravels and alluvial fan material derived from sediment generated by failure of the unstable valley sides. However, the relatively large size of the Boulder Creek catchment compared to adjacent stream basins in the Moeraki River valley indicates that other factors in addition to ice erosion have contributed to slope instability.

Aerial photograph evidence (Appendix 4 details aerial photograph coverage of Boulder Creek) shows that the current episode of slope activity commenced sometime during the 1950's. Prior to 1949 the stream catchment area contained only 4 relatively small areas of bare ground, which suggests only limited slope activity, and the alluvial fan surface was fully vegetated with a narrow, partially entrenched streambed. The 1949 photographs do, however, show a definite line of revegetation outlining areas of past slope movement activity, and this revegetated zone covers an area of about one half of the present active slope area. This in turn suggests that the current period of slope activity is the most intense undergone by Boulder Creek in recent history (last 100-200 years).

Fig. 4.2 Boulder Creek study catchment showing the outline of the escarpment slope undergoing slope activity. Vertical elevation from the bottom of the photograph to the top of the ridge is approx. 600m. Oblique view looking north-northeast. (N.Z. Geological Survey photo CN 5850a, photographer: D.L. Homer)

Fig. 4.3 Boulder Creek alluvial fan, looking upstream from the State Highway 6 bridge crossing. Top of escarpment slope is visible in the top left corner of the figure.

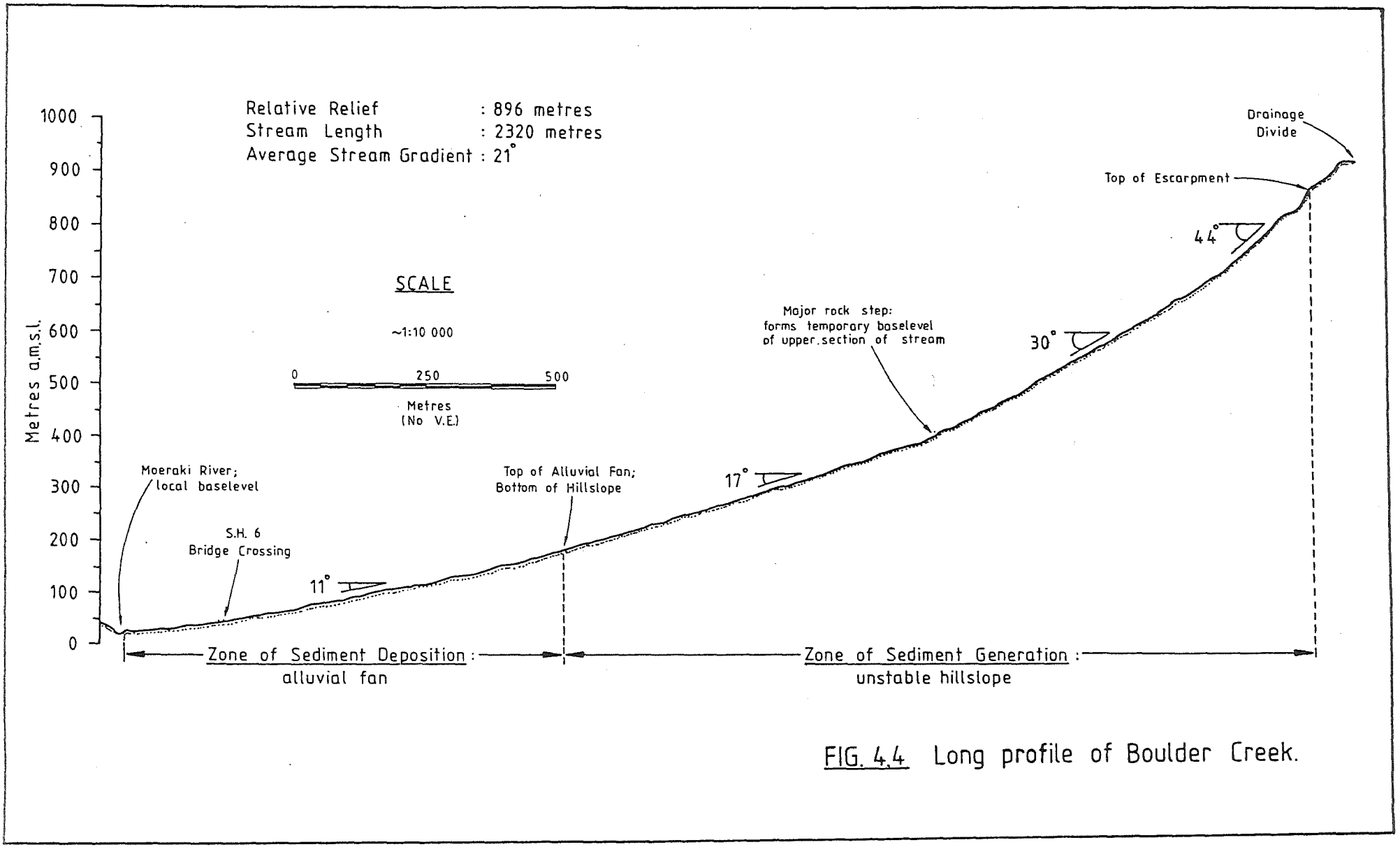

FIG. 4.4 Long profile of Boulder Creek.

4.3 ENGINEERING GEOLOGY INVESTIGATIONS

4.3.1 Investigation Programme

The main method of investigation was engineering geological mapping at a scale of 1:2000. Field mapping was carried out using 1981 aerial photograph enlargements (see section 1.4.2) during March 1985 and February 1986, and the photogrammetric base maps were compiled from 1984 photographs. This combination of field and base maps made compilation of the final maps difficult due to the highly dynamic nature of the Boulder Creek catchment, where slope failure and stream erosion is occurring continuously, constantly changing the distribution of materials and the slope morphology. Two maps have been compiled based on this mapping, which show the conditions of the stream catchment as they existed in 1985:-

1. A 1:2000 engineering geology plan showing the distribution of bedrock and surficial materials, basic morphological features, and hydrogeological features (Fig. 1, map pocket);
2. A 1:2500 engineering geology assessment of slope movement and hydrologic processes (Fig. 2, map pocket).

The engineering geology features shown on the 1:2000 plan are discussed in Sections 4.3.2 to 4.3.5. This work identified a number of features which required further field investigation within the scope of the study. Listed below are the additional field methods used, their purpose, and where the results of this work are reported:-

1. Rock defect survey: four tape traverses at varied orientations were made measuring rock defects for stability assessment of intact bedrock slopes; survey results are reported in Section 4.4.6 (ii);
2. Face log of bedrock: to investigate the nature and origin of the crushed bedrock mass; results are presented in Section 4.4.3 (i);
3. Face log of stream gravels: to investigate hydrologic processes controlling the transportation and deposition of stream gravels on the alluvial fan surface; results are given in Section 4.3.3 (iv) and interpretation discussed in Section 4.5.3.

Limited laboratory testing was carried out on fault gouge and tectonic breccia matrix samples with the primary objectives of:-

1. characterising these materials according to standard geotechnical tests, and;
2. allowing a preliminary assessment of their engineering properties.

Methods and results of these investigations are reported in Section 4.3.6.

4.3.2 Bedrock Geology

The main engineering geology mapping unit was hornfelsed sandstone, corresponding with the single rock formation mapped at Boulder Creek as Greenland Group by Wellman (1955) and Mutch & McKellar (1965). This map unit is divided into two sub-units based on the quality of the rock mass: crushed hornfelsed sandstone and intact hornfelsed sandstone. Two further map units are distinguished: fault gouge and tectonic breccia. The distribution and occurrence of these units together with summary rock mass and material descriptions are given on the 1:2000 engineering geology plan of Boulder Creek presented in Figure 1 (map pocket) with more detailed descriptions of rock material given in Table 4.1. Each of these rock units and sub-units are described below in terms of their material and mass properties.

(i) Hornfelsed Sandstone Basement Rock

Greenland Group as exposed in Boulder Creek is a very strong, dark greenish-grey crystalline siliceous sandstone and mudstone, which has largely been recrystallised to a biotite hornfels by contact metamorphism from intruding Tuhua Group granite. Small scale sedimentary structures can still be identified in places where the rock mass has remained relatively intact and graded bedding and sole marks indicate younging to the north. Bedding is complexly folded both microscopically and macroscopically, whilst cleavage is moderately well developed and dips to the northeast. This corresponds well with observations made in Collie Creek, located immediately north over the drainage divide, where bedding dips dominantly to the north and cleavage to the east.

PROPERTY	HORNFELSED SANDSTONE	TECTONIC BRECCIA	FAULT GOUGE
WEATHERING	Slightly weathered: Grade 2 (some staining of defect surfaces).	Slightly weathered: Grade 2 (minor alteration of matrix).	Unweathered to slightly weathered: some parts of material discoloured.
WATER CONTENT	N/A	Sandy matrix moist (- wet): adheres & is darkened in colour; feels cold	Wet: in places free water forms on surface when sample disturbed.
STRENGTH	Very strong 3 - 10 MPa point load strength.	Matrix hard (- stiff): indented by hand pressure; only remoulded on immersion in water.	Firm (- soft): moulded by hands; extrudes between fingers after immersiom in water.
COLOUR	Dark greenish grey; fault altered: light greyish green.	Light greyish brown.	Light greyish green.
FABRIC	Well cleaved; original bedding occasionally visible.	Massive - faintly coarsely layered.	Massive - finely laminated.
ROCK NAME	Crystalline siliceous hornfelsed SANDSTONE.	Hornfelsed sandstone puggy TECTONIC BRECCIA.	FAULT GOUGE: clayey silt with some sand (ML).

Table 4.1 Summary of rock material properties for bedrock map units at Boulder Creek.

Division of hornfelsed sandstone basement into two sub-units (intact and crushed rock) based on rock mass quality is important in terms of slope movement processes. Table 4.2 compares various rock mass parameters of the intact and crushed hornfelsed sandstone. Intact rock contains moderately spaced, moderately persistent closed joints while crushed rock consists of closely spaced, very low persistence open joints up to 30mm in width and the defects are often infilled with loose granular and coarse sand material (Fig. 4.5). The result is a very loose rock mass consisting of angular blocks up to 500mm equivalent cube size, but generally less than 100 mm, surrounded by a matrix of loose coarse sand.

The origin of the crushed rock mass may be attributed to three possible alternatives:-

1. Tectonic movement caused by fracturing of basement rock due to fault movement;
2. Rock creep involving disruption of the rock mass in the zone of loosening due to deep reaching gravitational deformations of the steep valley slopes (see Section 4.4.3 (i));
3. Slope movement involving disruption of the rock mass by large-scale, deep-seated, ancient movement(s) of valley slopes (see Section 4.4.5).

Evidence exists for the operation of all three mechanisms (which are discussed elsewhere): the presence of fault gouge and tectonic breccia indicates faulting, release jointing indicates rock creep, and possible ancient scarp systems may indicate large-scale slope failure(s).

(ii) Fault Gouge & Tectonic Breccia

Fault gouge and associated tectonic breccia have been mapped as bedrock units in the Boulder Creek catchment. Fault gouge occurs in zones up to 6.0m wide outcropping mainly in the streambed or in slopes immediately above the streambed (Fig. 4.6). As a consequence exposure is relatively short-lived and changes constantly, only surviving during periods of downcutting by the stream to expose bedrock beneath stream gravels and rock debris alluvium. Fault gouge is dominantly a

CRITERIA	INTACT HORNFELSED SANDSTONE		CRUSHED HORNFELSED SANDSTONE
DEFECT TYPE	Closed joint	Shear zone	Open joint
DEFECT SPACING	Wide to v. close (20-400mm), average: moderate (100-200mm); zones of intense jointing: v. close to extremely close (<5-20mm).	Extremely wide (>2000mm)	Close to v. close (5-100mm)
DEFECT PERSISTENCE	Low to moderate (c. 2.0m); intense zones: low to very low (<0.5-2.0 m)	Very high (>10 m)	Very low (<0.5m)
AVERAGE UNIT BLOCK SIZE	Medium (average 100-150mm)	Very large (>1000mm)	Small (10-100mm)
GROUNDWATER	Dry	Generally dry, occasional seepage from some zones	Dry to low flow

Table 4.2 Summary of rock mass properties for two types of hornfelsed sandstone bedrock map units at Boulder Creek.

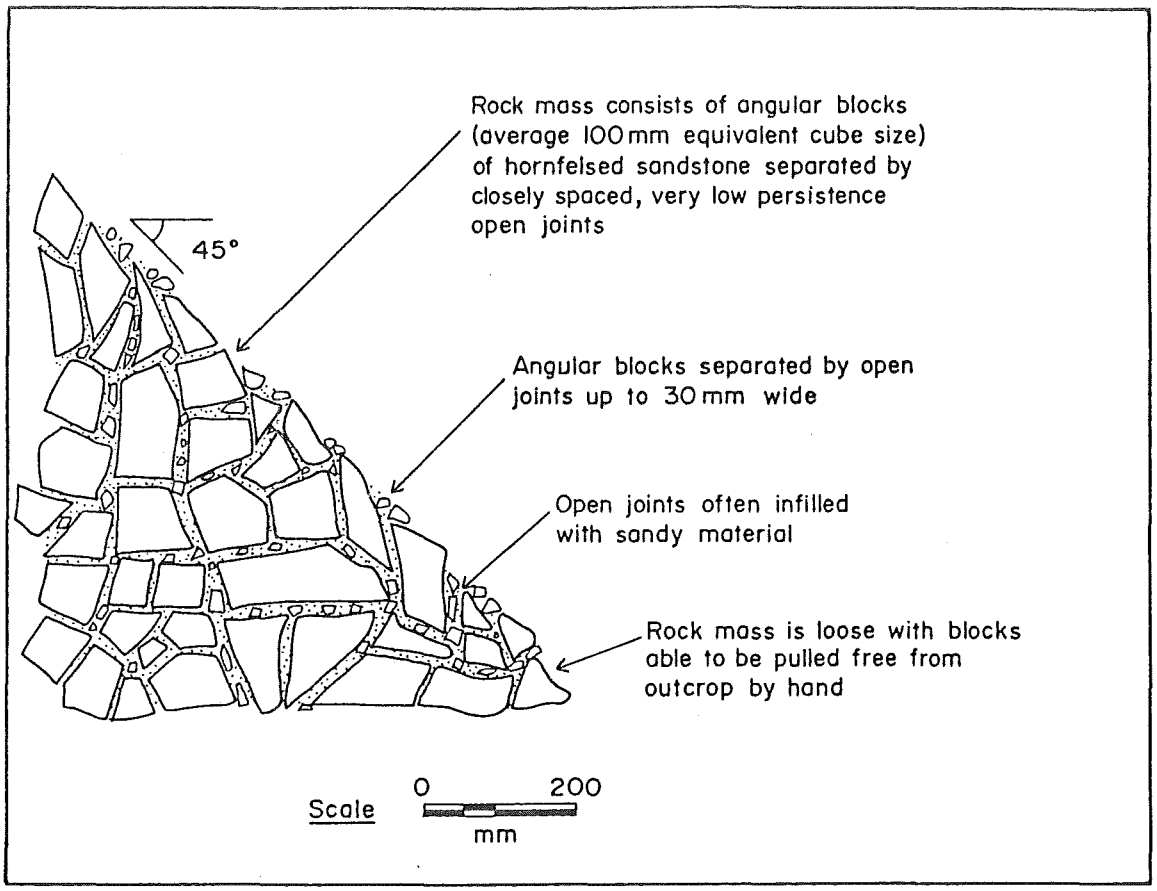

Fig. 4.5 Sketch diagram illustrating the loose, crushed bedrock mass at Boulder Creek

A

B

Fig. 4.6 Light greyish green and light greenish brown fault gouge material as exposed at localities BE 1 (photo A) and BE 4 (photo B).

wet, firm, light greyish green, occasionally light greenish brown, clayey silt material. It often contains disorientated sub-angular fine gravel-sized fragments of bedrock scattered within the clayey silt.

According to the Bell & Pettinga (1985) rock mass classification the "fault gouge zone" would be termed a crush zone, but the former name is preferred here to avoid confusion with the use of "crush zone" to define the lateral extent of rock crushing due to tectonic movement outside of the zone of fault-altered materials (see Section 2.5.1).

Associated with two southeast dipping fault gouge zones located at BE 1 (Fig. 4.7) and BE 9 is a puggy tectonic breccia extending laterally up to 50m from the gouge zone. This is a weak, light greyish brown breccia comprised of angular, fine to coarse gravel size fragments of bedrock in a matrix of muddy sand. The matrix is moist to wet, hard (to stiff) and easily remoulded on immersion in water.

The nature of the gouge and tectonic breccia materials suggests that there may be a continuum from fault gouge to tectonic breccia depending on the relative proportions of matrix to rock fragments. Gouge is dominantly fine-grained matrix, and the tectonic breccia is dominantly coarse-grained rock fragments with the boundary between the two materials ranging from sharp to gradational in character.

(iii) Structure

The attitude of the gouge zones suggests there are two main fault systems which cross Boulder Creek:-

1. $056^{o}\pm4^{o}/45^{o}\pm23^{o}$SE;
2. $353^{o}\pm7^{o}/58^{o}\pm12^{o}$W.

The southeast dipping system has associated with it a tectonic breccia zone as described above, but despite a faint fine lamination fabric of the gouge material no sense of movement could be determined. This system appears to be part of a set of NE-SW striking faults which controls the drainage pattern in the Whakapohai River catchment. These faults

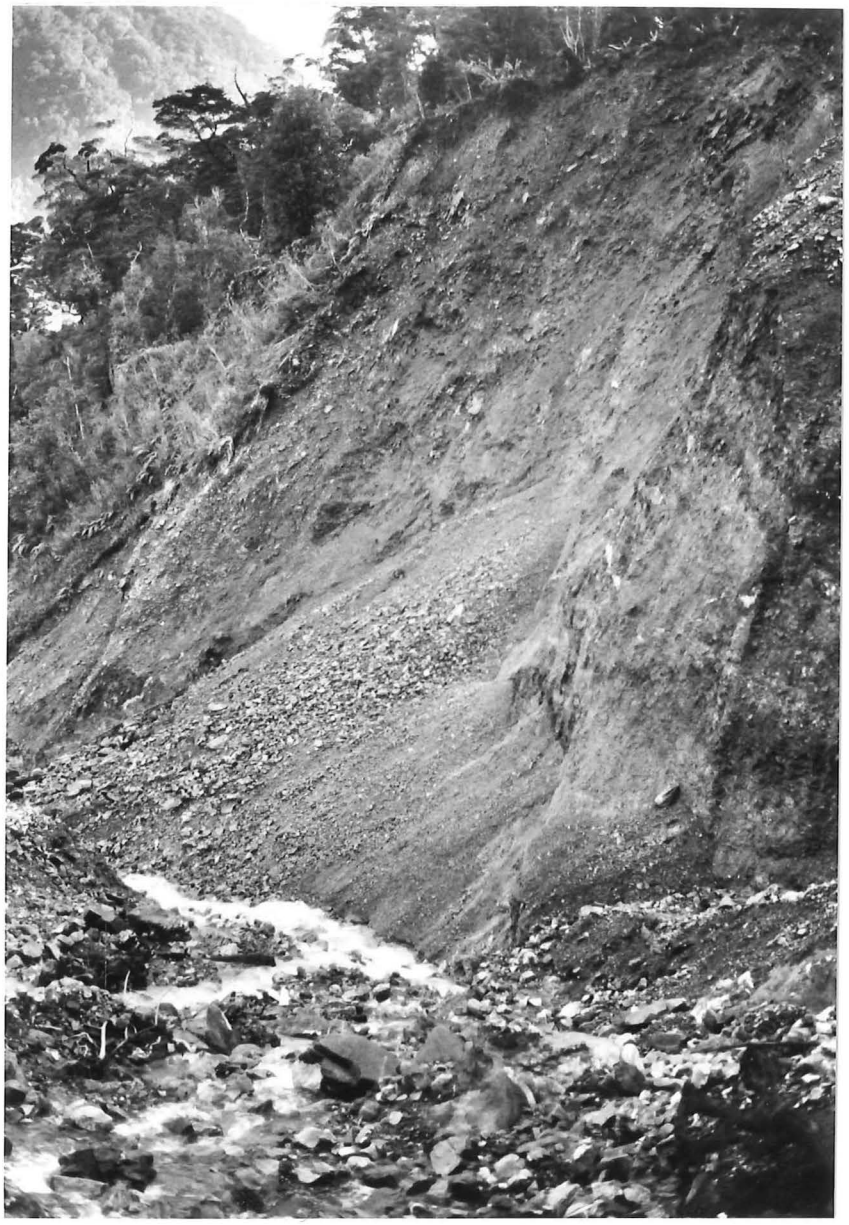

Fig. 4.7 Puggy tectonic breccia bedrock exposed in approx. 20m high escarpment slope at locality BE 1.

strike sub-parallel to faults controlling the distribution of Cretaceous-Tertiary sediments to the northwest of Boulder Creek along the coast and also strikes sub-parallel to the Alpine Fault. This series of faulting may be due to sympathetic tectonic movement to the Alpine Fault Zone.

The westerly dipping fault system has no puggy tectonic breccia material associated with it. Its gouge zone strikes roughly up the centre of the gully being exposed for long distances (up to 165m) in the streambed or immediately above it, and has no internal fabric from which possible sense of movement could be determined. Bedrock east of the zone is relatively undisturbed whereas rock west of the zone is highly fractured and crushed.

The nature of this zone and lack of tectonic breccia may indicate that it is a very large slope movement shear zone. However, for such a thickness of shear material to be generated there would had to be considerable movement producing substantial morphological features, and the only aerial photographic evidence for such a slope movement feature is a lineament which trends across the top of the catchment near BE 11. It is considered that this feature is not extensive enough to be related to this shear zone, and also the attitude of the zone does not suggest a failure surface to this possible headscarp feature.

4.3.3 Surficial Geology

Choice of surficial geology mapping units was based on the objective of adopting a material terminology which identified the origins of deposits located on different parts of the slope and in the streambed. The surficial mapping units selected were:-

1. Slope storage debris;
2. Debris accumulation;
3. Rock debris alluvium, and;
4. Stream gravels.

(i) Slope Storage Debris

This is defined as colluvial material lying temporarily in storage on the slope that has been derived from failure of bedrock and other similar materials further upslope. Being derived mainly from crushed hornfelsed sandstone, the most widely occurring bedrock material, it dominantly consists of angular coarse gravel sized blocks of bedrock with a minor sandy matrix.

Differentiation between crushed hornfelsed sandstone material and slope storage debris was difficult on most upper portions of the escarpment slope due to their similar surface character. Many of the upper slopes were inaccessible due to steepness of the slope and danger from rock and debris fall and where slopes could not be field checked, identification of the surface material was based on aerial photograph interpretation. In reality the distribution of slope storage debris over crushed bedrock slopes is probably far more complex than that indicated on the 1:2000 engineering geology plan. However, only those slopes which could be positively identified as being covered with slope storage debris were mapped as such, resulting in a conservative assessment of the distribution of slope storage debris in the catchment.

(ii) Debris Accumulations

Slope storage debris passes downslope into debris accumulations (Fig. 4.8). The main difference between the two types of surficial deposits is their relative position on the slope, debris accumulations forming debris fans at the base of the slope below slope storage areas. Consequently, slope storage is the primary source of material supply to debris accumulations, usually from debris infilled gullies, but on some slopes slope movement processes directly contribute material to debris accumulations, by-passing the slope storage stage. This usually occurs where the slope is of insufficient height to store slope movement material other than at the base of the slope (Fig. 4.9).

The type of material is similar to slope storage debris being predominantly coarse gravel size, sub-angular blocks of hornfelsed sandstone with minor interstitial fines. There is

Fig. 4.8 Debris accumulation at the base of the escarpment slope at BE 6, and rock debris alluvium overloading the streambed area; view looking downstream.

Fig. 4.9 Approx. 40m high escarpment slope at locality BE 2 covered with debris accumulations.

a grading of block size from coarse gravel size at the base of the accumulation fan to fine gravel size near the top.

(iii) Rock Debris Alluvium

Rock debris alluvium is an alluvial fill deposit which overloads the streambed with material directly supplied from debris accumulations during phases of sediment generation (Fig. 4.10). Again there is a continuum from debris accumulation to rock debris alluvium, reflecting the change in process of origin from dominantly gravitational processes on the slopes to dominantly fluvial processes in the streambed.

Rock debris alluvium consists of the same material as slope storage debris and debris accumulation. However, all of the fines have been removed leaving a deposit of loosely packed, sub-angular to sub-rounded large gravel size blocks of bedrock. During normal stream flow no surface channel is formed with the stream being entirely groundwater flow.

(iv) Stream Gravels

Stream gravels occupy the streambed in the catchment area between rock debris alluvium deposits, and also occur on the alluvial fan surface. The unit dominantly consists of sub-angular to sub-rounded, small to coarse gravel with a poorly sorted sandy matrix. Figure 4.11 illustrates and describes stream gravels exposed in a stream bank approximately 550m above the State Highway 6 bridge crossing on the alluvial fan surface. Processes governing the nature and origin of these materials are discussed in Section 4.5.

4.3.4 Slope Morphology

The basic morphological feature at Boulder Creek is the distinct convex angular break in slope which marks the boundary between forested stable slopes and bare unstable slopes (Fig. 4.2). The forested slopes are steep, around 36-39°, whilst the area of slope instability forms a deeply incised gully system, which disrupts the otherwise uniform hillside and within which is a complex of slope features and forms.

Fig. 4.10 Rock debris alluvium overloading the streambed area above a 2.0m high waterfall formed by a log jam.

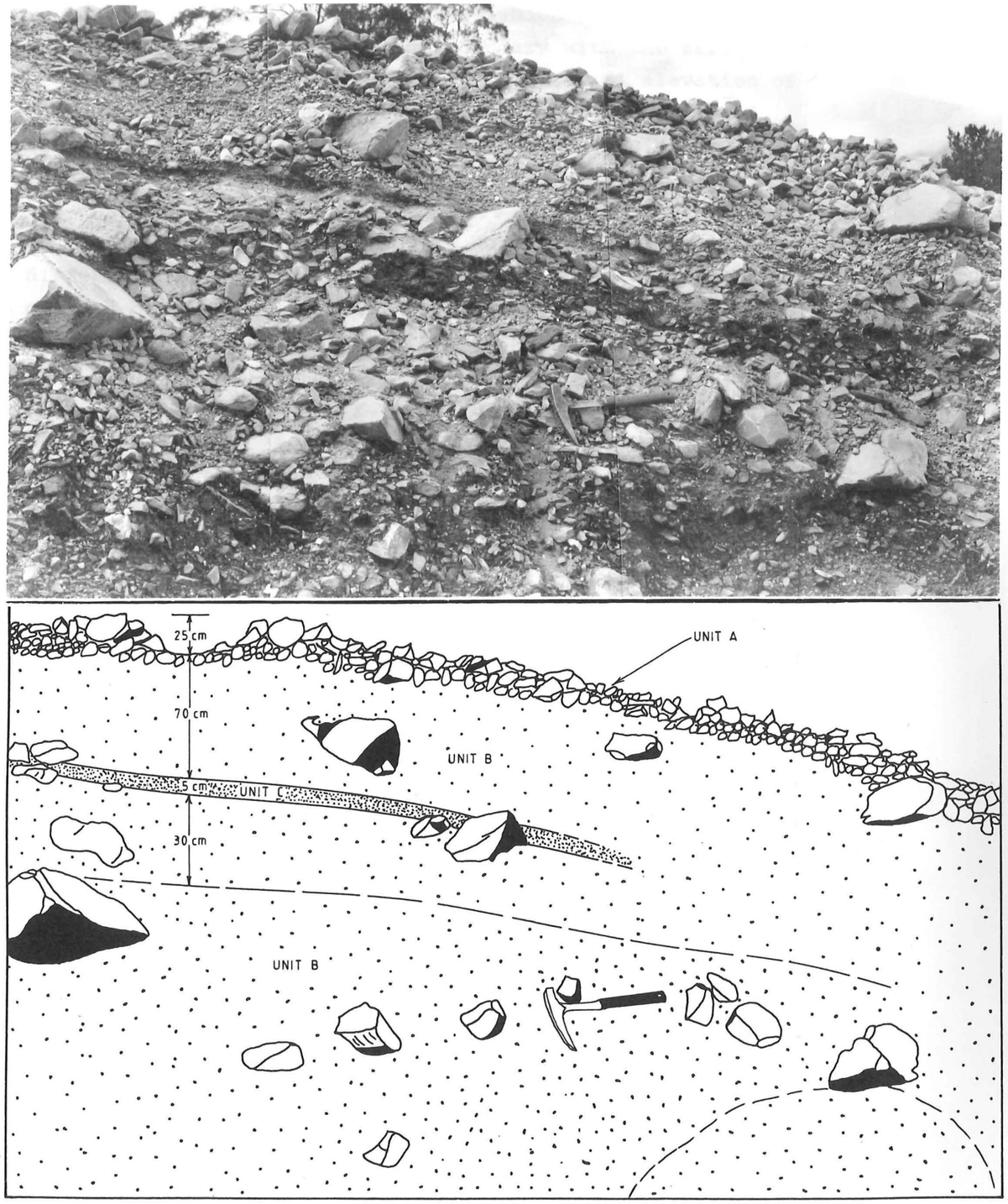

Fig. 4.11 Face log illustrating stream gravels exposed in stream bank on alluvial fan surface, approx. 550m above the S.H. 6 bridge crossing.

ENGINEERING GEOLOGICAL DESCRIPTIONS

UNIT	DESCRIPTION
A	Unweathered, moist, loose, grey, massive, COARSE GRAVEL with some boulders (GP). Unit contains no fines and consists of poorly packed, very loose, angular to sub-angular crystalline siliceous horn-felsed sandstone and mudstone clasts which armour the streambed surface.
B	Unweathered, moist, loose, grey, massive, sandy MEDIUM GRAVEL with some coarse gravel (GM). Unit consists of poorly packed, very loose, angular to sub-angular clasts surrounded by a matrix of poorly sorted, loose sand with occasional bands of sand.
C	Unweathered, moist, loose, grey, faintly layered, faintly imbricated fine to coarse SAND (SW). Sand is poorly sorted, angular, quartzo-micaceous with some coarse sand being lithoclastic.

The principal surface feature is the extensive escarpment slope which forms the area within which slope activity is taking place. It extends from the boundary with the forested slopes above down to streambed level, a vertical elevation of up to 170m, and is confined largely to the west hillside of the gully. Escarpment slope angles are steep ranging from 42 -65°.

The escarpment slope area can be divided into a number of different morphological features. Gullying has developed in crushed bedrock material at BE 8, dissecting the slope and creating a sharp ridge-gully surface form (Fig. 4.12). Isolated outcrops of intact bedrock have formed rock buttresses on slopes composed dominantly of crushed bedrock. The base of the escarpment slope is mantled with debris fans coalescing to form debris aprons, and slope angles of these fans varies from 28 to 39°, averaging 33°.

In the streambed lobes of rock debris alluvium have overloaded the stream where there is a large supply of sediment in storage on adjacent escarpment slopes (Fig. 4.10). During periods of sediment supply to the rock debris lobes, debris fans and aprons coalesce with the lobes to produce a continuous expanse of debris from hillslope to stream channel. During periods of little or no sediment supply the debris lobes separate from the debris fan and move downstream as pulses of sediment. As they move on to the alluvial fan surface they lose their lobate form and become broad fronts termed sediment "waves".

4.3.5 Geohydrology

There are three main features of hydrologic importance at Boulder Creek: water springs, groundwater flow in the streambed, and waterfalls.

Water springs have been found to occur in association with the presence of gouge zones, particularly at BE 10, with flow rates being generally low, ranging from seepage up to approximately 100mls^{-1}. Most commonly the springs are situated immediately above the gouge zone which may indicate that the relatively impervious gouge material is creating a

Fig. 4.12 Extensive gully erosion in crushed hornfelsed sandstone bedrock at the top of the escarpment gully complex at BE 11. Vertical elevation from streambed (bottom of photograph) to top of escarpment slope approx. 150m.

drainage barrier to groundwater flow, directing water to the surface (Fig. 4.13).

Where the stream channel is overloaded with rock debris alluvium, stream water flow is entirely underground. Surface water flow in the stream channel disappears beneath the surface immediately above the rock debris material and emerges from the base of the rock debris lobe front further downstream (Fig. 4.10). This change from surface water flow to groundwater flow through highly pervious rock debris alluvium is of significance to the hydrologic mechanism moving this material, which is discussed in Section 4.5.

Numerous waterfalls have formed along the stream channel length which control the channel grade in the upper part of the stream. A major rock step occurs at BE 7 where the stream flows through a short gorge incised into intact bedrock containing three 2-5m high waterfalls (Fig. 4.4). This rock step forms a local baselevel towards which the stream channel above it is graded. Above this major rock step small 1-2m high waterfalls comprised of log jams and minor rock steps form a series of riffle zones which controls the channel morphology (Fig. 4.10).

4.3.6 Laboratory Investigations

(i) Laboratory Programme

Laboratory testing was carried out on fault gouge and tectonic breccia materials. The objective of the laboratory programme was to characterise these materials according to standard geotechnical tests in order to allow a preliminary assessment of their engineering properties. Disturbed bag samples, collected from surface outcrop exposures, were tested to determine grain size distribution, in-situ moisture content, Atterberg limits and derived consistency indexes, and clay mineralogy according to the methods given in Appendix 5. Results obtained for two tectonic breccia and four fault gouge samples are summarised in Table 4.3, and these results are discussed below.

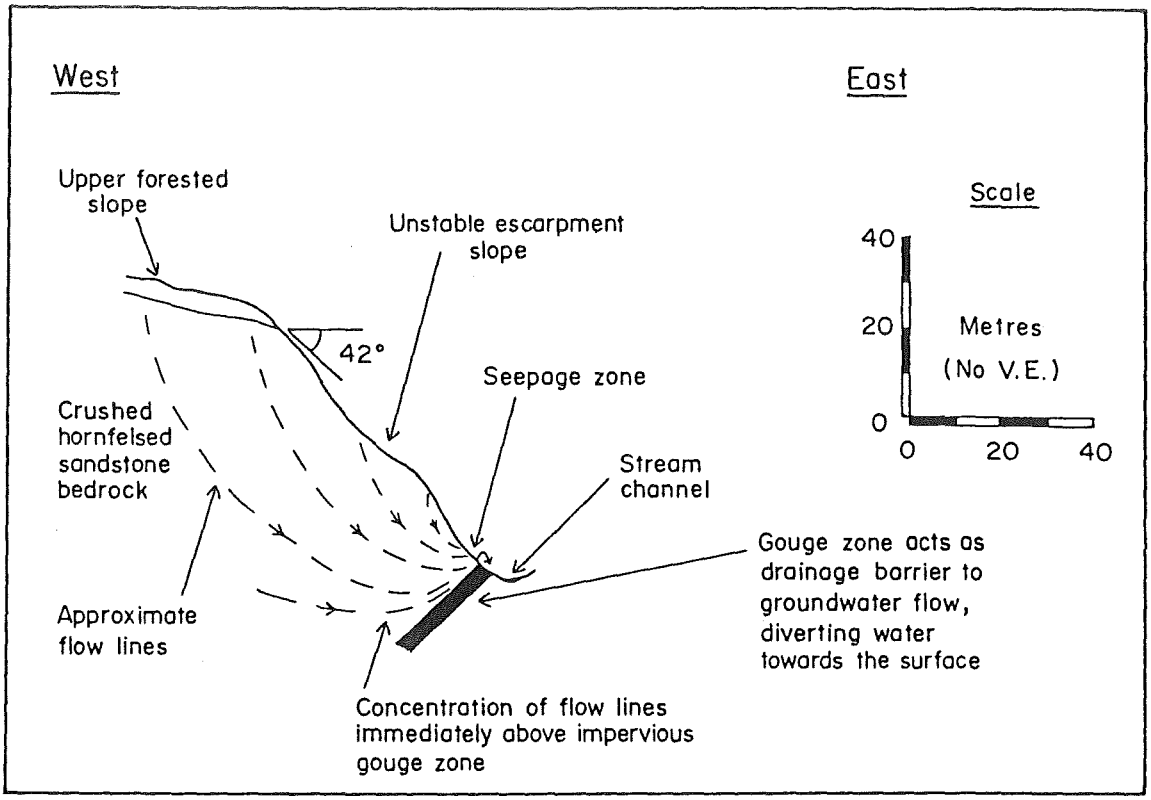

Fig. 4·13 Sketch diagram illustrating the occurrence of water springs immediately above fault gouge zones in Boulder Creek

Sample Number	Sample Origin and Description	Water Content %	Grain Size Analysis				Atterberg Limits				Activity	Soil Class[n]	Clay Mineralogy
			Gravel %	Sand %	Silt %	Clay %	LL	PL	PI	LI			
BS 1	BE 1, S.E. dipping fault zone, clayey silt FAULT GOUGE.	12	15	22	38	25	21	11	10	0.10	0.40	CL	n.d.
BS 3	BE 4, W. dipping fault zone, clayey silt FAULT GOUGE.	20	16	20	36	28	35	17	18	0.17	0.64	CL	illite>chlorite >quartz
BS 4	BE 9, S.E. dipping fault zone, clayey silt FAULT GOUGE.	19	18	21	33	28	31	16	15	0.20	0.54	CL	n.d.
BS 6	BE 10, W. dipping fault zone, clayey silt FAULT GOUGE.	24	13	23	29	35	46	22	24	0.08	0.69	CL	n.d.
BS 2	BE 1, S.E. dipping fault zone, gravelly sand TECTONIC BRECCIA.	13	37	38	21	4	14	13	1	0	0.25	SM	n.d.
BS 5	BE 9, S.E. dipping fault zone, gravelly sand TECTONIC BRECCIA.	16	18	33	33	16	19	15	4	0.25	0.25	SM	chlorite>illite >swelling chlorite>quartz

Note - n.d. - not determined

Table 4.3 Summary of laboratory test results for fault gouge and tectonic breccia matrix samples, Boulder Creek.

(ii) Grain-size Distribution

Semi-log plots of samples analysed are presented in Appendix 5. Grain-size distribution allows the engineering properties of coarse-grained soils (gravels and sands) to be estimated.

Tectonic breccia samples dominantly consists of coarse-grained material, with 50-75% of the sample larger than 0.06mm and a clay fraction generally less than 16%, more commonly around 4%. Gouge material, on the other hand, is fine-grained, with 60-65% of the sample smaller than 0.06mm and a clay fraction ranging from 25-35%, averaging 28%.

(iii) In-situ Moisture Content and Atterberg Limits

The results of in-situ moisture content and Atterberg limit tests allow fine-grained soils to be classified, since variation in moisture content in these soils can produce significant changes to their engineering properties.

The tectonic breccia samples had liquid limits less than 20% with a corresponding low plasticity index (1-4), and are classed as inactive. On the Plasticity Chart (Fig. 4.14) they plot to the left of the "A" line and according to the Unified Soil Classification System they are sands with silt (SM).

The liquid limits for the fault gouge samples range from 21-46%, and they plot above the "A" line on the Plasticity Chart, being classified as inorganic clay with low plasticity (CL). All are inactive clays with liquidity indexes ranging from 0.08-0.20, in the plastic solid phase under normal (12-24%) moisture conditions.

There is a certain amount of variation in the consistency limits between fault gouge samples despite all being low plasticity clays. However, there may be some correlation within localities as gouge and breccia from BE 1 have low plasticity and low liquidity indexes compared with samples from BE 9, which may reflect the higher clay content and higher natural moisture content of the material at BE 9.

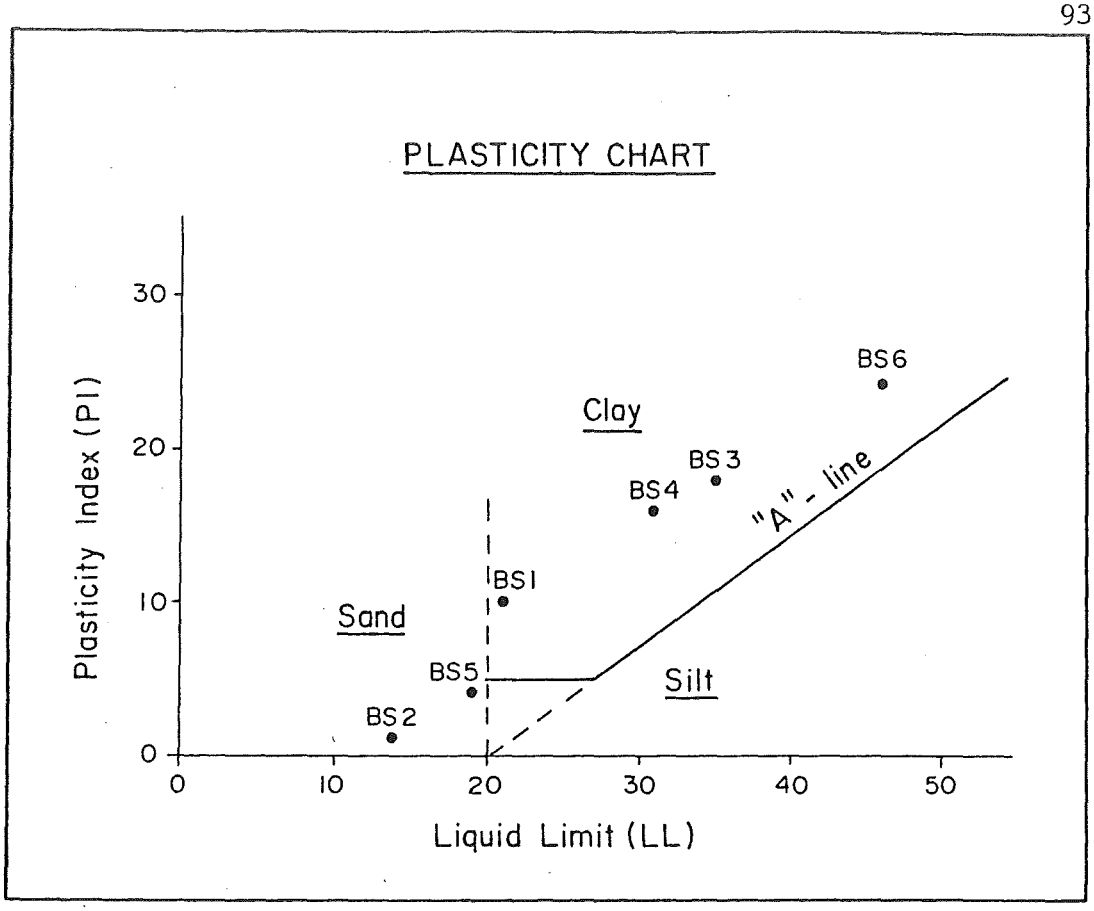

Fig. 4·14 Fault gouge and tectonic breccia samples plotted on the Plasticity Chart

The liquid limit, plasticity index, and activity ratio for samples from the westerly dipping gouge zone are all higher than the southeasterly dipping gouge samples. This is due to the higher clay content of the westerly dipping gouge zone giving this material a relatively higher plasticity.

(iv) Clay Mineralogy

Clay mineralogy was determined by X-ray diffraction analysis according to the methods outlined in Appendix 5. The objective of this analysis was to relate behaviour of the material to its clay mineralogy. One sample each of the tectonic breccia matrix and fault gouge material was tested, and diffractograms for these tests are presented in Appendix 5. Table 4.4 lists the d-spacings and possible minerals present for both samples run.

The assemblage illite-chlorite-quartz is interpreted for the fault gouge material, and chlorite-illite-swelling chlorite-quartz for the breccia matrix sample. Chlorite is preferred over the combination vermiculite and kaolinite since chlorite is present in thin section of bedrock samples and since it is more likely than the latter two minerals in relatively unweathered hornfelsed sandstone. In addition, Velde (1985) states that illite-rich sediments typically develop the assemblage chlorite-illite-quartz upon epi-metamorphism, and quartz is interpreted to exist in trace quantities combined with illite at 3.34A to form a broad peak.

Upon glycolation of the breccia matrix sample there was a small shift in part of the 14A peak to 16A. This is either due to minor smectite or swelling chlorite, the latter being preferred since normal chlorite occurs in the sample and no smectite was found in the gouge sample upon glycolation.

The non-swelling illite-chlorite-quartz assemblage accounts for the low activity ratio of both the gouge and breccia matrix samples. The trace quantities of swelling chlorite found in the breccia matrix does not seem to be of sufficient quantity to alter behaviour of the clay fraction.

SAMPLE	PEAK d-SPACING[1]	MINERAL(S)
BS 3 Fault Gouge	14.37	Chlorite or Vermiculite
	10.11	Illite
	7.14	Chlorite or Kaolinite
	4.99	Illite
	4.73	Chlorite
	3.55	Chlorite or Kaolinite
	3.34	Illite & trace of Quartz
BS 5 Puggy Tectonic Breccia	15.92[2]	Smectite or swelling Chlorite
	14.25	Chlorite or Vermiculite
	10.05	Illite
	7.11	Chlorite or Kaolinite
	5.01	Illite
	4.73	Chlorite
	3.55	Chlorite or Kaolinite
	3.34	Illite & trace of Quartz

[1] measured in Angstrom units

[2] shifted peak upon glycolation

Table 4.4 d-spacings of peaks obtained from diffractograms and possible mineral combinations.

4.4 SLOPE MOVEMENT PROCESSES

4.4.1 Objectives

The primary objective of this section is to describe the slope movement processes operating in Boulder Creek under the three slope settings within which they occur:-

1. intact hornfelsed sandstone slopes;
2. crushed hornfelsed sandstone slopes, and;
3. tectonic breccia slopes.

These processes are discussed in terms of the slope movement types, mechanisms, and causes of failure which are interpreted to occur. Ancient slope movement features are also described, followed by an assessment of slope instability. The distribution of slope movement processes are illustrated on the 1:2500 engineering geological plan presented in Figure 2 (map pocket).

4.4.2 Slopes in Intact Hornfelsed Sandstone

Due to the limited distribution of intact bedrock, its importance in respect to the present slope instability at Boulder Creek is not as great relative to the instability of the crushed bedrock slopes. However, the occurrence of intact bedrock disrupts the distribution of crushed bedrock, and influences the mode of failure for crushed bedrock slopes.

Intact bedrock slopes fail by two main types of slope movement (viz. rock fall and rock slide), and both reflect the importance of rock mass defects in controlling failure.

(i) Rock Falls

Rock falls occur on the outer slopes of the intact bedrock buttresses where the slope angle approaches vertical. Blocks of rock detach from the rock mass along a defect surface and fall to the slopes below, which in turn are usually covered by slope storage debris or debris accumulations. In some cases where the underlying slope is sufficiently steep the falling block may continue downslope by leaping, bouncing, or rolling, and come to rest in the streambed below. In this way rock fall can supply material directly to the streambed, by-passing the slope storage and debris accumulation stages.

(ii) Rock Slide

The basic mechanism of failure of a rock slope is simple gravitational sliding where a single block of rock slides down an inclined plane. Two basic types are distinguished (Hoek & Bray 1981):-

1. plane failure, where a rock defect strikes parallel to the slope face and dips out of the slope at an angle greater than the angle of friction, and;
2. wedge failure, where the line of intersection of two defects daylights in the slope face and is inclined at a greater angle than the angle of friction.

Either of these two mechanisms may operate on the intact bedrock slopes, but in reality the failure process is probably more complex, involving a combination of these two failure modes. Only the rock buttress at BE 6 is probably of large enough size to produce a significant rock slide failure. Field investigations of this slope found that a number of joint defect sets had favourable orientations for planar failure to occur, which provided a surface of sliding and a tension crack along which the moving block could be released from the rock mass. This observation is supported by stereographic analysis of rock defects (Appendix 6) which found that conditions are favourable for rock sliding by planar failure.

Two main factors are contributing to both the rock fall and the rock sliding failures:-

1. Removal of lateral and underlying support: creation of steep, high slopes by slope failure and stream erosion, increasing the total shear stress, and;
2. Nature of the rock mass: rock defect surfaces providing planes of weakness along which failure can occur.

Secondary (triggering) causes are earthquake shaking and the influence of water providing uplift forces along defect surfaces.

4.4.3 Slopes in Crushed Hornfelsed Sandstone

Crushed hornfelsed sandstone is the most widely occurring slope setting in Boulder Creek, and as such is the most important in terms of slope stability. Three types of slope movement are considered to be the dominant modes of failure:

rock creep, debris fall, and debris slump/slide-avalanche.

(i) Rock Creep

The removal of rock from the Boulder Creek catchment by slope failure and stream erosion has created slopes up to 600m high at angles <65°. Such slopes are susceptible to deep-reaching gravitional deformations due to the release of horizontal stresses and unloading (Fig. 4.15).

The removal of rock causes a redistribution of internal stresses and subsequent deformation may take place in the vicinity of the slope surface. The new, secondary state of stress includes a relaxation of stress near the slope surface producing a zone of loosening. In this zone, the deformation manifests itself by disrupting the rock mass into blocks due to release jointing, usually parallel to the slope face (Fig. 4.16). Either new joints are created or the rock mass uses pre-existing, suitably oriented rock defects which widen and progressively disintegrate the rock mass into individual blocks. These blocks undergo creep movement which may pass into a faster motion (sliding or falling) depending on the time or the action of a suitable triggering event (Slivovsky 1977).

Figure 4.17 illustrates a section of the rock face at BE 2. A number of statements relating to the nature of the rock mass can be made from this face log:-

1. The top surface of the rock outcrop seems to be composed of "rock pinnacles" with debris infilling gaps in between. This may be due to extension or loosening of the rock mass near the free surface leading to toppling;
2. The upper portions of the joint defects are slightly bent downhill indicating creep (extremely slow) movement near the surface;
3. Most joint defects are open and have been infilled with sandy slope debris. This again is due to loosening of the rock mass;
4. The rock mass is of a loose nature - blocks can be pulled from outcrop by hand;

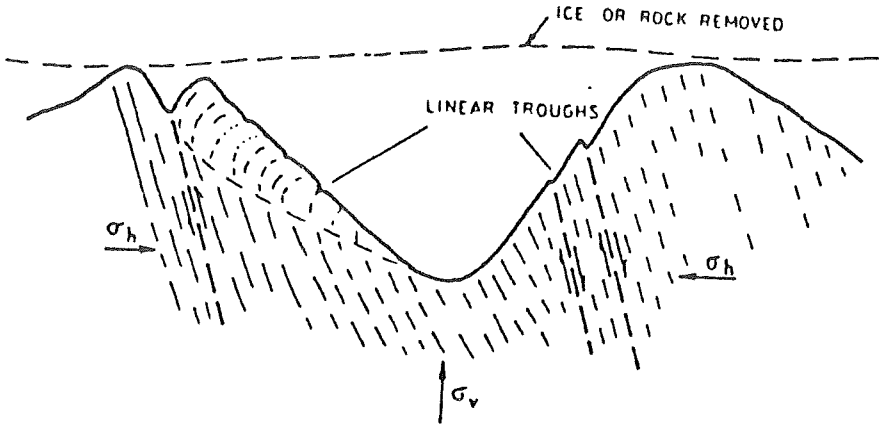

Fig. 4.15 Large-scale deformational features of a valley which has been unloaded by erosion or deglaciation. σ_h - horizontal stress
σ_v - vertical stress
(from Mahr 1977)

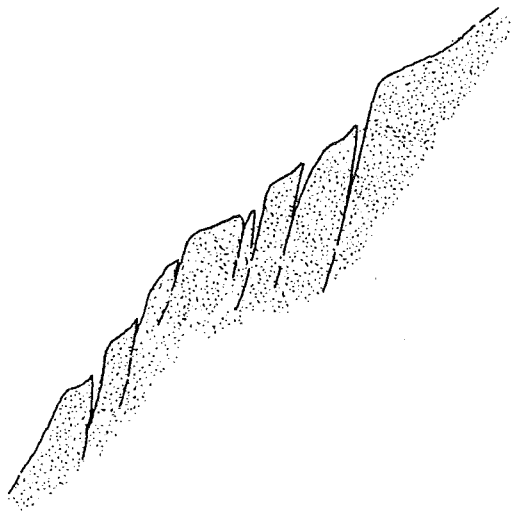

Fig. 4.16 Gravitional deformation by release jointing parallel to the surface on valley slopes in the zone of loosening (after Slivovsky 1977).

5. Joint sets B and C are parallel to the slope face, acting as release surfaces in the zone of loosening.

These features indicate that gravitational deformation by rock creep is operating on these slopes. Apart from the high, steep slopes, other factors contributing to rock creep movement may be earthquake shaking imposing transitory earth stresses on the slope materials, the release of residual stresses from tectonic pressures after valley deepening, and the existence of suitable tectonic dispositions for the occurrence of deep-reaching gravitational deformations (Mahr 1977).

(ii) Debris Falls

Debris falls involve the gravitational downslope movement of individual blocks or groups of blocks moving independently. Blocks are derived from the loose, crushed and fractured bedrock mass, separating from the mass along closely spaced, low persistence open joints with block size reaching up to 50cm equivalent cube size. Once movement is initiated, the blocks fall downslope by leaping, bouncing, or rolling, often disintegrating into small fragments and coming to rest either on the slope (to become slope storage debris), at the bottom of the slope (to become debris accumulation), or if movement is sufficient, in the streambed itself.

Although the material involved in failure is bedrock derived, the term debris fall was preferred over rock fall since the material involved is essentially composed of detrital fragments prior to movement. Also, it was necessary to distinguish the fall of material derived from crushed bedrock from that of intact bedrock on the 1:2500 plan (Fig. 2, map pocket). Debris fall is considered here to be equivalent to the process of ravelling (as described by Hoek & Bray 1981).

Steep, high slopes and the loose, crushed rock mass are the principal causes of failure. The influence of water pressure in the open joints, earthquake shaking, and ground disturbance from passing, falling blocks may act as triggering mechanisms.

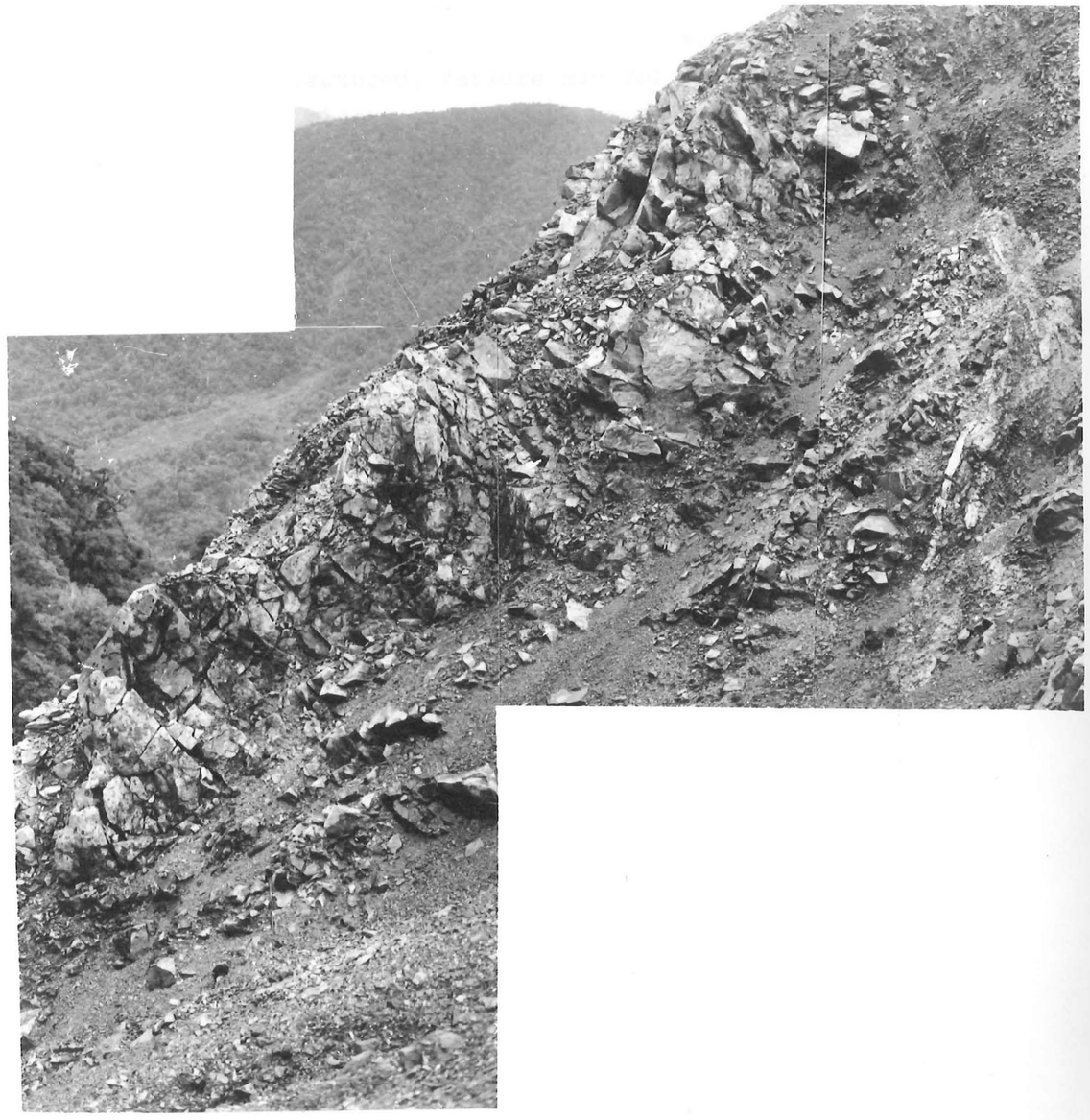

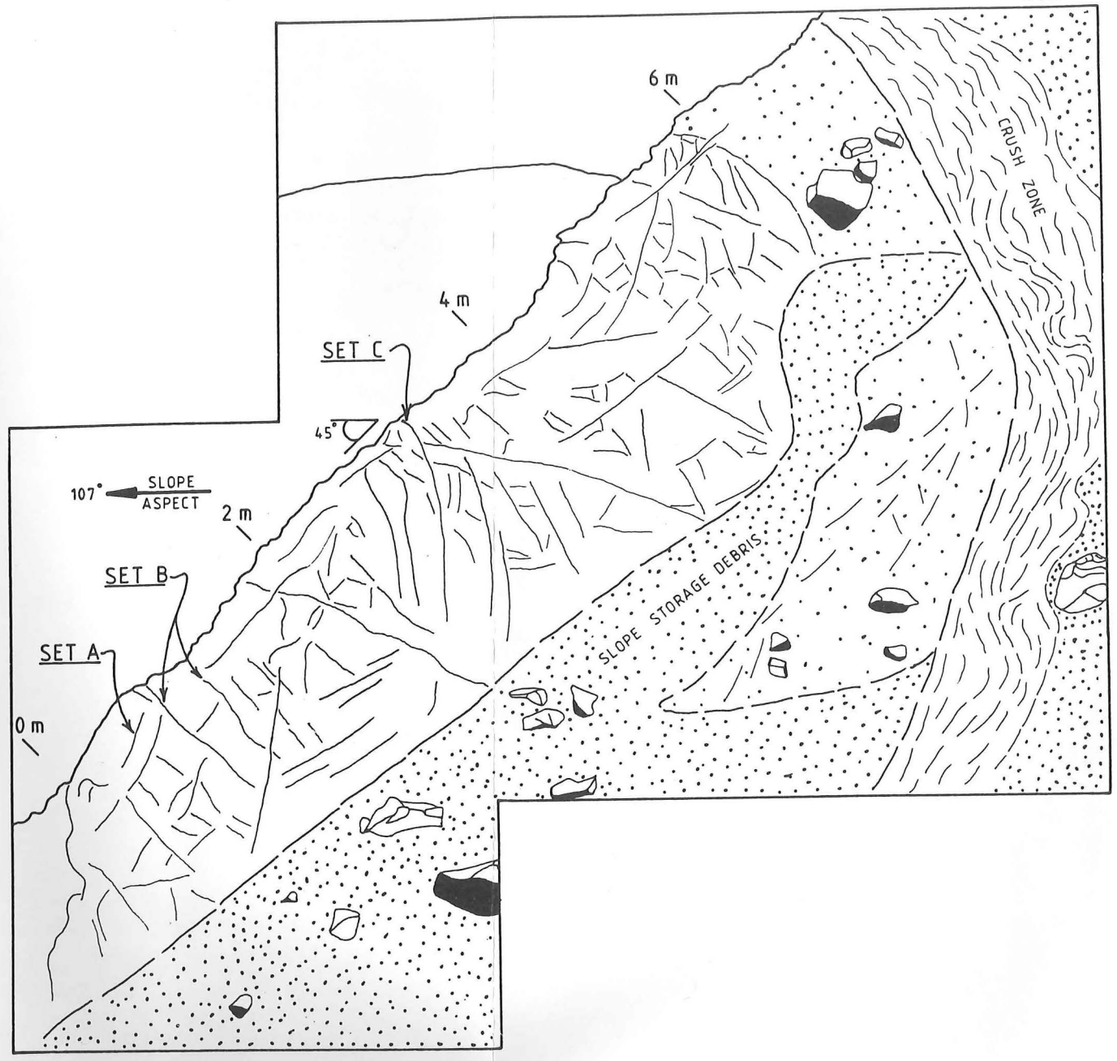

Fig. 4.17 Face log illustrating crushed hornfelsed sandstone in escarpment slope at locality BE 2.

ROCK MASS DESCRIPTION

DEFECT SET	DEFECT TYPE	DEFECT SPACING	DEFECT PERSISTENCE	DEFECT ORIENTATION
A	Joint	Moderate	Low	038°/52°SE
B	Joint	Close	Low	002°/37°W
C	Joint	Close	Low	112°/84°NE
-	Crush Zone	Extremely Wide	Very High	060°/48°SW

(iii) Debris Slump/Slide-Avalanches

When a material is very weak or a rock mass is very closely jointed or fractured, failure may follow a circular path. If individual blocks in the rock mass are very small compared to the size of the slope, and if these blocks do not interlock as a result of their shape, the crushed rock mass will tend to behave as a "soil" and slope failure will occur in a circular mode (Hoek & Bray 1981).

Rock mass conditions at Boulder Creek are suitable for circular sliding of the crushed hornfelsed sandstone. On slopes generally less than 45^{0}, circular headscarps were observed after rainstorm events suggesting a spoon-shaped failure surface. These features were short-lived, quickly destroyed by debris fall movements or covered with slope storage debris. Greater than around 48^{o}, failure scars were always planar shaped with an apparent transition zone between $45\text{-}48^{o}$. These observations compare well with Hoek & Bray (1981), who suggest that failure surfaces on weak or "soil" slopes less than 45^{o} would have a circular shape, and a planar shape on slopes steeper than 45^{o}.

These observations suggest that the basic failure mechanism of crushed bedrock slopes is by debris slide which may alter to debris slump at lower slope angles (less than 45^{o}). Due to the poor quality of the rock mass and the steep, high slopes, once failure is initiated by sliding the moving mass quickly accelerates and disintegrates to form an avalanche of sliding, flowing, and falling blocks. Observations suggest that failure takes place during rainstorm events, therefore sufficient water content would be present to allow an avalanche-type mechanism (Fig. 4.18).

At the downstream end of the escarpment slope at BE 2 the slope height is only 15m. At this locality "rafts" of vegetation have detached from the slope above the escarpment head and moved down and over the crushed bedrock, coming to rest near the base of the slope (Fig. 4.19). This debris sliding of the forested regolith/colluvium cover seems to be the main mechanism for retrogressive extension of the escarpment system upslope. Once the protective regolith/colluvium

Fig. 4.18 Debris slide-avalanche in crushed hornfelsed sandstone bedrock at locality BE 6: failure was initiated by debris sliding on upper crushed bedrock escarpment slopes which degenerated into an avalanche of falling blocks and flowing debris on lower debris accumulation slopes.

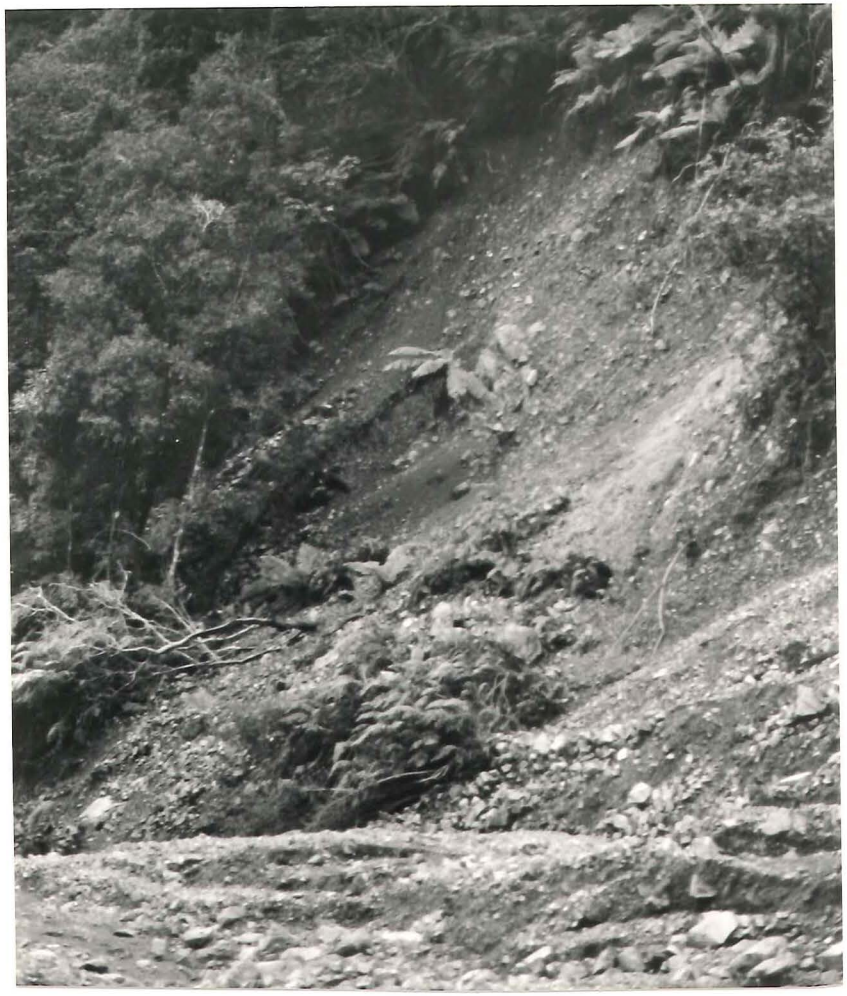

Fig. 4.19 Shallow debris sliding of the forested regolith/colluvium cover at locality BE 2: rafts of vegetation have detached from the slope above the escarpment head and moved down and over the crushed bedrock.

cover has been removed and the crushed bedrock has been exposed, water infiltration is increased which in turn increases positive pore pressures, resulting in a decrease in the effective normal stress rendering the slope more unstable.

Causes of failure are basically the same as debris fall: oversteepened, high slopes have removed lateral and underlying support, and the loose, crushed rock mass has decreased bedrock shear strength. Rainstorms act as triggering events suggesting that the crushed bedrock slopes are potentially unstable under wet and/or saturated conditions. Observations suggest that debris falls act as precursor events to debris slump/slide-avalanches. Either the displacement of material by debris fall removes underlying support of higher slopes, or the passage of falling debris disturbs lower slopes, in either case initiating failure.

4.4.4 Slopes in Tectonic Breccia

Tectonic breccia forms the slope material at two localities, BE 1 and BE 9. The dominant mechanism of slope failure in this setting is debris slump/slide-avalanching. Few debris fall failures occur on the puggy breccia slopes since the muddy sand matrix imparts a certain amount of cohesion to the rock material, not allowing individual blocks to be released as easily as on the crushed hornfelsed sandstone slopes.

The muddy sand matrix gives the breccia material a "soil-like" character which enables circular failure to take place. However, the breccia slopes range from 45 to 65°, therefore planar sliding is inferred to be the most common failure mode, based on observations made in crushed bedrock slopes and suggestions made by Hoek & Bray (1981). The presence and nature of the matrix would allow flowage, with sufficient water content available, once failure was initiated and the rock mass disturbed. On such steep slopes, this movement would manifest itself as an avalanche-type failure.

The causes of failure are similar to crushed bedrock material: lack of lateral and underlying support due to high, steep slopes produced by slope movement and stream erosion is the principal cause. The nature of the rock material, earth-

quake shaking and rainstorm events are additional factors which aid and trigger failure conditions.

4.4.5 Ancient Slope Movement Features

Two features were identified by aerial photograph interpretation which may relate to ancient slope movements at Boulder Creek. Both of these are mapped on the 1:2500 engineering geological assessment of slope and hydrologic processes presented in Figure 2 (map pocket).

The first feature is a lineament which trends across the top of the escarpment slope at an elevation of 720m and appears as a short, sharp break in slope through the forest vegetation on all aerial photographs studied (Appendix 4 details aerial photograph coverage of Boulder Creek). Three explanations are offered concerning its origin:-

1. Glacial feature: the lineament maybe a kame terrace, however no glacial deposits were found in the catchment and it is considered that Boulder Creek is a post-glacial feature;
2. Fault trace: the lineament maybe a fault trace, however, it is discontinuous and does not extent beyond the catchment and it is therefore unlikely that this is an active fault scarp;
3. Ancient slope movement: possible degraded, revegetated headscarp of a large-scale, deep-seated ancient slope movement, or a linear trough or "ridge rent" (Fig. 4.15) due to deep reaching gravitational movements; this would contribute to the origin of the crushed and fractured nature of the bedrock.

The second feature is an area of depressed topography surrounded by steep slopes above the escarpment slope at BE 2 which may be either a slumped block, part of larger movement, or a separate movement event in itself. Alternatively, the depressed area may have been lowered by past stream erosion during times when stream level was at that higher elevation.

No field evidence for either features being slope movement-derived was found and in fact it is difficult to recognise them on the ground beneath the heavy vegetation

cover. The interpretation that they are both ancient slope movement features therefore remains conjecture.

4.4.6 Assessment of Slope Instability

(i) Scope

Individual failure mechanisms operating in Boulder Creek can be summarised as follows:-

1. Intact Bedrock Slopes
   (a) Rock fall;
   (b) Rock slide;
2. Crushed Bedrock Slopes
   (a) Rock creep;
   (b) Debris fall;
   (c) Debris slump/slide-avalanche;
3. Tectonic Breccia Slopes
   (a) Debris slump/slide-avalanche.

Analysis of a failure or calculation of the factor of safety for a particular slope requires that the shear strength of the failure surface (defined by C and ϕ) be known. However, for some slope movements where failure does not involve sliding along a failure plane, factors of safety cannot be calculated which include rock and debris fall. Assessment of slope instability is limited to the rock slide and debris slump/slide-avalanche failure types with the following objectives:-

1. To find if rock sliding in intact bedrock is kinematically possible and if so, whether the failure would be planar or wedge shaped;
2. To obtain an indication of the factor of safety of the crushed bedrock and puggy tectonic breccia slopes which fail by debris slump/slide-avalanche, in both fully drained and saturated groundwater conditions, using published typical shear strength values.

(ii) Rock Slide in Intact Bedrock Slopes

Assessment of the instability of intact bedrock slopes was made by stereographic analysis utilising rock defect data collected during engineering geology field investigations. Appendix 6 details the analysis which was limited to ascer-

taining whether failure by sliding is kinematically possible and if so, whether planar or wedge shaped. Results of this analysis are reproduced below.

Marklands test for the intact bedrock slope at BE 6 showed that the plunge of the lines of intersection of joint defect sets do not fall in the zone of instability, although the intersection between sets A and C may be marginally significant, plunging just 4° steeper than the average slope angle. The Hocking refinement to the Markland test showed that failure is kinematically possible by plane sliding, however in both cases, the slope angle must be greater than 50°. Marklands test also showed that joint set C has the potential to produce a toppling failure which may initiate rock fall movements producing a complex topple-fall failure.

(iii) Failures in Crushed Bedrock & Tectonic Breccia Slopes

The main mechanism of failure in crushed bedrock and tectonic breccia slopes was described as a debris slump/slide -avalanche in Sections 4.4.3 and 4.4.4. Analysis of this movement mechanism assumes that failure is initiated by circular sliding to allow the use of the circular failure charts produced by Hoek & Bray (1981). This assumption is not completely geotechnically valid as field observations indicate that the initial failure is dominantly by translational sliding, especially on slopes >48°. This would limit the accuracy of the results, however, assuming a direct relationship in the condition of limiting equilibrium between circular and planar sliding mechanisms, the results are considered to be applicable within the accuracy of the analysis where shear strength data have been estimated from published typical rock property values. Details of the analysis are presented in Appendix 7 with the main conclusions being reproduced below.

Both crushed bedrock and tectonic breccia slopes were found to be stable under dry (fully drained) conditions with factors of safety ranging from 1.0-1.4, but under saturated conditions they become unstable with the factor of safety dropping to 0.9-0.6. This principal conclusion confirms field observations that failure occurs during rainstorm events when groundwater conditions approach the saturated state.

4.5 HYDROLOGIC PROCESSES

4.5.1 Objectives

Lobes of rock debris alluvium were described in Sections 4.3.3 (iii) and 4.3.4 as being an alluvial fill deposit overloading the streambed with material supplied principally by debris accumulations. As this material moves downstream on to the alluvial fan surface the lobate form is lost and the pulse of sediment becomes a sediment "wave". The purpose of this section is to describe the processes responsible for moving this material which are illustrated on the 1:2500 plan of engineering geology assessment of slope and hydrologic processes presented in Figure 2 (map pocket).

4.5.2 Development of Debris Lobes & Sediment "Waves"

During the course of fieldwork, the following chronology of slope and stream channel activity was recorded:-

March 1985: the stream channel had incised into its own alluvial deposits and in some places into bedrock below with limited debris accumulation development;

July 1985: a significant quantity of debris accumulation had built up throughout the catchment as a result of major slope activity during the period March-July 1985, which in turn correlated with a period of heavy rainfall; the stream channel remained relatively "empty" of material;

February 1986: material had moved from debris accumulation to the stream channel, forming a series of debris lobes which were moving downstream during flood events (Fig. 4.20); Table 4.5 lists the position of these lobes and correlates them to the slope area where the material originated from (the position of these lobes and of sediment "waves" which existed on the alluvial fan surface during February 1986 are given on the 1:2500 plan in Figure 2, map pocket).

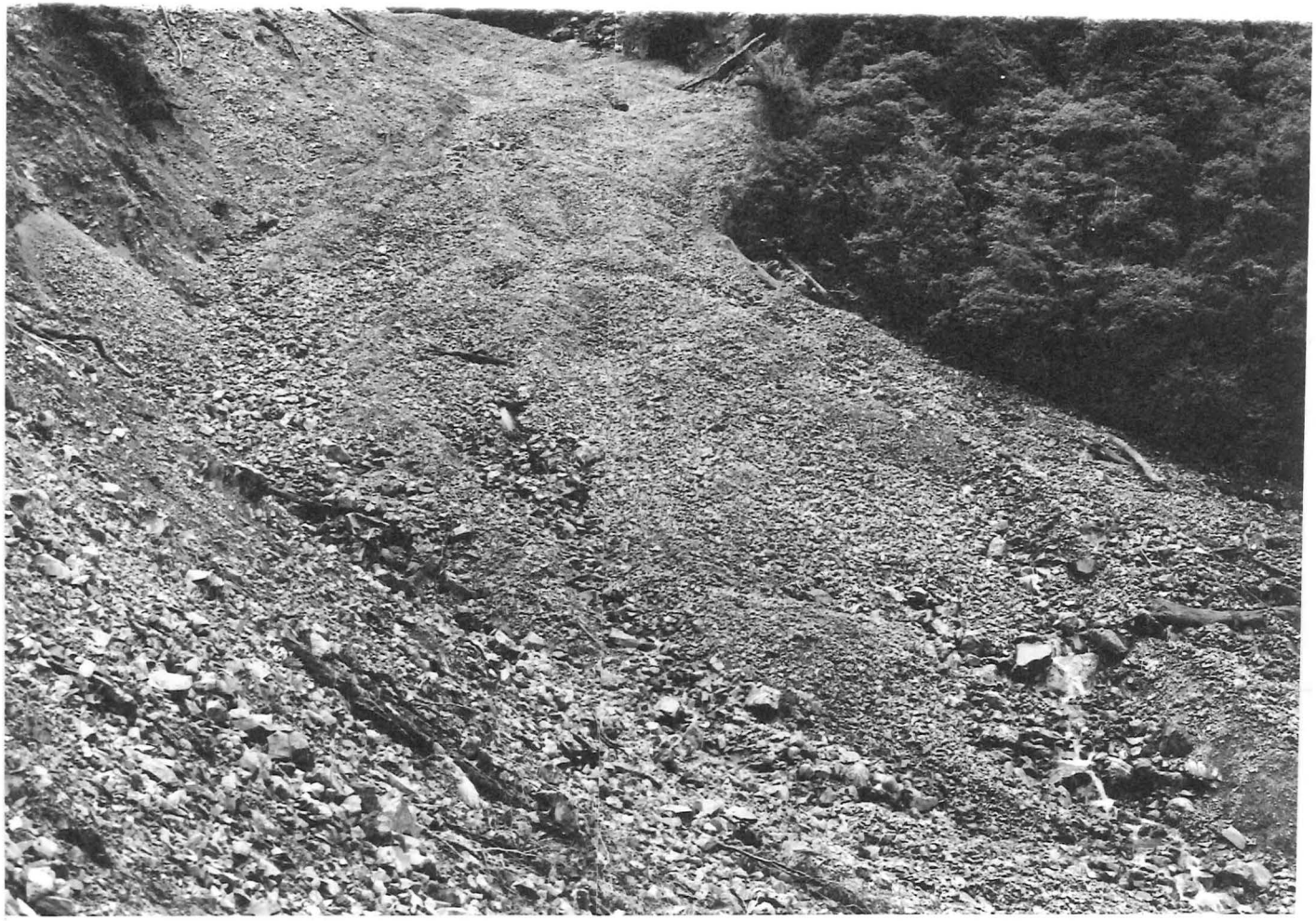

Fig. 4.20 Front of debris lobe 3 (1100m position, near locality BE 2) during February 1986; note the emergence of stream flow at the base of the lobe front, and the coalescence of debris accumulations with rock debris alluvium to produce a continuous expanse of debris from hillslope to stream channel.

POSITION OF SEDIMENT PULSES*		SLOPE SOURCE AREA
Debris Lobe 1:	1720 metres	BE 8
Debris Lobe 2:	1220 metres	BE 6
Debris Lobe 3:	1100 metres	BE 6 & BE 3
Sediment "Wave" 4:	780 metres	Not Known
Sediment "Wave" 5:	550 metres	Not Known
Sediment "Wave" 6:	220 metres	Not Known
Sediment "Wave" 7:	125 metres	Not Known

* Positions given as they occurred during February 1986 as ground distance measured along the streambed above the S.H. 6 bridge crossing.

Table 4.5 Correlation of sediment pulses with slope source area.

4.5.3 Description of Transported Material

A face log illustrating the structure and material descriptions of the stream gravels was given in Figure 4.11, Section 4.3.3 (iv). This log shows that the stream gravels are a coarsely layered, poorly sorted gravel unit which is randomly packed and loose in character. The surface of the streambed has an armour of coarse gravel with no interstitial fines, and on parts of the alluvial fan surface small lobate masses have formed with the outer perimeter of the lobe lined with boulder-sized clasts (Fig. 4.21). These lobate masses are up to 5.0m wide and occur on the fan surface between sediment "wave" fronts.

4.5.4 Rock Debris Lobe Movement & Sieve Deposition

Lobes of debris similar to the rock debris lobes of Boulder Creek were observed by Hayward (1980) in the Torlesse Stream catchment, Canterbury, which is situated in well indurated quartzo-feldspathic sandstones and mudstones of the Torlesse Supergroup. During a rainstorm event, fine gravel deposits in the Torlesse Stream catchment were seen by Hayward to move downstream in a similar manner to debris lobes seen in Boulder Creek during periods of high flow.

Hayward (1980) observed that water from heavy rainfall drains rapidly into and through coarse gravel material in Torlesse Stream with no indication of movement. However, transmission rates for water in fine gravel deposits are relatively lower allowing pore-water pressures to increase and the deposit becomes more fluid. Hayward (1980) describes the movement of this material as follows:-

> "Debris on its leading face ... moves in a series of amoeba-like advances ... As sections of leading face collapse a small flow of water entrains debris from the new channel and from the body of the deposit and transports it rapidly down the oversteepened face. The stream continues to cut through the unconsolidated debris until its oversteepened sides collapse inward and divert its flow back into the body of the deposit. A quiescent period will follow

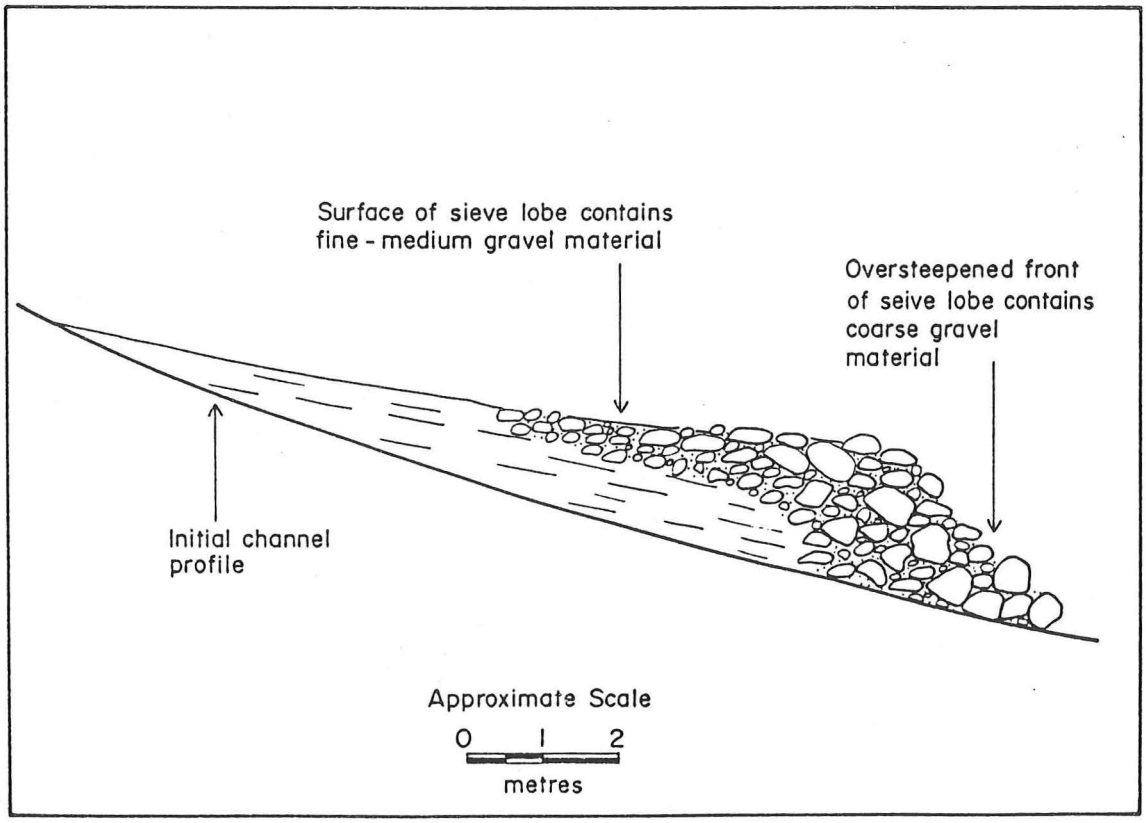

Fig. 4.21 Cross-section of a debris lobe on the alluvial fan surface situated at the same locality as Figure 4.11.

until a new section of leading face attains a fluidity that will cause it to slump and repeat the process."
(Hayward 1980, pp.38)

This same type of process was observed to move the rock debris lobes in Boulder Creek (Fig. 4.22 & 4.23), except that this material is coarse gravel rather than fine gravel. This implies that greater stream energy in the Boulder Creek system must be available to transport the larger bed load particle size, and this energy could be provided by the submergence of the pool-riffle channel morphology by rock debris overloading the stream channel. Modification of the steep stream gradient by a pool-riffle morphology allows the dissipation of potential energy of stream flow via a series of hydrologic jumps. If the pools are filled with debris their effectiveness in dissipating energy by turbulent mixing is impaired and flow energies increase (Hayward 1980). This increase in the capacity of the stream to do work may be sufficient to drive the mechanism to transport the coarse rock debris material.

This process also occurs on the alluvial fan surface at Boulder Creek forming coarse gravel lobate masses which are similar to those termed sieve lobes or sieve deposits by Hooke (1967). The mechanism Hooke describes closely resembles the processes observed in Boulder Creek where the gravels are so coarse the entire flow infiltrates before reaching the bottom of the fan. These deposits act as strainers or sieves by permitting water to pass while holding back the coarse material in transport, and under these conditions a lobe of debris is deposited at the point where water is unable to effect further transport (Hooke 1967).

4.5.5 Rheologic Motion

As defined by Moss (1972), water-laid sands and gravels are almost invariably composed of three depositional populations, designated A, B, and C:-

A - Framework: builds the sediment framework, attributed to saltation combined with packing processes;

B - Interstitial: composed of finer particles deposited interstitially to the A framework;

A

B

Fig. 4.22 Rock debris lobe No. 2 at locality BE 4:
A. Oversteepened front of the debris lobe.
B. Section of the leading face transporting debris down the oversteepened front.

Fig. 4.23 Rock debris lobe No. 1 above locality BE 7 during high flow: transportation of debris down the leading face of the debris lobe.

C - Contact: particles large enough to be rolled into position over the surface made by A.

According to Moss (1972), bed load sedimentation is naturally divided into a number of discrete bed stages, viz:-

1. fine ripple bed stage;
2. coarse ripple bed stage;
3. dune bed stage;
4. rheologic bed stage.

Mountain streams, such as Boulder Creek, are dominated by the rheologic bed stage and are floored by, "C-dominated, monolayer-capped, traction clog gravels", (Moss 1972, pp.214). Apart from sufficient finer material to fill the gravel interstices and some interbedded sands, all finer material is transported downstream.

Traction clog gravels are formed by the collective halting of rolling C particles in a concentrated juxtaposition (clogged). In response to erosion, the finest particles are removed from traction clog gravels, leaving a monolayer of the coarsest contact population particles available to the flow. These monolayers cause extreme bed roughness and act as flow energy dissipaters (Moss 1972).

The stream gravels described in the face log presented in Figure 4.11 are interpreted to be rheologic bed stage gravels with a clogged contact population. The mechanism of transport is rheologic motion described as follows.

When saltation becomes intense, intergranular collisions above the bed eventually become inevitable and the bed load changes its nature. Particles move collectively (not individually), gravitationally pulled towards the bed but maintained in a dispersed state. A layer is formed which flows like a viscous fluid called the rheologic layer (Moss 1972).

Provided that bed load free water applies shear to the rheologic layer from above, the tendency of particles to become dispersed is balanced against gravity. However, if the dispersion reaches the surface, conditions change and the mass

is driven by gravity alone. Under these conditions bed loads lose their identities and transport approaches slope movement in nature (Moss & Walker 1978; Moss & Walker 1980). Rheologic bed load transport probably grades into debris flow movement, and debris flow has been claimed to occur on some alluvial fans in California by Bull (1963) and Hooke (1967).

To summarise; sediment supplied to the stream system in Boulder Creek is transported out of the catchment area by a series of debris lobes and moves down the alluvial fan in sediment "waves". These pulses of sediment are dependent primarily on the rate of supply of material from the active escarpment slopes, and also on flood magnitude and frequency. Sediment is transported by water flow mechanisms involving sieve deposition and rheologic motion which may rarely pass into debris flow movement.

4.5.6 State Highway 6 Bridge Crossing

State Highway 6 crosses the Boulder Creek alluvial fan approximately 150m upstream from the Moeraki River. The bridge, a concrete slab structure, is presently being threatened by the unstable nature of stream channels on the alluvial fan surface and two problems are being experienced.

Firstly, the large amounts of sediment being transported down the fan in the form of sediment "waves" are blocking the bridge waterway opening and threaten to swamp the bridge deck. Secondly, the ability of stream channels on the fan surface to suddenly change course during high flow events (Fig. 4.24 & 4.25) is threatening the bridge road approaches. Figure 2 (map pocket) shows the direction of streamflood flows adjacent to the bridge crossing where unstable stream channels on the southeastern side of the fan are encroaching onto forest lands and cutting off the southeastern roadway approach (Fig. 4.26).

To reduce both problems, the Ministry of Works & Development groomed the entire alluvial fan surface from the top of the fan to the bridge in October 1985, in an attempt to train the stream and direct the flow into a single straight channel down the middle of the fan surface. Apparently the main

Fig. 4.24 Boulder Creek during high flow on the alluvial fan surface adjacent to the State Highway 6 bridge crossing: stream channels continually migrate across the fan surface by sudden changes in channel course, threatening the bridge road approaches.

Fig. 4.25 Encroachment of alluvial fan onto adjacent forest lands depositing stream gravels beneath the forest canopy.

Fig. 4.26 Deposition of stream gravels immediately adjacent to the southeastern bridge road approach by unstable stream channels during high flow.

purpose of this work was to facilitate movement of sediment down the fan and under the bridge waterway opening, however, in effect the slope or energy gradient was increased by shortening the river course and as a result this work was destroyed by the first flood event after construction was completed. Consequently, remedial measures have been restricted to repairing the road approaches and clearing the waterway opening after each flood event.

The most permanent solution would be to construct a series of debris detention dams down the alluvial fan surface which trap passing sediment behind a structure (such as willowpole scrub and netting, and concrete and earthfill dams) but allow water discharge downstream. This prevents streambed aggradation and decreases the energy gradient of the stream. Economically this is not a very viable solution for Boulder Creek considering the size of the stream system and the limited use of State Highway 6. More realistically, the unstable stream channels on the fan surface could be controlled by a series of guide banks to confine the flow towards the bridge waterway opening and away from the southeastern side of the fan.

4.6 SLOPE INSTABILITY ON GREENLAND GROUP HILL COUNTRY

4.6.1 Objectives

The extensive development of slope failures operating at Boulder Creek is indicative, although an exceptional example, of slope instability on Greenland Group Hill Country. The study of regional slope stability identifies fundamental causes of failure; however, when the emphasis shifts from the slope failure population to the site, additional variables become operative and the population data must be qualified by the site conditions. The objectives of this section are to:-

1. illustrate how specific site conditions combine with the fundamental causes of slope instability in a slope evolution model for Boulder Creek;
2. describe other slope movements occurring on Greenland Group Hill Country;

3. discuss the implications of this slope instability to future forest management of Greenland Group Hill Country.

4.6.2 Slope Evolution of Boulder Creek

The slope evolution model interpreted for Boulder Creek, summarised in Figure 4.27, identifies a series of processes and events which have combined to form the present system of sediment generation, transportation, and deposition, and divides the causes of these processes into fundamental and site specific causes. Figure 4.28 summarises the present system of sediment movement, dividing the processes moving the sediment into gravitational and hydrologic types, and identifies four stages of sediment movement from the stream catchment to the alluvial fan: sediment generation, storage, transportation, and deposition.

The slope evolution model identifies three key elements which are considered relevant to the slope instability of all Greenland Group Hill Country:-

1. decrease in the total shear strength by the crushed nature of the rock mass due to faulting, large-scale ancient slope movement(s), and deep rock creep;
2. increase in total shear stress by removal of lateral and underlying support due to oversteepening of slopes by ice erosion, deep stream incision, and past failure of catchment slopes (feedback loop - see Fig. 4.27);
3. high intensity rainstorm events and seismic events provide triggering mechanisms of slope failure.

4.6.3 Slope Movements on Greenland Group Hill Country

During preliminary fieldwork, most of the major streams in Greenland Group Hill Country were covered at a reconnaissance level. The objective of this section is to summarise observations and the salient conclusions on slope stability in Greenland Group Hill Country in South Westland based on this fieldwork and on results of more detailed investigations at Boulder Creek.

The majority of South Westland hill country is covered in heavy forest vegetation, and coupled with the high infil-

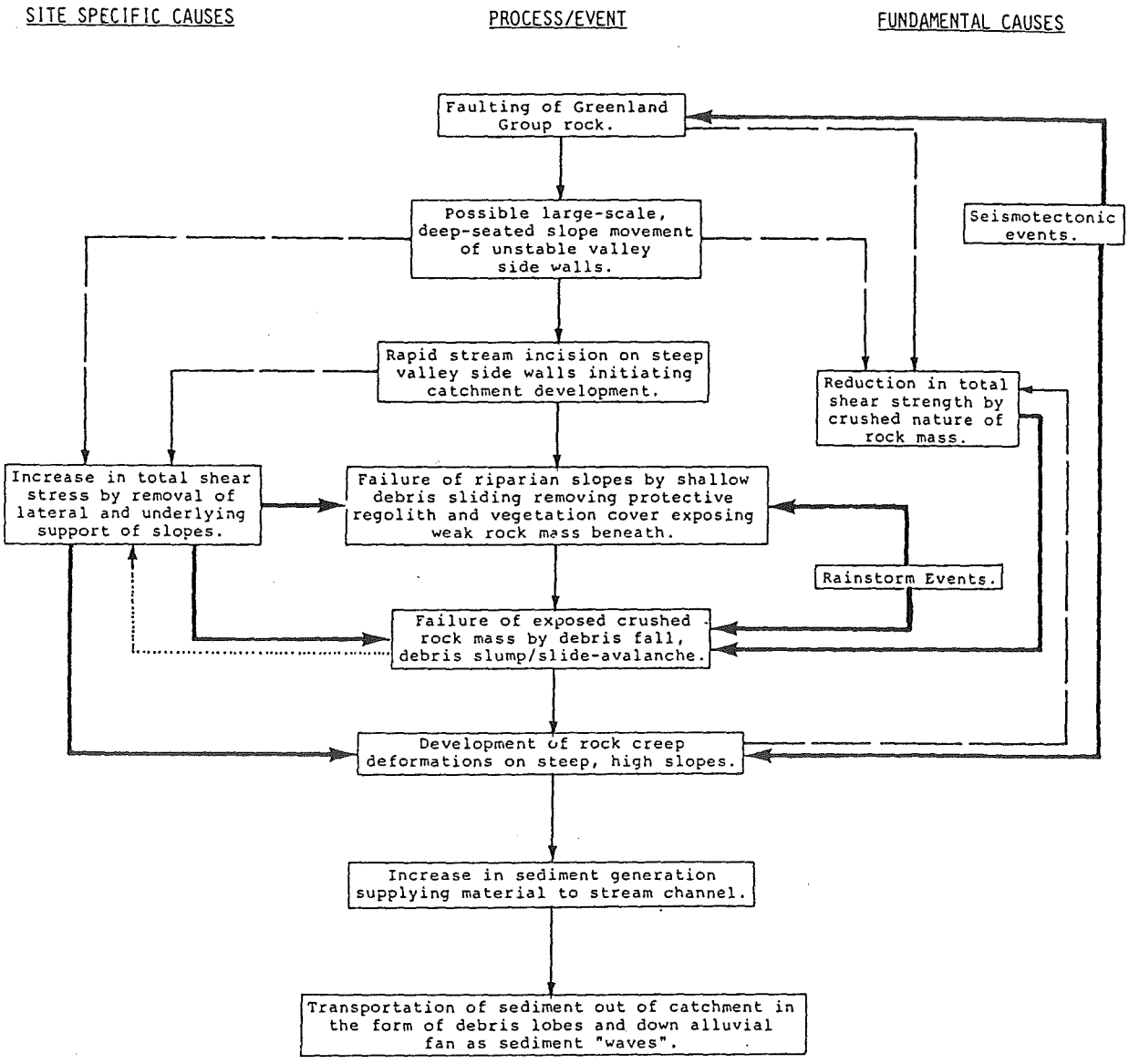

Fig. 4.27 Slope Evolution Model for Boulder Creek.

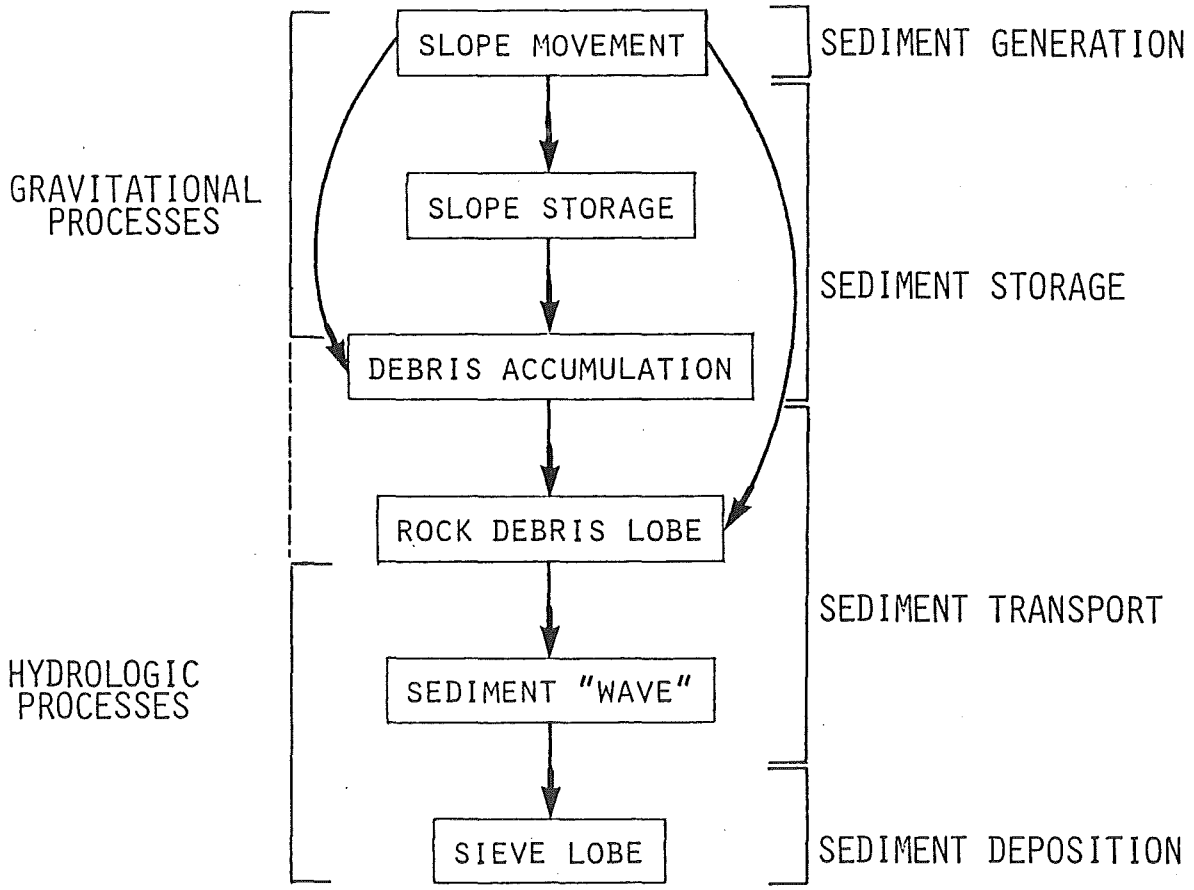

Fig. 4.28 Summary of sediment movement processes from catchment to alluvial fan.

tration capacity of the regolith/colluvium cover, this protects the slopes from surface erosion. However, it is this combination of factors which results in slope movement processes generally being the dominant mechanism of sediment generation and transport from hillslopes to stream channel.

The dominant slope failure mechanism is shallow debris slide-avalanche of the regolith/colluvium surficial cover, commonly along the regolith/colluvium-bedrock interface. Failure occurs on slopes ranging from 34 to 60°, with movement being mainly confined to the riparian zone extending up to 60m above stream level, but generally less than 40m. Few failures occur above this zone where the toe of the failure lies in a mid-slope position.

Often a large fallen tree was found lying at the base of a failure suggesting that removal of this tree by natural fall had initiated failure. This may be caused by rainwater infiltrating into the bare ground created and/or by the cessation of the binding effects of the tree roots. Figures 4.29 and 4.30 illustrates typical debris slide-avalanche failures in Greenland Group Hill Country from Mistake Creek (Whakapohia River catchment) and Power Creek.

Greenland Group Hill Country recorded a high 14.8 slope failures per km^2 in the Moeraki Hill - Collie Creek and Whakapohia River catchment areas, which contrasts to 3.1 in the Power Creek catchment (see Section 3.1.2). These are the two highest slope movement densities recorded in South Westland. This high density of slope failures south of the Paringa River seems to be related to the long life of the failure scars. Bedrock is typically crushed and fractured with numerous faults producing tectonic breccia material, with Boulder Creek being an exceptional example of these slope settings. Once the protective regolith/colluvium cover has been removed, bedrock is exposed to secondary failure by the mechanisms described for Boulder Creek in Section 4.4.

In the Power Creek catchment, bedrock has a higher rock mass quality corresponding to the intact bedrock type at Boulder Creek. As a result, shallow debris slide-avalanche

Fig. 4.29 Shallow debris slide-avalanche failures over Greenland Group bedrock on slopes up to 40m high at Mistake Creek, Whakapohai River catchment. Oblique view looking south-east. (N.Z. Geological Survey photo CN 5917a, photographer: D.L. Homer)

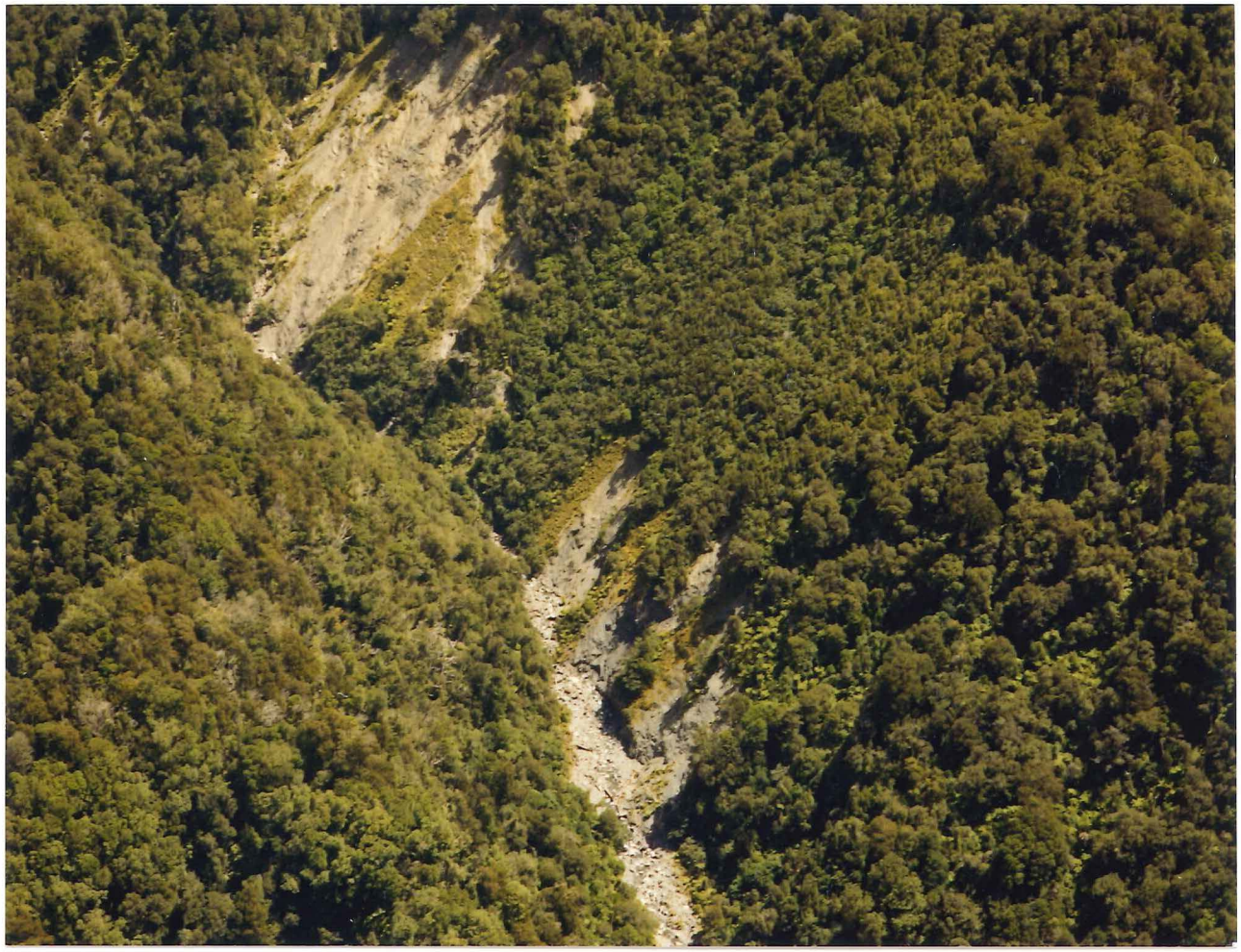

Fig. 4.30 Shallow debris slide-avalanche failures over Greenland Group bedrock on slopes up to 30m high at Power Creek. Oblique view looking west. (N.Z. Geological Survey photo CN 5887b, photographer: D.L. Homer)

failure scars do not commonly undergo secondary failure of the rock mass, allowing the scar to become revegetated and stabilised. The slope failure density of the Power Creek catchment (3.1 failures per km^2) probably reflects the true frequency of debris slide-avalanche failures in Greenland Group Hill Country south of the Paringa River as well.

Boulder Creek is an exceptional example of these slope instability problems in Greenland Group Hill Country, and the main reason for this can be explained by its geomorphic setting. Boulder Creek is situated on the flanks of a glaciated valley (see Section 4.2), and ice erosion has produced slopes which are higher and steeper than in the unglaciated hill country. Combined with two major fault systems which have crushed and weakened the bedrock mass, these have contributed to an unusual combination of geomorphic and geologic conditions resulting in a severe slope instability problem.

4.6.4 Implications For Forest Management

Swanston & Swanson (1976) estimated the net impact of forest management activities by determining the rate of debris avalanching in clearcut areas and road right-of-ways, and comparing these with the rate of slope activity for forested areas during the same time period. This analysis showed that clearfelling commonly results in an increase in debris avalanche activity by a factor of 2 to 4. In some cases, road related debris avalanche activity increased by factors ranging from 25 to 340 times the rate of activity in forested areas, and clearly this type of slope failure mechanism is highly susceptible to forest management activities.

When planning a timber harvesting operation, the most important consideration in terms of slope stability is determining the steepest slope that could be logged without causing failure. Two mechanisms of failure are relevant to analysing this problem for Greenland Group Hill Country: shallow debris slide-avalanche in the regolith/colluvium cover, and debris slump/slide-avalanche in crushed hornfelsed sandstone and puggy tectonic breccia bedrock materials. The steepest slope that could be logged without causing failure would correspond to the failure mechanism with the lowest slope angle at limit-

ing equilibrium (F.S = 1.0) under the worst groundwater conditions (saturated slope).

Table 4.6 summarises the critical slope angle data at the above conditions for a slope 40m high. This height was chosen because this was the average height observed in the field for the shallow debris slide-avalanche failures (see Section 4.6.3). A critical slope angle of 34^{o} for the debris slide-avalanche mechanism is taken from the worst case measured in the field. Critical slope angle data for the debris slump/slide-avalanche mechanism was taken from the slope height versus slope angle graphs presented in Appendix 7.

Table 4.6 shows that the steepest slope that could be logged without causing slope failure is 30^{o} for crushed bedrock slopes and 40^{o} for tectonic breccia slopes. These values are based on average slope height and worst groundwater conditions and as such they should be regarded only as general guidelines. More detailed analysis of specific sites is required before clearfelling is considered.

Assessment of the impact of bush-mill logging, involving single tree or small groups of trees removal, is more difficult. No information is available in the literature regarding the impact of this type of activity on slope stability. However, a number of general statements can be made which would apply equally to any type of forest management activity:

1. Timber should not be harvested from slopes over 60m above stream level (that is, within the riparian zone); even single tree removal may initiate failure on these slopes;
2. In general, slopes above the riparian zone greater than 30^{o} should be managed with care; slopes greater than 50^{o} should be undisturbed;
3. In any case, care should be taken in any forest operation not to remove the protective regolith/colluvium cover over crushed and brecciated bedrock.

FAILURE MECHANISM & SLOPE SETTING	CRITICAL SLOPE ANGLE (DRY CONDITIONS)	CRITICAL SLOPE ANGLE (SATURATED CONDITIONS)
1. Shallow debris slide -avalanche in regolith/colluvium.	Not estimated	34°
2. Debris slump/slide - avalanche in crushed bedrock.	51°	30°
3. Debris slump/slide - avalanche in tectonic breccia.	65°	40°

Table 4.6 Critical slope angles (F.S.=1.0) for the three types of failure mechanisms analysed in Greenland Group Hill Country based on a slope height of 40m.

4.7 SYNTHESIS

Engineering geology investigations at Boulder Creek identified three main slope settings within which specific slope failure mechanisms are operating:-

1. Intact Hornfelsed Sandstone Bedrock Slopes
   (a) Rock fall;
   (b) Rock topple-fall;
   (c) Rock slide;
2. Crushed Hornfelsed Bedrock Slopes
   (a) Rock creep;
   (b) Debris fall;
   (c) Debris slump/slide-avalanche;
3. Tectonic Breccia Slopes
   (a) Debris slump/slide-avalanche.

Fundamental causes of slope failure interpreted are:-

1. Reduction in total shear strength by the crushed and fractured rock mass due to faulting, rock creep, and possibly by disruption due to large-scale ancient slope movement(s);
2. Increase in total shear stress and reduction in total shear strength by increased water content and pore water pressure due to rainstorm events.

The geomorphic setting of Boulder Creek provides specific site conditions which are contributing to failure, which are not typical of Greenland Group Hill Country. The steep, high slopes produced by ice erosion, past slope failure, and stream erosion has removed lateral and underlying support increasing the total shear stress.

The hydrologic processes operating in Boulder Creek were investigated to complete the system of sediment generation, transportation, and deposition. Sediment moves out of the catchment as a series of pulses in the form of debris lobes, and on to the alluvial fan as sediment "waves". These pulses of sediment are dependent primarily on the rate of supply of material from active escarpment slopes and also on flood magnitude and frequency. Sediment is transported by water flow mechanisms involving sieve deposition and rheologic

motion which may pass into debris flow movement.

Results of geotechnical assessment of slope instability support field observations that both crushed bedrock and tectonic breccia slopes are stable under fully drained conditions but are unstable under saturated conditions. As a general guideline, according to this preliminary assessment and field observations, the steepest slope that could be logged without causing slope failure is 30^{o} for a saturated, 40m high slope. Detailed analysis of specific sites is required, however, to assess more accurately their stability and likely response to logging and roading activities.

CHAPTER FIVE

ALPINE FAULT ZONE SLOPES: HAVELOCK CREEK

5.1 OUTLINE OF APPROACH

Selection of a detailed investigation site for Alpine Fault Zone slopes was based on reconnaissance level investigations of slope instability in South Westland, and Havelock Creek was chosen for the following main reasons:-

1. the presence of all major slope settings identified on Alpine Fault Zone slopes;
2. the high severity of the slope instability problem, and;
3. good access to the site from State Highway 6.

The method of approach to investigations was based on the scheme outlined in Section 3.6 with investigations reported under two main headings:-

1. Engineering geology field and laboratory studies;
2. Slope movement processes.

A summary of observations made during reconnaissance field work of Alpine Fault Zone slopes follows the main discussion of Havelock Creek investigations, and the possible implications for future forest management are reviewed by way of conclusion.

5.2 GEOMORPHIC & GEOLOGIC SETTING

5.2.1 Topography & Vegetation

Havelock Creek (Fig. 5.1) drains the northern slopes of the Copland Range in mountainous schist terrain, flowing northwest to cross State Highway 6 approximately 8km north of the Karangarua River bridge (S78/553566). The site of investigation is the catchment of the first major northeastern (true right) tributary approximately 2000m upstream from the State Highway 6 bridge crossing. Figure 5.2 delineates the study site and shows the position of localities mentioned in the text.

Fig. 5.1 Havelock Creek study catchment showing the large (240m vertical elevation) rock slide and other slope movements in the Alpine Fault Zone. Oblique view looking southeast. (N.Z. Geological Survey photo CN 5824a, photographer: D.L. Homer)

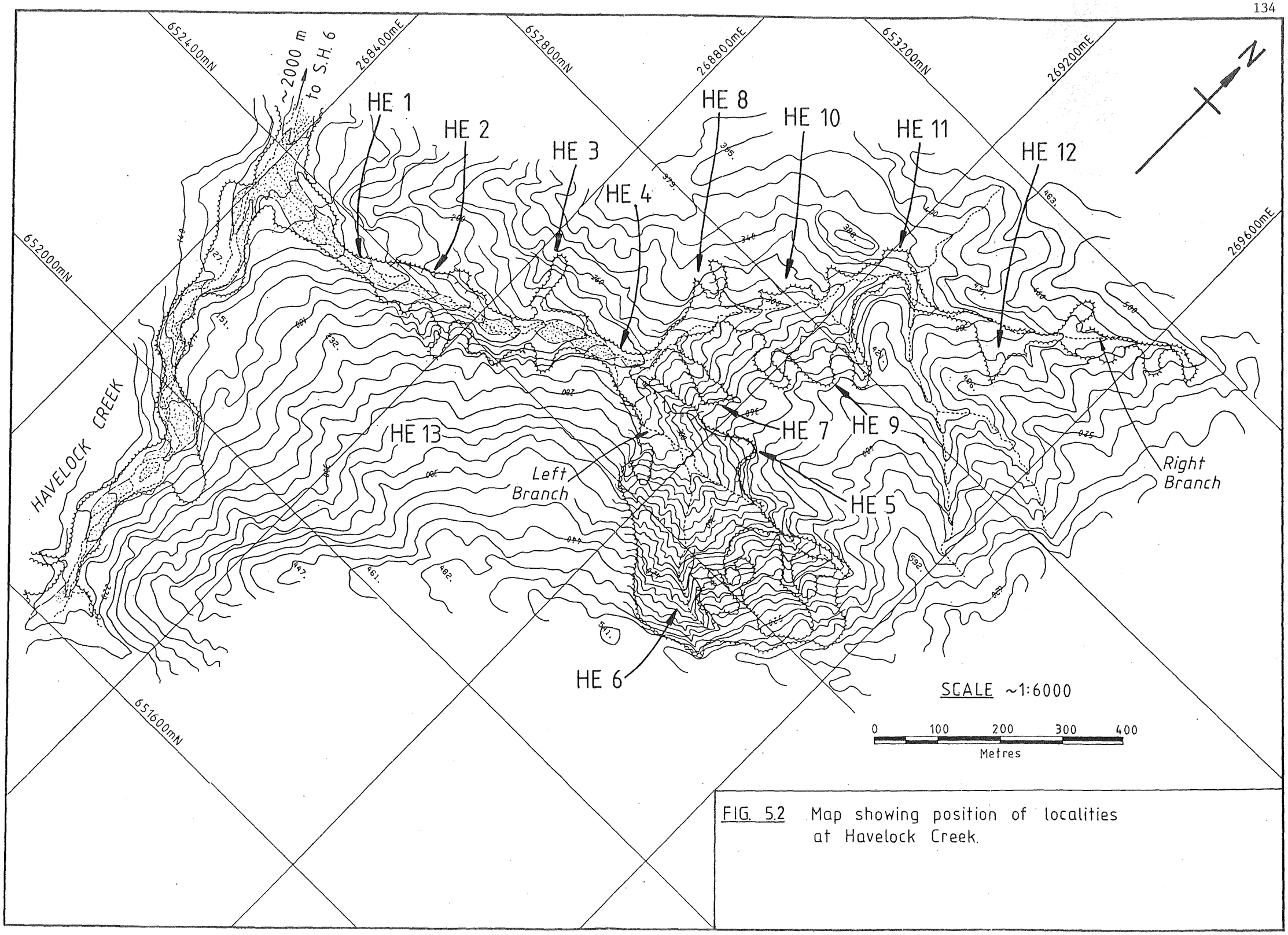

FIG. 5.2 Map showing position of localities at Havelock Creek.

Total catchment area of the study site is 877 000m^2 of which 186 000m^2 (21%) is bare ground and 691 000m^2 (79%) is forested slopes. Catchment relief ranges from 120m (above sea level) at the tributary junction with Havelock Creek to 640m at the highest point on the drainage divide, a relative relief of 520m. The stream divides into left and right branches some 720m up the tributary from Havelock Creek (see Fig. 5.1), the right branch continuing as the main stream for 1025m to the drainage divide, giving a total stream length of 1745m. Over this 1745m, the stream drops from 520m to 120m above sea level, with an average stream gradient of 13^o.

The dominant forest type is Kamahi/Rimu-Blechnum Forest with smaller areas of Rimu/Kahikatea-Phyllocladus Forest and Kamahi/Rata/Rimu-Pseudopanax Forest. This gives way to dominantly Rata/Kamahi Forest in the higher slopes in schist mountain country (J. Pfaflert NZFS pers. comm.).

5.2.2 Fault Movement

The tributary in the study catchment is structurally controlled by the Alpine Fault and trends subparallel to the strike of the Fault Zone. The geology of the fault zone is complex, and with little exposure is difficult to determine. Two major fault gouge zones were mapped and are shown on the 1:2000 plan in Figure 3 (map pocket), whilst aerial photograph interpretation identified two lineaments in the study catchment which may be fault traces (Fig. 5.3). Field checking revealed no extra information due to the difficulty of recognising these features beneath heavy forest vegetation cover. The most significant feature at Havelock Creek is the presence of a large "bulge" which lies on the surface of moraine hill country immediately northwest of the study catchment (see Fig. 5.3). This feature is considered to be a gravity collapse napplet with schist overthrusting glacial gravels, as described elsewhere along the Alpine Fault by Wellman (1955) and Suggate (1963).

The history of fault movement at Havelock Creek is difficult to ascertain. The gravity collapse napplet thrust over glacial gravels limits fault movement producing this

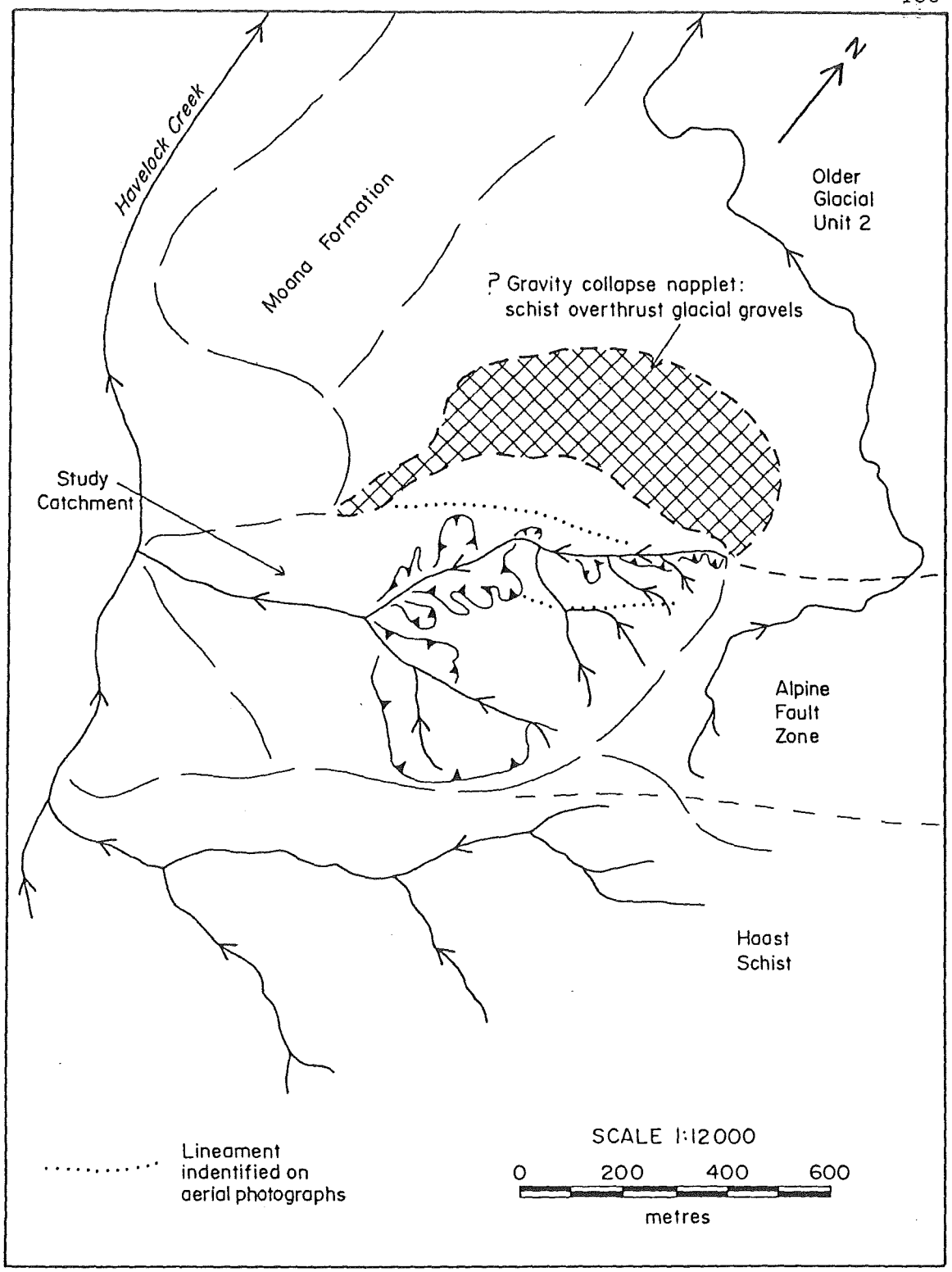

Fig. 5·3: Sketch map illustrating the occurrence of possible gravity collapse napplet with schist overthrusting glacial gravels, Havelock Creek

feature to post-glacial times (post 14 000 years B.P.), and at least one further major movement has taken place since then, thrusting fault gouge over post-glacial gravels at locality HE 4.

5.2.3 Recent History of Slope Activity

The age of the catchment is post-glacial, the tributary stream quickly establishing preferentially along the line of the Alpine Fault Zone soon after retreat of ice after the last glaciation (Moana Glaciation c.14 000 years B.P.). Stream incision would have been rapid, downcutting into weak fault zone materials creating steep, high slopes which were susceptible to slope movement.

Aerial photograph evidence suggests that slope movement activity occurs episodically. 1942 photography (Appendix 4 details aerial photograph coverage of Havelock Creek) shows minor amounts of bare ground (<5%) relative to the 21% present today but with distinct areas of regenerating vegetation outlining slopes which had undergone past activity. 1965 photograph coverage shows the catchment to be fully vegetated with no bare ground, and since then, slope activity has increased to 21% of the slope area experiencing failure or stream erosion based on 1984 aerial photography.

5.3 ENGINEERING GEOLOGY INVESTIGATIONS

5.3.1 Investigation Programme

The Havelock Creek investigation site was mapped in terms of engineering geological at a scale of 1:2000 and two maps have been compiled based on this information:-

1. a 1:2000 engineering geology plan showing the distribution of bedrock and surficial materials, basic morphological features, and hydrogeological features (Fig. 3, map pocket), and;
2. a 1:2500 engineering geology assessment of slope movements showing the distribution of interpreted failure types and processes (Fig. 4, map pocket).

The engineering geological features shown on the 1:2000 plan are discussed in Sections 5.3.2 to 5.3.5. Limited laboratory testing was carried out on fault gouge and tectonic breccia matrix samples with the primary objectives of:-

1. characterising these materials according to standard geotechnical tests, and;
2. allowing a preliminary assessment of their engineering properties.

Methods and results of this work are reported in Section 5.3.6.

5.3.2 Bedrock Geology

The basic bedrock lithology at Havelock Creek is laminated garnet schist mapped as Haast Schist by Gair (1967). This lithology has been altered to mylonite schist, tectonic breccia, and fault gouge materials within the Alpine Fault Zone. The distribution and occurrence of these bedrock units, together with summary rock material and mass descriptions are given on the 1:2000 plan (Fig. 3, map pocket) and more detailed material descriptions given in Table 5.1. Each of these bedrock units is described below in terms of their material and mass properties.

(i) Garnet Schist

Unaltered garnet-biotite schist outcrops in the main (right) branch of the Havelock Creek tributary upstream from locality HE 12, and in the large slope movement scar up the left branch (HE 6). The dominant rock type is a grey (to dark brown), thinly laminated quartzo-feldspathic schist with alternating light and dark bands 1-3mm thick. Near the toe of the slope movement scar, light and dark layering in the schist becomes less marked and the laminae are reduced to very thin (<1mm) lensoidal wispy streaks. This rock is termed wispy schist and represents the first stage of mylonitisation (see Fig. 2.5.2 (iv)).

The garnet schist has been divided into two sub-units based on quality of the rock mass:-

1. intact schist, and;
2. Crushed schist.

PROPERTY	GARNET SCHIST	MYLONITE SCHIST	TECTONIC BRECCIA	FAULT GOUGE	GLACIAL GRAVELS
WEATHERING	Slightly weathered: Grade 2 (some staining of defect surfaces)	Unweathered	Unweathered	Unweathered	Unweathered; slightly weathered matrix.
WATER CONTENT	N/A	N/A	Matrix: moist to saturated	Moist to saturated	Matrix: moist
STRENGTH	Strong to very strong (1-10 MPa point load strength)	(Moderately strong to) strong (0.3-3 MPa point load strength)	Matrix: stiff	Hard to very soft	Compact
COLOUR	Grey (to brown)	Dark greenish grey	Light greyish green to dark greenish grey	Light greyish green	Matrix: brown
FABRIC	Finely laminated	Faintly finely laminated	Faintly coarsely layered	Finely laminated	Faintly coarsely layered
ROCK NAME	Garnet-oligoclase SCHIST	MYLONITE SCHIST	Mylonite schist puggy TECTONIC BRECCIA	FAULT GOUGE: silty clay (CL)	Sandy, fine to coarse GRAVEL

Table 5.1 Summary of rock material properties of bedrock map units at Havelock Creek.

Intact schist contains dominantly widely spaced, closed joints and outcrops only in the main (right) branch beyond HE 12. The large slope movement scar at HE 6 is entirely composed of crushed schist in which the rock mass consists of very closely spaced, low persistence joints which are mostly closed with some occasional open fractures. Poor quality of the crushed rock mass is due to tectonic deformation from the Alpine Fault movements and forms the most eastern rock type in the Alpine Fault Zone.

(ii) Mylonite Schist

Mylonite schist occurs widely in the Havelock Creek tributary as the most common hard rock type. It is exposed in the stream eroded gullies on the southeastern (true left) bank of the tributary stream opposite localities HE 1 to HE 4, forms the high (up to 100m) scarp at HE 5, and outcrops in the headscarps and slopes at localities HE 7 and HE 9.

The mylonite schists show little layering in hand specimen but are highly schistose. In thin section, grain size is seen to be greatly reduced and individual grains are oriented parallel to schistosity. Mineralogy and metamorphic grade of the mylonite schists is very similar to that of the unaltered schist, both biotite and garnet present in most samples (Nathan 1984). Interlayered within the mylonite schist are dark greenish grey to black amphibolite rocks which show no metamorphic layering, have a poorly developed schistosity, and in thin section these rocks show little textural evidence of deformation (Nathan 1984).

The mylonite schists have been severely crushed and fractured producing extremely close to very closely spaced closed and open joints of very low persistence. Joint opening averages 5-10mm and is occasionally infilled with fine sandy material. Very widely spaced shear zones 5-10m apart strike sub-parallel (approx. 060^{o}) to the Alpine Fault Zone within the crushed rock mass. These zones average 50mm in width and consist of small (average 10mm equivalent cube size) mylonite schist rock fragments surrounded by a puggy matrix with a very fine laminar fabric.

The structure of the schists defines a synform within the fault zone. In the headscarp region of the slope failure at HE 6, schistosity dips at a shallow angle of 10-12° to the northwest. Near the base of the slope, schistosity steepens to 45°NW before overturning to the southeast in the mylonite zone, as illustrated in cross section A-A', Figure 3 (map pocket).

(iii) Fault Gouge & Tectonic Breccia

Two major fault gouge zones are exposed in the Havelock Creek tributary at localities HE 1 and HE 4, and in addition, fault gouge material is exposed at the base of the slope at HE 7-HE 9. All these exposures are at streambed level and are subject to rapid change due to streambed aggradation-degradation and stream channel shifts.

At HE 1 and HE 4, the material is described as an unweathered, moist to wet, hard, light greyish green, finely laminated silty clay. At HE 1 the gouge zone also contains fine irregular laminae of brown and dark bluish grey material which are either weathered zones, or more likely, derived from thin bands of inclusion material interbedded within the original quartzo-feldspathic sediment from which the schist is derived. Scattered within the gouge material are occasional small (average 10mm equivalent cube size) angular fragments of mylonite schist rock. As exposed, the two gouge zones are 1.5-2.0 and 3.0m wide at HE 1 and HE 4 respectively and dip to the southeast at 24 and 55° respectively.

The fault gouge material at HE 7 and HE 9 occurs as a low 1.0m high exposure above streambed level which extends for 125m. The material is massive, wet to saturated, and easily moulded by hand pressure (soft to very soft strength). Numerous water springs emerge from this low bank and the gouge material in places is seen to flow onto the streambed and cover stream boulders (Fig. 5.4).

To the east of the gouge zone is a belt of tectonic breccia which forms the slope material at localities HE 2, HE 7 and HE 10. This material consists of angular to sub-angular, fine to coarse gravel size blocks of mylonite schist

in a moist to wet, stiff, puggy clayey silt matrix. At HE 2 there seems to be a gradation in colour from light greyish green adjacent to the fault gouge zone to dark greenish grey next to mylonite schist rock. This may reflect a gradual increase in mylonite schist clast content towards the south-east with a corresponding decrease in puggy matrix away from the gouge zone.

(iv) Glacial Gravels

Glacial gravels are exposed at three localities, all on the northern bank, at HE 3, HE 8, and HE 11 and have been mapped as Older Glacial Unit 2 by Mortimer et al. (1984). This gravel is dominantly clast supported and is faintly coarsely layered suggesting that it maybe outwash material. The clasts are sub-angular to sub-rounded, poorly sorted schist gravels ranging from fine to coarse in size with a slightly weathered, moist, compact, brown quartzo-micaceous sand matrix.

At HE 11 glacial gravels directly overlie mylonite schist, whereas at HE 8 puggy tectonic breccia is seen to overlie glacial gravels. It is inferred that schist has been thrust over the gravels forming the gravity collapse napplet described in Section 5.2.2, and that the gravels have been exposed as "windows" through the fault zone materials (see cross section C-C', Fig. 3, map pocket).

5.3.3 Surficial Geology

The surficial geology has been divided into three units:-

1. slope storage debris;
2. debris accumulation, and;
3. stream gravels.

This classification reflects both the position of surficial material on the slope and the type of material involved; each of the units are described below.

(i) Slope Storage Debris & Debris Accumulation

Any debris covering bedrock material on fresh (unvegetated) slopes or infilling gullies is classified as slope storage debris. It may include regolith, derived from in-situ

weathering of bedrock, or more commonly, colluvium derived from slope failure. Slope storage debris dominantly consists of broken fragments of bedrock and disrupted vegetation debris ranging from dry on fresh slopes to saturated in gully depressions. This material is held temporarily in storage on the slope until moved further downslope to eventually become incorporated as slope storage accumulation material.

Many of the crushed garnet schist and crushed mylonite schist slopes are partially mantled by slope storage debris that consists of broken fragments of bedrock similar in appearance to the crushed rock mass. Consequently, it is difficult to distinguish between these two slope materials on inaccessible slopes, and therefore where slopes have simply been mapped as crushed bedrock they may also contain certain quantities of slope storage debris overlying them.

(ii) Stream Gravels

Stream gravels occupy the permanent streambed areas and are formed and transported by normal mountain stream pool and riffle type fluvial processes. Basically they consist of sub-angular to sub-rounded, small to large gravel with a poorly sorted sandy matrix. Large glacial erratic boulders up to 10-20m^3 in size lie in the streambed below locality HE 8, having fallen from the glacial gravel deposit that form the stream bank on the northwestern side.

5.3.4 Slope Morphology

The most dominant morphological feature in the study site is a vertical 240m high slope movement scar up the left branch (Fig. 5.1). This failure has a 10-30m high headscarp which extends along the top of the ridgeline for approximately 350m, and gully erosion on the southwestern flank has removed a substantial amount of crushed schist bedrock leaving a sharp ridge-gully topography. The northeastern flank is separated into two blocks by a major scarp, the lower block undergoing active gully erosion while the upper block still supports the original forest vegetation cover, with incipient slope storage-infilled gullies developing on the surface (perhaps signifying future erosion potential). Average slope angle of this displaced block is 40^o, while adjacent slopes average 38^o.

Throughout the rest of the catchment both fresh and eroding escarpments, resulting from slope failure and gully erosion, form the most obvious surface morphological features (Fig. 5.5). These are often mantled at the base of the slope by debris accumulation deposits in the form of debris fans. All these features have been mapped on the 1:2000 engineering geology plan (Fig. 3, map pocket).

5.3.5 Geohydrology

Numerous cold water mineral springs which occur in the catchment are characterised by a brownish yellow precipitate deposited on surrounding rocks and a pungent "rotten egg" smell indicating hydrogen sulphide (H_2S) gas (Fig. 5.6). Similar cold water H_2S mineral springs have been noted elsewhere within the Alpine Fault Zone in South Westland. These springs are thought to originate from deep-reaching circulating groundwater which is heated by frictional mechanisms, dissolving mineral material from surrounding country rock. These solutions travel to the surface along the line of weakness provided by the fault plane, decreasing in temperature and becoming cold (similar temperature to stream water) by the time they reach the surface.

As noted in Section 5.3.2 (iii), a line of groundwater springs emerge from gouge and tectonic breccia material along the base of the slopes at HE 7 and HE 9. Flow rates are low (less than $100ml.s^{-1}$) in dry weather, increasing during and immediately after rainstorm events to a moderate flow (up to $1l.s^{-1}$). The only other water spring noted was a seepage at the base of a headscarp at HE 9 situated 30m upslope from the basal springs.

There is presently a substantial quantity of sediment in storage in the streambed area which has been generated by the current episode of slope activity. Although the smaller of the two branches, the left branch is contributing an estimated 70-80% of the sediment emerging from this tributary with most originating from erosion of the large slope movement scar. This large quantity of sediment is having significant downstream effects on the State Highway 6 bridge crossing

Fig. 5.4 "Rafts" of vegetation sliding over wet to saturated gouge material which is flowing onto the streambed and covering stream boulders.

Fig. 5.5 Gully erosion on escarpment slope in crushed mylonite schist bedrock at locality HE 5.

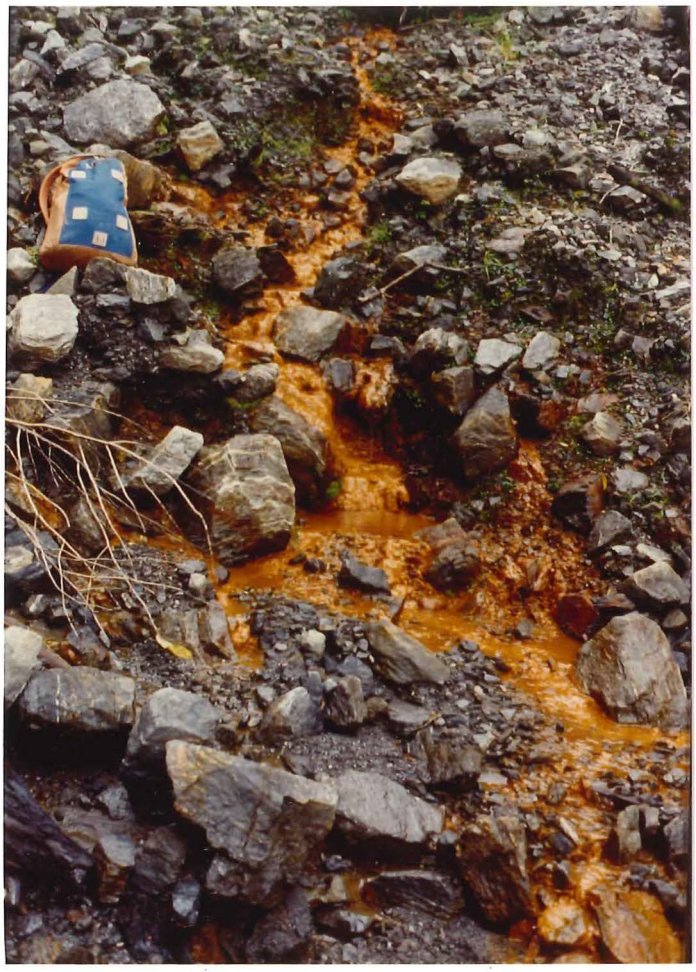

Fig. 5.6 Cold water H_2S spring depositing a brownish yellow precipitate on surrounding stream gravels at Havelock Creek.

which is situated on the Havelock Creek alluvial fan. During times of high flow (Fig. 5.7), substantial quantities of sediment are being transported on to the fan surface threatening the bridge crossing in two ways:-

1. By aggradation of the streambed, which blocks the bridge waterway opening and swamps the bridge decking, and;
2. By migration of unstable stream channels, which may cut-off the bridge road approaches.

Current short-term solutions by the Ministry of Works and Development involve:-

1. grooming the stream channel on the alluvial fan surface to direct the flow through the waterway opening (Fig. 5.8);
2. constructing uncompacted gravel levees where flood channels have deviated away from this straight course, and;
3. clearing the bridge waterway opening after each major fresh and flood.

5.3.6 Laboratory Investigations

(i) Laboratory Programme

Disturbed bag samples of fault gouge and tectonic breccia matrix were collected from surface outcrop exposures and tested to determine grain-size distribution, in-situ moisture content, Atterberg limits, and clay mineralogy. The main objective of this limited laboratory programme was to characterise these materials according to some standard geotechnical tests which would allow a preliminary assessment of their engineering properties. Results obtained for three gouge and two tectonic breccia matrix samples, summarised in Table 5.2, are discussed below.

(ii) Grain-Size Distribution

Methods used to determine grain-size distribution and semi-log plots of results are given in Appendix 5. Coarse-grained engineering soils (sands and gravels) can be classified according to their grain-size distribution.

Fig. 5.7 State Highway 6 bridge crossing of Havelock Creek minutes after flood waters passed over the concrete slab structure, flooding the bridge decking.

Fig. 5.8 Bulldozers clearing and realigning the stream channel to flow through the bridge waterway opening at Havelock Creek after a major fresh.

Sample Number	Sample Origin and Description	Water Content %	Grain Size Analysis				Atterberg Limits				Activity	Soil Class[n]	Clay Mineralogy
			Gravel %	Sand %	Silt %	Clay %	LL	PL	PI	LI			
HS 1	HE 1, silty clay FAULT GOUGE.	9.4	0	21	40	39	25	9	16	0.02	0.41	CL	n.d.
HS 2	HE 2, sandy gravel TECTONIC BRECCIA.	8.7	65	24	8	3	11	10	1	-1.3	0.33	GM	chlorite>illite >quartz
HS 3	HE 4, silty clay FAULT GOUGE.	14	2	25	35	38	34	12	22	0.09	0.58	CL	chlorite>illite >quartz
HS 4	HE 7, silty sand TECTONIC BRECCIA.	13	19	45	28	8	15	13	2	0	0.25	SM	n.d.
HS 5	HE 9, silty clay FAULT GOUGE.	34	1	23	36	40	38	14	24	0.83	0.60	CL	n.d.

Note - n.d. - not determined

Table 5.2 Summary of laboratory test results for fault gouge and tectonic breccia matrix samples, Havelock Creek.

Fault gouge materials are fine-grained with 73-79% of the sample finer than 0.06mm of which about 40% is in the clay fraction. The remaining 20-30% is mostly sand with little or no gravel content.

Tectonic breccia matrix samples, on the other hand, are coarse-grained with 64-89% of the sample coarser than 0.06mm. Within the coarse fraction, the most dominant size varied from gravel (65%) in the sample from HE 2, to sand (45%) in the sample from HE 7. This variation probably reflects the distance the sample was taken from the gouge zone, the finer sandy sample being taken closer to the gouge zone than the gravelly sample. According to the Unified Soil Classification system, sample HS 2 is a poorly graded silty gravel (GM), while HS 3 is a poorly graded silty sand (SM).

(iii) In-situ Moisture Content & Atterberg Limits

Appendix 5 details methods used to determine in-situ moisture content and Atterberg limits. The results of these tests allow the fine-grained soils to be classified since variation in moisture content in these soils can produce significant changes to their engineering properties.

Both tectonic breccia matrix samples have low Atterberg limits, plotting to the left of the "A" line on the Plasticity Chart (Fig. 5.9). Liquidity indexes are at or below unity, indicating that natural water contents are at or below the plastic limit.

Atterberg limits for the fault gouge samples are comparatively higher, plotting above the "A" line (Fig. 5.9) as clays of low to medium plasticity (CL). Sample HS 5 from HE 9 has an activity ratio of 0.60 and a liquidity index of 0.83. This characterises the material as a marginally active clay of medium plasticity, with natural water content approaching the liquid limit. This relatively higher activity and plasticity properties compared to the other gouge samples corresponds well with its observed field behaviour as described in section 5.3.2 (iii).

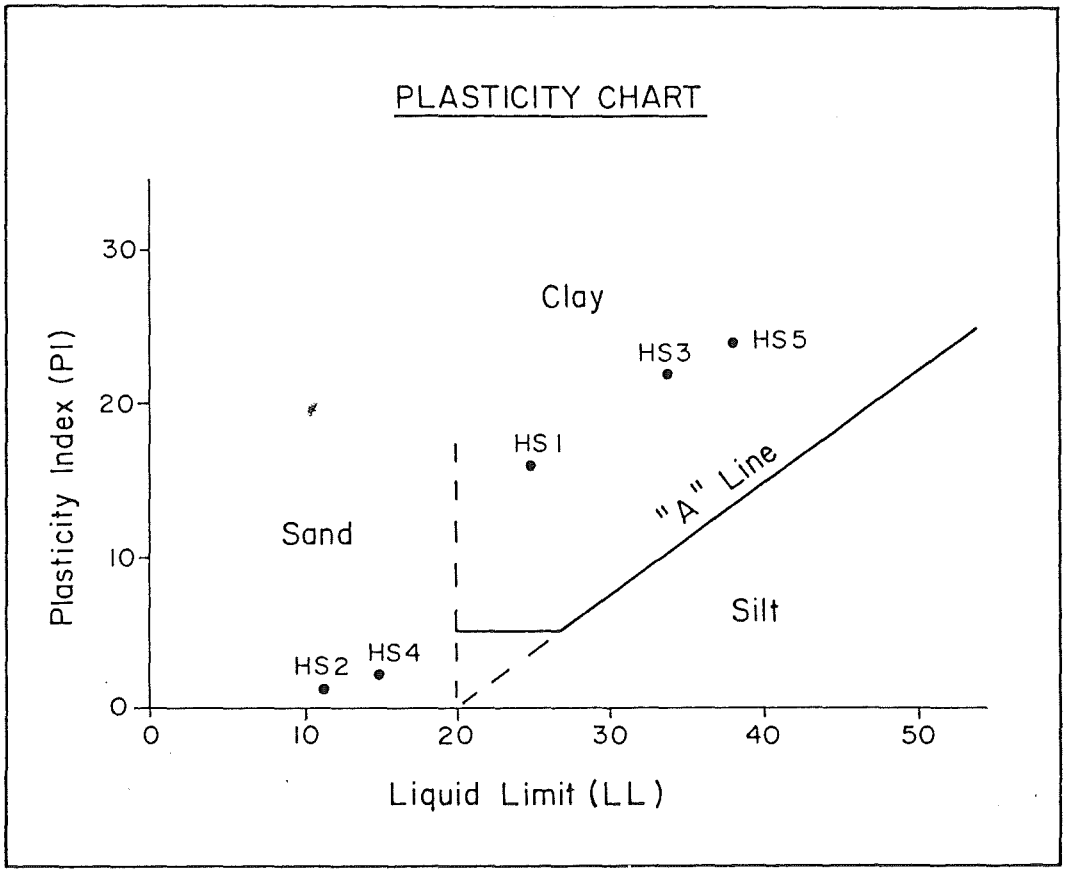

Fig. 5·9 Fault gouge and tectonic breccia matrix samples plotted on the Plasticity Chart, Havelock Creek

(iv) Clay Mineralogy

One sample each of the gouge and breccia matrix materials were tested by X-ray diffraction analysis to determine the clay mineralogy. Methods of the analysis and representative diffractograms are given in Appendix 5 and Table 5.3 lists d-spacings of peaks obtained and possible mineral assemblages present for both samples tested.

For both gouge and breccia materials a chlorite-illite-quartz assemblage is interpreted. The initial expectation was to obtain some amphibole as it was thought that the green colouring of the gouge and breccia materials may be due to the presence of these minerals derived from the amphibolites interbedded with the mylonite schist. However, amphiboles are heavy minerals and they would have settled out in the column before a sample was extracted. Chlorite is interpreted over the vermiculite-kaolinite combination since it is more likely to be present in a high grade rock such as garnet schist. This non-swelling clay mineral assemblage of chlorite-illite-quartz accounts for the low activity of the fine-grained materials.

5.4 SLOPE MOVEMENT PROCESSES

5.4.1 Objectives

Detailed engineering geological mapping identified five slope settings at the study site within which slope movement processes are operating, and the objective of this section is to describe these processes, their failure mechanisms, and the causes of failure, and to qualitatively assess the slope instability. The distribution of slope movement processes are illustrated on the 1:2500 engineering geology plan presented in Figure 4, map pocket.

5.4.2 Slopes in Intact Schist

The distribution of intact schist is restricted to the upstream end of the main (right) branch, as discussed in section 5.3.2 (i). Three types of slope activity are operating on these slopes:-

SAMPLE	PEAK d-SPACING[1]	MINERAL
HS 3 Fault Gouge	14.25	Chlorite or Vermiculite
	10.11	Illite
	7.11	Chlorite or Kaolinite
	5.01	Illite
	4.73	Chlorite
	4.26	Quartz
	3.50	Chlorite or Kaolinite
	3.35	Illite & Quartz
HS 2 Puggy Tectonic Breccia	14.25	Chlorite or Vermiculite
	10.11	Illite
	7.14	Chlorite or Kaolinite
	4.74	Chlorite
	3.55	Chlorite or Kaolinite
	3.34	Illite & trace of Quartz

[1] measured in Angstrom units

Table 5.3 d-spacings of peaks obtained from diffractograms and possible mineral combinations, Havelock Creek.

1. rock falls in eroding stream banks;
2. shallow debris slides in slope storage debris, and;
3. deep-seated rock slides.

Minor rock falls are occurring on oversteepened stream banks which have been undercut by stream erosion. Failure is mostly by rolling and bouncing downslope, with little free-fall, to form a debris accumulation deposit at the base of the slope.

Three shallow debris slide failures occur on 37-39^{o} slopes. These movements involve disruption of the regolith/colluvium surficial cover and are interpreted to involve sliding along the interface with underlying bedrock. Similar failures of this type have been recorded elsewhere in New Zealand as being initiated by high intensity rainstorms (Bell 1976; Rogers & Selby 1980) where shallow, unconsolidated slope debris overlies relatively impermeable bedrock. Water infiltration into unsaturated slope debris reduces the pore suction (negative pore pressures), or into saturated slope debris increases pore water pressure, which results in a decrease in the effective normal stress which may lead to failure (Brand 1981).

At locality HE 12 a more deep-seated movement is inferred to have taken place, producing a 1-2m high headscarp and displacing a single block of bedrock which has been degraded by post-failure gully erosion separating the displaced block from the headscarp, and making interpretation of the failure mechanism difficult. The nature of the failure surface is unknown as schistosity dips moderately to the northeast, not being favourable as a failure surface for a northwesterly facing slope.

5.4.3 Slopes in Crushed Schist

Crushed schist covers a substantial area of the south-eastern slopes in the study site and two types of failure are inferred to be operating:-

1. deep-seated rock block slide, and;
2. debris slide-avalanche.

(i) Rock Block Slide

A large slope movement feature was described at locality HE 6 (Section 5.3.4) and is interpreted as a deep-seated rock block slide which has been partially degraded by post-failure gully erosion (Fig. 5.1 & 5.10). Many of the original failure features have been obscured by this erosion, making reconstruction of the initial failure mechanism difficult, but a number of features still provide evidence for a deep-seated rock slide type movement.

The most obvious of these is a 10-30m high headscarp which extends along the top of the ridgeline for approximately 350m. On the western flank where extensive gully erosion has removed a substantial part of the upper displaced block, the base of the headscarp is marked by the tops of sharp ridges of debris which are remnants of a formerly more extensive slope before post-failure erosion (Fig. 5.11). A second major scarp approximately half way down the slope separates the entire displaced rock mass into two blocks. Within the displaced rock mass, "pinnacles" of crushed rock can be recognised with "sag" deposits in between (Fig. 5.12) and this indicates that the rock has been extended in a downslope direction, separating sections of the rock mass into "pinnacles" and loosening the rock mass along defects.

Sliding is inferred to have occurred by translational spreading downslope along schistosity which dips 10-12^{o}NW and daylights in the more steeply dipping slope face (37^{o}). However, adopting a residual friction angle of 24½ for schist (Ackroyd 1985), according to the Marklands test the line of sliding does not fall in the zone of instability indicating that failure is not kinematically possible (Fig. 5.13). A complex step-like failure surface is therefore interpreted, which would increase the dip of the surface of rupture to greater than the residual friction angle. Small steps formed by schistosity defects are connected by the numerous fractures which exist in the crushed rock mass, defining a failure surface with a dip steeper than schistosity but less than the slope angle. Cross section B-B', Figure 4 (map pocket) illustrates the geometry of the inferred failure surface.

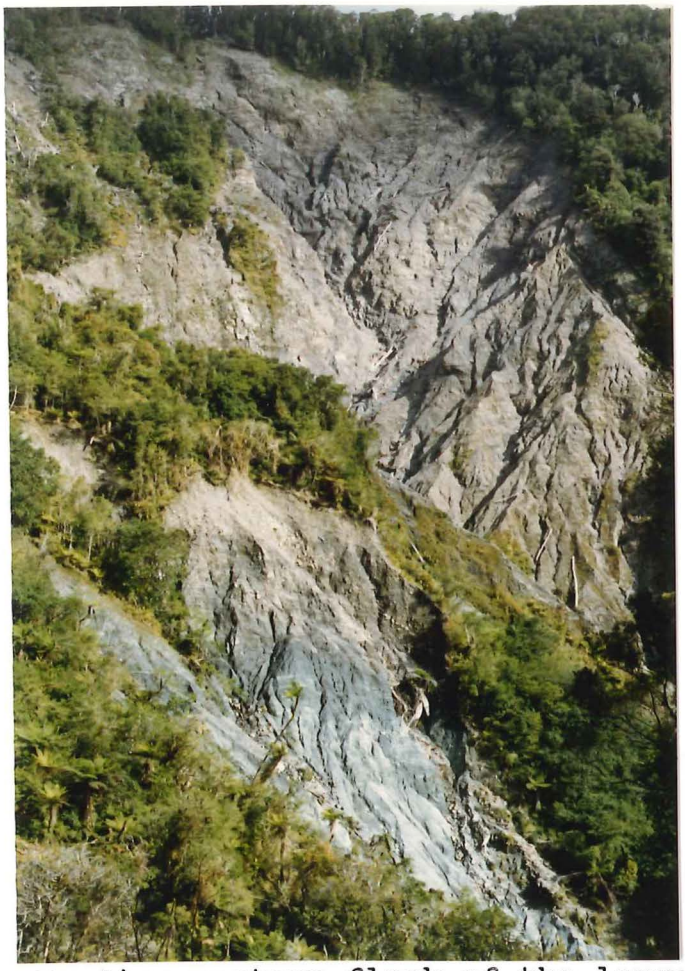

Fig. 5.10 Eroding western flank of the large rock slide at locality HE 6, and crushed mylonite schist at locality HE 7 (foreground).

Fig. 5.11 Approx. 20m high headscarp of rock slide at HE 6 with the base of the scarp marked by the tops of sharp ridges of debris, remnant of a formerly more extensive slope before post-failure erosion.

Fig. 5.12 Eroding western flank of large rock slide with "pinnacles" of crushed rock and sag deposits in between indicating extension and loosening of the rock mass along defects.

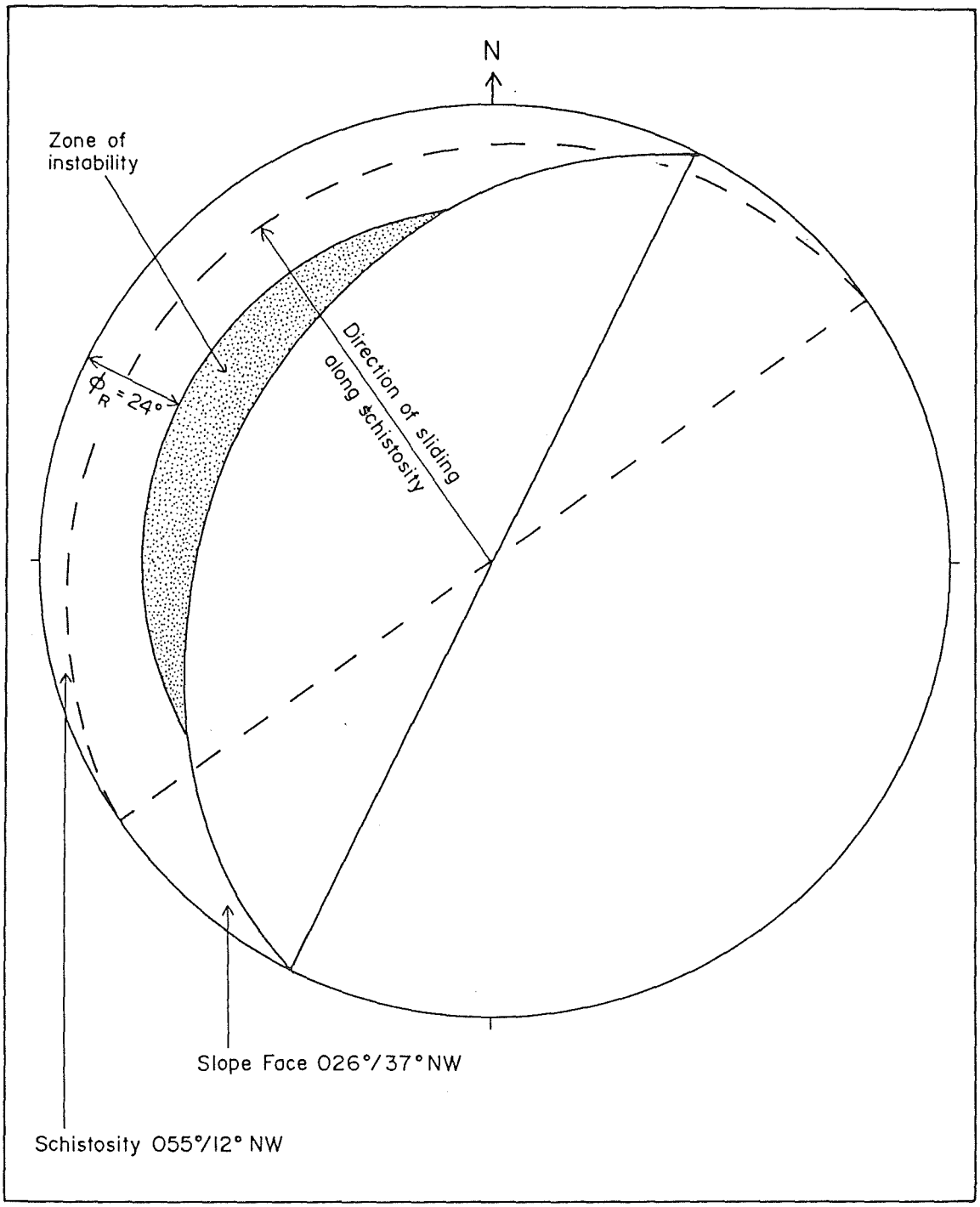

Fig. 5·13: Stereoplot of rock block slide at locality HE6, Havelock Creek

Limited evidence can be obtained from aerial photograph interpretation as to the history of movement. 1942 photography (Appendix 4 details aerial photograph coverage of Havelock Creek) clearly shows in outline the present area of the landslide scar with a headscarp which does not seem to be as fully developed as is currently. No major scarp is visible, the landslide being comprised of a single block, and limited erosion activity had taken place on the western flank. A lineament, extending southwestwards from the headscarp just below the top of the ridgeline almost to Havelock Creek (see Fig. 4, map pocket), can be identified below which is an area of depressed topography. 1965 photography shows the landslide scar to be fully vegetated, although the headscarp and lineament are still discernible. 1983 coverage shows the present day situation with the fully developed headscarp, the major scarp, and the eroding western flank.

It is inferred from this information that the present day active slope is a reactivation of a much larger, ancient slope movement which involved the entire hillslope, and that the lineament is a degraded, revegetated headscarp of this failure. The present failure seems to have reactivated at least twice, once pre-1942 to produce the fresh headscarp, and again during the period 1965-1983, to enlarge the headscarp and produce the major scarp which divided the displaced rock mass into two blocks. Figure 5.14 diagrammatically illustrates the evolution of this rock block slide.

A combination of factors is inferred to have initiated this large-scale, deep-seated movement. Likely fundamental causes are the steep, high slopes created by stream incision into weak fault zone materials increasing total shear stress conditions, and the crushed rock mass decreasing the total shear strength of the rock. The initial triggering event of the ancient movement may have been a large seismic event, with subsequent reactivations due to seismic shaking or large rainstorm events.

(ii) Debris Slide-Avalanches

Aerial photograph interpretation identified a series of sharp ridge and narrow gullies on the fully vegetated north-

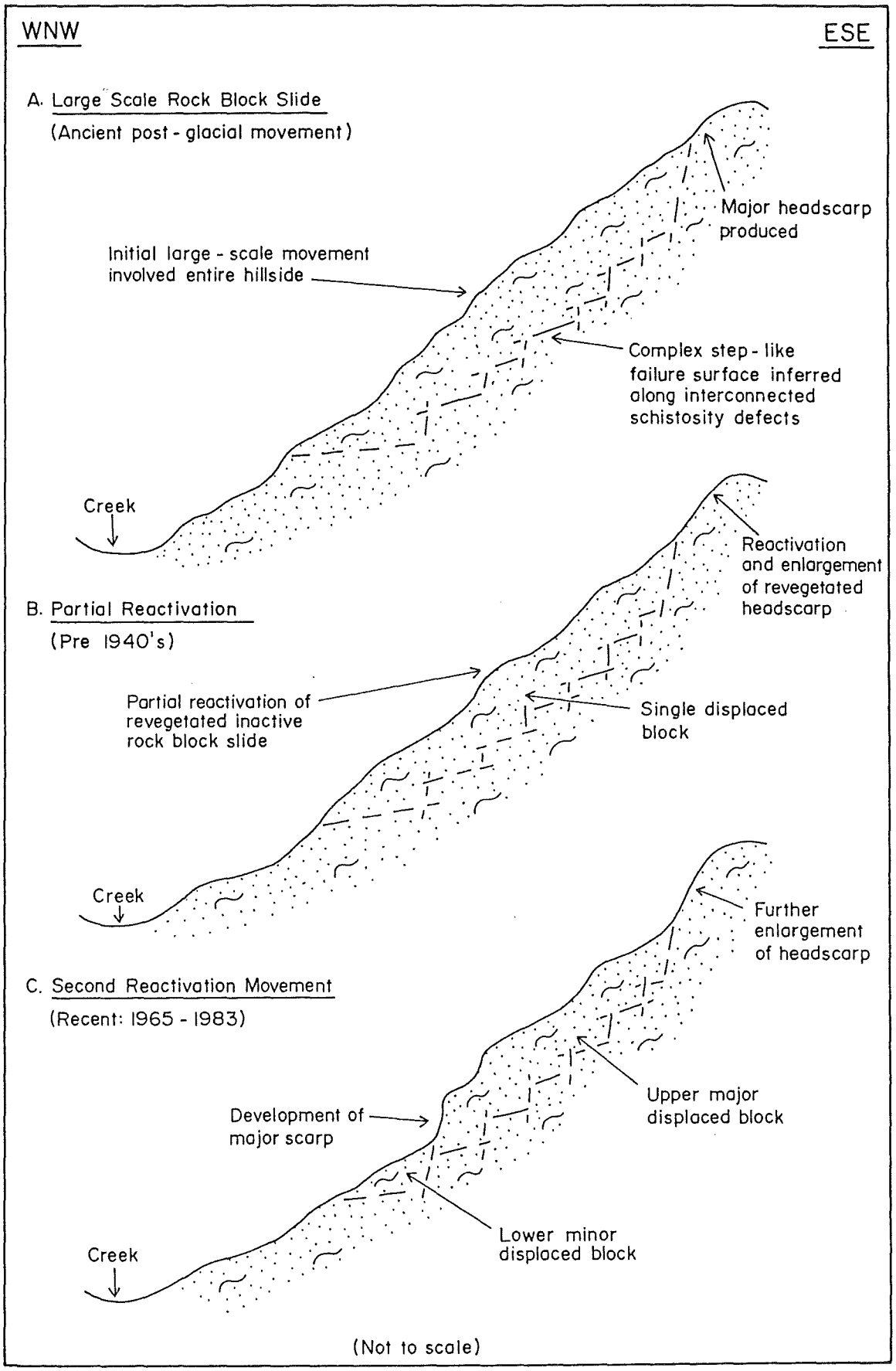

Fig. 5·14: Sketch diagram illustrating movement history of rock block slide in crushed normal schist at locality HE 6, Havelock Creek

west facing slope at locality HE 13. It is inferred from the "trail" nature of the surface morphology that this topography was produced by ancient debris slide-avalanche failures. These "trails" are clearly visible in the field at a distance through the heavy forest cover, although no indication as to their nature can be found on the ground beneath the forest canopy.

5.4.4 Slopes in Crushed Mylonite Schist

Crushed mylonite schist slopes undergo two basic types of slope activity:-

1. debris slide and debris falls in association with gully erosion on steep, high escarpment slopes, and;
2. deep-seated rock block slides.

(i) Debris Slide and Debris Falls

At locality HE 5 crushed mylonite schist forms a steep escarpment slope up to 100m high (Fig. 5.5). The crushed nature of the rock mass allows slope failure by debris slide and debris fall in a similar manner to failure in crushed hornfelsed sandstone at Boulder Creek (Section 4.4), but little or no debris accumulation has formed at the base of this slope due to its rapid removal by the stream. Similar slope activity is occurring in a gully in mylonite schist immediately upstream of HE 9, although at this locality stream erosion is the dominant type of slope activity followed by debris fall.

The crushed rock mass at both these localities is wet, emphasising the importance of water in contributing to the debris slide failures. Other factors contributing to failure are the due to the crushed rock mass which decreases the total shear strength, and due to the removal of lateral and underlying support by stream undercutting and past slope failures which increases total shear stress.

(ii) Rock Slide

At HE 9, the crushed mylonite schist slope has undergone a more deep-seated movement (compared with the debris slide failures) interpreted as a rock block slide. Two separate failures have occurred, both involving displacement of a

single block of bedrock producing two major headscarp features (8m and 35m high respectively). Cross section D-D', Figure 4 (map pocket) details the upstream slide, while Figure 5.15 illustrates the downstream slide.

The mechanism of failure is difficult to determine. Schistosity dips to the northeast which is unfavourable to promote failure in respect of the northwesterly aspect of the slope. Failure can probably be attributed to the presence of wet to saturated fault gouge material at the base of the slope forming a zone of weakness along which movement could propagate. Joining of this weak zone and the headscarp by the failure surface would then involve a complex series of interconnected defect surfaces through the crushed rock mass (Fig. 5.15).

5.4.5 Slopes in Tectonic Breccia & Fault Gouge

Failures in tectonic breccia and fault gouge materials are restricted to the following movement types:-

1. shallow debris slides in slope storage debris, and;
2. debris flow in saturated slope storage debris and underlying puggy breccia or gouge bedrock.

(i) Debris Slides

Shallow debris failures have occurred on slopes at HE 2 and HE 7. At HE 7 a complex gully system exposes a section through the fault zone from fault gouge to mylonite schist (Fig. 5.10). The upper mylonite schist slopes are undergoing stream erosion, while the lower slopes in puggy breccia and gouge are failing by shallow debris sliding of the vegetation mat and <1.0m thick regolith/colluvium cover. "Rafts" of vegetation separate from the gully side slopes and move downslope to the stream channel over wet to saturated puggy breccia and gouge (Fig. 5.4).

At locality HE 2 a 150m long scarp has developed in puggy tectonic breccia which has been dissected by post-failure gully erosion (Fig. 5.16). Initial failure was by shallow sliding of the debris cover along the interface with underlying bedrock, and once this protective cover had been removed the underlying weak fault zone materials were exposed

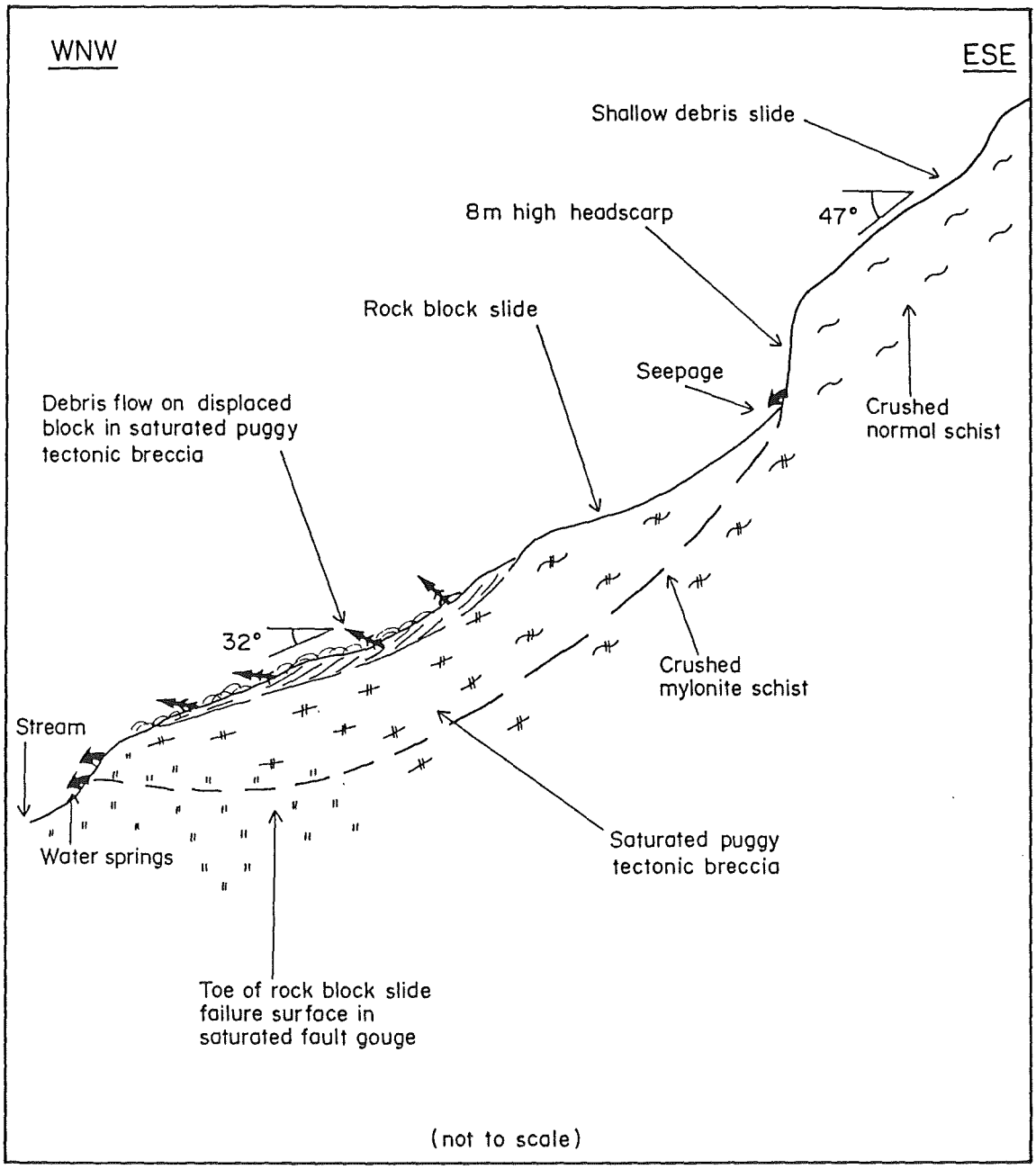

Fig. 5·15: Sketch diagram illustrating rock block slide in crushed mylonite schist and debris flow in puggy tectonic breccia at locality HE9, Havelock Creek

Fig. 5.16 150m long shallow debris slide failure scar in puggy tectonic breccia at locality HE 2 which has been dissected by post-failure gully erosion.

to erosion, destroying most of the original failure features. A number of sharp ridges produced by this erosion still carry the original regolith/colluvium cover (Fig. 5.17), being remnants of the initial failure surface, and the dips of these surfaces indicate a slope angle of 28° for the failure surface (Fig. 5.18). Failure of the back scarp by headward erosion is bringing fresh debris on to the scarp face (Fig. 5.18), and the initial failure mechanism is similar to the shallow debris slides over intact schist that were triggered by high intensity rainstorms.

(ii) Debris Flows

Minor debris flow failures are located at the upstream end of HE 2, on the displaced block at HE 9, and at HE 10. The failures at HE 2 and HE 9 both involve flow movement in saturated slope storage debris over saturated puggy tectonic breccia or fault gouge bedrock in gully depressions. Water originates both from the collection of surface run-off, and from groundwater sources which are in ample supply at both these slopes as indicated by the numerous groundwater and mineral springs.

A larger debris flow failure is occurring at HE 10 in an area of depressed topography as illustrated by cross-section D-D' in Figure 4 (map pocket). Failure involves movement of a block of highly disturbed vegetation which is partially surrounded by low angle (20°) scarps in puggy tectonic breccia bedrock. This displaced block seems to be undergoing creep movement creating tilted vegetation and broken ground beneath the forest cover.

5.4.6 Assessment Of Slope Instability

Analysis of a failure or calculation of the factor of safety for a particular slope requires that the shear strength of the failure surface (defined by C and ø) be known. No typical shear strength values for fault zone materials are available, and it is beyond the scope of this investigation to derive these values. Assessment of slope instability on Alpine Fault Zone slopes is therefore limited to evaluating slope angle data measured in the field for each slope setting identified.

Fig. 5.17 Remnant initial failure surface preserved on sharp ridge on dissected shallow debris slide failure scar at locality HE 2.

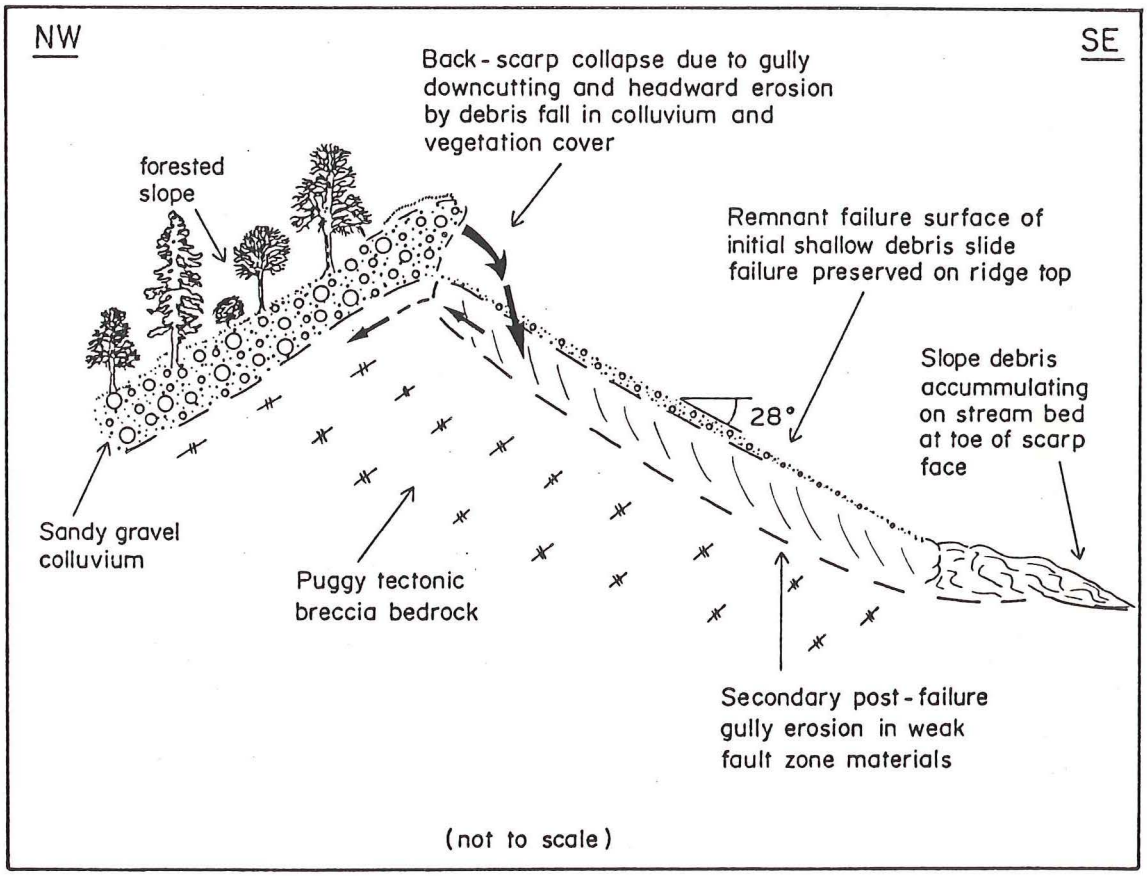

Fig. 5.18: Sketch diagram of shallow debris slide and secondary post-failure gully erosion at locality HE 2, Havelock Creek

Table 5.4 summarises slope angle data for the major slope movements at the study site. According to this data, puggy tectonic breccia and fault gouge slopes are the least stable, failing by shallow debris slide of the surficial regolith/colluvium cover at 28° and by debris flow at 20-32°. Crushed mylonite schist and crushed garnet schist fail at 36-40° by rock block slide and at 38-47° by debris slide and debris slide-avalanche, while intact schist slopes are susceptible to shallow debris slides at 36°. Maximum stable slope angles for these materials can be summarised as:-

1. Puggy tectonic breccia & fault gouge: 20°;
2. Crushed mylonite schist & crushed normal schist: 35°;
3. Intact schist: 35°.

5.5 SLOPE INSTABILITY ON ALPINE FAULT ZONE SLOPES

5.5.1 Objectives

Investigations at Havelock Creek identified a number of important factors which are contributing to the slope instability of Alpine Fault Zone slopes. The objectives of this section are to:-

1. summarise the causes of slope instability at Havelock Creek in a slope evolution model;
2. summarise observations made in terms of slope instability on Alpine Fault Zone slopes during reconnaissance investigations to extend the Havelock Creek discussions, and;
3. discuss the implications of this slope instability to future forest management of Alpine Fault Zone slopes.

5.5.2 Slope Evolution of Havelock Creek

The slope evolution model interpreted for the Havelock Creek tributary is summarised in Figure 5.19. The model summarises the series of processes and events which have occurred to form the present geomorphic and geologic setting at Havelock Creek, indicating processes which have produced fundamental causes of slope instability and illustrating how these fundamental causes and external triggering events contribute to slope failure.

LOCALITY	SLOPE SETTING	SLOPE MOVEMENT TYPE	SLOPE ANGLE
Above HE 12	Intact schist	Shallow debris slide	36-38°
HE 13	Crushed schist	Debris slide-avalanche	38°
HE 6	Crushed schist	Rock block slide	37°
HE 5	Crushed mylonite schist	Debris slide	42-47°
HE 9	Crushed mylonite schist	Rock block slide	40°
HE 2	Puggy tectonic breccia	Shallow debris slide	28°
HE 9	Puggy tectonic breccia	Debris flow	32°
HE 10	Puggy tectonic breccia	Debris flow	20°
HE 9	Fault gouge	Debris flow	30°

Table 5.4 Summary of slope angle data for major slope movements in Havelock Creek.

Slope instability is attributed to two main factors:-

1. A reduction in total shear strength due to the crushed nature of the rock mass caused by tectonic deformation within the Alpine Fault Zone.
2. An increase in total shear stress by removal of lateral and underlying support as a result of deep stream incision into weak fault zone materials, the rate of which is in turn controlled by local base level changes induced by tectonic uplift.

Two types of triggering mechanisms are inferred to have initiated slope failure:-

1) Seismic events causes ground shaking, producing transitory earth stress which increases the total shear stress;
2) High intensity rainstorm events increases water infiltration which causes a reduction in pore suction (negative pore pressure) in unsaturated material, or an increase in positive pore pressures in saturated material, resulting in a decrease in the effective normal stress.

5.5.3 Slope Movements on Alpine Fault Zone Slopes

Alpine Fault Zone slopes can be divided into two geomorphic settings and slope instability on this landform type is discussed according to these two settings:-

1. catchment slopes of streams which cross or flow along the fault zone, and;
2. fault-bounded mountain front slopes.

(i) Catchment Slopes

Almost all the slope failures are located in the first type of geomorphic setting, for which Havelock Creek is an example. In most of these streams, exposure of fault zone materials is restricted to mylonite schist and crushed schist, with tectonic breccia and fault gouge materials on the northwestern edge of the fault zone commonly being buried by postglacial alluvial gravels. Consequently, the dominant type of slope movement on these stream catchment slopes is debris slide-avalanche in crushed mylonite schist and crushed schist

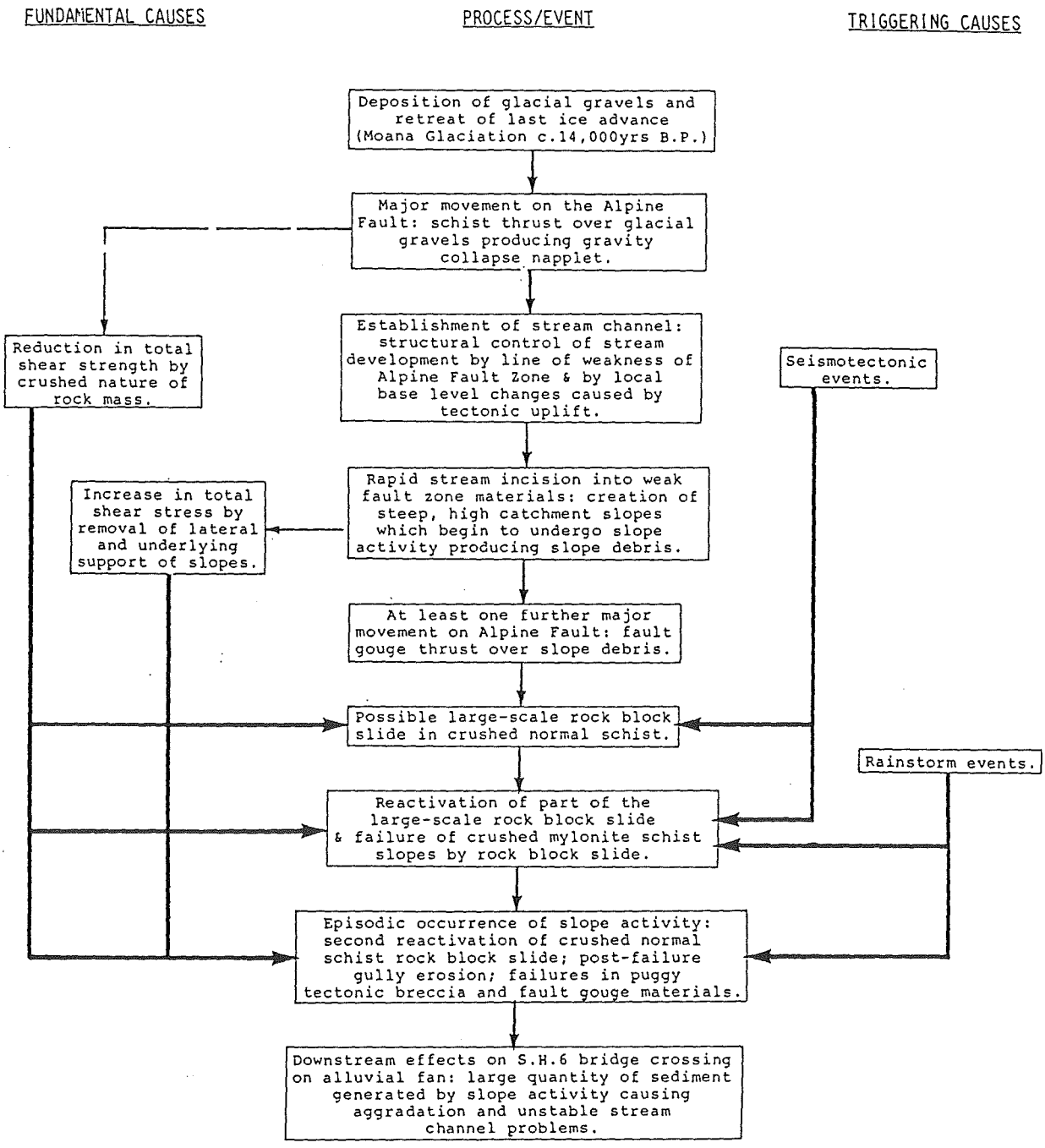

Fig. 5.19 Slope Evolution Model for Havelock Creek Tributary.

bedrock. No deep-seated failures such as the rock block slides in Havelock Creek were seen to occur anywhere else on Alpine Fault Zone slopes.

The debris slide-avalanche failures occur on both riparian slopes (up to approximately 70m above stream level) with the toe of the slide scar at stream level (Fig. 5.20), and on mid-slope positions where slide materials form debris torrents down to stream level (Fig. 5.21). Slope angles for these failures vary from 32 to over 45°, averaging around 38°. Failure commonly occurs in pre-existing gully depressions where water has accumulated, and sliding of the gully head wall region quickly degenerates into an avalanche-type movement due to the high water content of the slide debris and the steep, high slopes. Due to the high regional rainfall, secondary gully erosion rapidly degrades the failure scar, deepening and extending the scar surface.

Where puggy tectonic breccia and fault gouge bedrock do form slope materials, as in Havelock Creek, these are prone to shallow debris slide and debris flow failure. Riparian puggy tectonic breccia slopes fail by shallow debris slide of the regolith/colluvium cover along the interface with underlying bedrock, exposing the weak fault zone material to post-failure gully erosion. In gully depressions, saturated puggy tectonic breccia and fault gouge bedrock may form debris flow failures (Fig. 5.22).

A particularly large failure scarp has developed within the crush zone of the Alpine Fault at Robinson Creek (Fig. 5.23), a tributary of the Waita River on the northwestern slopes of the Mataketake Range, where the cattle track crosses the stream (S87/993168). This locality is known as Slippery Face, named by trackmen in the early 1900's who had difficulty in maintaining this section of the track due to the unstable nature of the slopes. The scarp, exposing fault gouge thrust over alluvial gravels, is 60-80m high and approximately 350m long, extending from the fault gouge zone through to crushed schist. This feature is an exceptional example of debris slide-avalanche type failure which are inferred to be the result of a combination of movements within the crush zone.

Fig. 5.20 Debris slide-avalanche in crushed mylonite schist in the Alpine Fault Zone at Bullock Creek (person at top of slide scar for scale).

Fig. 5.21 Debris torrent on approx. 120m high slope at Saltwater Creek in the Alpine Fault Zone.

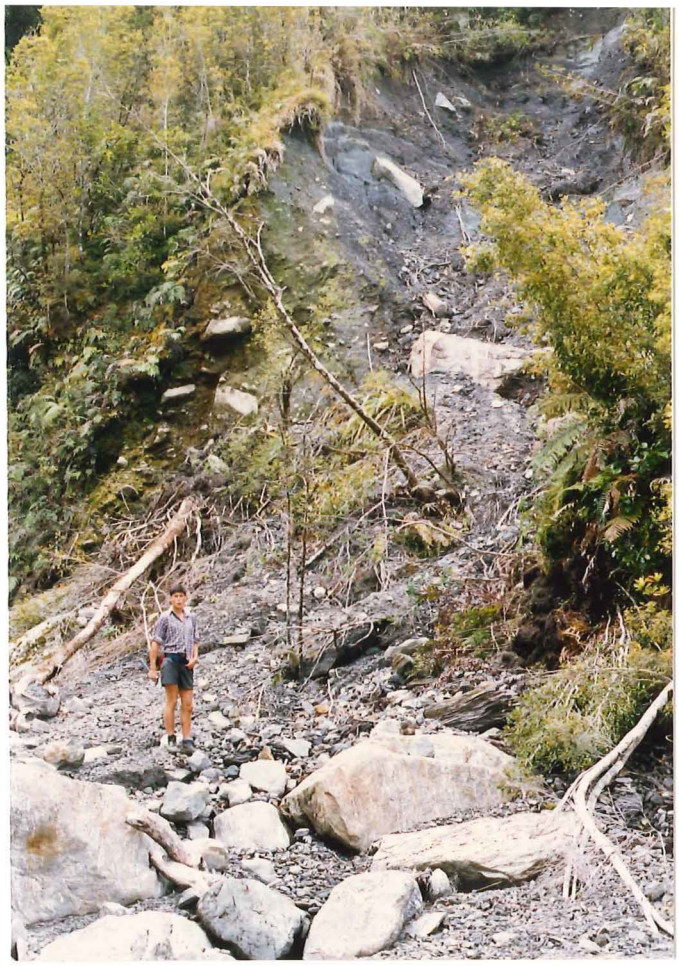

Fig. 5.22 Debris slide-flow in puggy tectonic breccia at Saltwater Creek.

Fig. 5.23 Slope failure scarp (approx. 350m long) in the Alpine Fault Zone at Slippery Face, Robinson Creek. Oblique view looking south-southwest.

Intact schist and alluvial fan gravel slopes immediately upstream and downstream respectively are stable on the same 35° slope.

(ii) Fault-bounded Mountain Front Slopes

Few failures occur on the fault-bounded mountain front slopes because extensive alluvial fans have formed at the base of these slopes covering and protecting the weak fault zone materials from slope activity. However, a recent extensive failure has occurred on mountain front slopes at an unnamed creek northwest of Flagstaff Creek near the Mahitahi River (Fig. 5.24) (S78/345405). Failure occurred during a high intensity rainstorm sometime in 1978 (J. Condon pers. comm.), producing a failure scarp approximately 150-200m high on a 34° slope in crushed mylonite schist and crushed garnet schist bedrock. Movement was by debris slide-avalanche, producing a substantial debris torrent which narrowly missed a farmers house. Fundamental causes of this failure were the steep, high slopes along the active fault scarp and the crushed fault zone bedrock mass due to tectonic deformation, while the triggering mechanism was the high intensity rainstorm event.

5.5.4 Implications for Forest Management

The scope of evaluating slope movements on forest lands at the resource allocation level is limited to providing an overview of slope movement potential adequate for development planning. Slope movement potential on Alpine Fault Zone slopes is evaluated by assessing slope angle data of slope failures measured in the field to find the steepest slope that could be logged without causing failure.

As described in Section 5.5.3 (i), debris slide-avalanche in crushed mylonite schist and crushed normal schist is the most dominant failure type on Alpine Fault Zone slopes. This failure mechanism was found by Swanston & Swanson (1976) to be highly susceptible to forest management activities (see section 4.6.4), and is therefore regarded as being the most probable response of slopes to timber harvesting activities on Alpine Fault Zone slopes.

Fig. 5.24 Debris slide-avalanche on fault-bounded mountain front slope in crushed mylonite schist and crushed garnet schist which failed in 1978 producing a debris torrent narrowly missing farm buildings (arrowed). Oblique view looking south-southeast. (N.Z. Geological Survey photo CN 5914a, photographer: D.L. Homer)

Debris slide-avalanche movements occur on 36-38° slopes at Havelock Creek (Table 5.4) and on 32 to over 45° slopes (averaging around 38°) in other streams within the Alpine Fault Zone, while the recent failure near Flagstaff Creek occurred on a 34° slope. It can be concluded from this data that slopes generally over 32° in crushed mylonite schist and crushed normal schist are susceptible to debris slide-avalanche failure.

Slopes in puggy tectonic breccia and fault gouge fail dominantly by shallow debris slide and debris flow movements. Data from Havelock Creek (Table 5.4) suggests that slopes composed of these materials over 20° are susceptible to these types of failures.

Based on the above information, Alpine Fault Zone slopes over 32° (or in the case of puggy tectonic breccia and fault gouge slopes over 20°) are susceptible to slope movement and should be managed accordingly. Due to tectonic uplift and stream incision into weak fault zone materials, most of these slopes are over this value, therefore it is recommended that the Alpine Fault Zone slopes are not suitable for large-scale (clearfelling, selective logging, and associated road development) timber harvesting activities.

5.6 SYNTHESIS

Engineering geology investigations at Havelock Creek identified five major slope settings within which specific slope movement mechanisms are operating. These can be grouped as follows:-

1. Intact schist slopes
   a) Shallow debris slide;
   b) Rock slide;
   c) Rock fall;
2. Crushed garnet schist & crushed mylonite schist slopes
   a) Rock block slide;
   b) Debris slide-avalanche;
   c) Debris fall;

3. Tectonic breccia & fault gouge slopes
   a) Shallow debris slide;
   b) Debris flow.

Factors contributing to slope failure can be separated into fundamental causes and triggering mechanisms:-

1. Fundamental causes
   a) A reduction in total shear strength due to the crushed nature of the rock mass caused by tectonic deformation within the Alpine Fault Zone;
   b) An increase in total shear stress by removal of lateral and underlying support as a result of deep stream incision into weak fault zone materials, the rate of which is in turn controlled by local base level changes induced by tectonic uplift;
2. Triggering mechanisms
   a) Seismic events causes ground shaking, producing transitory earth stress which increases the total shear stress;
   b) High intensity rainstorm events increases water infiltration which causes a reduction in pore suction (negative pore pressure) in unsaturated material, or an increase in positive pore pressures in saturated material, resulting in a decrease in the effective normal stress.

Implications of slope instability on forest lands for forest management of Alpine Fault Zone slopes has been evaluated by assessing slope angle data for natural failures measured in the field to find the steepest slope that could be logged without causing failure. Debris slide-avalanche in crushed mylonite schist and crushed normal schist is regarded as the most probable response of slopes to timber harvesting activities (including roading), and this type of failure may occur in this slope setting on slopes greater than 32^{o}. Since nearly all slopes in the Alpine Fault Zone are greater than 32^{o}, it is recommended that this landform unit is not suitable for large-scale timber harvesting activities.

CHAPTER SIX

CRETACEOUS-TERTIARY HILL COUNTRY: GRAVE CREEK

6.1 OUTLINE OF APPROACH

Grave Creek was selected as the main investigation site for slope instability assessment on Cretaceous-Tertiary Hill Country based on preliminary reconnaissance fieldwork which identified Grave Creek as having a geomorphic and geologic setting typical of this landform type. A serious slope instability problem (the Grave Earthflow) affects State Highway 6 and this is directly relevant to forest management activities in this terrain unit.

Engineering geology investigations at Grave Creek are reported under three main headings:-

1. Grave Creek site geology and geomorphology, which describes the geologic and geomorphic setting as background to more detailed studies of the Grave Earthflow;
2. Earthflow description, which discusses engineering geological mapping, subsurface investigation, and laboratory studies of the Grave Earthflow;
3. Earthflow stability and remedial options, in which are included discussion of surface movement monitoring investigations, stability assessment, and possible remedial options for the earthflow.

Following the main discussion of the Grave Creek investigations, slope instability on Cretaceous-Tertiary Hill Country in general is summarised. Aspects discussed include the geomorphic evolution of Grave Creek, slope movements elsewhere on the landform unit, and possible implications these may have for future management of forestry activities in this type of terrain.

6.2 SITE GEOLOGY & GEOMORPHOLOGY

6.2.1 Location and Objectives

Grave Creek drains coastal hill country between the Whakapohai and Waita Rivers, flowing north-northwest to cross State Highway 6 approximately 28km north of Haast, and then flowing into the Tasman Sea between Knight and Arnott Points (S77/989304). The study site is centred around State Highway 6, with the Grave Earthflow located on the western side of Grave Creek immediately above the road.

The objectives of this section are to describe the bedrock and surficial geology at Grave Creek, and to discuss the geomorphology of the site with respect to slope morphology and slope processes. This provides a background for more detailed investigations and is necessary to understand the development of the Grave Earthflow. Figure 5 (map pocket) summarises engineering geology data for the Grave Creek area, incorporating:-

1. a 1:2000 engineering geology plan and cross section;
2. a 1:3000 geological map and cross section, and;
3. engineering geological descriptions of bedrock and surficial materials.

6.2.2 Bedrock Geology

Five bedrock mapping units have been recognised at Grave Creek, the distribution of these being shown on the 1:3000 geological map together with brief engineering geological descriptions (Fig. 5, map pocket). Table 6.1 gives a stratigraphic summary of these units and more detailed engineering geological descriptions.

The main structural features at Grave Creek are the two northeast-striking faults which bound the lower member of the Otumotu Formation (see geological map in Fig. 5, map pocket). The nature of these faults is uncertain, but based on stratigraphic evidence they are interpreted as steeply dipping normal faults. The more inland fault is interpreted as uplifting basement Greenland Group, and is correlated with Nathan's (1977) Arnott Fault (Fig. 6.1). The Greenland Group rocks are highly sheared and crushed, this condition extending

MAP UNIT	ENGINEERING GEOLOGICAL DESCRIPTION
ARNOTT BASALT (late Haumarian or early Teurain)	Slightly weathered, strong to very strong, dark bluish brown, coarsely interlayered BASALT and VOLCANIC BRECCIA. Unit overlies highly weathered, very weak, yellowish brown, massive, basaltic TUFF. Tuff is dry with occasional small to medium gravel-sized clasts of slightly weathered basalt. Tuff forms a 5-20m band at base of Arnott Basalt.
WHAKAPOHAI SANDSTONE (Haumarian)	Slightly to moderately weathered, strong to very strong, light yellowish brown and dark reddish brown, coarsely bedded, quartzo lithic glauconitic medium and fine SAND-STONE. Unit is burrowed abd bioturbated.
TAUPERIKAKA FORMATION (Haumarian)	Highly weathered, moderately weak, light yellowish brown, coarsely bedded, quartzo lithic glauconitic medium and fine SANDSTONE interbedded with grey carbonaceous MUDSTONE.
Upper Member OTUMOTU FORMATION (Piripauan)	Moderately weathered, moderately strong, light brown, coarsely bedded, medium and fine SANDSTONE and grey MUDSTONE with occa-sional cobble-pebble CONGLOMERATE lenses, coaly layers and plant fragments.
Lower Member	Unweathered to slightly weathered, strong to very strong, bluish grey, massive, rounded lithic cobble CONGLOMERATE with a grey sand-stone matrix. Occasional angular to sub-rounded lithic cobble-pebble conglomerate, pebbly sandstones, and carbonaceous mudstone layers.
GREENLAND GROUP (Ordovician)	Moderately weathered, strong to very strong, light greenish grey or weathered light red-dish brown, interbedded crystalline sili-ceous SANDSTONE and MUDSTONE. Unit is locally highly sheared and crushed due to intense faulting.

Table 6.1 Stratigraphic summary and engineering geological descriptions of bedrock units at Grave Creek.

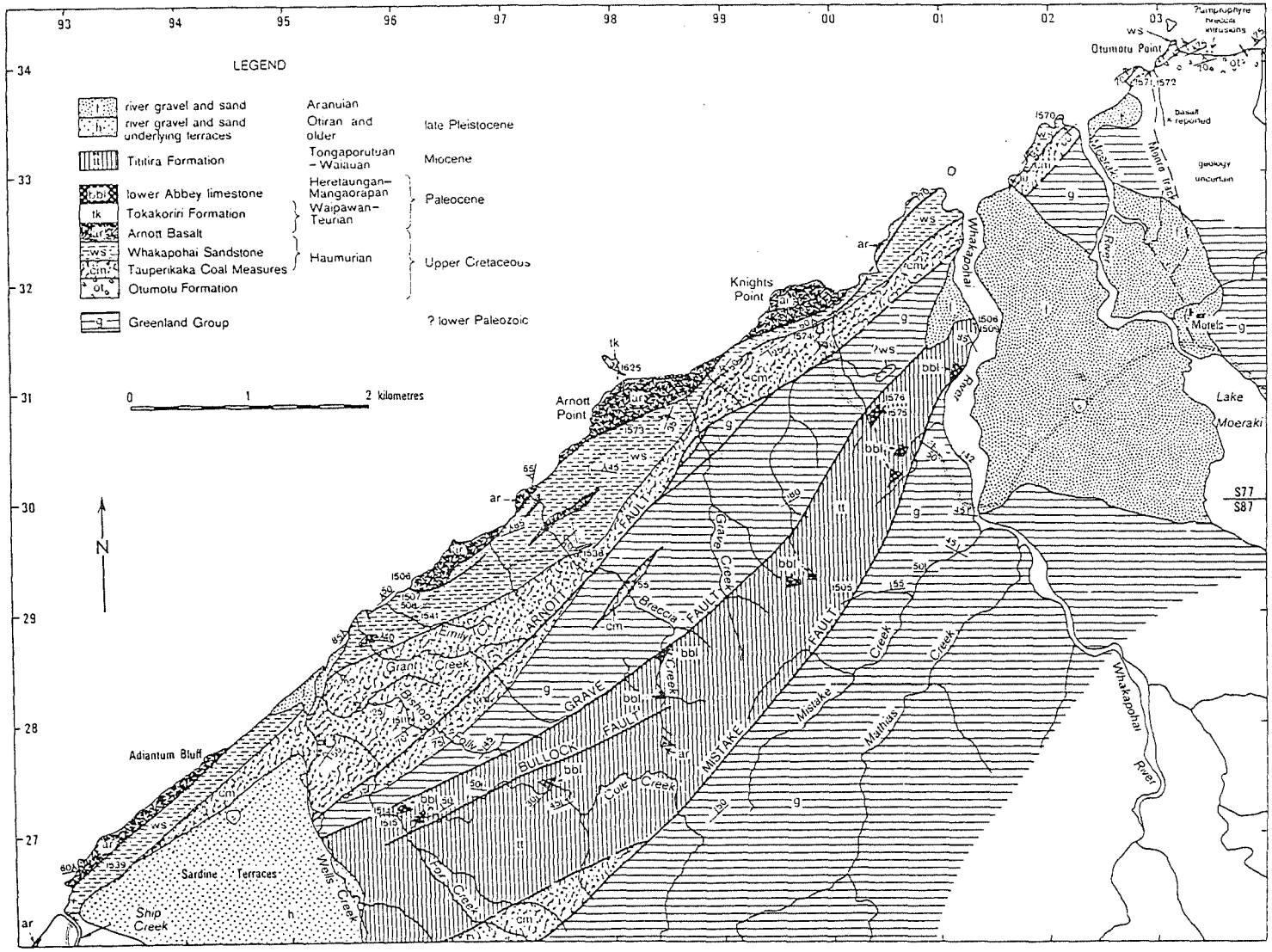

Fig. 6.1 Geological map of the coastal area between Ship Creek and Otumotu Point (from Nathan 1977).

for at least 500m upstream from the Grave Creek culvert crossing and indicating intense faulting throughout this block of basement rock. Following Nathan (1977) the second fault is interpreted as a splinter from the Arnott Fault, uplifting a sliver of lower Otumotu rock which is highly sheared, producing a grey muddy gouge material.

Northwest of this fault outcrops a sequence of rocks that extend from the upper member of the Otumotu Formation through to the Arnott Basalt, which has been folded and overturned. In the northern part of the 1:3000 map (Fig. 5, map pocket), weathered sandstone and mudstone with coaly layers and plant fragments of the upper Otumotu Formation have been mapped against the splinter fault along State Highway 6 as overturned and dipping to the southeast. Downslope in Grave Creek, no upper Otumotu Formation is seen, with Tauperikaka Coal Measures mapped against the splinter fault right way up, dipping steeply to the northwest. This structure is interpreted as an inclined fold with the upper limb overturned, and as such, the disconformable contact between upper Otumotu Formation and Tauperikaka Coal Measures is inferred to terminate against the splinter fault, as shown on the 1:3000 geological map and cross section (Fig. 5, map pocket).

6.2.3 Surficial Deposits

Two surficial deposit units are identified on the 1:2000 engineering geology plan (Fig. 5, map pocket):-

1. Raised beach deposits;
2. Coal measures/sandstone derived colluvium.

Raised beach deposits consist of loose to compact, weathered reddish brown interbedded fine gravel, coarse sand, and medium-fine sand. They underlie flat to gently inclined ($<10^{o}$ NW) terrace surfaces at an altitude of approximately 140m above sea level, and are correlated with the Knights Point interglacial terrace of pre-Terangian age (Nathan 1975)

On the southwestern side of Grave Creek a highly weath ered, loose, light greyish white and yellowish brown, massive quartzose coarse to fine sand deposit is found in association with the terrace surface. Figure 6.2 illustrates this expo-

Fig. 6.2 Sandstone colluvium overlying raised beach deposits exposed in failed road batter at the southern approach to Grave Creek along S.H. 6.

sure and shows the weathered sand deposit overlying raised beach deposits. This is interpreted as a slope movement deposit (colluvium) derived from failure of an ancient sea cliff formed in Tauperikaka Coal Measures and/or Whakapohai Sandstone during the pre-Terangian interglacial. Nathan (1975) recognised a similar deposit, described as a muddy breccia overlying the Knights Point terrace, exposed sporadically along State Highway 6 south of Knights Point. Nathan also interpreted this deposit as slump and landslide material derived from steep cliffs behind an interglacial marine cut platform.

6.2.4 Geomorphology

(i) Slope Morphology

The 1:2000 engineering geology plan (Fig. 5, map pocket) illustrates the slope morphology of the Grave Creek site. The Grave Creek gully forms the basic morphological feature, draining steep coastal slopes with deeply incised first order tributary streams which dissect the second order stream gully slopes. Hillslopes are high and steep, ranging up to 310m above sea level at the study site and averaging around 30^{o}. The Arnott Basalt, which outcrops along the coast, has formed a 30-90m high seacliff over which Grave Creek and other streams fall to beach level. The slopes are heavily vegetated with riparian lands covered by Kahikatea/Kamahi Forest and the remaining slopes covered with Rimu/Kahikatea-Phyllocladus Forest with occasional stands of Rata/Silver Beech Forest on the tops of high ridges (J. Pfaflert, NZFS, pers. comm.). This geomorphic setting has been interrupted by State Highway 6, which contours around coastal slopes between the Whakapohai River and Ship Creek producing made ground, spoil tips, and cut batter slopes.

(ii) Slope Movement

The 1:2000 engineering geology plan is divided into three slope areas which relate to the present slope activity:-

1. a recent slope movement area;
2. a stabilised, revegetated slope movement area, and;
3. a forested undifferentiated slope area.

The stabilised, revegetated slope movement area indicates slopes that were active during and immediately after construction of State Highway 6 in 1963-65 and which have subsequently stabilised and become revegetated. Figure 6.3 illustrates the unstable state of slopes east of Grave Creek in highly sheared Greenland Group bedrock immediately above the Grave Creek culvert during the construction period, which are now revegetated. Initial failure by debris sliding moved approximately 6800m^3 of material downslope into the culvert excavation (P. Hardie, MWD Haast, pers. comm.).

Major slope movements are continuing on both sides of Grave Creek and have been identified as multiple rotational slides in lower Otumotu bedrock which is bounded by the Arnott Fault and the splinter fault. Both these movements were initiated by construction of State Highway 6, with the northwestern bank failure providing greater problems during construction (P. Hardie, MWD Haast, pers. comm.). This failure has subsequently become less active and the southwestern bank failure (the Grave Earthflow) is presently undergoing a period of increased activity, causing slide debris to move onto the road pavement surface during rainstorm events. The surface of rupture of both these failures is inferred to be in grey mud material derived from highly sheared lower Otumotu bedrock (see 1:200 engineering geology cross section, Fig. 5, back pocket). Other slope movements in the study site are confined to shallow debris slides over lower Otumotu Formation, Greenland Group, and Arnott Basalt bedrock.

6.3 EARTHFLOW DESCRIPTION

6.3.1 Objectives

This section reports engineering geological mapping, subsurface, and laboratory investigations carried out on the Grave Earthflow, with the principal objective being to describe the earthflow in terms of its:-

1. history of movement;
2. bedrock and surficial geology (including subsurface and geotechnical information), and ;
3. surface morphology.

Fig. 6.3 Debris slide in sheared Greenland Group bedrock on eastern slopes above the Grave Creek culvert during construction of S.H.6 in 1963-1965 (from Young 1968).

The distribution of bedrock and surficial materials as well as surface morphological features were mapped at a scale of 1:250, and this is presented in Figure 6 (map pocket) along with summary excavation logs of shallow surface trenching carried out to determine the subsurface geology. Discussion of these investigations is followed by description of laboratory tests which were carried out to allow a preliminary assessment of the geotechnical characteristics of surficial materials.

6.3.2 History of Movement

The Grave Earthflow is a very recent feature which was triggered by construction of State Highway 6 in 1963-1965 (P. Hardie, MWD Haast, pers. comm.). This is confirmed by aerial photograph evidence, 1949 photography (Appendix 4 details aerial photograph coverage of Grave Creek) showing no sign of the earthflow complex. However, this low level 1949 photography (scale approximately 1:16 000) showed a series of raised features on a broad spur which leads down from the main ridgeline above the present position of the earthflow. These features may possibly be degraded, revegetated scarps of displaced blocks of bedrock, indicating possible ancient movement of this section of the hillside, and in fact this interpretation is confirmed by field observations, as discussed in Section 6.3.4(ii).

Since 1965, the Grave Earthflow has developed from essentially a rotational slide movement into a complex rotational slide-earthflow. Initial slide movement was along the main headscarp which has since remained inactive, with current activity now taking place on the southeastern side of the earthflow complex. This active area has apparently become increasingly unstable providing maintenance problems with State Highway 6 until December 1984 when the road batter was recut and benched to produce a catchment area for debris between the road and earthflow. Figure 6.4 shows the earthflow before December 1984, and Figure 6.5 one month after, illustrating the changes made by the Ministry of Works and Development which had a significant effect on movement rates as discussed in Section 6.4.3. The present situation is that

Fig. 6.4 Grave Earthflow in August 1984 before the road batter at the toe of the earthflow was cut and benched.

A

B

Fig. 6.5 Grave Earthflow in January 1985, one month after the road batter was cut and benched; the batter face was already beginning to degrade by minor sliding of debris onto the bench. Note the wet (darkened) zone immediately above the yellowish brown slide deposit-grey mud boundary.

this catchment area has now been infilled with slide debris, and the Grave Earthflow is once again edging on to the road pavement surface (Fig. 6.6).

6.3.3 Earthflow Materials

Within the Grave Earthflow complex, lower Otumotu Formation and Tauperikaka Coal Measures bedrock materials are exposed. Lower Otumotu bedrock, a grey, massive cobble conglomerate, outcrops in major lateral scarps either side of the cut road batter at the toe of the earthflow. It is also seen on the northwestern (true left) side of the earthflow exposed between a tension crack and minor scarp which makes up the northwestern lateral shear zone of the current active system (Fig. 6, map pocket).

Tauperikaka Coal Measures forms the major bedrock lithology within the earthflow from which the large rotated blocks are derived. This lithology is not in-situ within the fault-bounded sliver of uplifted lower Otumotu Formation bedrock. It is inferred that the Tauperikaka Coal Measures bedrock originates from west of the splinter fault which swings south above the earthflow, terminating against the Arnott Fault bringing coal measures against Greenland Group basement. Ancient slope movements have transported coal measures bedrock downslope and over sheared lower Otumotu Formation bedrock.

Two engineering soil deposits, associated with the earthflow, are derived from the two bedrock lithologies described above. An unweathered grey mud outcrops in the cut road batter at the toe of the earthflow and has been derived from shearing within lower Otumotu bedrock (Fig. 6.7): it is interpreted that this forms the zone within which basal sliding is taking place, thereby defining the surface of rupture. It is not known whether this grey mud is solely derived from fault pug material or also incorporates sheared material derived from slide movement of coal measures sandstone over lower Otumotu bedrock.

A

B

Fig. 6.6 Grave Earthflow in February 1986, 14 months after the road batter was cut and benched; the catchment area has infilled with debris and the toe of the flow is edging on to the road pavement surface. Note also the increase in bare ground since January 1985.

Fig. 6.7 Saturated grey mud in the east lateral shear zone, derived from intense shearing in lower Otumotu Formation bedrock.

The second engineering soil deposit is described as a highly weathered, light yellowish brown sand and is derived from the disintegration of the Tauperikaka Coal Measures ancient slide deposit within the earthflow. This material forms the majority of surficial material exposed in the earthflow, the distribution of which is shown on the 1:250 plan (Fig. 6, map pocket). Detailed engineering geological descriptions of both soil materials are given in Section 6.3.4 (subsurface investigations), and their geotechnical characterisation is described in Section 6.3.5 (laboratory investigations).

6.3.4 Slope Morphology

(i) Topographic Surveys

Surface morphology features of the Grave Earthflow were surveyed and mapped in March 1985 using a Wild Citation CI-450 EDM and T16 theodolite, and again in February 1986 using a Nikon NTD-3 uniaxial theodolite-distancemeter (Appendix 8 details survey methods and instruments used). A topographic base plan at a scale of 1:250 was prepared from these two surveys using a 2.5m contour interval, and this plan was used for detailed mapping of individual slope movement features during February 1986. The following descriptions correspond to the condition of the earthflow at that time.

(ii) Slope Morphology Features

The headscarp of the Grave Earthflow is located 80-135m above State Highway 6 on a 27^{o} northwest-facing slope, and forms a distorted square shape in plan view. The hillside on which the earthflow is located can be divided into the following three areas, which are discussed separately below:-

(a) Hillslope above the main headscarp, extending up to the ridgeline;

(b) Original failure active during road construction 1963-1965, which is outlined by the main headscarp system and has a total area of approximately 10 200m^2 (1.02ha);

(c) Currently active portion on the eastern flank outlined by a major scarp, with a total area approximately 5,200m^2 (0.52ha).

(a) Hillslope above main headscarp

A walk-over survey of the hillslope above the main headscarp up to the ridgeline identified a number of possible degraded revegetated scarps previously interpreted from 1949 aerial photography (see Section 6.3.2). These were mapped by tape and compass methods and are shown in Figure 6.8, a sketch map of the surface morphology of the Grave Earthflow hillslope.

The main headscarp is constrained for most of its length by an angular convex break of slope immediately behind it, except for the most uphill point where a narrow stretch of slope extends up to the ridgeline. On this narrow hillslope, a series of four degraded scarps were recognised which are semicircular in outline and surround areas of depressed ground, suggesting a rotational slide type of movement. The degraded, revegetated nature of these features suggest that they are ancient, inactive slope movements.

(b) Headscarp Area

This includes the area between the main headscarp and the currently active portion of the earthflow, as illustrated in Figure 6.8. The main headscarp ranges from 1.5-4.0m high and extends for a distance of 135m from survey base station GE 3 up to survey monitoring station GEM 16, trending along a ridge top which drops away sharply southwest of the earthflow (as described above). A shallow (<1.0m deep) graben has developed between the bottom of the main headscarp and the back of an incipient displaced block, extending for 50m from base station GE 3. At the uphill end of this graben, a tension crack begins which connects the graben structure with a scarp system, the northwestern portion of which has recently been active, developing into a debris slide in yellowish brown sandy slide material (see section 6.3.3). Behind this incipient slide, a second major tension crack connects the main headscarp with a large degraded debris slide on the western edge of the main landslide area. A second, older, but still active debris slide occurs below the relatively recent incipient debris slide.

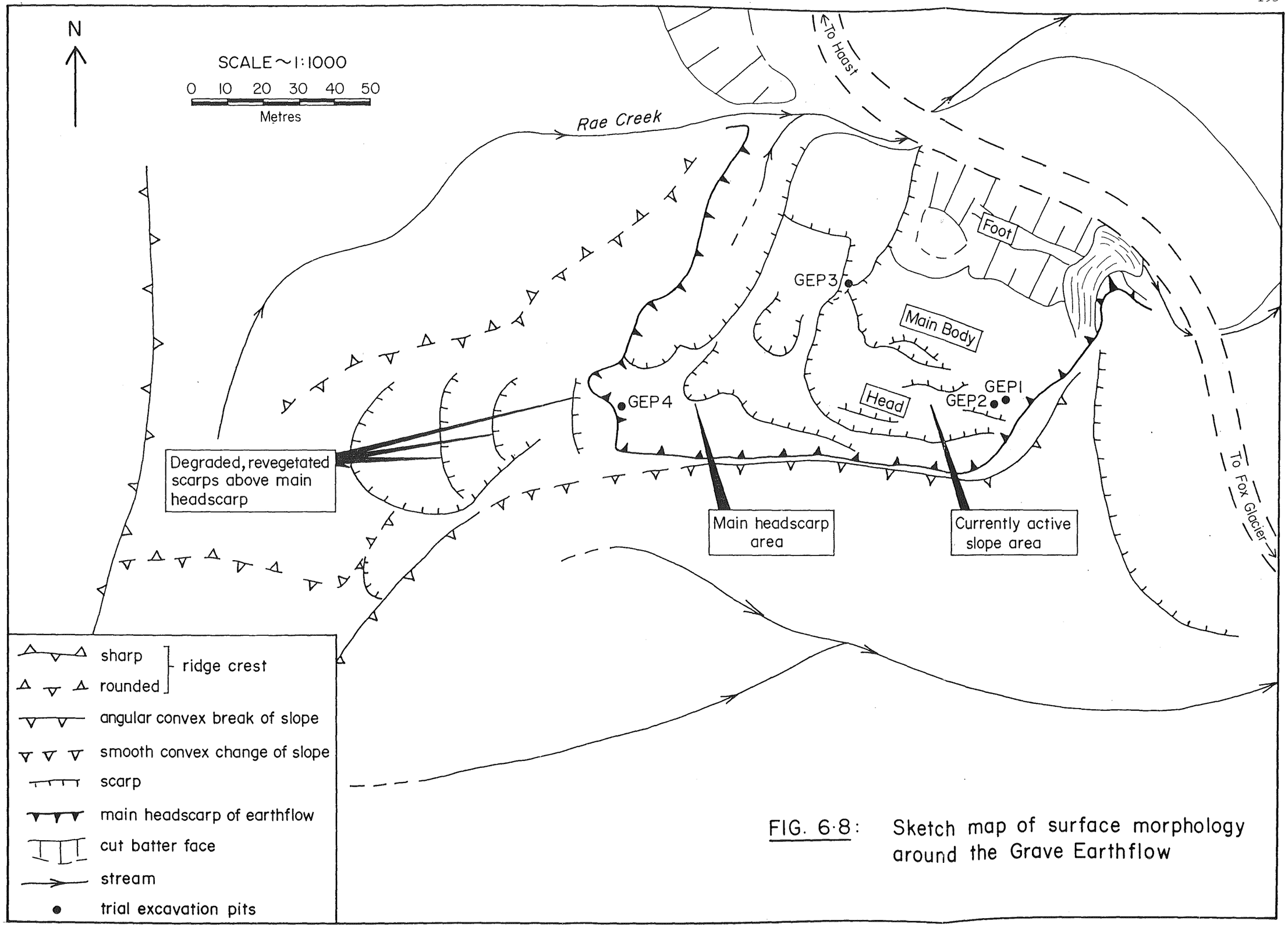

FIG. 6·8: Sketch map of surface morphology around the Grave Earthflow

c) Currently active System

This is confined to the eastern flank of the total earthflow system and is bounded on the southeast by the true right lateral shear zone of the total earthflow system; in the head area and on the northwest side by a major scarp; and at the toe by State Highway 6 (Fig. 6.5b). This currently active system can broadly be divided into three areas: the head, main body and foot.

The head area contains a series of displaced blocks in Tauperikaka Coal Measures ancient slide deposit with rotated, vegetated ground surfaces and major scarps bounding their fronts.

The main body is characterised by a series of transverse tension cracks, some of which are discontinuous, whilst others interconnect and link scarp systems. The majority of this area is bare ground composed of yellowish brown sandy slide material.

The foot area consists of a degraded road batter which was cut and benched in December 1984. It is bounded on both sides by major scarps in lower Otumotu bedrock, with both flanks undergoing secondary slope movements. The top of the cut batter and the true left side have enlarged into a major scarp formed by downslope movement of a block of sandy slide deposit, and the true right side is undergoing secondary movement by debris flow failure (Fig. 6.9). This southeastern (true right) flank is slightly depressed in topography, allowing groundwater to collect and to saturate the sandy slide deposit and underlying grey mud material which forms the debris flow. A large lobe (approx. 20m across) has formed at the base of this flow which encroaches on to the road pavement surface during rainstorm events.

Sandy slide material is seen to overlie grey mud material in the cut road batter, with water springs occurring immediately above the contact between these two materials in a wet zone which extends along the top of this boundary. This wet zone is probably the result of a perched water table, the relatively impervious grey mud preventing infiltration of

Fig. 6.9 Debris flow lobe approx. 20m wide on the eastern flank of the road batter.

water below the sand:mud boundary.

6.3.5 Subsurface Investigations

(i) Objectives and Methods

The objective of the subsurface investigations was to determine the geology of the Grave Earthflow and to ascertain the nature of the failure surface. Four methods were considered to achieve this:-

1. hand augering;
2. seismic refraction survey;
3. open excavations;
4. mechanical drilling.

Hand augering was attempted, but the maximum depth reached was only 1.2m due to the presence of large coal measure sandstone blocks incorporated in the slide deposit, and this prevented penetration to greater depths. Seismic refraction surveying was rejected due to the presence of these sandstone blocks, which would provide "false refractors", and also because the grey mud material, inferred to form the zone of failure beneath the coal measure derived slide deposit, was considered to be a poor seismic transmitter.

Backhoe trench excavations and mechanical drilling methods were also rejected, as these methods of investigations were considered to be beyond the scope of this study. In addition, it is envisaged that both these methods would have difficulties due to the steep nature of the ground surface and the very soft, wet to saturated slope materials which could cause trench wall instability problems and restrict the movement of heavy equipment.

(ii) Shallow Trial Pit Excavations

Carefully positioned hand-dug trial excavation pits were the main method of subsurface investigation, these being located where depth to the grey mud material was thought to be shallow (within 1-2m). Maximum depth reached was only 1.8m due to difficulties with unstable pit side-walls, but four pits were dug, their position shown on the 1:250 engineering geology plan (Fig. 6, map pocket) and in Figure 6.8. Figures

6.10 to 6.16 illustrate the trial pit excavations which are described below.

GEP 1 (Fig. 6.10) was located approximately 8m from the eastern lateral shear zone in the middle of bare ground. The upper 0.8m consisted of highly weathered, yellowish brown, silty sand with some gravel derived from disintegration of coal measure sandstone bedrock. At 0.35 to 0.8m depth, substantial groundwater seepage (low to moderate flow) into the pit occurred causing rapid collapse of the pit side-walls and preventing excavation beyond 1.2m depth. Below a sharp boundary at 0.8m depth, dark grey silt occurs.

GEP 2 (Figs 6.11 & 6.12) was located approximately 5.5m upslope from GEP 1 at the base of a major scarp. Below broken coal measure sandstone in the scarp, yellowish brown, wet to saturated, gravelly sand slide deposit occurred to a depth of 0.6m. As in GEP 1, a saturated zone existed immediately above the yellowish brown slide deposit and grey mud material boundary. Below this contact was a 0.15m band of carbonaceous mud, which contained small angular fragments of coal up to 20mm long, and below this, grey sandy silt material with layers of carbonaceous mud occurred to a depth of 1.1m where the excavation ended.

GEP 3 (Figs 6.13 & 6.14) was situated 2.5m from the western lateral shear zone. Below a 0.15m cover of wet, yellowish brown silty sand a light and dark grey, mottled sandy silt with lenses of dark reddish brown and black muddy layers occurs. This passes into a light grey silty sand with angular quartz and lithic clast fragments up to 25mm long derived from the lower Otumotu cobble conglomerate.

GEP 4 (Figs 6.15 & 6.16) was located at the base of the 4m high headscarp in the southwestern corner of the earthflow complex. Below the broken coal measures sandstone exposed in the headscarp, three highly to completely weathered units occur: a 0.3m thick soft, light brown, massive sand, a 0.2m thick stiff, light green and dark reddish brown, massive silt, and a firm, yellowish brown, reddish brown and black, mottled fine sandy silt. All three units are inferred to be derived

Trial Pit No. GEP 1

METHOD OF EXCAVATION: Hand dug

DATE EXCAVATED: 20/3/85

COORDINATES
Metres N: 299 669·50
Metres E: 700 324·25

REDUCED LEVEL: 111 m (a.s.l.)

LOCATION: Grave Earthflow, Grave Creek, South Westland

SAMPLE	WATER CONT-ENT (%)	ATTERBERG LIMITS LL	PL	PI	DEPTH (m)	PROFILE LOG	ENGINEERING GEOLOGICAL DESCRIPTION
					0		
GS1	25	27	26	6	0·8		Highly weathered, moist to saturated, soft, light yellowish brown, massive, silty SAND, with some gravel (SM).
GS2	21	31	19	12	1·0		Unweathered, saturated, very soft, dark grey, massive, clayey SILT with some sand (ML).
					1·2	? ? ?	

PLAN:

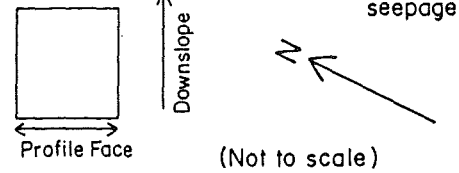

LOGGED BY: Mark J Eggers
DATE: 20/3/85

SCALE: 1:20

FIG. 6·10

Trial Pit No. GEP 2

METHOD OF EXCAVATION: Hand dug

DATE EXCAVATED: 20/3/85

COORDINATES
Metres N: 299 666·50
Metres E: 700 324·75

REDUCED LEVEL: 112 m (a.s.l.)

LOCATION: Grave Earthflow, Grave Creek, South Westland

SAMPLE	WATER CONTENT (%)	ATTERBERG LIMITS LL	PL	PI	DEPTH (m)	PROFILE LOG	ENGINEERING GEOLOGICAL DESCRIPTION
					Ground level 0		Moderately weathered, moist, loose, light yellowish brown, massive, sandy GRAVEL (GP). Broken Tauperikaka Coal Measures bedrock exposed in major scarp approx. 3m high.
							Highly weathered, wet to saturated, very soft, yellowish brown, massive, gravelly SAND (SP).
					0·60		
GS 3	22	39	18	21	0·75		Unweathered, moist, soft, black, finely laminated, clayey SILT (OL). Contains small angular fragments of coal up to 20mm long.
					1·0		Unweathered, moist, soft, dark grey, finely laminated, sandy SILT (ML). Contains layers of black carbonaceous silt.
					1·1		
GS 4	16	26	16	10			Unweathered, wet, very soft, grey, massive, sandy SILT (ML).
					1·8	? ? ?	
					2·0		

PLAN:

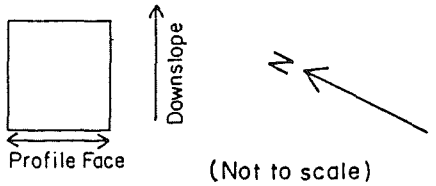

LOGGED BY: Mark J Eggers
DATE: 20/3/85

SCALE: 1:20

FIG. 6·11

Fig. 6.12 Trial pit GEP 2: note the wet zone in yellowish brown gravelly sand slide deposit immediately above the band of black carbonaceous mud.

Trial Pit No. GEP 3

METHOD OF EXCAVATION: Hand dug

DATE EXCAVATED: 20/3/85

COORDINATES
Metres N: 299 644·25
Metres E: 700 273·00

REDUCED LEVEL: 119 m (a.s.l.)

LOCATION: Grave Earthflow, Grave Creek, South Westland

SAMPLE	WATER CONTENT (%)	ATTERBERG LIMITS LL	PL	PI	DEPTH (m)	PROFILE LOG	ENGINEERING GEOLOGICAL DESCRIPTION
GS5	26	29	24	5	0		Highly weathered, wet, soft, light yellowish brown, massive, silty SAND with some gravel (SM).
					0·15		Unweathered, moist, soft to firm, light and dark grey, mottled, sandy SILT (ML). Contains reddish brown lens and black carbonaceous lens.
GS6	14	27	18	9			
					1·0		
GS7	6·3	19	15	4			Unweathered, moist, firm, light grey, massive, silty SAND, with some fine gravel (SM). Contains angular quartz and lithic clast fragments up to 25mm long.
					1·8	? ? ?	
					2·0		

PLAN:

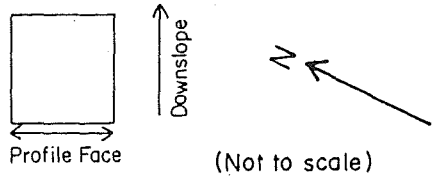

LOGGED BY: Mark J Eggers
DATE: 20/3/85

SCALE 1:20

FIG. 6·13

Fig. 6.14 Trial pit GEP 3: note the mottled grey and dark reddish brown sandy silt with angular quartz and lithic clasts.

Trial Pit No. GEP 4

METHOD OF EXCAVATION: Hand dug

DATE EXCAVATED: 20/3/85

COORDINATES
Metres N: 299 568·75
Metres E: 700 275·00

REDUCED LEVEL: 157 m (a.s.l.)

LOCATION: Grave Earthflow, Grave Creek, South Westland

SAMPLE	WATER CONTENT (%)	ATTERBERG LIMITS LL	PL	PI	DEPTH (m)	PROFILE LOG	ENGINEERING GEOLOGICAL DESCRIPTION
					Ground level 0	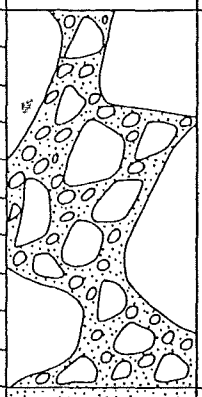	Moderately weathered, dry to moist, compact, brown, massive, sandy GRAVEL (GP). Disintegrated Tauperikoka Coal Measures exposed in headscarp approx. 4m high.
					0·3		Highly weathered, moist, soft, light brown, massive SAND with some fine gravel (SP).
					0·5		Completely weathered, moist, stiff, light green and dark reddish brown, massive SILT with some sand (ML).
					1·0		Highly weathered, moist, firm, yellowish brown and reddish brown mottled, fine sandy SILT with some clay (ML). Contains mottles of black, reddish brown, yellowish brown material up to 20mm long.
					1·2		
					2·0		

PLAN:

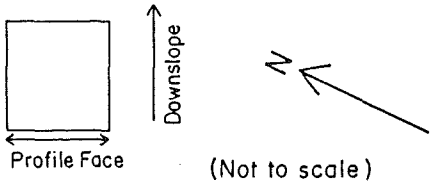

LOGGED BY: Mark J Eggers
DATE: 20/3/85

SCALE: 1:20

FIG. 6·15

Fig. 6.16 Trial pit GEP 4: highly to completely weathered sand and silt materials underlying broken coal measures sandstone exposed in the headscarp.

from Otumotu Formation bedrock.

Although of shallow depth limiting detailed investigations, the trial excavation pits allowed the following observations to be made:-

1. A wet to saturated zone 0.4-0.6m thick in weathered yellowish brown sandy slide deposits is present immediately above the contact with underlying grey mud material;
2. Black carbonaceous mud and dark reddish brown layers in grey mud material occur immediately below the sandy slide contact, which passes down into grey sandy silt deposit;
3. The occurrence of angular quartz and lithic clast fragments in the grey mud deposit suggests it is derived from shearing in lower Otumotu bedrock.

6.3.6 Laboratory Investigations

(i) Laboratory Programme

Disturbed bag samples collected from trial excavation pits were tested to determine grainsize distribution, in-situ moisture content, Atterberg Limits and clay mineralogy. The primary objective of this programme was to characterize the materials according to standard geotechnical tests to allow a preliminary assessment of their engineering properties. Results obtained from seven samples, summarised in Table 6.2, are discussed below.

(ii) Grain Size Distribution

Appendix 5 details methods used and gives semi-log plots of results obtained from grainsize analysis. Yellowish brown sandy slide material is coarse-grained, containing 47-50% sand and 30-32% gravel with the remaining 20-21% of fine-grained material being mostly silt (17%). According to the Unified Soil Classification system, they are poorly graded silty sands (SM). The grey mud material, on the other hand, is dominantly fine-grained with 39-75% finer than 0.06mm, the clay content averaging 9% (apart from the carbonaceous mud sample (GS 3) which contained 27% clay).

Sample Number	Sample Origin and Description	Water Content %	Grain Size Analysis				Atterberg Limits				Activity	Soil Class[n]	Clay Mineralogy
			Gravel %	Sand %	Silt %	Clay %	LL	PL	PI	LI			
GS 1	GEP 1, 0.6m deep, yellowish brown gravelly SAND.	25	32	47	17	4	27	21	6	0.67	1.5	SM	chlorite>illite >quartz
GS 2	GEP 1, 1.1m deep, dark grey, sandy SILT.	21	18	34	39	9	31	19	12	0.17	1.3	CL	illite>chlorite
GS 3	GEP 2, 0.7m deep, black carbonaceous MUD.	22	6	19	48	27	39	18	21	0.19	0.78	OL	illite>chlorite >quartz
GS 4	GEP 2, 1.6m deep, grey sandy SILT.	16	23	38	31	8	26	16	10	0	1.2	CL	n.d.
GS 5	GEP 3, 0.1m deep, yellowish brown silty SAND.	26	30	50	17	3	29	24	5	0.40	1.7	SM	n.d.
GS 6	GEP 3, 0.7m deep, grey sandy SILT.	14	25	30	36	9	27	18	9	-0.44	1.0	CL	chlorite>illite
GS 7	GEP 3, 1.2m deep, grey silty SAND.	6.3	26	50	20	4	19	15	4	-2.17	1.0	SM	n.d.

Note - n.d. - not determined

Table 6.2 Summary of laboratory test results from trial excavation pit samples, Grave Earthflow.

(iii) In-Situ Moisture Content and Atterberg Limits

Methods used to determine in-situ moisture content and Atterberg Limits are detailed in Appendix 5. The results of these tests allow fine-grained soils to be classified since variation in moisture content in these soils can produce significant changes to their engineering properties.

The yellowish brown sandy slide deposit has a low plasticity index (5-6) but high activity (1.5-1.7) and relatively high liquidity index (0.40-0.67). This is due to the low clay content of these materials (3-4%) but high in-situ moisture content bringing the material close to its liquid limit (27-29%).

The grey mud material has a higher plasticity index (4-21) but lower liquidity index (-2.17-0.19) due to the relatively lower in-situ moisture contents being below or just above the plastic limit. Activity ranges from normal to high (0.78-1.3) which suggests a low permeability resistance to shear, with cohesion responsible for strength (Grim 1962). According to the Unified Soil Classification the grey mud is a clay with low plasticity (CL) which contrasts to field identification as silt with low plasticity (ML). The carbonaceous mud sample (GS 3) is classified as organic silt of low plasticity (OL).

(iv) Clay Mineralogy

Clay mineralogy was determined by x-ray diffraction analysis as outlined in Appendix 5, and one yellowish brown sandy slide deposit and three grey mud deposit samples were analysed. A chlorite-illite-quartz clay mineral assemblage is inferred for all samples, with relative quantities for each sample as indicated in Table 6.2. No swelling clays were identified upon treatment of the samples with glycol indicating a completely non-swelling clay mineral assemblage.

6.4 EARTHFLOW STABILITY AND REMEDIAL OPTIONS

6.4.1 Objectives

The main objectives of this section are:-

1. to discuss the present stability of the Grave Earthflow, and;
2. to describe possible remedial options in terms of preventing damage to State Highway 6.

The present stability of the Grave Earthflow was assessed by surface movement monitoring investigations, and methods and results of these investigations are reported together with a stability assessment which describes the failure model inferred for the earthflow. Discussion of remedial options follows this and is based on the understanding of instability and the nature of the surface morphology and slope materials.

6.4.2 Grave Creek Survey Network

The Grave Creek Survey network was installed in March 1985 to monitor ground surface movements, and to provide a local base grid for topographical mapping of the earthflow. Appendix 8 details the methodology of installation and the survey system used.

Two major problems were experienced in setting up the network. Firstly, the unstable nature of the slopes around Grave Creek gully provided a lack of suitable stable base station sites. As a result base stations GE 1 and GE 2, providing the baseline for the local coordinate grid system, were installed on raised beach surfaces situated on the northeastern corner of the gully approximately 470m from the earthflow (Fig. 6.17), increasing the distance of the closed traverse survey system more than was originally planned, and so increasing the likely survey error.

Secondly, positioning of monitoring stations parallel and perpendicular to the axis of the earthflow to provide a regular system of monitoring was hampered by the presence of vegetation cover within the earthflow which obscured the line of sight. Allowance for probable future movement was also

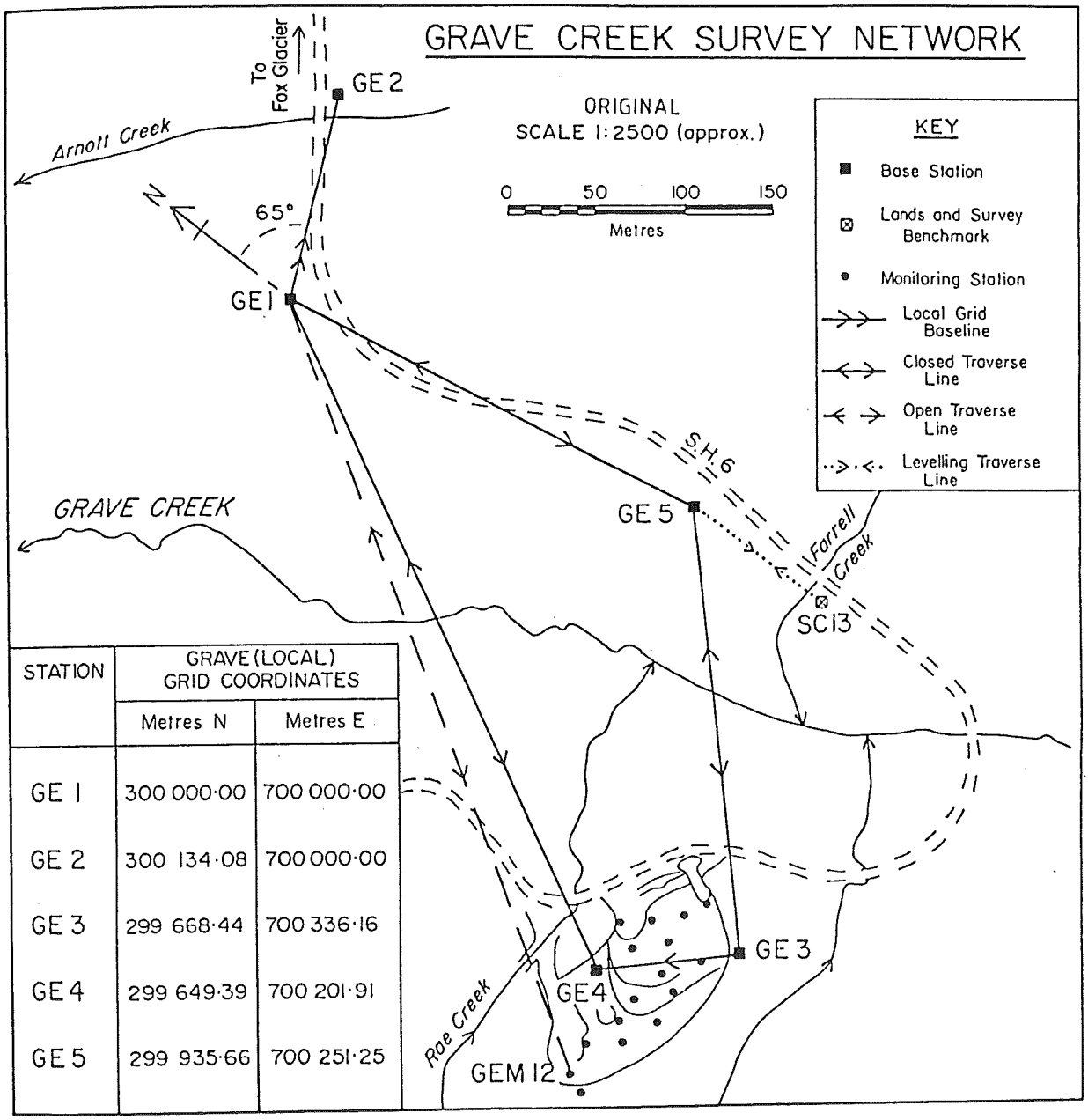

STATION	GRAVE (LOCAL) GRID COORDINATES	
	Metres N	Metres E
GE 1	300 000·00	700 000·00
GE 2	300 134·08	700 000·00
GE 3	299 668·44	700 336·16
GE 4	299 649·39	700 201·91
GE 5	299 935·66	700 251·25

Fig. 6.17 Grave Creek Survey Network

made to ensure a line of sight was maintained to each station.

Initially nine monitoring stations (GEM 1 - GEM 9) were installed in March 1985, all positioned in the currently active slope area. This system was extended to 16 stations in October 1985 (Fig. 6.18) to include the main headscarp area which was thought to be experiencing a re-initiation of movement due to the development of fresh tension cracks and minor scarps after commencement of monitoring the initial nine station system. Establishment of monitoring stations in the main headscarp area was excluded from the March 1985 installation due to difficulties in siting monitoring stations and a closed traverse base station in this area, as described above. However, subsequent installation and monitoring was attempted using an open (hanging) traverse line from base station GE 1 to monitoring station GEM 12, which therefore limited the accuracy of results obtained. Seven surveys were completed, three prior to October 1985 with the last survey made in June 1986.

6.4.3 Surface Movement Monitoring Investigations

(i) Movement Data

The main aim of the surface movement monitoring investigations was to ascertain the areas of instability within the earthflow complex, and to define patterns of movement within the active areas which may help identify the nature of the failure surface. Movement data obtained from surveying (coordinates: metres E, metres N and reduced level) are presented in tables given in Appendix 9 together with the following calculated parameters:-

1. components of displacement (x, y, z directions): recent (since the last survey) and cumulative;
2. horizontal displacement (combined x and y directions): recent, cumulative, and average;
3. total displacement (combined x, y, and z directions): recent, cumulative, and average;
4. rate of displacement (x, y, z, horizontal, total): recent, cumulative, and average;
5. direction of displacement: recent and average.

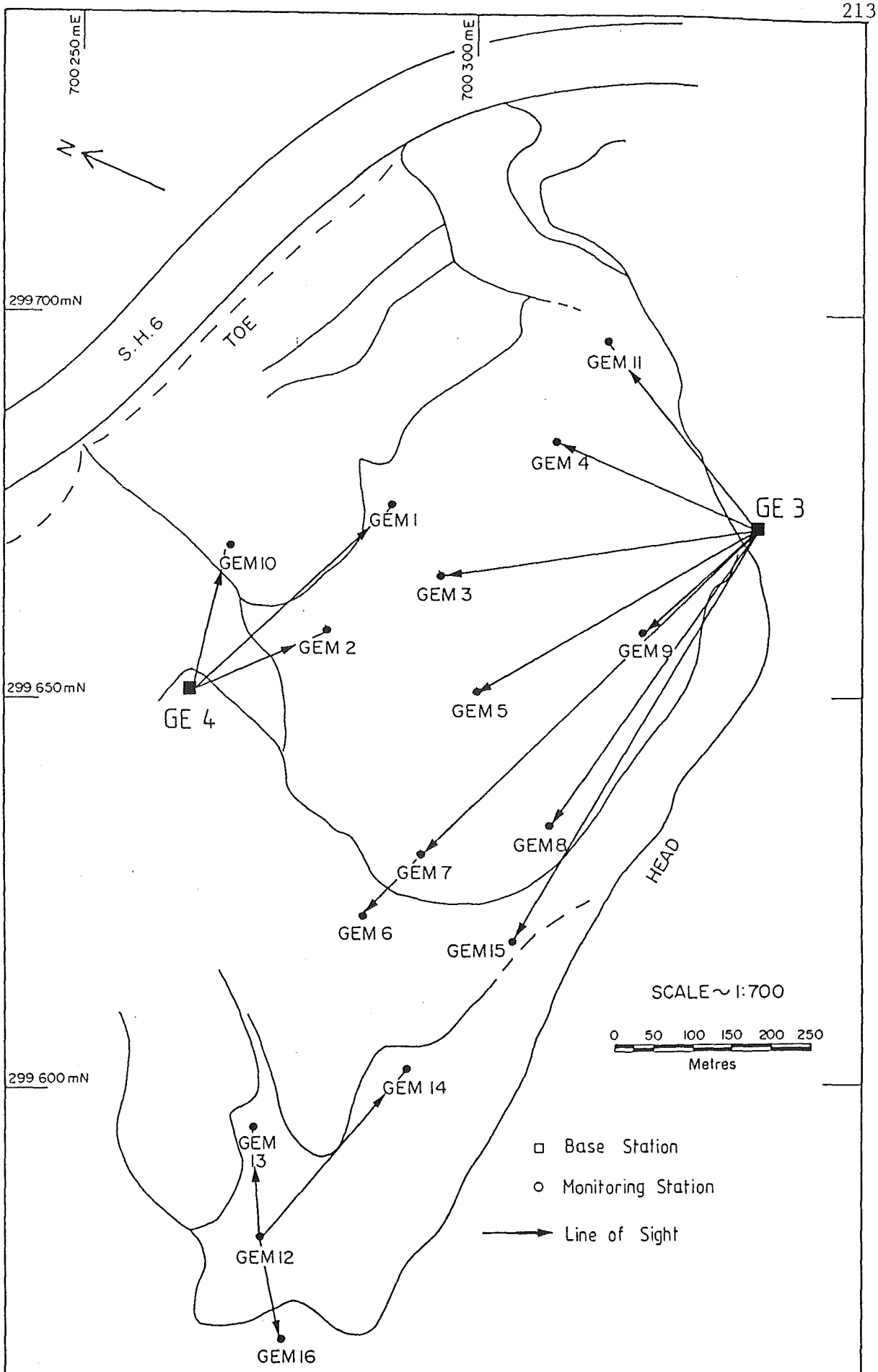

Fig. 6.18 Grave Earthflow Monitoring Network

(ii) Total Displacement

Table 6.3 lists the rate of total cumulative displacement for each monitoring station on the earthflow as measured during the monitoring period, and Figure 6.19 shows these data as vectors of rate of total cumulative displacement.

The greatest amount of movement was measured at the foot of the earthflow, with GEM 2 recording the highest total displacement rate of 419cm/year. This is a high movement rate producing substantial displacements at the toe of the earthflow and causing movement to extend on to the pavement surface of State Highway 6 during periods of heavy rainfall, which in turn provides continual maintenance problems. Rates of displacement decreased toward the head region of the active earthflow area, with GEM 8 recording the lowest of 108cm/year. Direction of displacement (Fig. 6.19) in the head area is east-northeast and this swings slightly to the northeast at the foot of the earthflow, which is directly downslope but acute to the aspect of the earthflow complex (north-northeast).

Beyond the active earthflow area, two monitoring stations (GEM 6 and GEM 15) also recorded movement. These are separated from the other monitoring stations in the main headscarp area (GEM 12,13,14) by a tension crack - scarp system along which the movement is inferred to be occurring. The one monitoring station (GEM 16) located outside of the earthflow complex above the main headscarp, recorded no movement.

Figure 6.20 illustrates the change in rate of total, recent (since the last survey) displacement during the monitoring period. The foot region (Graph A) shows a rapid decline in rate before increasing to the rates indicated in Table 6.3, for example, GEM 3 fell from 720cm/year on 4/6/85 to 200cm/year on 9/4/86, then climbed to 382cm/year on 28/6/86. The head region (Graph B, Fig. 6.20) also declined over approximately the same period, but not to the same degree; in fact GEM 7 and 5 increased from 290cm/year on 4/6/85 to 360 and 320cm/year respectively on 7/9/85 before declining to 150cm/year each on 6/2/86. They then increased

MONITORING STATION	MONITORING PERIOD (days)	TOTAL CUMUL. DISPL. (cm)	RATE OF TOTAL CUMUL. DISPL. (cm/year)
GEM 1	389	363	341
GEM 2	459	527	419
GEM 3	459	481	382
GEM 4	459	293	233
GEM 5	459	301	239
GEM 6	459	173	138
GEM 7	459	327	260
GEM 8	459	136	108
GEM 9	459	157	125
GEM 10	269	264	358
GEM 11	269	147	199
GEM 12	269	Nil	Nil
GEM 13	269	Nil	Nil
GEM 14	269	Nil	Nil
GEM 15	269	86	117
GEM 16	269	Nil	Nil

Table 6.3 Rate of total cumulative displacement for each monitoring station on the Grave Earthflow.

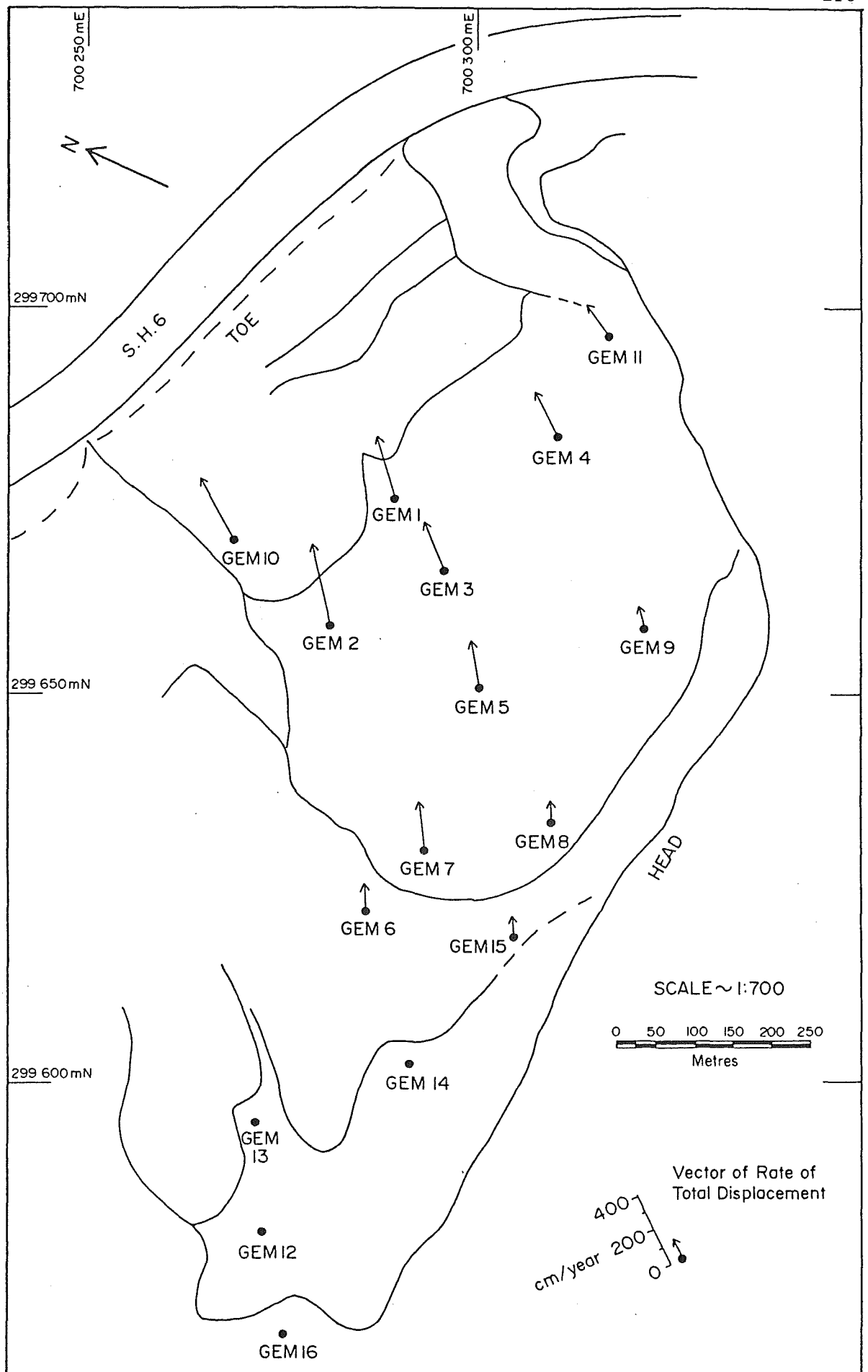

Fig. 6·19: Rate of total displacement vectors for monitoring period 26/3/85 - 28/6/86, Grave Earthflow

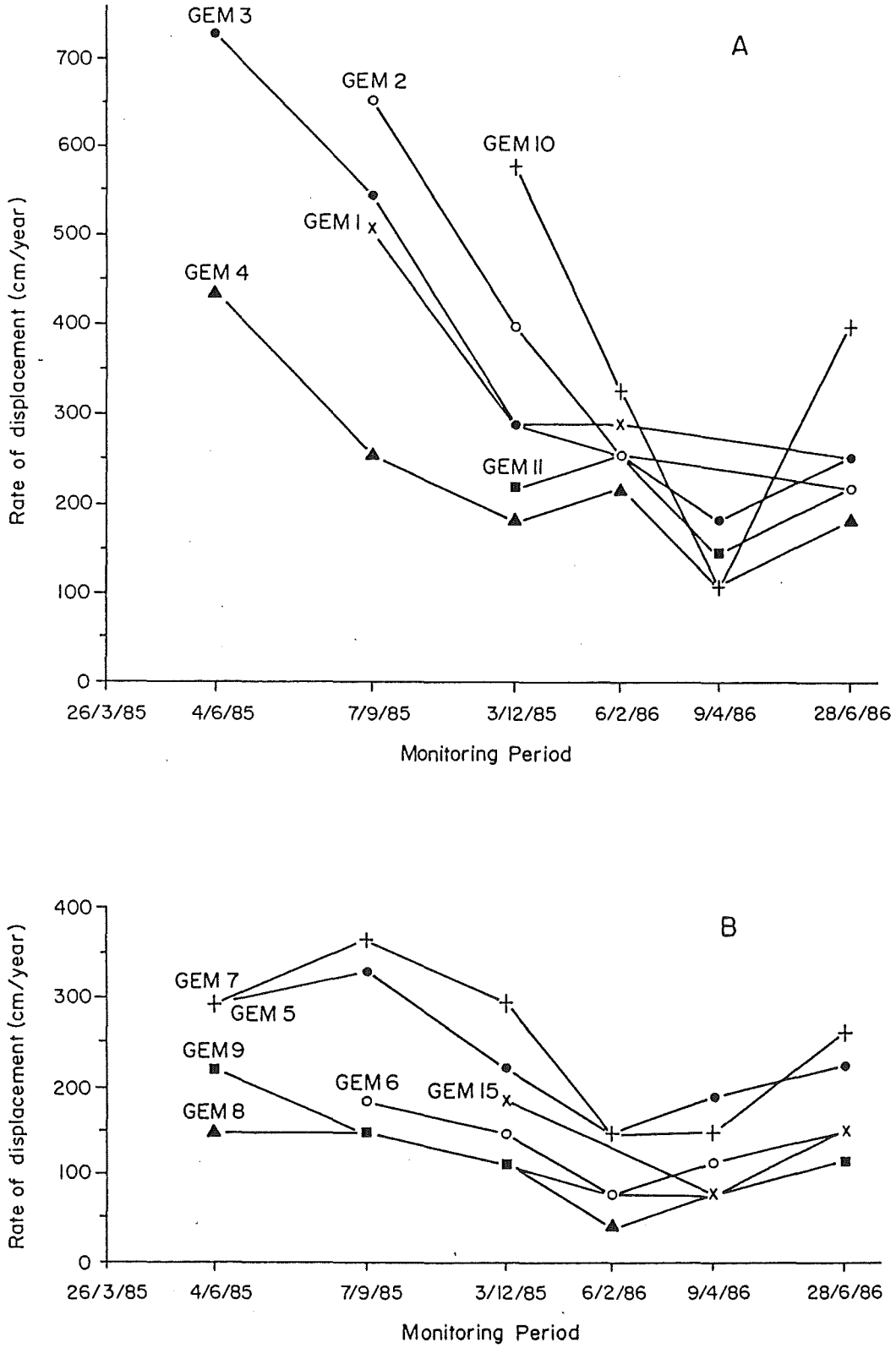

Fig. 6·20: Change in rate of total (recent) displacement during the monitoring period 26/3/85 - 28/6/86 for the Grave Earthflow

A = Foot region B = Head region

to 200cm/year (GEM 7) and 239cm/year (GEM 8) on 28/6/86.

This pattern of movement is interpreted to be the response of the earthflow to unloading of toe support in December 1984 when the road batter was cut and benched (see Section 6.3.2). Removal of toe support in effect caused an instantaneous acceleration in movement rates in the foot region, which then retrogressively moved towards the head region. Monitoring, which began in March 1985 (3 months later), picked up the deceleration of movement rates from the initial high value caused by the instantaneous acceleration, and this obscured any other variation in movement rates which may have been present. Near the end of the monitoring period, movement rates had declined to what is inferred to be "normal" levels that seemed to be influenced by seasonal variations, as discussed below.

(iii) Correlation of Movement with Rainfall

Figure 6.21 illustrates a correlation of rainfall with total displacement during the period of earthflow monitoring. Rainfall data, taken from daily observations made at the new Haast station (station number F39802), is plotted as total recent rainfall since the last survey, as is total displacement. The two total displacement curves, one each from the foot and head regions, show a similar pattern to the rate curves in Figure 6.20, declining from a high to a low value before increasing to a moderate ("normal") level. The rainfall curve shows a similar pattern, with a winter maximum coinciding with the maximum displacement value (on 7/9/85), and the summer minimum coinciding with minimum displacement (on 9/4/86). There is no lag or delay in movement following rainfall variations, suggesting that rainfall effects on movement are immediate. However, this apparently good correlation is interrupted by two anomalies:-

1. GEM 3 total displacement does not recover to its 4/6/85 high on 28/6/86, and;
2. an increase in rainfall during the period 3/12/85-6/2/86 did not produce a corresponding increase in movement.

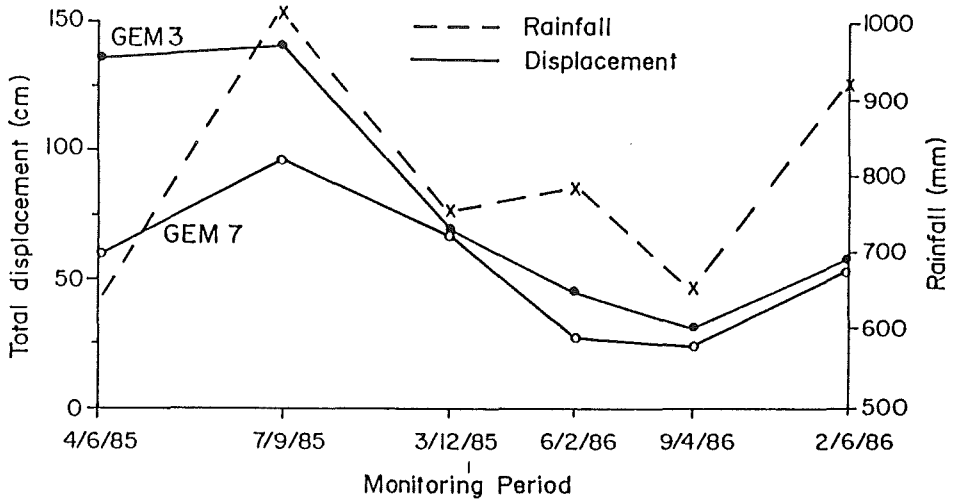

Fig. 6·21: Correlation of rainfall with total (recent) displacement during the monitoring period for the Grave Earthflow

The first anomaly was caused by the effect of unloading toe support on movement during the 1985 season which produced an unusually high displacement rate. The second anomaly is probably due to the fact that either movement was still primarily being influenced by the deceleration process, overriding rainfall effects, or possibly the increase in rainfall may not have been sufficient to increase movement rates, suggesting that there is a threshold value of rainfall that causes movement. The most likely explanation would be a combination of these two ideas.

(iv) Hodographs of Movement

Ter-Stepanian and Goldstein (1969) and Ter-Stepanian and Ter-Stepanian (1971) analyse average displacement rates of monitoring points in slope movement areas to study the mechanism of sliding. The average displacement rate vector is resolved into x, y and z components:-

$V_x=x/t$; $V_y=y/t$; $V_z=z/t$;

where t is the time interval between measurements (the monitoring period). The horizontal projection (V_h) of the average displacement rate vector is determined from this data:-

$$V_h=(V_x^2+V_y^2)^{1/2}$$

Two diagrams were drawn, one showing the horizontal plane (with coordinate axes V_x and V_y) and the other showing the vertical plane (coordinate axes V_h and V_z), which are termed hodographs of the displacement rates of sliding which assume that displacement is continuous (steady creep). Figure 6.22 illustrates hodographs constructed for the Grave Earthflow, plotted from data presented in the movement tables given in Appendix 9. Interpretation of these diagrams has been based on examples described by Ter-Stepanian and Goldstein (1969) and Ter-Stepanian and Ter-Stepanian (1971), and is discussed below.

Several groups of topographically closely related monitoring stations were separated on the diagrams which show various features of the mechanism of failure of the earthflow:-

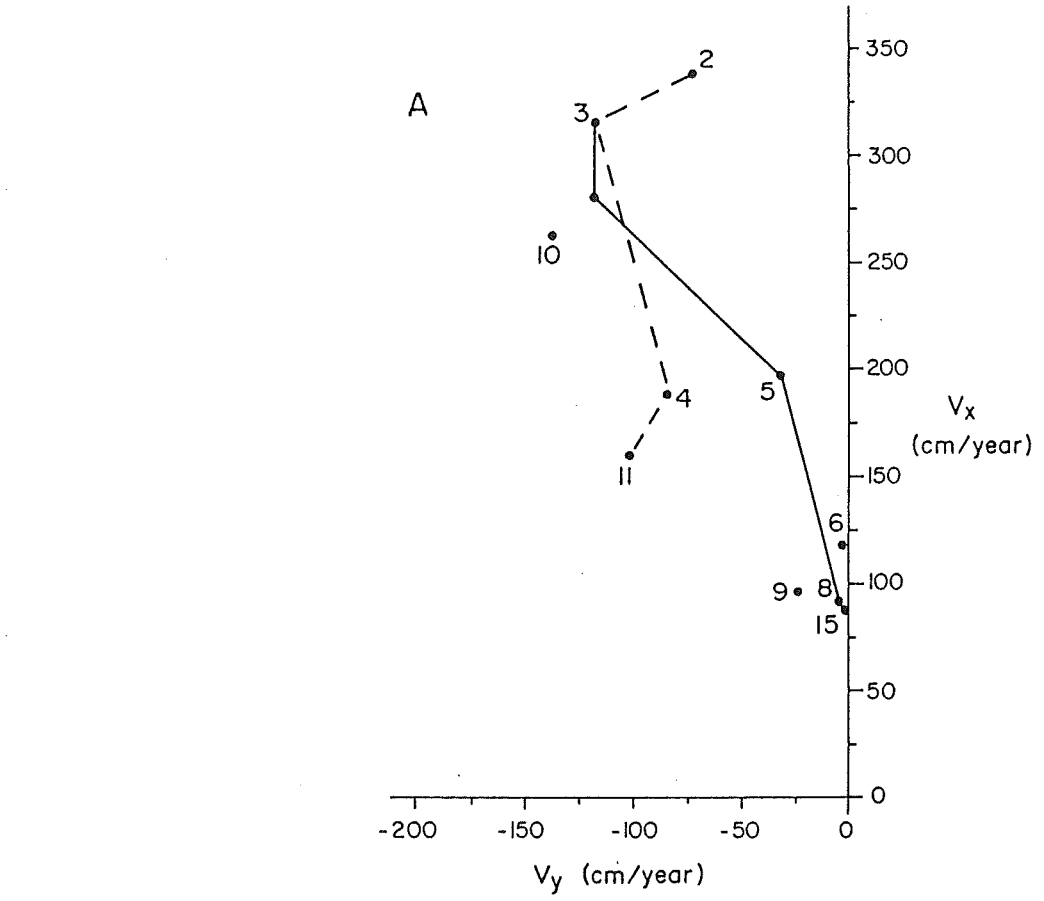

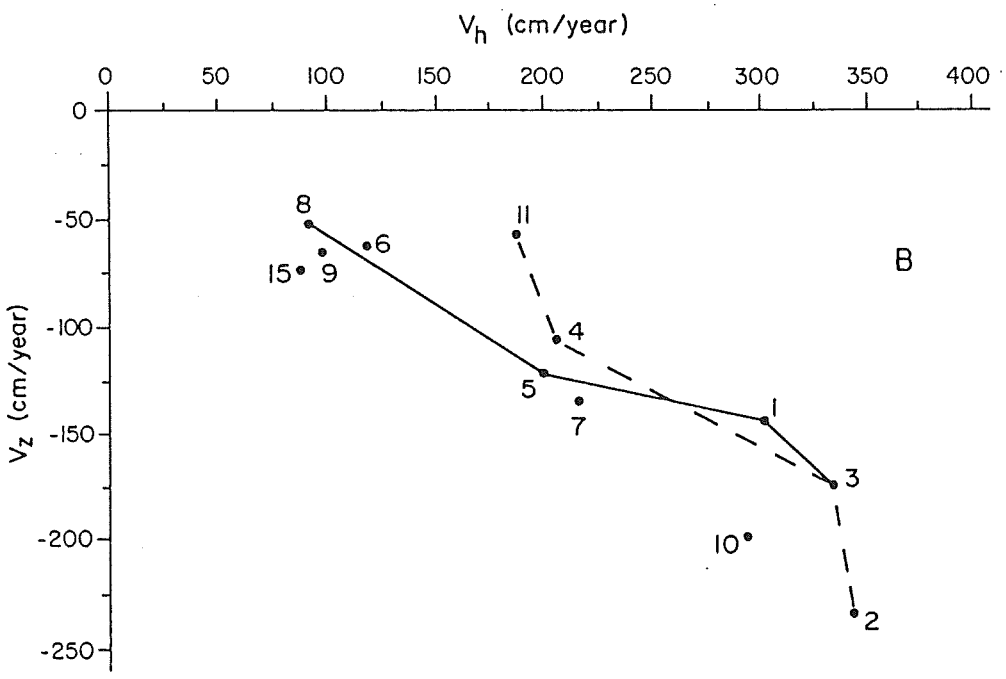

Fig. 6·22: Hodographs of average displacement rates of monitoring stations on the Grave Earthflow, measured between 26/3/85 - 28/6/86

A = Horizontal Plane B = Vertical Plane

1. Stations GEM 15,8,5,3 and 1 are located along a line parallel to the earthflow axis. They plot as rectilinear hodographs with the foot region stations (3 and 1) showing the greatest movement and the head region stations (15 and 8) showing the least. This is indicative of a retreating flow failure with the seat of failure located in the lower part of the slope.
2. Stations GEM 2,3,4 and 11 are located across the earthflow axis with their hodographs showing a part rectilinear, part fan-like arrangement indicating failure is part-rotational, part-translational.

(v) Synthesis

Surface movement monitoring investigations have identified a high rate of movement of the earthflow near the toe, up to 419cm/year, which is significant in terms of maintenance of State Highway 6. Movement is confined to the current active zone, with little or no movement in the main headscarp area. However, movement in stations GEM 6 and 15, along with field evidence of fresh tension crack and minor scarp development, may indicate that this area is beginning to reactivate.

Unloading of toe support in December 1984 was interpreted to have caused an instantaneous acceleration in movement rates which subsequently declined during the monitoring period. This deceleration process obscured any climatic influences on movement, however, by the end of the monitoring period, movement rates had decreased to the point where climatic influences were once again the primary factor controlling movement. This climatic influence has an immediate effect on movement, with no lag or delay, although there may also be a threshold rainfall value which must be exceeded before movement increases. Hodographs of movement suggest that failure is taking place by retreating part-rotational, part-translational failure, with the seat of failure located in the lower part of the slope.

6.4.4 Stability Assessment

(i) Quantitative Analysis

A quantitative stability analysis involving limit equilibrium theory and computed factors of safety was not carried out due to the lack of geotechnical information for the Grave Earthflow. Such a stability analysis requires adequate subsurface data from the zone of failure, but subsurface investigations did not intercept or positively identify the failure zone and therefore approximate strength parameters could not be determined. Stability assessment is restricted to a qualitative appraisal of movement mechanisms, and the causes of slope instability.

(ii) Failure Model

On the basis of engineering geological mapping, subsurface, laboratory and surface movement monitoring investigations, a failure model for the Grave Earthflow can be constructed describing the failure mechanisms and causes of slope instability.

a) Failure Mechanisms and Sequence of Movement

Failure is inferred to be taking place by a complex rotational slide (slump) - earthflow type movement, as shown on the engineering geological cross-section in Figure 6 (map pocket). This involves multiple rotational sliding of an ancient slide deposit in Tauperikaka Coal Measures near the headscarp, which degrades into an earthflow movement in the main body and foot of the slope movement complex, and which fails on a planar zone of sliding in sheared grey mud of the lower Otumotu Formation daylighting in the cut batter face. As such, it is also a compound movement with the failure surface formed of a combination of curved and planar elements giving the movement a part-rotational, part-translational character. Movement may also be considered as multi-storied (see Section 3.2.5), with a debris flow occurring on the batter face developed on top of the main earthflow movement. Presently, movement is retrogressive (rather than uniform), retreating upslope opposite to the direction of movement of material.

(b) Causes of Failure

Factors contributing to failure can be separated into fundamental causes, which combine to produce a slope at limiting equilibrium (factor of safety close to 1.0), and triggering mechanisms, which initiates the critical slope to fail. Figure 6.23 illustrates the interrelationships of causes of the Grave Earthflow and these are described below under the two above headings:-

FUNDAMENTAL CAUSES

1. Reduction in shear strength of lower Otumotu Formation bedrock by faulting, producing a weak grey mud gouge material;
2. Increase in shear stress by removal of underlying support produced by over steepened slopes of deeply incised coastal stream, and;
3. Removal of lateral support in the head region by movement of material downslope.

TRIGGERING MECHANISMS

1. Undercutting of the critical slope by construction of State Highway 6 which removed underlying support;
2. Water infiltration during high intensity rainstorms, which increases positive pore pressures (resulting in a decrease in the effective normal stress) and increases the surcharge on the slope, and;
3. Seismic events produce transitory earth stresses which may increase the shear stress.

6.4.5 Remedial Options

(i) Potential Remedial Measures

Five potential remedial measures are recognised for the Grave Earthflow:-

1. dewatering, using surface and subsurface drainage;
2. planting of trees;
3. buttressing of toe;
4. relocation of highway, and;
5. maintaining the present situation.

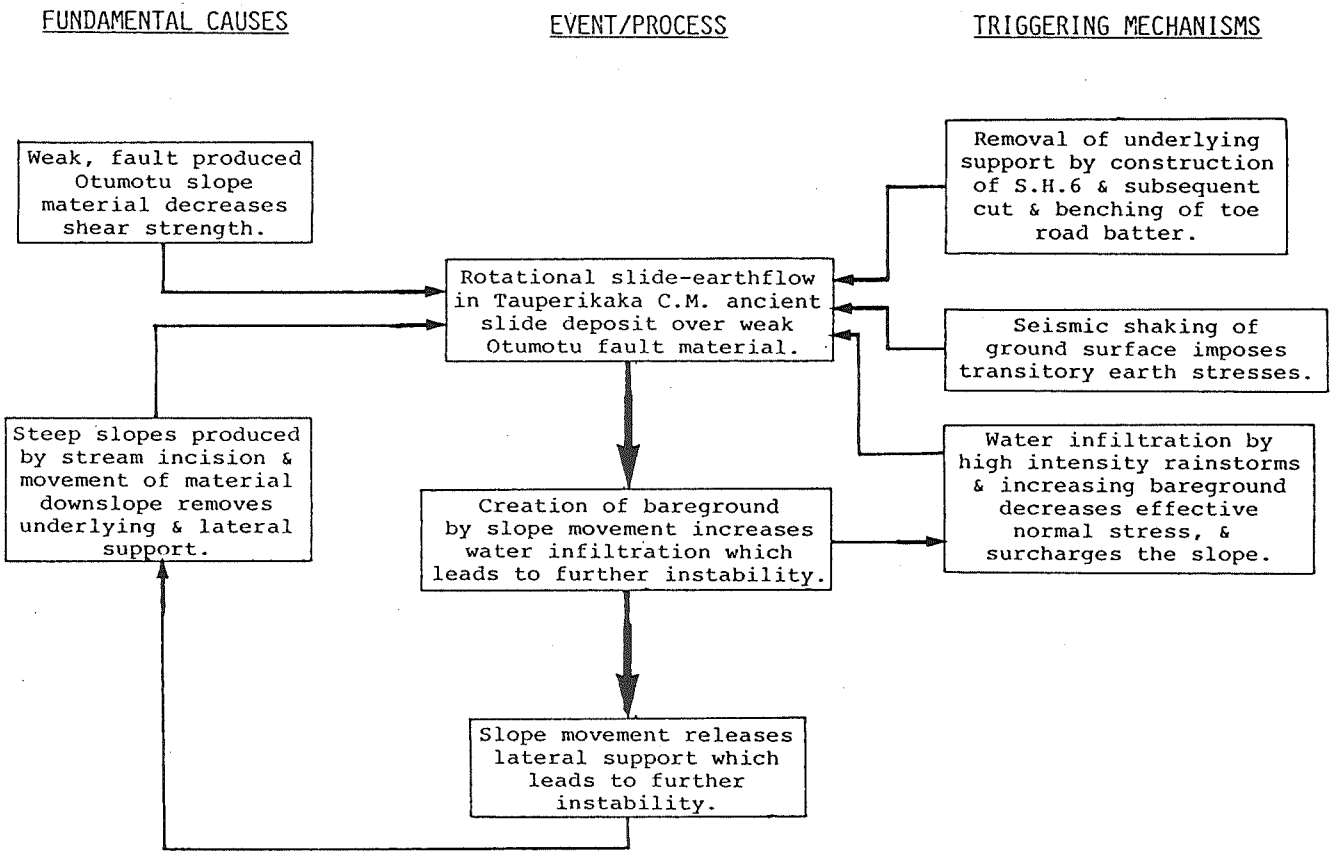

Fig. 6.23 Model of interrelationships between factors contributing to failure.

Each of these potential remedial measures are discussed separately, concluding with a list of recommendations which recognise that complete stabilization of the earthflow may not be economically viable.

(ii) Dewatering

Dewatering of the earthflow mass would have three effects in stabilising the slope:-

1. reduce positive pore water pressures, consequently increasing the effective normal stress;
2. reduce the surcharge on the slope caused by the weight of water;
3. reduce the "lubricating" effect water has in contributing to flow-type movements.

Two methods of dewatering are surface and subsurface drainage. Surface drainage ditches, both upslope and at the toe, reduce groundwater infiltration and recharge from rainfall by increasing run-off and preventing surface ponding. Subsurface drainage, by counterfort drains, horizontal and vertical gravity drains, and pump wells intercept and remove groundwater flow. These would be very beneficial measures for the Grave Earthflow but could be very difficult to implement for the following reasons:-

1. construction of surface drains and deep trenches for counterfort drains would be difficult on the steep slopes and weak surficial materials, causing access problems to the earthflow and collapse of drain sidewalls;
2. steady creep and local secondary failures would damage and infill surface and gravity drains quickly, rendering them ineffective.

(iii) Planting

The planting of trees on the earthflow surface would decrease the amount of bare ground, with the following advantageous effects:-

1. an increase in interception of rainwater, retaining it by wetting leaves, branches, trunks and eliminating water by evapotranspiration, which effectively lowers infiltration into the slope;

2. immobilises water that reaches the ground by the high retention capacity of vegetal debris on the ground surface, and;
3. a root system which would help establish the underflow, and create negative pore pressures by biological suction, increasing soil cohesion using water that would otherwise be part of the effective infiltration.

An adverse effect of planting may be surcharging the slope by large (heavy) trees.

(iv) Buttressing

The purpose of buttress or counterweight fills are to provide sufficient dead weight or artificially reinforced restraint near the toe of the unstable mass to prevent movement. Buttressing of the toe of the Grave Earthflow would be difficult due to the high batter slope which would have to be re-cut in the design of a retaining structure, and the retention of earthflow materials would be difficult due to the high movement rate which could cause overtopping of the structure by flow movements.

(v) Relocation of Highway

Relocating the highway to avoid the unstable slope would be the most permanent, but also probably the most expensive solution. Two alternatives routes across Grave Creek gully are possible:-

1. Above the Earthflow: the main disadvantage of this route is that it would involve crossing Grave Creek further upstream than at present, increasing the distance the alternative road would traverse across highly sheared Greenland Group rock, and therefore increasing the risk of further slope instability problems;
2. High bridge across Grave Creek avoiding the gully entirely.

(vi) Maintaining the Present Situation

At present, the policy of the Ministry of Works and Development is to clear the road right-of-way after material has moved on to the road pavement surface, pushing the debris on to the opposite side of the road which is building a large area of made ground and spoil. Another measure tried was

benching of the batter face at the toe, the purpose of this being to produce a large catchment area into which advancing debris would be collected, and thereby preventing material from blocking the road. However, this catchment area was not maintained and quickly infilled due to the acceleration of movement caused by unloading of toe support.

(vii) Recommendations

Based on the above engineering geological investigations and the potential remedial options reviewed, the following recommendations for controlling the Grave Earthflow are made:-

1. close planting of appropriate tree types on the bare ground within the earthflow complex;
2. the maintenance a small catchment area and drainage ditch between the toe of the flow and the road alignment;
3. continued monitoring of surface movement to allow the effectiveness of remedial measures to be assessed, to detect any future extension of the active movement area upslope, and to refine investigations of movement mechanisms;
4. further investigations, especially subsurface studies, after the effects of planting had decreased the effective infiltration of water permitting movement of heavy equipment on the weak slope materials and the construction of excavations without causing slope failure, with the following objectives:-
   a) to define the nature and geometry of the failure surface more precisely;
   b) to allow a quantitative analysis of instability;
   c) to allow installation of piezometers to monitor groundwater levels, and;
   d) to experiment with possible horizontal and vertical gravity drains and counterfort drains.

6.5 SLOPE MOVEMENT ON CRETACEOUS-TERTIARY HILL COUNTRY

6.5.1 Objectives

Cretaceous-Tertiary Hill Country can be divided into two different geomorphic settings:-

1. catchment slopes of coastal streams, and;
2. sea eroded coastal slopes.

Engineering geological investigations at Grave Creek, an example of the first type of geomorphic setting, identified a number of important factors which contributed to slope instability and are considered relevant to the stability of Cretaceous-Tertiary Hill Country as a whole. The objectives of this section are to:-

1. summarise the causes of slope instability at Grave Creek in a slope evolution model;
2. describe other slope movements occurring on Cretaceous-Tertiary Hill Country in the second type of geomorphic setting, and;
3. discuss the implications of this slope instability to future forest management of Cretaceous-Tertiary Hill Country.

6.5.2 Slope Evolution of Grave Creek

The slope evolution model interpreted for the Grave Creek study site is presented in Figure 6.24. The model summarises the series of processes and events which have formed the present geomorphology of Grave Creek, and indicates how the Grave Earthflow evolved as part of this system. The model identifies three key elements of this geomorphic setting which are considered relevant to the slope instability of all Cretaceous-Tertiary Hill Country:-

1. major faulting has decreased the shear strength of the rock mass producing weak fault zone materials;
2. sea erosion since the last glacial period has produced steep coastal slopes and seacliffs, and;
3. rapid stream incision since the last glacial advance has deeply dissected coastal catchment slopes producing steep, high slopes.

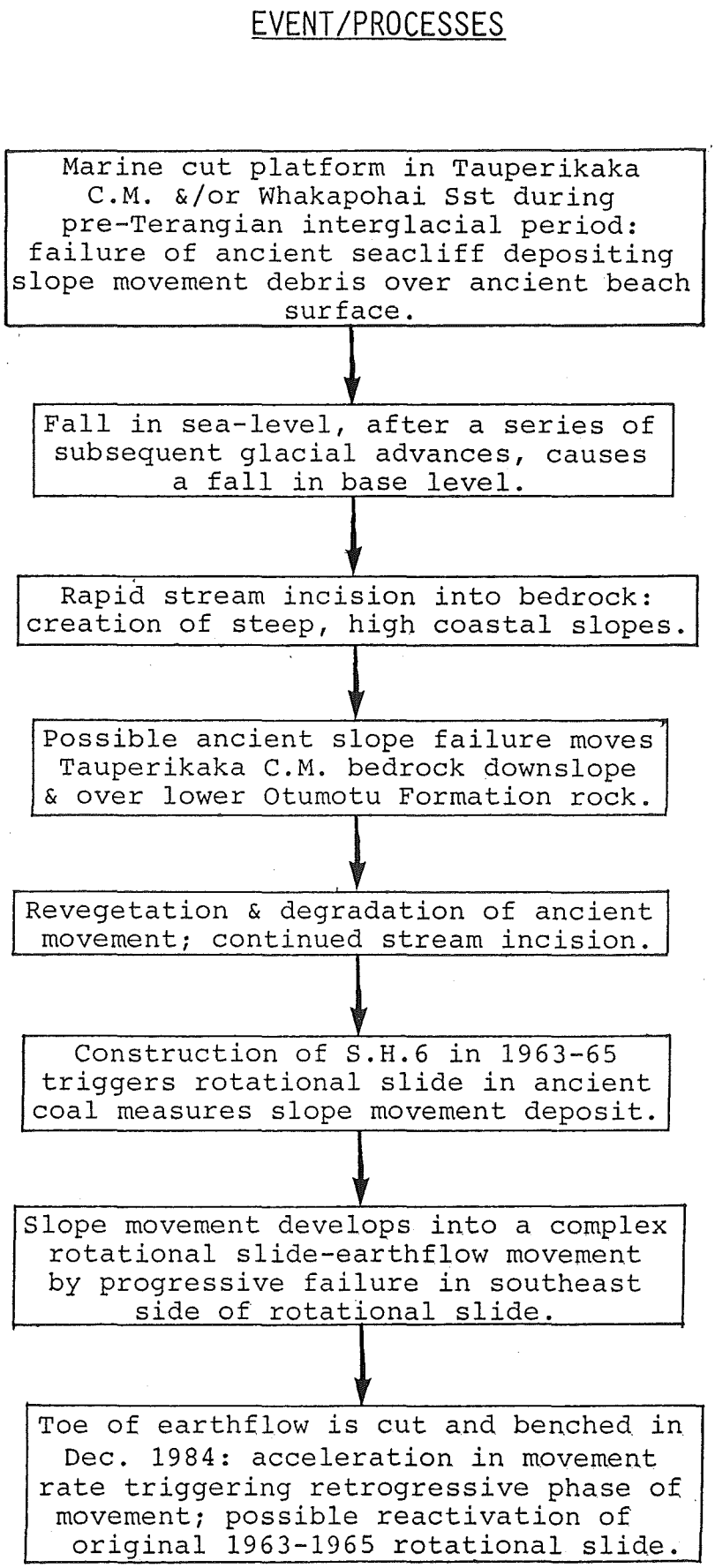

Fig. 6.24 Slope evolution model for Grave Creek.

6.5.3 Slope Movement on Coastal Slopes

This section describes slope movement features between Otumotu Point (S77/032343) and Flaggy Point (S77/058356), which are located north of the Moeraki River mouth, on sea eroded coastal slopes, in the second type of geomorphic setting. Three slope movement types are operating on these slopes:-

1. rock fall;
2. shallow debris slide, and;
3. rock slide.

(i) Rock Fall & Shallow Debris Slide

The most common mode of slope failure is rock fall on oversteepened seacliffs in Otumotu Formation and Tokakoriri Formation bedrock. Seacliffs in Otumotu Formation are not presently undergoing active sea erosion and are partly degraded and revegetated. Figure 6.25 illustrates rock fall in cobble conglomerate of the lower Otumotu Formation, which has been controlled by rock defect orientation.

Seacliffs in calcareous mudstone of the Tokakoriri Formation are undergoing active sea erosion, which undercuts the base of the slope causing defect controlled rock fall (Fig. 6.26a). Rock fall debris, which accumulates at the base of the slope, protects the cliff face from further erosion and oversteepening, thereby allowing the slope to grade to a more stable angle (Fig. 6.26b). In places this ancient, degraded seacliff slope setting has accumulated a surficial layer of regolith/colluvium which undergoes shallow debris slide failure along the regolith/colluvium - bedrock interface (Fig. 6.26c).

(ii) Flaggy Point Rock Slide

On the northwestern side of Flaggy Point a deep-seated rock slide has occurred on coastal slopes along a carbonaceous mudstone layer which is interpreted as a low angle thrust fault between Tokakoriri Formation and lower Abbey Formation limestone (M. Aliprantis pers. comm.) (Figs 6.27 & 6.28). Movement was by translational sliding of a single block of calcareous mudstone of the Tokakoriri Formation over lower Abbey Limestone, creating a 2-4m deep graben at the head of

Fig. 6.25 Rock fall in lower Otumotu Formation bedrock on seacliffs north of Otumotu Point.

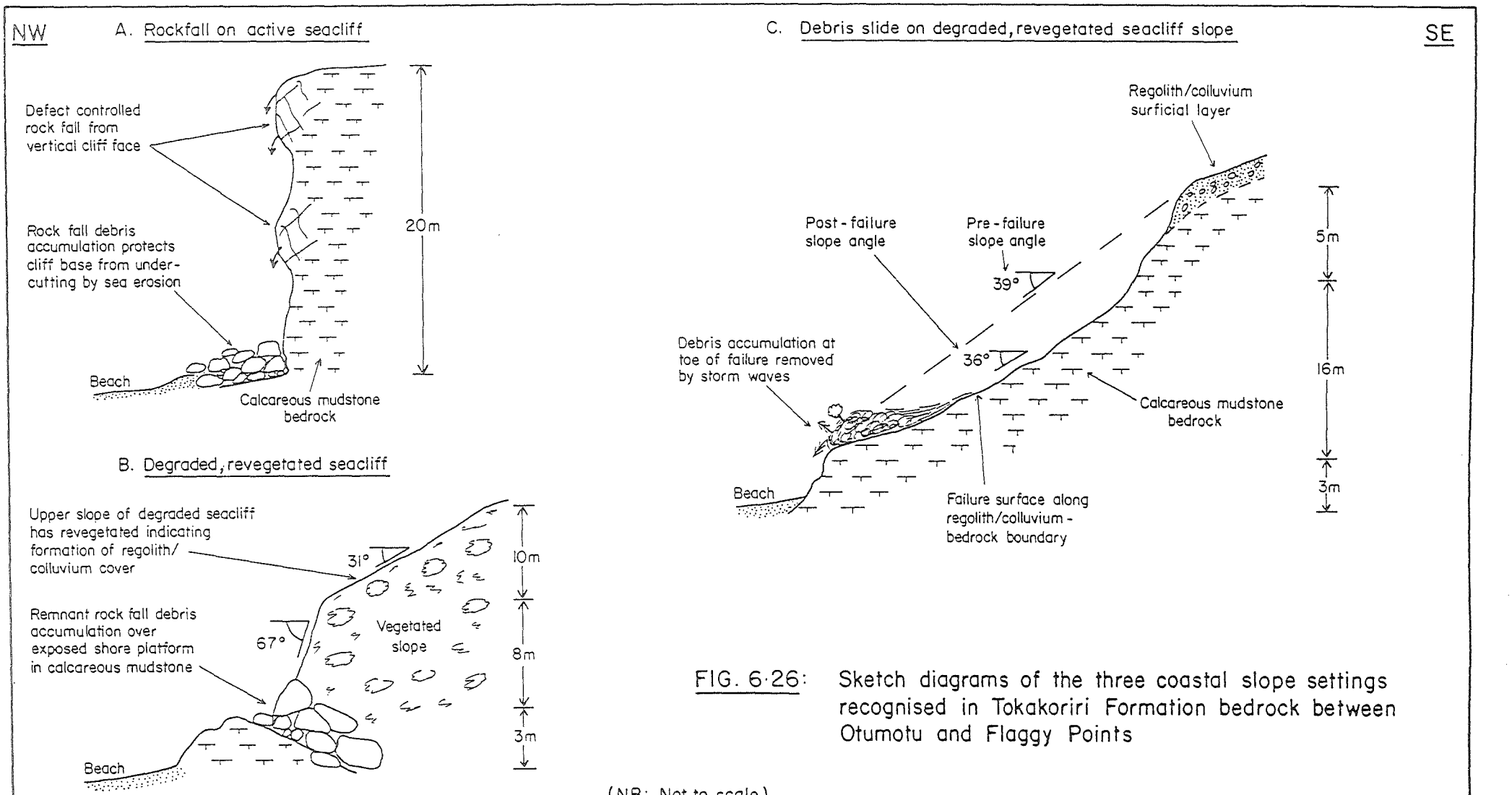

FIG. 6·26: Sketch diagrams of the three coastal slope settings recognised in Tokakoriri Formation bedrock between Otumotu and Flaggy Points

(NB: Not to scale)

Fig. 6.27 Rock slide on coastal slopes at Flaggy Point. Oblique view looking east.

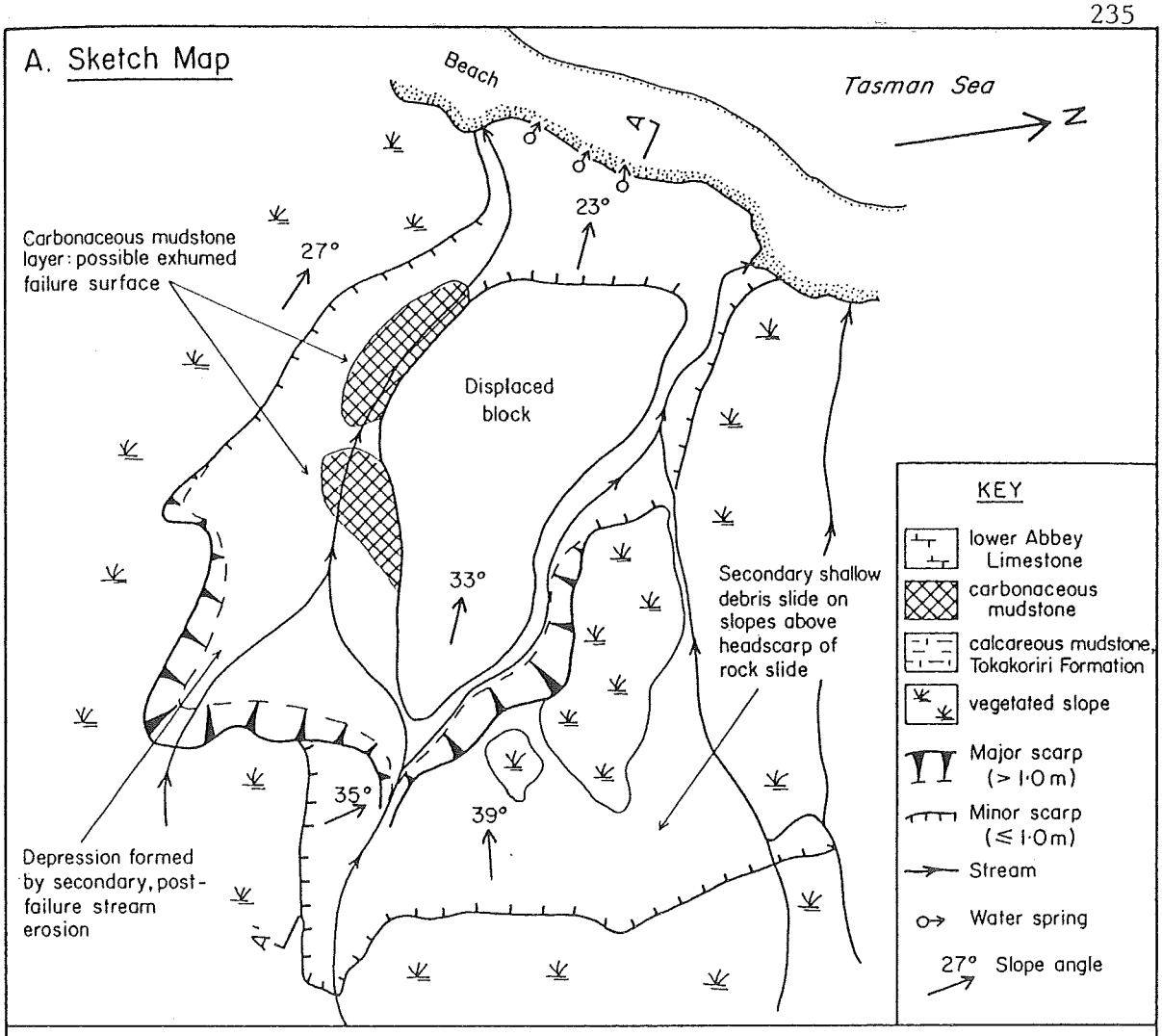

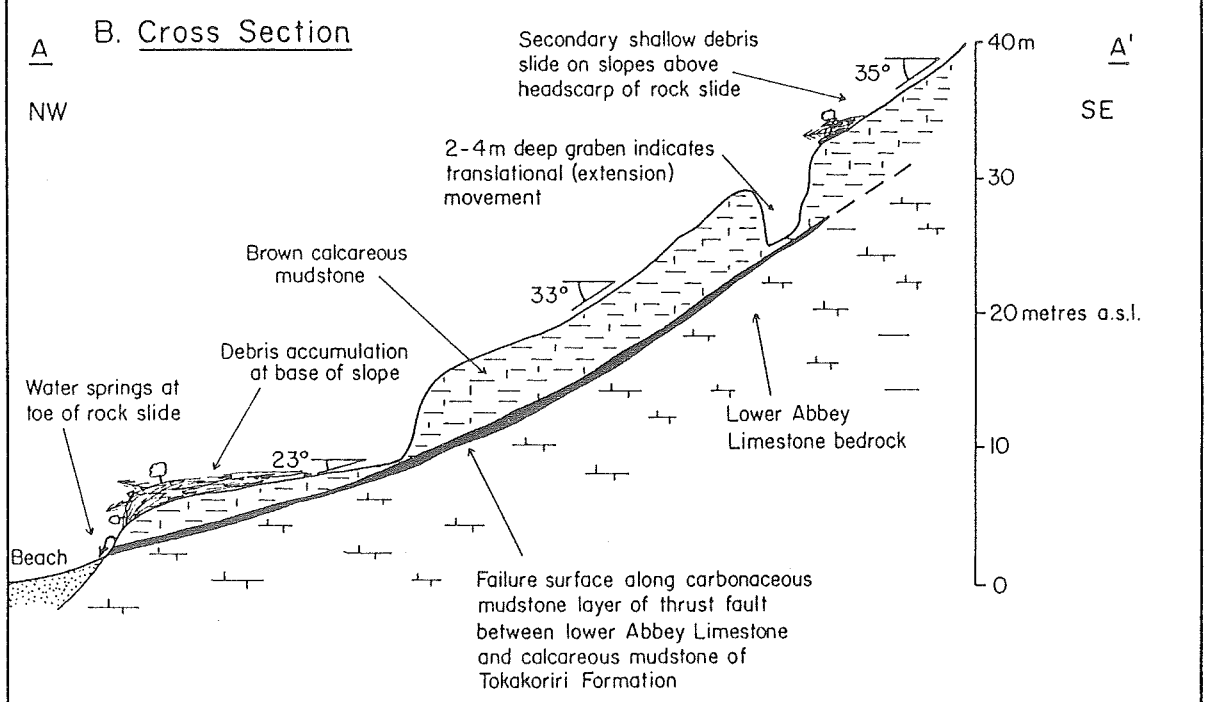

SCALE 1:1000 (approx.)

0 10 20 30 40

Metres

FIG. 6·28 Sketch diagram of the Flaggy Point rock slide

the failure. The carbonaceous mudstone thrust fault acts as an aquifer, this being evidenced by a line of water springs that emerge from the toe of the slope at beach level.

Above the main slide failure a number of secondary "sympathetic" shallow debris slide movements have occurred along the regolith/colluvium - bedrock interface. These post-date the rock slide movements, and were triggered in response to changes in slope conditions caused by the initial deep-seated movement, such as the removal of basal toe support and oversteepening of the slope.

6.5.4 Implications For Future Forest Management

The purpose of this section is to provide an overview of slope movement potential on Cretaceous-Tertiary Hill Country that is adequate for development planning at the resource allocation level of evaluating slope movement on forest lands. Table 6.4 summarises the slope movement types recognised and the slope angles at which they occurred for the two geomorphic settings recognised in Cretaceous-Tertiary Hill Country.

Shallow debris slide failures were found to occur in both types of geomorphic settings on slopes as low as 30^{o}, and in all Cretaceous-Tertiary bedrock types. Fundamental causes of failure are oversteepened slopes and removal of underlying support, for example by road construction at Grave Creek, or by sea or stream erosion while, the main triggering mechanisms are inferred to be high intensity rainstorms and seismic ground shaking. Rock fall occurs on coastal seacliffs (steeper than 65^{o}) as a result of the removal of underlying support by sea erosion, and a consequent decrease in rock mass strength along defects.

The most important slope movement process in terms of forest management and slope movement potential is the occurrence of deep-seated failures such as the Grave Earthflow and the Flaggy Point Rock Slide. The fundamental causes of both these failures is the presence of large-scale fault structures which have produced weak fault zone materials, this lowering the strength of slope forming materials. Critical slopes in these materials may be triggered move by a number of mecha-

GEOMORPHIC SETTING	SLOPE MOVEMENT TYPE	SLOPE ANGLE
A. Catchment slopes of coastal streams	Rotational slide - earthflow	27^0
	Shallow debris slide	30^0
B. Sea-eroded coastal slopes	Rock fall	$>65^0$
	Shallow debris slide	$36-39^0$
	Rock (block) slide	33^0

Table 6.4 Summary of geomorphic settings and slope movement types in Cretaceous-Teriary Hill Country.

nisms including removal of underlying support, high intensity rainstorms, or seismic ground shaking.

The potential of Cretaceous-Tertiary Hill Country to fail by the above slope movement processes is governed by the following factors:-

1. distribution of fault-derived slope materials, and;
2. slope steepness.

Due to the intense faulting in Cretaceous-Tertiary bedrock and the highly dissected hill country which they form, this landform type is regarded as having a high potential for slope instability, and is recommended as not being suitable for large-scale timber harvesting operations (clear-felling and selective logging, including road development). Impacts of small-scale bush-mill harvesting systems, however, are not very well known. Removal of a single tree or small groups of trees is unlikely to cause slope failure unless on very steep ground (>45^{o}) and/or fault zone bedrock materials. This type of activity maybe feasible and should be considered for development planning for Cretaceous-Tertiary Hill Country.

6.6 SYNTHESIS

Two geomorphic settings were recognised in Cretaceous-Tertiary Hill Country within which specific slope movement mechanisms are operating:-

1. Catchment slopes of coastal streams
   a) Rotational slide-earthflow;
   b) Shallow debris slide;
2. Sea-eroded coastal slopes
   a) Rock fall;
   b) Rock slide;
   c) Shallow debris slide.

The Grave Earthflow, located within the first type of geomorphic setting, was triggered by construction of State Highway 6 in 1963-1965, as a result of removal of underlying support. Failure is taking place by a complex rotational slide-earthflow type of movement along a zone of basal sliding within grey mud material derived from faulting in lower Otumotu Formation bedrock. Ground surface movement monitoring

investigations measured a high rate of movement at the toe (419cm/year), which is causing problems with slide debris moving on to the road pavement surface and blocking the right-of-way. Remedial options recommended include:-

1. close planting of appropriate tree types on the bare ground within the earthflow complex to decrease the effective infiltration;
2. maintenance of a small catchment area between the toe and road surface to catch debris;
3. continued monitoring of surface movement, and;
4. further investigations to define the nature and geometry of the failure surface more precisely, and to experiment with dewatering techniques.

Engineering geology investigations at Grave Creek and reconnaissance level investigations of slope instability on Cretaceous-Tertiary Hill Country identified two main factors which control slope movement potential on this landform type:-

1. intense faulting in Cretaceous-Tertiary bedrock, which has produced widely distributed weak fault zone materials, and;
2. highly dissected hill country, created by deep stream incision and sea erosion, have produced steep, high slopes which increased the shear stress on slope-forming materials.

Based on this high potential for slope instability, it is recommended that large-scale timber harvesting operations (clear-felling and selective logging, including road development) are not suitable activities on Cretaceous-Tertiary Hill Country. However, small-scale bush milling activities may be feasible, but are dependent on project planning investigations (the next level of investigation) adequately defining specific site conditions, especially the distribution of fault zone materials and slope steepness, to be sufficiently stable to allow this type of operation to be carried out.

CHAPTER SEVEN

SUMMARY AND CONCLUSIONS

7.1 ENGINEERING GEOLOGY INVESTIGATIONS AND METHODOLOGY

The purpose of this thesis study was to investigate the geological nature and origin of slope instability on three landform types in South Westland, which had been identified by FRI landform studies as having major slope instability problems that could influence or limit future forest operations. The scope of the study was limited to the resource allocation phase of forest land management activity, which provides an overview of slope movement potential adequate for development planning.

Field reconnaissance was carried out to investigate each of these three landform units regionally, and on the basis of this preliminary fieldwork one site on each of these three landform types was selected for detailed investigation. Selection was influenced by geomorphic setting, severity of the slope instability problem, bedrock exposure and accessibility. The three landform units and the selected study sites were:-

1. Greenland Group Hill Country - Boulder Creek;
2. Alpine Fault Zone Slopes - Havelock Creek;
3. Cretaceous-Tertiary Hill Country - Grave Creek.

Engineering geology site investigations were divided into three stages:

1. Engineering Geology Field and Laboratory Studies, which involved collection of data on bedrock geology and basic geotechnical properties, surficial geology, slope morphology, slope movement features and hydrogeology. The main purpose of this stage of the investigation was to identify the slope settings within which slope failure was occurring;

2. Assessment of Slope Movement Processes operating within each slope setting identified, incorporating interpretative information on slope movement types, mechanisms and factors contributing to failure;
3. Assessment of Slope Instability using qualitative methods.

Slope movement on each landform type was assessed by discussing the slope evolution of the respective study site, summarising slope movements elsewhere on the landform (based on preliminary reconnaissance field work), and finally by discussing possible implications the slope instability may have to future forest management of the particular landform unit.

7.2 SLOPE FAILURE MECHANISMS

7.2.1 Greenland Group Hill Country: Boulder Creek

Boulder Creek, located in the glaciated Moeraki River valley, was chosen as the investigation site for Greenland Group Hill Country primarily because of the high severity of the slope instability problem. Engineering geological mapping identified three main slope settings within which specific slope failure mechanisms are operating.

(i) Slopes in Intact Hornfelsed Sandstone

Intact hornfelsed sandstone bedrock, composed dominantly of moderately spaced, moderately persistent closed joints, outcrops in isolated rock buttresses. These slopes fail by rock (topple-) fall and planar rockslide, both of these movement types reflecting the importance of rock mass defects in controlling failure.

(ii) Slopes in Crushed Hornfelsed Sandstone

Crushed hornfelsed sandstone bedrock consists of closely spaced, very low persistence open joints producing a loose rock mass consisting of angular blocks up to 500mm equivalent cube size surrounded by a matrix of loose coarse sand. The origin of this crushed rock mass is attributed to a combination of tectonic deformation, disruption by ongoing

rock creep, and disturbance by large-scale, ancient slope movements. Apart from rock creep, slopes in crushed bedrock fail by debris fall, which involves the gravitational downslope movement of individual blocks or groups of blocks moving independently by leaping, bouncing or rolling; and by debris slump/slide-avalanche which involves circular or planar sliding of the closely jointed or fractured rock mass which may disintegrate into an avalanche-type movement involving sliding, flowing and falling of blocks.

(iii) Slopes in Tectonic Breccia

Tectonic breccia and fault gouge material, formed by tectonic deformation of the rock mass within two major fault zones, fails by debris slump/slide-avalanche.

Reconnaissance preliminary fieldwork recognised shallow debris slide-avalanche of the regolith/colluvium surficial cover, commonly along the regolith/colluvium-bedrock interface, as the dominant slope failure mechanism on Greenland Group Hill Country. Boulder Creek is an exceptional example of slope instability on this landform unit, explained by the oversteepened sides of the glaciated Moeraki River valley in fault-crushed bedrock.

7.2.2 Alpine Fault Zone Slopes: Havelock Creek

The five slope settings identified at Havelock Creek were combined into three groups within which specific slope movement mechanisms are operating, viz:-

(i) Slopes in Intact Schist

Intact garnet-biotite schist bedrock fails by rock falls in eroding stream banks, shallow debris slides in the regolith/colluvium cover and deep-seated rockslides.

(ii) Slopes in Crushed Schist and Mylonite Schist

Crushed schist and altered mylonite schist bedrock, consisting of very closely spaced, low persistence, open and closed joints, was created by tectonic deformation from Alpine Fault movements. This weakened bedrock material fails by large-scale rock (block) slides involving translational extension downslope along a complex step-like failure surface,

debris slide-avalanches, and debris falls of loosened blocks.

(iii) Slopes in Tectonic Breccia and Fault Gouge

Slopes in tectonic breccia and fault gouge are restricted to shallow debris slide failures in the regolith/colluvium surficial cover and debris flows in saturated regolith/colluvium material and underlying puggy breccia or gouge bedrock.

Alpine Fault Zone slopes were divided into two geomorphic settings, catchment slopes of streams which cross or flow along the fault zone, of which Havelock Creek is an example, and fault-bounded mountain front slopes. Debris slide-avalanche failures were the most common movement type identified with most failures occurring within the first geomorphic setting (catchment slopes).

7.2.3 Cretaceous-Tertiary Hill Country: Grave Creek

The Grave Earthflow was chosen as the main investigation site for Cretaceous-Tertiary Hill Country, based on preliminary reconnaissance fieldwork which recognised Grave Creek as having a geomorphic and geologic setting considered typical for this landform unit. This setting has contributed to the initiation of the earthflow failure causing maintenance problems for State Highway 6, which is directly relevant to forest management activities. The earthflow was triggered by construction of State Highway 6 in 1963-65, with failure taking place by a complex rotational slide-earthflow type of movement along a zone of basal sliding within grey mud material derived from faulting in lower Otumotu Formation bedrock.

Cretaceous-Tertiary Hill Country was divided into two different geomorphic settings, catchment slopes of coastal streams (of which Grave Creek is an example) and sea-eroded coastal slopes. Slope movement types occurring in the second type of geomorphic setting were identified as rock falls on oversteepened seacliffs, shallow debris slides in the regolith/colluvium surficial layer on degraded seacliff slopes, and deep-seated rockslides along zones of weakened fault-zone material.

7.3 CAUSES OF SLOPE FAILURE

7.3.1 Fundamental Causes

Fundamental causes of slope instability can be divided into factors which have contributed to an increase in the total shear stress and factors which have contributed to a reduction in the total shear strength of slope forming materials. Both of these types of factors were found to be important in contributing to all slope failures recognised.

Reduction in total shear strength of slope forming materials is due to the crushed and fractured nature of the rock mass caused by:-

1. tectonic deformation within fault zones;
2. disruption of the rock mass by rock creep, and;
3. disruption of the rock mass by large-scale, deep-seated ancient slope movements.

Increase in total shear stress on slope forming materials by the removal of lateral and underlying support of slopes as a result of deep stream incision and coastal sea-erosion, the rate of which is in turn controlled by:-

1. weak crushed rock mass and fault-zone materials, and;
2. (local) base level changes induced by tectonic uplift and sea level changes since the last glaciation.

7.3.2 Triggering Mechanisms

Slope failures on critical slopes are interpreted to be triggered by three main mechanisms:-

1. High intensity rainstorm events where increased water infiltration into a slope causes a reduction in pore suction (negative pore pressure) in unsaturated material, or an increase in positive pore pressures in saturated material, resulting in a decrease in the effective normal stress;
2. Seismic events where earthquake shaking produces transitory earth stresses which increases the total shear stress acting on slope materials;
3. Undercutting of critical slopes by stream erosion or road construction, which removes underlying support.

Large-scale, deep-seated slope movement types such as rock (block) slides were inferred to be triggered by relatively infrequent seismic events, whereas the more commonly occurring shallow debris slide-avalanche failures were interpreted, and observed, to be triggered by high intensity rainstorm events.

7.4 CONCLUSIONS

7.4.1 Current Slope Instability

FRI landform studies analysed historical aerial photograph records extending back to 1947 in an attempt to outline the recent erosion history of South Westland. In general, the investigation concluded that both individual and groups of slope instability features develop very rapidly and active instability periods occur in short-lived episodes. Revegetation of slope movement scars is rapid with a good cover over scar surfaces within five years after a failure event. Rainfall data indicate an approximate correlation of instability and the incidence of heavy precipitation periods. Currently, Greenland Group Hill Country and Alpine Fault Zone slopes are undergoing a period of increased slope activity, in the case of Boulder Creek beginning sometime during the 1950's whilst Havelock Creek commenced increased activity in the late 1970's (approximately 1978).

Engineering geological investigations identified a number of large-scale, deep-seated ancient slope movements at each study site which indicate past slope activity. These large-scale, infrequent movements are inferred to be caused by discrete seismic events due to their high magnitude and low frequency nature, causing large-scale infrequent slope activity.

7.4.2 Implications for Forest Management

(i) Resource Allocation Evaluation

The scope of this study was limited to resource allocation, the first level of evaluating slope movements on forest lands, which provides an overview of slope movement potential

adequate for development planning. The potential of South Westland slopes to undergo slope failure is governed by the occurrence of factors which contribute to failure, which can be summarised as follows:-

1. distribution of weak fault zone materials and crushed and fractured rock mass, and;
2. slope steepness.

In all three landform units investigated (Greenland Group Hill Country, Alpine Fault Zone slopes and Cretaceous-Tertiary Hill Country) both these factors are important; faulting is intense, being the most important structural style in South Westland bedrock, and the hill country is highly dissected, caused by rapid stream incision induced by tectonic base level changes. The potential for slope movement on these landform units, based on the high incidence of both these factors, is therefore high as evidenced by the high occurrence of natural episodic instability.

On both Greenland Group Hill Country and Alpine Fault Zone slopes, the most commonly occurring slope movement type was found to be debris slide-avalanche in the regolith/colluvium surficial cover and/or crushed bedrock (hornfelsed sandstone, mylonite schist, or unaltered schist bedrock types). The steepest slope that could be logged without causing failure would correspond to the slope angle at limiting equilibrium (FS = 1.0) under the worst groundwater conditions (saturated slope).

Geotechnical assessment of crushed hornfelsed sandstone slopes suggest a critical slope angle for debris slump/slide-avalanche of around 30^{o} under saturated conditions, whilst crushed mylonite schist and crushed unaltered schist slopes fail by debris slide-avalanche on slopes over 32^{o}, based on field observations of natural failures. Slopes in puggy tectonic breccia and fault gouge materials fail dominantly by shallow debris slide and debris flow movements which occur on slopes over 20^{o}.

In Cretaceous-Tertiary Hill Country, deep-seated failures (rotational slide-earthflows, rock slides) in fault zone bedrock materials are the most important slope movement processes in terms of production management activities and were observed to occur in slopes over 27°.

A number of general statements can be concluded from this qualitative assessment of slope instability which are relevant to any production forestry management type activity:

1. Slope movement potential on forest lands in South Westland is primarily governed by:
   a) condition of the bedrock, and;
   b) slope steepness.
2. Due to the intense faulting of all bedrock types and highly dissected hill country, Greenland Group Hill Country, Alpine Fault Zone slopes and Cretaceous-Tertiary Hill Country are all regarded as highly unstable landform units and are unsuitable for large-scale (clear-felling, selective logging and associated road development) production management forestry activities.
3. Small-scale timber harvesting systems (bush-mill logging) may be applicable to Cretaceous-Tertiary Hill Country and Greenland Group Hill Country landform units and should be considered for development planning for this type of activity.
4. Alpine Fault Zone slopes, due to their steepness and fault-altered bedrock, should be managed by protection forestry methods.

(ii) Recommendations

It is proposed that evaluation of slope instability on forest lands follows the system of providing information at three levels of land management activities:-

1. Resource allocation;
2. Project planning;
3. Critical site stabilisation.

This study has provided information at the resource allocation phase, and also a preliminary assessment at the project planning level, delineating areas susceptible to slope movements and assessing the severity of instability identified

by reconnaissance investigations. Based on this information, the following recommendations can be made whether to limit development or to continue to more detailed level 2 and level 3 evaluation:-

1. Alpine Fault Zone slopes should be limited to protection forestry management practices and no timber extract activities be planned for these slopes.
2. Greenland Group Hill Country and Cretaceous-Tertiary Hill Country should be evaluated for transport planning, timber harvesting techniques and route locations so critical sites can be isolated along several routes where level 3 analysis will have most benefit. It is further recommended that small-scale (bush-mill) harvesting methods are the most suitable and should be given priority for investigation.

7.4.3 Engineering Geological Approach to Evaluating Slope Instability on Forest Lands

Engineering geology methods of investigation and data presentation can make a valuable contribution towards the evaluation of slope movement potential on forest lands, dividing investigations into 5 stages:-

1. Reconnaissance and Selection

At the resource planning level, reconnaissance of forest lands delineating the areas or landforms which are susceptible to slope movement on a broad scale, enabling selection of study site(s) for stage 2 investigations.

2. Feasibility Investigations

Collection of field and laboratory information to allow an assessment of areas of instability identified during reconnaissance investigations. This enables decisions to be made at the project planning stage on whether to limit development or continue to level 3 investigations, to allow evaluation of alternative timber harvesting techniques and route locations, and to isolate critical sites along selected routes for level 3 studies.

3. Design Investigations

The geotechnical design of slope and road stabilisation measures at selected sites, as part of the level 3 critical site evaluation.

4. Construction/Harvesting Investigations

Monitoring of slopes and roads during harvesting operations to confirm satisfactory design performance of stabilisation measures.

5. Post-Construction/Harvesting Investigations

Design and implementation of remedial stabilisation measures after completion of harvesting to ensure the sustained stability of slopes until reforestation is complete.

ACKNOWLEDGEMENTS

Many people and organisations have assisted me in the preparation of this thesis to whom I am very grateful. In particular, the following people deserve special thanks.

N.Z. Forest Service for providing funding for the project through the South Westland Management Evaluation Programme. Special thanks go to Mike Orchard, John Pfaflert, Doug McNabb, the late Kirk Gleason (NZFS Hokitika), Dave Hilliard (NZFS Harihari), and John Mead (NZFS Haast).

Colin O'Loughlin (FRI) for assistance in establishing the project and for encouragement and guidance throughout.

Simon Nathan for introducing me to South Westland and for helping with countless problems.

To my supervisors Dave Bell and Jarg Pettinga for guidance and patient editing of drafts.

Simon Pease (MWD Greymouth) for assisting with the initial survey of the Grave Earthflow, and Peter Hardie (MWD Haast) for giving me a guided tour of State Highway 6 and for enlightening me on the numerous problems in maintaining the road.

To the technicians of the Geology Department who assisted in their various fields of expertise, especially to Chris Thornley who kindly made available his computer when all seemed lost.

Sean, John, Mike, Dave, Mark, and Udo (the South Westland "geology crew") for the great times and the many memories.

Ron and Toni Hoglund (Lakeside Motels, Lake Paringa) for providing a comfortable field base and useful local information and for the many hours of yarns.

To the many people who assisted me with surveying, often in "uncomfortable" conditions; especially Tim, Peter, Mal, Mark, Mike J., Mike S., and Andrea.

Mike J., Helen, Peter, and Janet for pulling me out of the muck at the end.

A special thanks to Andrea, for her tolerance, encouragement, and many hours of help, and to Sarah, for helping me put the whole thing in perspective and for being a great flatmate.

REFERENCES

ACKROYD, P. 1985: Engineering geology investigations of a proposed road alignment, Lake Wanaka, Central Otago. Unpublished M.Sc. thesis, Geology Department, University of Canterbury.

ADAMS, C. J. D. 1975: Discovery of Precambrian rocks in New Zealand: age relations of the Greenland Group and the Constant Gneiss, South Island. Earth and Planetary Science Letters 28: 98-104.

ADAMS, C. J. D. 1979: Age and origin of the Southern Alps. In: Walcott, R.I. & Cresswell, M.M. (eds), The Origin of the Southern Alps. Royal Society of New Zealand Bulletin 18: 73-78.

ADAMS, D. in prep.: The Cretaceous and Eocene Geology of South Westland. M.Sc. in geology, University of Canterbury.

ADAMS, J. 1980: Contemporary uplift and erosion of the Southern Alps, New Zealand. Geological Society of America Bulletin 91: 1-114.

ADAMS, J. 1984: Large-scale tectonic geomorphology of the Southern Alps, New Zealand. Tectonic Geomorphology, M. Morisawa and J. T. Hack (eds), Proceedings of the 15th Annual Binghamton Geomorphology Symposium September 1984: 105-128.

ALIPRANTIS, M. A. in prep.: Tertiary geology of the Paringa area, South Westland, with special attention to a structurally complex region. M.Sc in geology, University of Canterbury.

BELL, D. H. 1976: High intensity rainstorms and geological hazards: Cyclone Alison, March 1975, Kaikoura, New Zealand. Bulletin of the International Association of Engineering Geology 14: 189-200.

BELL, D. H. and PETTINGA, J. R. 1983: Presentation of geological data. Proceedings of the Symposium Engineering for Dams and Canals, New Zealand Geomechanics Society and New Zealand Society on Large Dams, Institute of Professional Engineers of New Zealand, Proceedings of Technical Groups 9 Issue 4(G): 4.1-4.36.

BOLITHO, W. J. 1937: Report on prospecting operations at Paringa, South Westland. Unpublished report, New Zealand Geological Survey, held on file G36/263.

BRAND, E. W. 1981: Some thoughts on rain-induced slope failures. Proceedings of the 10th International Conference on Soil Mechanics and Foundation Engineering 3: 373-376.

BULL, W. B. 1963: Alluvial-fan deposits in western Fresno County, California. Journal of Geology 71: 243-251.

CARTER, R. M. and NORRIS, R. J. 1976: Cainozoic history of southern New Zealand, an account between geological observations and plate-tectonic predictions. Earth and Planetary Science Letters 31: 85-94.

COOPER, A. F. 1974: Multiphase deformation and its relationship to metamorphic crystallisation at Haast River, South Westland, New Zealand. Journal of Geology and Geophysics 17(4): 855-880.

COOPER, A. F. and REAY, A. 1983: Lithology, field relationships, and structure of the Pounamu Ultramafics from the Whitcombe and Hokitika Rivers, Westland, New Zealand. New Zealand Journal of Geology and Geophysics 26(4): 359-80.

COOPER, R. A. 1974: Age of the Greenland and Waiuta Groups, South Island, New Zealand (Note). New Zealand Journal of Geology and Geophysics 17(4): 955-62.

COTTON, C. A. 1956: Coastal history of Southern Westland and northern Fiordland. Transactions of the Royal Society of New Zealand 83: 483-8.

COX, A. 1877: Report on the Westland district. New Zealand Geological Survey Report on Geological Exploration 1874-76 9: 63-93.

DEPARTMENT OF LANDS & SURVEY 1984: Register of Protected Natural Areas in New Zealand. Head Office, Wellington, New Zealand, 468p.

EGGERS, M. J. 1984: Notes on Alpine Fault traverses between Robinson and Wrong Creeks, Mataketake Range, South Westland. Unpublished report, New Zealand Geological Survey, Christchurch Office file G37/831.

FINDLAY, R. H. 1979: Summary of structural geology of Haast Schist terrain, Central Southern Alps, New Zealand: implications of structures for uplift and deformation within Southern Alps. In: Walcott, R.I. & Cresswell, M.M. (eds), The Origin of the Southern Alps. Royal Society of New Zealand Bulletin 18: 113-120.

FITZSIMONS, S. and O'LOUGHLIN, C. 1984: A classification of landform types and implications for forest management between the Cook and Paringa Rivers, South Westland. Forest Research Institute, Christchurch.

FITZSIMONS, S., O'LOUGHLIN, C. and EGGERS, M. J. 1985: Classification of landform types and implications for forest management between the Paringa and Haast Rivers, South Westland. Forest Research Institute, Christchurch.

GAIR, H. S. 1967: Sheet 20, Mt Cook, 'Geological Map of New Zealand 1:250 000'. New Zealand Department of Scientific and Industrial Research.

GAIR, H. S. and GREGG, D. R. 1962: Geology of the Whakapohai River to Bullock Creek section of the Paringa -Haast road. Unpublished report, New Zealand Geological Survey, Christchurch office files.

GEOLOGICAL SOCIETY 1972: The preparation of maps and sections in terms of engineering geology: report by the Geological Society Engineering Group Working Party. Quarterly Journal of Engineering Geology 5: 293-381.

GRIFFITHS, G. A. 1979: High sediment yields from major rivers of the Western Southern Alps, New Zealand. Nature 282(1): 61-63.

GRIM, R. E. 1953: Clay Mineralogy. McGraw-Hill Publishing Co. Ltd, London, 384p.

GRINDLEY, G. W. 1963: Structure of the Alpine Schists of South Westland, Southern Alps, New Zealand. New Zealand Journal of Geology and Geophysics 6: 872-930.

HAAST, J. von. 1879: 'Geology of the Provinces of Canterbury and Westland, New Zealand'. Times Office, Christchurch, 486p.

HALKETT, J. C. 1985: South Westland Management Evaluation Programme Reports and Technical Liason Committee Matters. Letter from Head Office, New Zealand Forest Service, Wellington.

HAYWORD, J.A. 1980: Hydrology and stream sediment from Torlesse Stream Catchment. Tussock Grasslands and Mountain Lands Institute Special Publication No.17, 236p.

HESSELL, J. W. D. 1982: The climate and weather of Westland. New Zealand Meteorological Service Miscellaneous Publication 115(10).

HOEK, E. and BRAY, J. 1981: Rock Slope Engineering. The Institution of Mining and Metallurgy, Third Edition, 358p.

HOOKE, R. LeB. 1967: Processes on arid region alluvial fans. Journal of Geology 75: 438-460.

HUTCHINSON, J. N. 1968: Mass Movement. In: Encyclopedia of Geomorphology F.W. Fairbridge (ed.), Reinhold Book Corporation, New York, pp.688-95.

INTERNATIONAL ASSOCIATION OF ENGINEERING GEOLOGY 1981: Recommended symbols for engineering geological mapping: report by the International Association of Engineering Geology Commission on Engineering Geological Mapping. Bulletin of the International Association of Engineering Geology 24: 227-234.

LAIRD, M. G. 1972: Sedimentology of the Greenland Group in the Paparoa Range, West Coast, South Island. New Zealand Journal of Geology and Geophysics 15: 372-93.

LAIRD, M. G. and SHELLEY, D. 1974: Sedimentation and early tectonic history of the Greenland Group, Reefton. New Zealand Journal of Geology and Geophysics 17: 839-54.

LEWIS, D. W. 1984: Practical Sedimentology. Hutchinson Ross Publishing Company, 229p.

MAHR, T. 1977: Deep-reaching gravitational deformations of high mountain slopes. Bulletin of the International Association of Engineering Geology 16: 121-127.

MASON, B. 1961: Potassium-argon ages of metamorphic rocks and granites from Westland, New Zealand. New Zealand Journal of Geology and Geophysics 4(4): 352-356.

McNAUGHTON, D. A. and GIBSON, F. A. 1970: Reef play developing in New Zealand. Oil and Gas Journal 68(45): 89-95.

MORTIMER, G., NATHAN, S., DAWSON, R. M. and EGGERS, M. J. 1984: Geology of the lowland area between the Cook and Paringa Rivers, South Westland. New Zealand Geological Survey Report G81.

MOSS, A. J. 1972: Bed-load sediments. Sedimentology 18: 159-219.

MOSS, A. J. and WALKER, P. H. 1978: Particle transport by continental water flows in relation to erosion, deposition, soils and human activities. Sedimentary Geology 20: 81-139.

MOSS, A. J., WALKER, P. H. and HUTKA, J. 1980: Movement of loose, sandy detritus by shallow water flows: an experimental study. Sedimentary Geology 25: 43-66.

MUTCH, A. and McKELLAR, I. C. 1964: Sheet 19, Haast, 'Geological Map of N.Z. 1:250 000'. New Zealand Department of Scientific and Industrial Research.

NATHAN, S. 1977: Cretaceous and Lower Tertiary stratigraphy of the coastal strip between Buttress Point and Ship Creek, South Westland, New Zealand. New Zealand Journal of Geology and Geophysics 20(4): 615-54.

NATHAN, S. 1984: Notes on mylonitic rocks along the Alpine Fault between the Cook and Paringa Rivers. Unpublished report, New Zealand Geological Survey, Christchurch office files.

NATHAN, S. and MOAR, N. T. 1975: Late Quaternary terraces between Ship Creek and the Whakapohai River, South Westland, New Zealand. Journal of the Royal Society of New Zealand 5: 313-27.

NEW ZEALAND METEOROLOGICAL SERVICE 1973: Rainfall normals for New Zealand 1941 to 1970. New Zealand Meteorological Service Miscellaneous Publication 145.

NEW ZEALAND STANDARD 4402 1980: Methods of testing soils for civil engineering purposes: Part 1 soil classification and chemical tests. Standards Association of New Zealand, 91p.

NORTHEY, R. D., HAWLEY, J. G. and BARKET, P. R. 1974: Classification and mechanisms of slope failures in natural ground. New Zealand Institute of Engineers, Proceedings of the Symposium on Stability in Natural Ground, Nelson 1 Issue 5(G): 3.1-3.8.

O'LOUGHLIN, C. L. and PEARCE, A. J. 1976: Influence of Cenozoic geology on mass movement and sediment yield response to forest removal, North Westland, New Zealand. Bulletin of the International Association of Engineering Geology 14: 41-46.

PALMQUIST, R. C. and BIBLE, G. 1980: Conceptual modelling of landslide distribution in time and space. Bulletin of the International Association of Engineering Geology 21: 178-186.

PASCOE, J. (ed.) 1957: Mr Explorer Douglas. A.H. and A.W. Reed, Wellington, 331p.

PRANDINI, L., GUIDICINI, G., BOTTURA, J. A., PONCANO, W. L. and SANTOS, A. R. 1977: Behaviour of the vegetation in slope stability: a critical review. Bulletin of the International Association of Engineering Geology 16: 51-55.

PRELLITZ, R. W. 1985: A complete three-level approach for analysing landslides on forest lands. Proceedings of the International Symposium on Erosion, Debris Flow and Disaster Prevention, Tsukuba, Japan: 475-479.

PRELLITZ, R. W., HOWARD, T. R. and WILSON, W. D. 1983: Landslide analysis concepts for management of forest lands on residual and colluvial soils. Evaluating Strength Parameters of Simple Clays: Geotechnical Considerations of Residual Soils. Transportation Research Record 919: 27- 6.

ROGERS, N. W. and SELBY, M. J. 1980: Mechanisms of shallow translational landsliding during summer rainstorms: North Island, New Zealand. Geografiska Annaler 62A: 11-21.

SCOTT, C. R. 1980: An Introduction to Soil Mechanics and Foundations. Applied Science Publishers Ltd, Second Edition, 406p.

SEWARD, D. and SIBSON, R. H. 1985: Fission-track age for a pseudotachylite from the Alpine Fault, New Zealand. New Zealand Journal of Geology and Geophysics 28: 553-557.

SHARPE, C. F. S. 1938: Landslides and Related Phenomena. A Study of Mass Movements in Soil and Rock. Columbia University Press, New York, 137p.

SIBSON, R. H., WHITE, S. H. and ATKINSON, B. K. 1979: Fault rock distribution and structure within the Alpine Fault Zone: a preliminary account. In: Walcott, R.I. & Cresswell, M.M. (Eds), The Origin of the Southern Alps. Royal Society of New Zealand Bulletin 18: 55-65.

SLIVOVSKY, M. 1977: Gravitational deformations of valley slopes in tectonically fractured rock masses. Bulletin of the International Association of Engineering Geology 16: 114-118.

STAUFFER, M. R. 1966: An empirical-statistical study of three-dimensional fabric diagrams as used in structural analysis. Canadian Journal of Earth Sciences 3: 473-498.

STEWART, M. and NATHAN, S. in prep.: Pre-Tertiary basement rocks between the Mahitahi and Waita Rivers, South Westland. New Zealand Geological Survey report.

SUGGATE, R. P. 1963: The Alpine Fault. Transactions of the Royal Society of New Zealand, Geology 2: 105-129.

SUGGATE, R. P. 1968: The Paringa Formation, Westland. New Zealand Journal of Geology and Geophysics 11: 345-55.

SWANSTON, D. N. and SWANSON, F. J. 1976: Timber harvesting, mass erosion, and steepland forest geomorphology in the Pacific Northwest. In: Coates, D.K. (ed.) Geomorphology and Engineering, Chapter 10 pp.199-221.

TECHNICAL LIAISON COMMITTEE 1984: Terms of Reference. Appendix to minutes of Technical Liason Committee meeting 8 February 1984, Wellington, New Zealand.

TER-STEPANIAN, G. and GOLDSTEIN, M. 1969: Multistoried landslides and strength of soft clays. Proceedings of the 7th International Conference on Soil Mechanics and Foundation Engineering, Mexico II: 693-700.

TER-STEPANIAN, G. and TER-STEPANIAN, H. 1971: Analysis of landslides. Proceedings of the 4th Conference on Soil Mechanics, Budapest: 499-504.

TERZAGHI, K. 1950: Mechanism of Landslides. In: Paige, S. (ed.) Application of Geology to Engineering Practice, Geological Society of America, Berkley Volume, pp. 83-123.

VARNES, D. J. 1958: Landslide Types and Processes. In: Landslides and Engineering Practice, Highway Research Board Special Report 29: 20-47.

VARNES, D. J. 1978: Slope Movement Types and Processes. In: Landslides Analysis and Control (R.L. Schuster and R.J. Krizek eds), Transportation Research Board Special Report 176: 12-33.

VELDE, B. 1985: Clay Minerals: A physico-chemical explanation of their occurrence. Elsevier, 427p.

WARREN, G. 1967: Sheet 17, Hokitika, 'Geological Map of N.Z. 1:250 000'. New Zealand Department of Scientific and Industrial Research, Wellington.

WATERS, J. C. 1983: The geology of the Paringa River, South Westland. Diploma of Science Thesis (in geology), University of Otago.

WELLMAN, H. W. 1955: The Geology Between Bruce Bay and Haast River, South Westland. New Zealand Geological Survey Bulletin 48 (2nd ed.).

WELLMAN, H. W. and WILLETT, R. W. 1942a: The geology of the West Coast from Abut Head to Milford Sound - Part 1. Transactions of the Royal Society of New Zealand 71(4): 282-306.

WELLMAN, H. W. and WILLETT, R. W. 1942b: The geology of the West Coast from Abut Head to Milford Sound - Part 2. Glaciation. Transactions of the Royal Society of New Zealand 72(3): 199-219.

YOUNG, D. J. 1968: Engineering Geology of the Paringa -Haast section of State Highway Six, South Westland. New Zealand Journal of Geology and Geophysics 11(5): 1134-58.

APPENDICES

APPENDIX ONE

TECHNICAL LIAISON COMMITTEE
TERMS OF REFERENCE

TECHNICAL LIAISON COMMITTEE
TERMS OF REFERENCE

1. To identify the areas and topics of study and the level of information required to facilitate the formulation of recommendations to the Ministers of Lands and of Forests on the future management of Crown owned land in the South Westland moratorium area.

2. (a) To determine the agencies and disciplines that should be encouraged to participate in the study and to outline the research and survey programmes to be undertaken, paying attention to the need to avoid overlaps or deficiencies.

   (b) To promote the need for scientific investigations designed to understand and evaluate physical and biological features and processes on a regional basis, over all land irrespective of tenure.

3. To provide liaison between the agencies involved, and the Hokitika Steering Committee and Wellington-based decision makers.

(4. To monitor and co-ordinate overall progress of the programme to ensure that the integration of the information gathered is completed by June 1986.)

5. To recommend to the Ministers of Lands and of Forests, through the respective Director-General, a management strategy for the Crown owned forest and non-forest areas. The strategy should allow for the incorporation of new research information from time to time.

6. To ensure that the management strategy adequately recognises the requirements of the moratorium area in respect of:

(a) identifying and protecting representative natural ecosystems, particularly those of natural significance;

(b) ensuring that the importance of the mountain lands and soil and water protection is recognised;

(c) providing for the maintenance of wildlife habitat;

(d) recognising the constraints on productive development imposed by topography, climate, soils and geology;

(e) identifying forest available for timber production management and indicating the likely sustainable level of such production in accordance with the Indigenous Forest Policy (1977);

(f) identifying land suitable and available for agricultural developments;

(g) providing opportunities for recreation and tourism;

(h) comparing the regional benefits of productive development, both forestry and agriculture, and other land within the framework of the approved West Coast United Council Regional Planning Scheme.

7. To ensure that the agencies and Ministers involved are aware of the necessity for the provision of adequate staffing and finance to achieve the objectives established by the Officials Committee on Assistance Options, and endorsed by the Minister of forests. Plus any further objectives identified by the current study.

(Appendix to minutes of committee meeting held on Wednesday 8 February 1984, TLC SWMEP. TLC 1984)

APPENDIX TWO

ROCK AND SOIL DESCRIPTION TERMINOLOGY

A2.1 Engineering Geological Field Description for Rock Material

A2.2 Engineering Geological Field Description for Soil Material

A2.3 Terminology for Rock Mass Description

A2.4 Terminology for Soil Mass Description

ENGINEERING GEOLOGICAL FIELD DESCRIPTION FOR ROCK MATERIAL

WEATHERING

	TERM	GRADE	ROCK DESCRIPTION
1.	residual soil (RW)	VI	discolouration and complete transformation to soil; original fabric destroyed
2.	completely weathered (CW)	V	discolouration and transformation to soil; original fabric largely preserved
3.	highly weathered (HW)	IV	discolouration; discontinuities open and rock fabric affected by deep alteration; lithorelicts present
4.	moderately weathered (MW)	III	discolouration, discontinuities open with discolouration and alteration penetrating inwards; loss of strength
5.	slightly weathered (SW)	II	slight discolouration on open discontinuities; no loss of material strength
6.	unweathered (UW)	I	no discolouration or loss of strength, or any other effects due to weathering

STRENGTH

	TERM	POINT LOAD STRENGTH INDEX $I_s(50)$	FIELD ESTIMATION OF STRENGTH
1.	extremely strong (ES)	more than 10	can only be chipped with geological hammer
2.	very strong (VS)	3 to 10	several blows of hammer required to break hand specimen
3.	strong (S)	1 to 3	few firm blows of hammer required to break specimen
4.	moderately strong (MS)	0·3 to 1	breaks readily with one blow of hammer
5.	moderately weak (MW)	0·1 to 0·3	broken by hand only with difficulty, small thin pieces broken by finger pressure
6.	weak (W)	0·03 to 0·1	broken by hand; pieces 25 mm or more broken by finger pressure
7.	very weak (VW)	less than 0·03	crushed or remoulded by hand (includes hard soils)

GEOLOGICAL CLASSIFICATION

CRYSTAL OR GRAIN SIZE	SEDIMENTARY		IGNEOUS				METAMORPHIC	
	CLASTIC	CHEM/ORGANIC		Silicic	Intermed.	Mafic	Ultramaf.	FOLIATED	MASSIVE
very coarse 64	CONGLOMERATE (1)		Mode of Occurrence: INTRUSIVE	(27)	(29)	(34)	(32)	GNEISS (34)	HORNFELS (39)
coarse 2	AGGLOMERATE (2)			(28)	(30)		(33)		
	BRECCIA (3)			GRANITE GRANODIORITE	SYENITE DIORITE	GABBRO	PERIDOTITE DUNITE	SCHIST (35)	MARBLE (40)
medium	SANDSTONE (4)	Calcareous LIMESTONE (9)						PHYLLITE (36)	QUARTZITE (41)
0·06		Siliceous CHERT (10) OTHER (11)							
fine	SILTSTONE (5)	Carbonaceous COAL (12) OTHER (13)	TUFFS (7)	(19) (20) (21)	(22) (23)	(24) (25)	(26)	SLATE (37)	AMPHIBOLITE (42)
	MUDSTONE (6)	Ferruginous LATERITE (14) OTHER (15)	Mode of Occurrence: EXTRUSIVE	RHYOLITE OBSIDIAN DACITE	TRACHYTE ANDESITE	DOLERITE BASALT	SERPENTINITE	MYLONITE (38)	
very fine 0·002 (mm)	CLAYSTONE (8)	Saline ROCK SALT (16) GYPSITE (17) OTHER (18)							

WEATHERING TERM → STRENGTH TERM → COLOUR → FABRIC → ROCK NAME

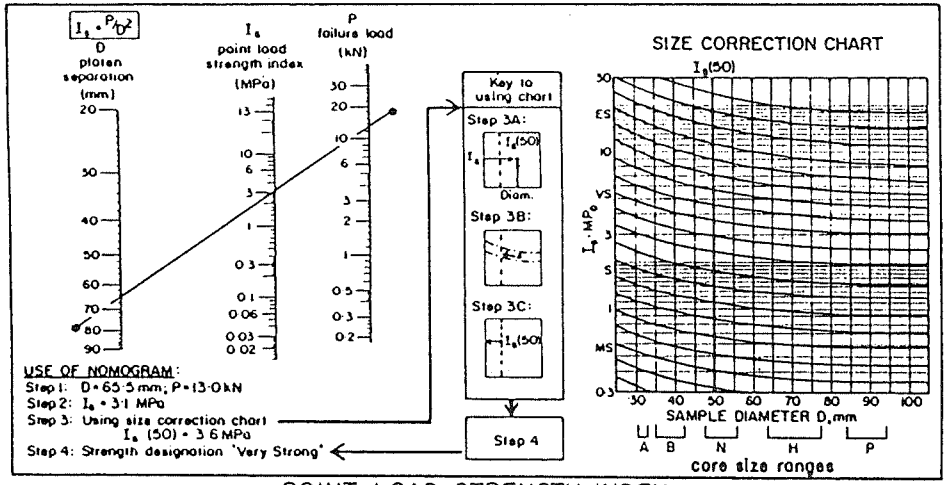

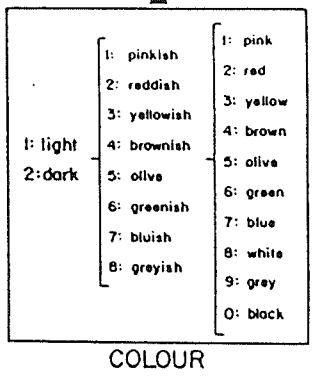

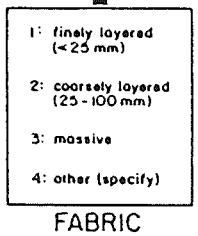

POINT LOAD STRENGTH INDEX

A2.1 Engineering Geological Field Description for Rock Material (from Bell & Pettinga 1983).

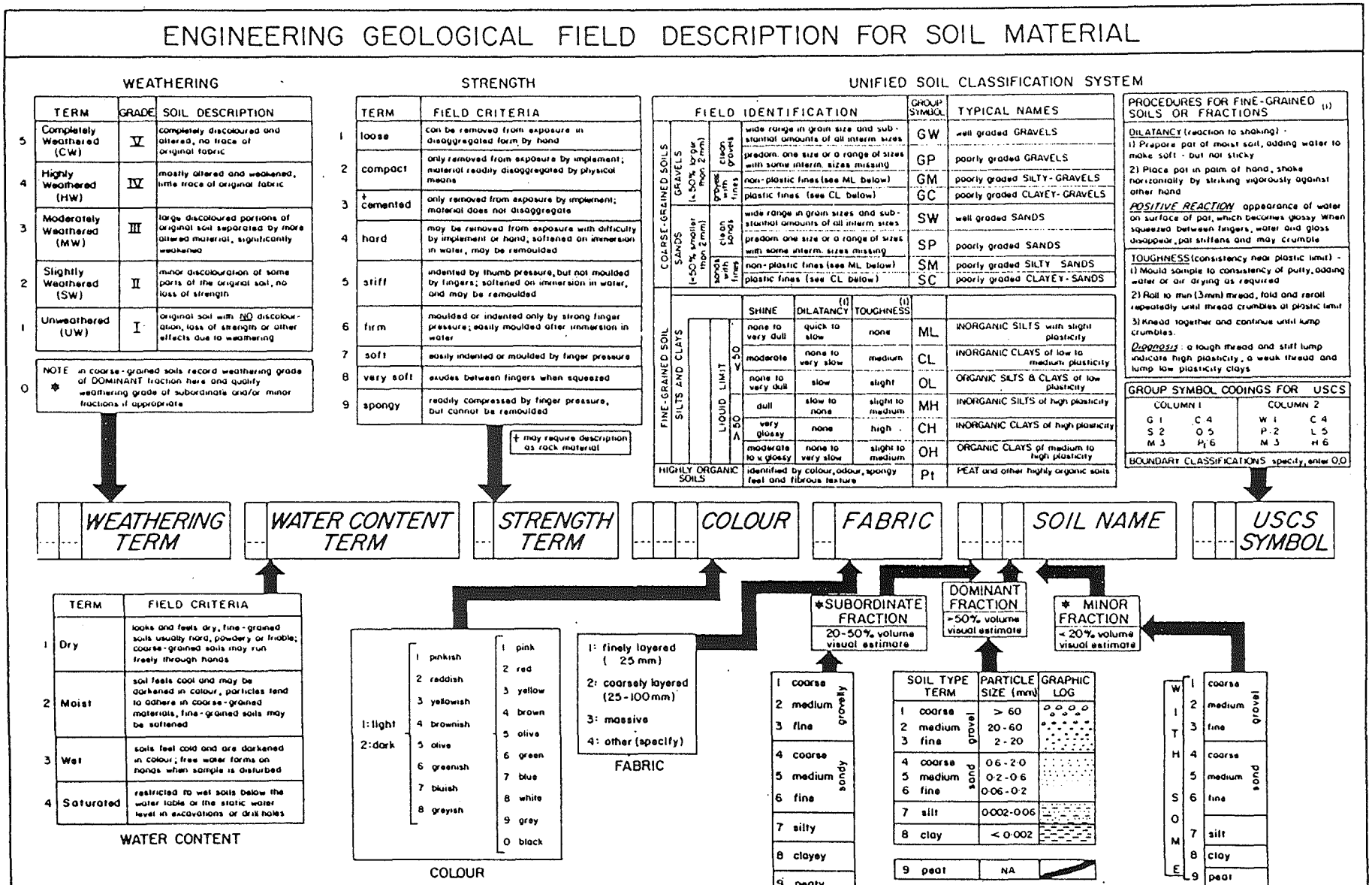

A2.2 Engineering Geological Field Description for Soil Material (from Bell & Pettinga 1983).

TERMINOLOGY FOR COMMON DEFECTS IN ROCK MASS

DEFECT TYPE	LAYERING (1)			FRACTURES AND FRACTURE ZONES (1)		WEAK SEAMS OR ZONES (1)		
	BEDDING (1)	FOLIATION (2)	CLEAVAGE (3)	JOINT / FAULT (4)	SHEARED ZONE (5)	CRUSHED (6)	DECOMPOSED (7)	INFILLED (8)
DESCRIPTION	I) Arrangement in layers of mineral grains or crystals of similar size or composition. II) Arrangement of elongated or platy minerals near parallel to one another and/or to the layers.			Single fracture across which rock has little tensile strength; planar, curved, or irregular; open, closed or incipient; surface rough, smooth or slickensided; fractures closed, open, weakly cemented or soil-coated.	Zone of multiple closely spaced (< 100 mm) fracture planes, with roughly parallel planar boundaries, blocks of intact material within zone typically lenticular or wedge shaped; fractures closed, open, weakly cemented or soil-coated.	Zone with roughly parallel planar boundaries:- I) Composed of disoriented, usually angular, rock fragments of variable size in a soil matrix. II) Some weathering of fragments possible, with soils either cohesive or non-cohesive. III) Lowest shear strength parallel to zone boundaries, which are commonly slickensided.	Zone of any shape, but commonly with roughly parallel planar boundaries:- I) Within zone rock moderately to completely weathered. II) At margins gradation into fresher rock.	I) Composed of soil materials which may show layering roughly parallel to zone boundaries. II) Rock fabric not present in infill zone.
MAP SYMBOLS with strike and dip	076 / 73	60 / 064	37 / 124	'open' 058 / 27; 'closed' 073 / 86	45 / 063	★ Record width of zone as required.	78 / 072	20 / 069	064 / 20

NOTE: materials forming zone require separate description as soil or rock

(1) OTHERS: Specify (9)

DEFECT DATA SUMMARY TABLE

ROCK UNIT No.	DEFECT SET No.	DEFECT TYPE	DEFECT SPACING	DEFECT PERSISTENCE	AV. UNIT BLOCK SIZE	DEFECT ORIENTATION: DIP DIRECTION	DEFECT ORIENTATION: DIP VALUE	GROUND-WATER	REMARKS
						±	±		
						±	±		
						±	±		
						±	±		
						±	±		
						±	±		
						±	±		
						±	±		
						±	±		
						±	±		

DEFECT ORIENTATION DIAGRAM

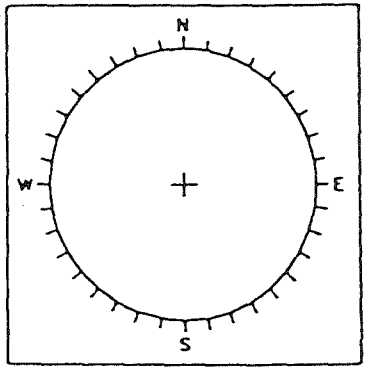

DEFECT SPACING

	TERM	SPACING (mm)
1	extremely wide	> 2000
2	very wide	500 - 2000
3	wide	200 - 500
4	moderate	100 - 200
5	close	25 - 100
6	very close	5 - 25
7	extremely close	< 5

DEFECT PERSISTENCE

	TERM	LENGTH (m)
1	very high	> 10
2	high	3 - 10
3	moderate	2 - 3
4	low	0.5 - 2
5	very low	> 0.5

AVERAGE UNIT BLOCK SIZE

	TERM	EQUIVALENT CUBE SIDE	APPROX. BLOCK VOLUME (m^3)
1	very large	1000 mm	> 1.0
2	large	500 mm	0.1 - 1.0
3	medium	100 mm	0.001 - 0.1
4	small	10 mm	< 0.001
5	very small		

GROUNDWATER

	TERM	FLOW RATE
1	dry	
2	seepage	< 1 $mL.s^{-1}$
3	very low flow	1 - 10 $mL.s^{-1}$
4	low flow	10 - 100 $mL.s^{-1}$
5	moderate flow	0.1 - 1 $L.s^{-1}$
6	large flow	1 - 10 $L.s^{-1}$
7	very large flow	> 10 $L.s^{-1}$

A2.3 Terminology for Rock Mass Description (from Bell & Pettinga 1983).

TERMINOLOGY FOR COMMON DEFECTS IN SOIL MASS

DEFECT TYPE	LAYERING (1) ✸		FRACTURES (1) ✸		CAVITIES (1) ✸	
	BEDDED/STRATIFIED(I)	LAYERED (2)(3)	JOINT/FISSURE(4)	SHEAR ZONE (5)	OPEN CAVITY (6)	INFILLED CAVITY (7)
DESCRIPTION	1) Arrangement in layers of soil particles of similar colour, size and composition 2) Arrangement of elongated or tabular particles or voids near parallel to one another or to the layers soil mass shows bedding or stratification with spacing > 100 mm	soil material is finely layered (<25mm) or coarsely layered (25-100mm)	Single fracture across which soil has little tensile strength; planar, curved or irregular; closed, open or partly infilled by soil or rock material; may be continuous over outcrop extent	Zone of multiple very closely spaced (<25mm) fracture planes either irregular, or with roughly parallel planar boundaries that are smooth or slickensided; lens shaped blocks of soil within zone, which may be softened or wetted	Opening within soil mass, commonly tubular; may occur singly or as multiple, separate or interconnected tubes; may occur also as sheet or wall-like openings within soil mass; walls of cavity may be coated with clay/silt or organic matter	Open cavities that have been partly or completely infilled by collapsed or transported material; infilling material may be partly cemented, softened or wetted
	NOTE: Indicate bed or layer description and defect spacing as shown below					
MAP SYMBOLS with strike and dip	081/21	32/076	'open' 060/27 'closed' 075/86	35/072 W	W denotes presence of 'wetted' zone or margin	where cavities identified indicate origin (e.g. dispersion)

SKETCH AS APPROPRIATE

(1) OTHERS (8): Specify

DEFECT DATA SUMMARY TABLE

SOIL UNIT No.	DEFECT SET No.	DEFECT TYPE	DESCRIPTION (II, III) LAYERING	DESCRIPTION (II, III) FRACTURE/CAVITY	DEFECT ORIENTATION DIP DIRECTION	DEFECT ORIENTATION DIP VALUE	GROUNDWATER	REMARKS
					±	±		
					±	±		
					±	±		
					±	±		
					±	±		
					±	±		
					±	±		
					±	±		

✸ NOTE I Where softened or wetted zones occur adjacent to layering, fractures or cavities, indicate on sketch and in remarks column

NOTE II Fracture/cavity description requires information on defect spacing, continuity and geometry. Sketch if appropriate

LAYERING DESCRIPTION

1: non-uniform
- 1: planar
- 2: curved
- 3: irregular
- 4: contorted
- 5: lensoidal
- 6: gradational
- 7: other (specify)

2: uniform

DEFECT SPACING

	TERM	SPACING (mm)
1	extremely wide	> 2000
2	very wide	500 - 2000
3	wide	200 - 500
4	moderate	100 - 200
5	close	25 - 100
6	very close	5 - 25
7	extremely close	< 5

DEFECT CONTINUITY

	TERM	LENGTH (m)
1	very high	> 10
2	high	5 - 10
3	moderate	2 - 5
4	low	0·5 - 2
5	very low	< 0·5

GROUNDWATER

	TERM	FLOW RATE
1	dry	
2	seepage	< 1 $ml.s^{-1}$
3	very low flow	1 - 10 $ml.s^{-1}$
4	low flow	10 - 100 $ml.s^{-1}$
5	moderate flow	0·1 - 1 $l.s^{-1}$
6	large flow	1 - 10 $l.s^{-1}$
7	very large flow	> 10 $l.s^{-1}$

A2.4 Terminology for Soil Mass Description (from Bell & Pettinga 1983).

APPENDIX THREE

GEOLOGICAL TIME SCALE

GEOLOGICAL TIME SCALE

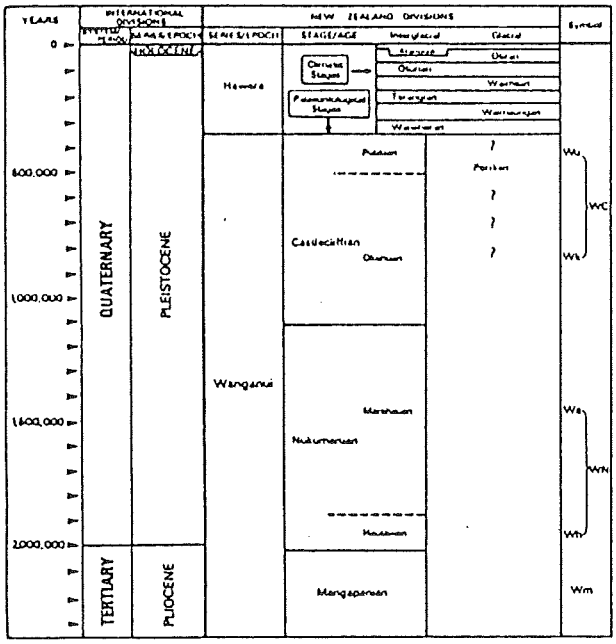

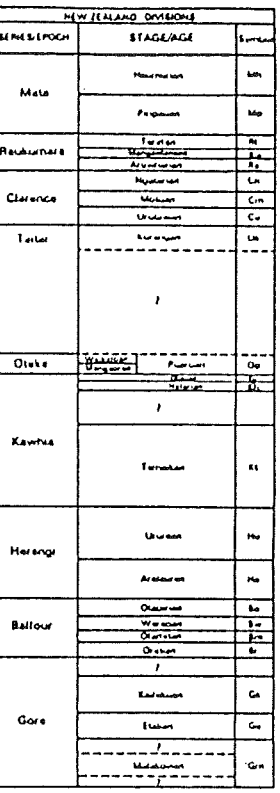

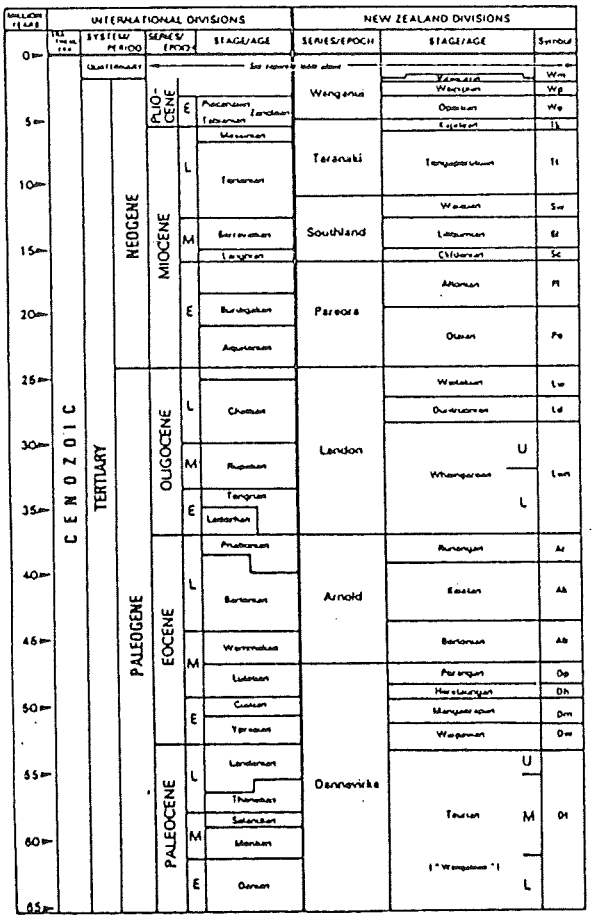

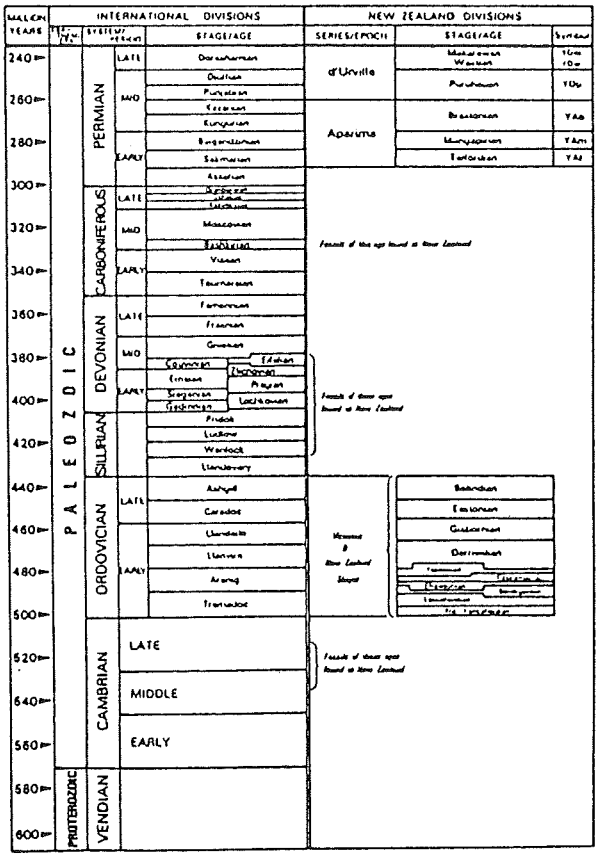

APPENDIX FOUR

VERTICAL AERIAL PHOTOGRAPHS

A4.1 Aerial Photograph Numbers

A4.1 AERIAL PHOTOGRAPH NUMBERS

The vertical aerial photographs used in this thesis study were flown by New Zealand Aerial Mapping Ltd and are as follows:-

A. Boulder Creek

Aerial	Survey	Number		945	(1946)	Run	Number	10,11
"	"	"		3718	(1965)	"	"	15,16
"	"	"	SN	5941	(1982)	"	"	C/1,2, C/41,42
"	"	"	SN	C8341	(1984)	"	"	C/7,8

B. Havelock Creek

Aerial	Survey	Number		922	(1942)	Run	Number	12,13, 14,15,16
"	"	"		3720	(1965)	"	"	11,12
"	"	"	SN	5941	(1983)	"	"	D/43,44

C. Grave Creek

Aerial	Survey	Number		948	(1949)	Run	Number	2,3
"	"	"		3717	(1965)	"	"	5,6
"	"	"	SN	5941	(1981)	"	"	A/20,21
"	"	"	SN	C8341	(1984)	"	"	A/5,6

APPENDIX FIVE

LABORATORY TESTS

A5.1 Grain-size Analyses

A5.2 Clay Mineral Identification

A5.3 Miscellaneous Tests

A5.1 GRAIN-SIZE ANALYSES

A5.1.1 Methodology

Grain-size analyses of whole samples were carried out using the techniques outlined in Lewis (1984). The gravel and sand fractions were determined by dry sieving for a standard 15 minutes using 1/2 phi interval sieves in the -3 to 4 phi range, and the silt and clay fractions by hydrometer analysis. Disaggregation of samples for hydrometer analysis was done by hand in a solution of distilled water and calgon (deflocculent).

A5.1.2 Results

Grain-size analyses were carried out on 18 samples from all three investigation sites (Boulder Creek, Havelock Creek, and Grave Creek). Gravel, sand, silt, and clay percentages for each of these analyses are presented in Tables 4.3, 5.2, and 6.2 and the grain-size distribution curves for each anaylsis are given in the following 4 pages.

UNIVERSITY OF CANTERBURY

DEPARTMENT OF GEOLOGY

PARTICLE SIZE DISTRIBUTION — SEMI LOG PLOT

PROJECT M.Sc ..... SAMPLE NO BS 1,2,3,4,5,6 ..... SAMPLED BY MJE ..... ANALYSED BY MJE .....

South Westland ..... LOCATION Boulder Creek ..... DATE May 1985 ..... DATE July 1985 ...

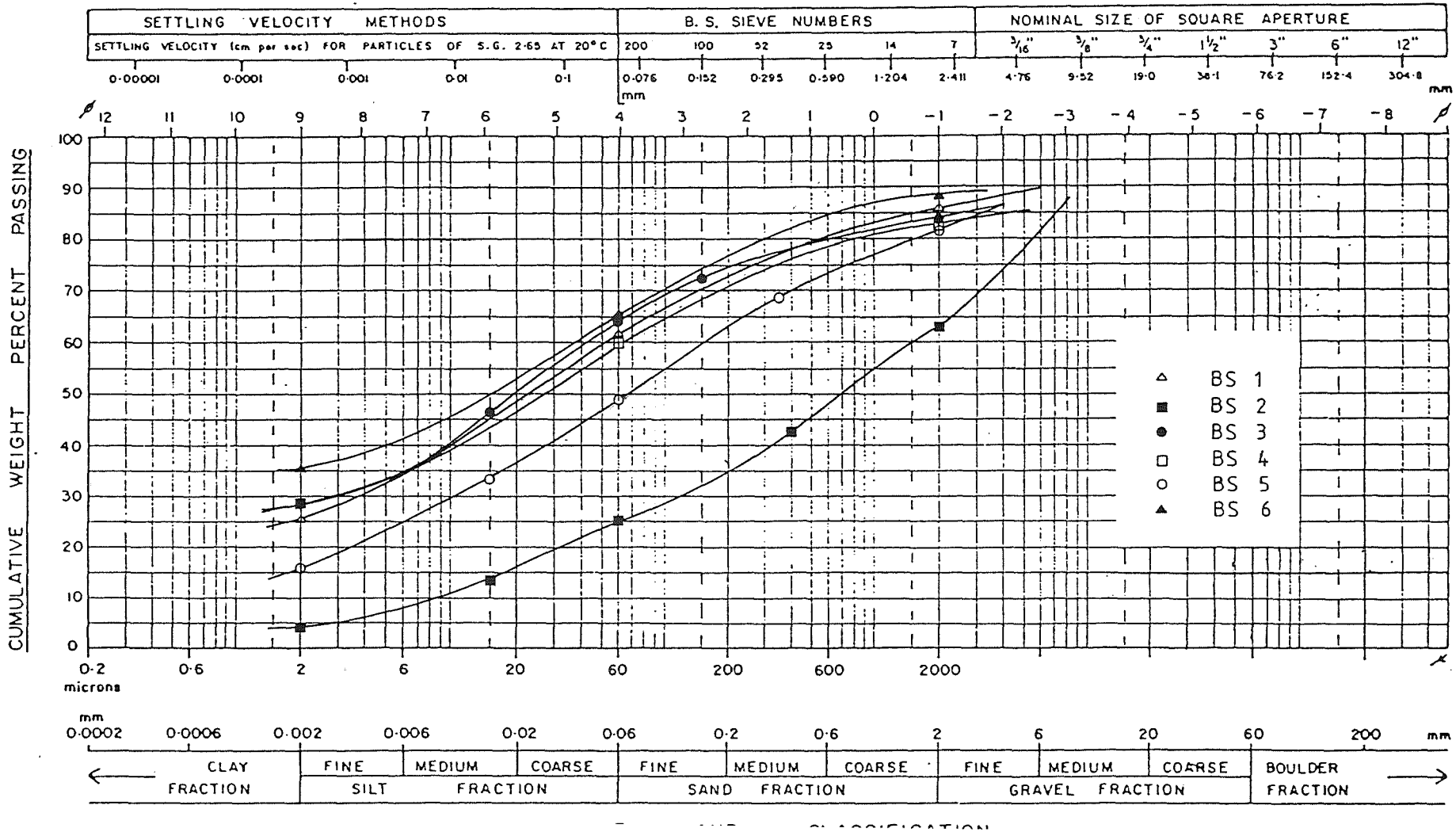

UNIVERSITY OF CANTERBURY

DEPARTMENT OF GEOLOGY

PARTICLE SIZE DISTRIBUTION — SEMI LOG PLOT

PROJECT M.Sc. Thesis ..... SAMPLE NO HS 1,2,3,4,5 ..... SAMPLED BY MJE ..... ANALYSED BY MJE .....

South Westland ..... LOCATION Havelock Creek ..... DATE May 1985 ..... DATE July 1985 ....

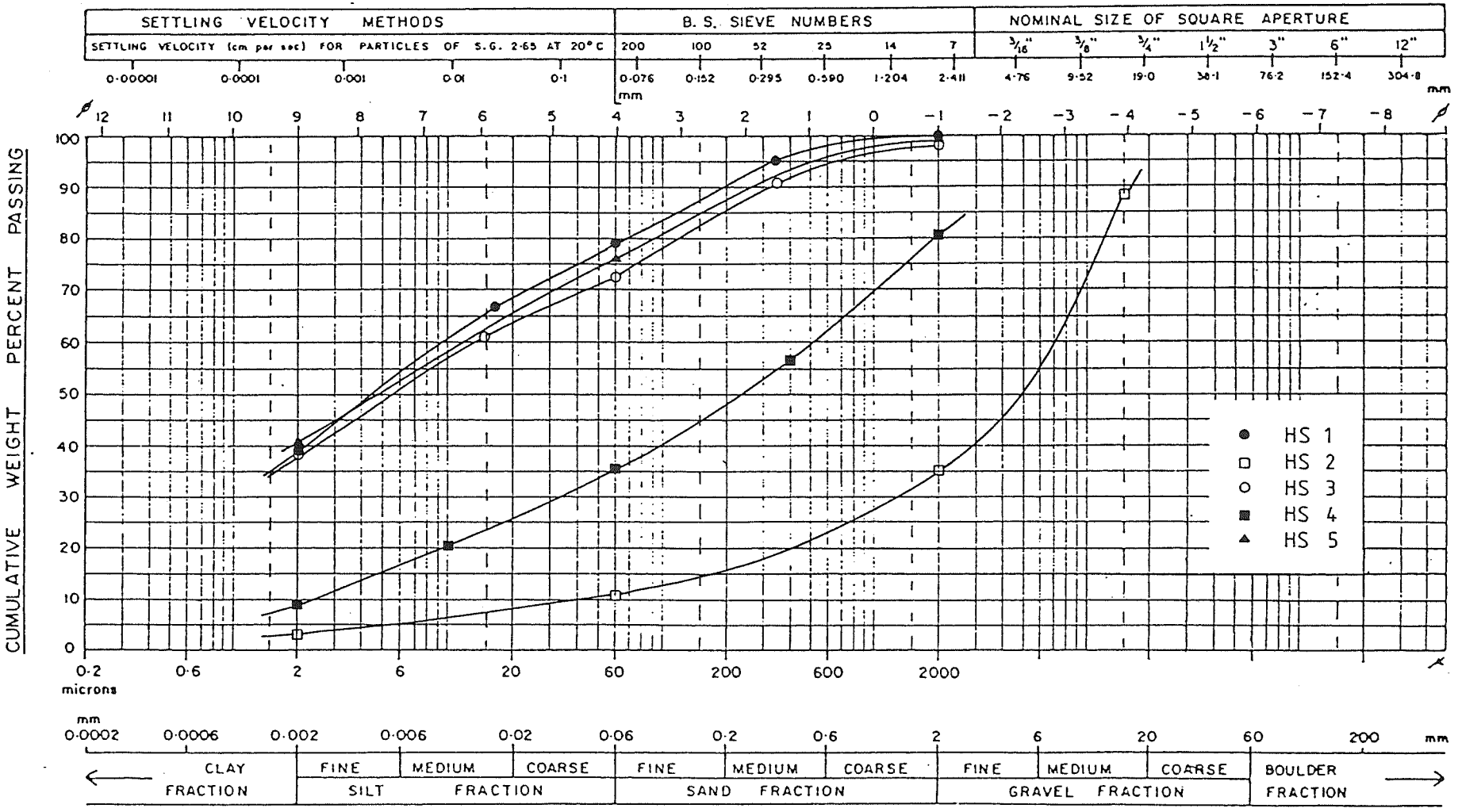

UNIVERSITY OF CANTERBURY

DEPARTMENT OF GEOLOGY

PARTICLE SIZE DISTRIBUTION — SEMI LOG PLOT

PROJECT M.Sc. Thesis ..... SAMPLE NO GS.1,5 ..... SAMPLED BY MJE ..... ANALYSED BY MJE .....

South Westland ..... LOCATION Grave Earthflow ..... DATE May 1985 ..... DATE July 1985 ...

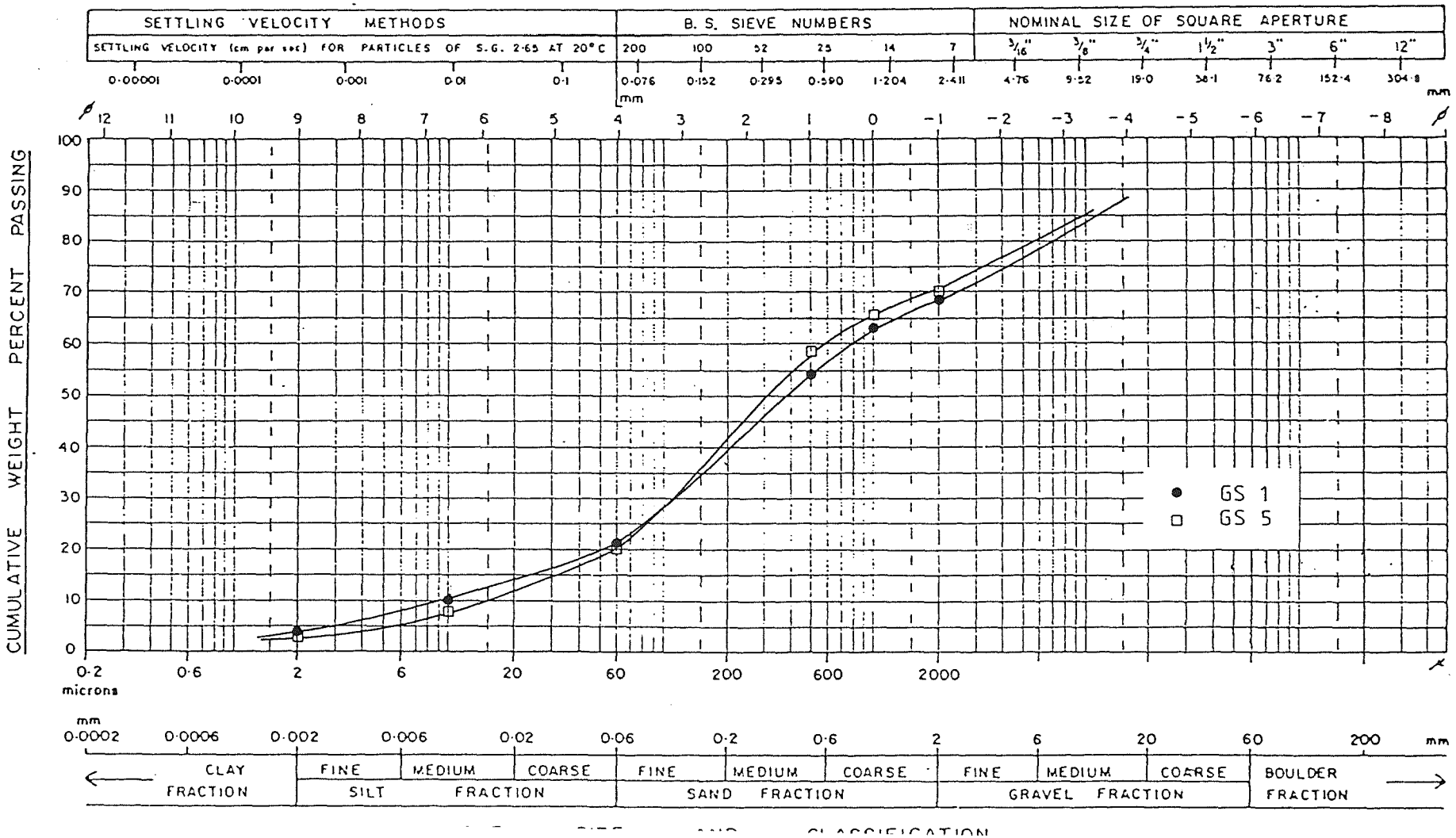

UNIVERSITY OF CANTERBURY

DEPARTMENT OF GEOLOGY

PARTICLE SIZE DISTRIBUTION — SEMI LOG PLOT

PROJECT M.Sc. Thesis ..... SAMPLE NO GS 2,3,4,6,7 ..... SAMPLED BY MJE ..... ANALYSED BY MJE .....

South Westland ..... LOCATION Grave Earthflow ..... DATE May 1985 ..... DATE July 1985 ...

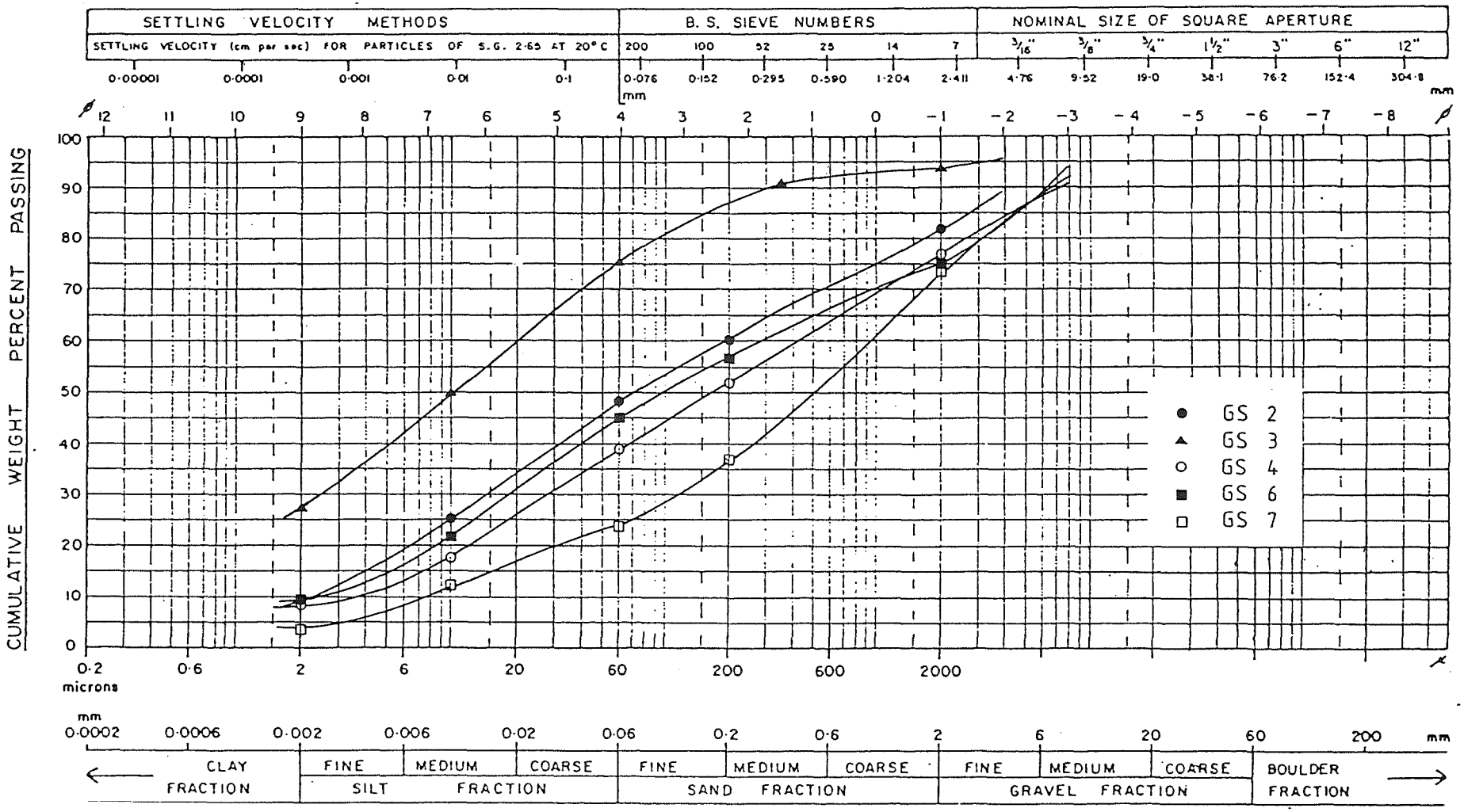

A5.2 CLAY MINERAL IDENTIFICATION

A5.2.1 Introduction

Clay mineral identification was carried out on the clay fraction of two samples each from Boulder and Havelock Creeks (one fault gouge and one puggy tectonic breccia) and on four samples from the Grave Earthflow using X-ray diffraction analysis. The objective of these analyses was to relate behaviour of the materials tested to their clay mineralogy.

A5.2.2 Sample Preparation

Oriented mounts were used because orientation (settlement) of the clay fraction enhances the basal reflections of the flaky clay minerals. The oriented slide mounts were prepared by taking a sample of the 0.002mm and finer fraction from settling columns during hydrometer analysis and were allowed to air dry on a slide over-night.

A5.2.3 Sample Testing

X-ray diffraction was carried out using a Phillips X-ray diffractometer and the samples were run from 2^{o} to about 35^{o}. The samples were then saturated with a fine spray of water and 10% glycol and retested, the glycol increasing the basal spacing of swelling clays allowing them to be distinguished from other minerals.

A5.2.4 Results

Basically the same minerals were identified in all the samples tested with minor variations in peak height, and are given in Tables 4.3, 5.2, and 6.2. Typical diffractograms, one each from the three investigation sites, are shown in Figure A5.1. Peak heights were used to give a general indication of the relative proportions of the different minerals present, but quantitative analysis was not undertaken as it was beyond the scope of this study.

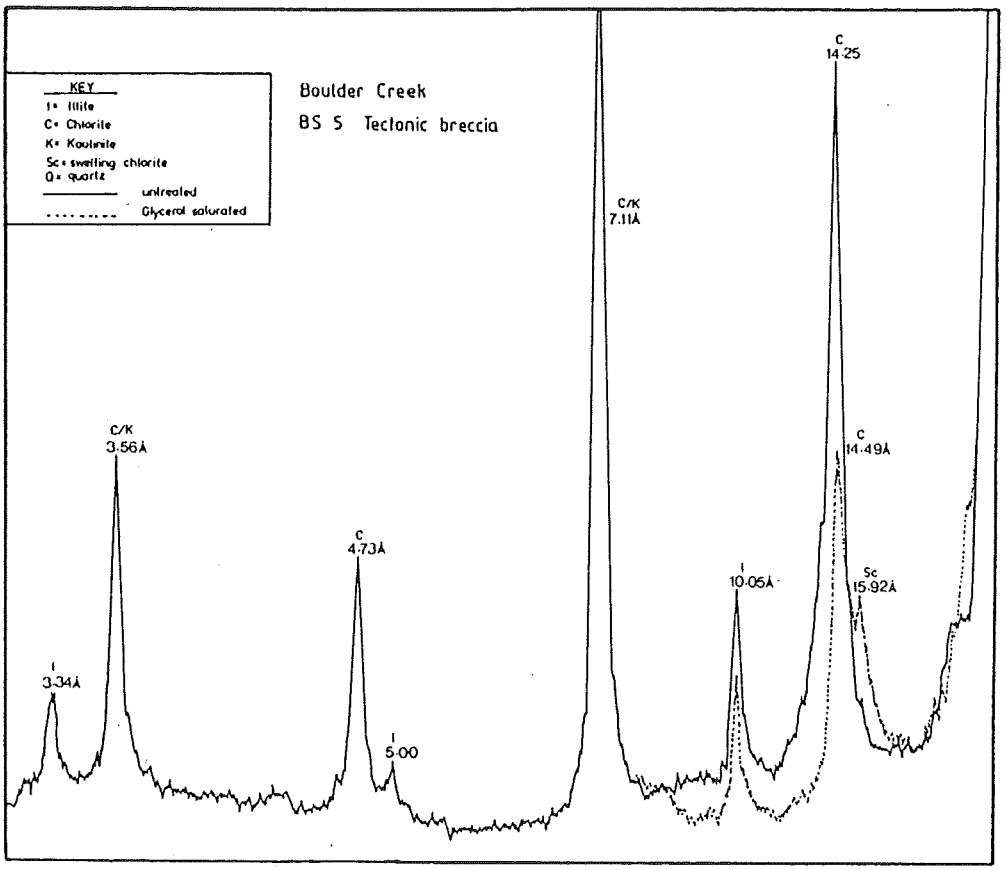

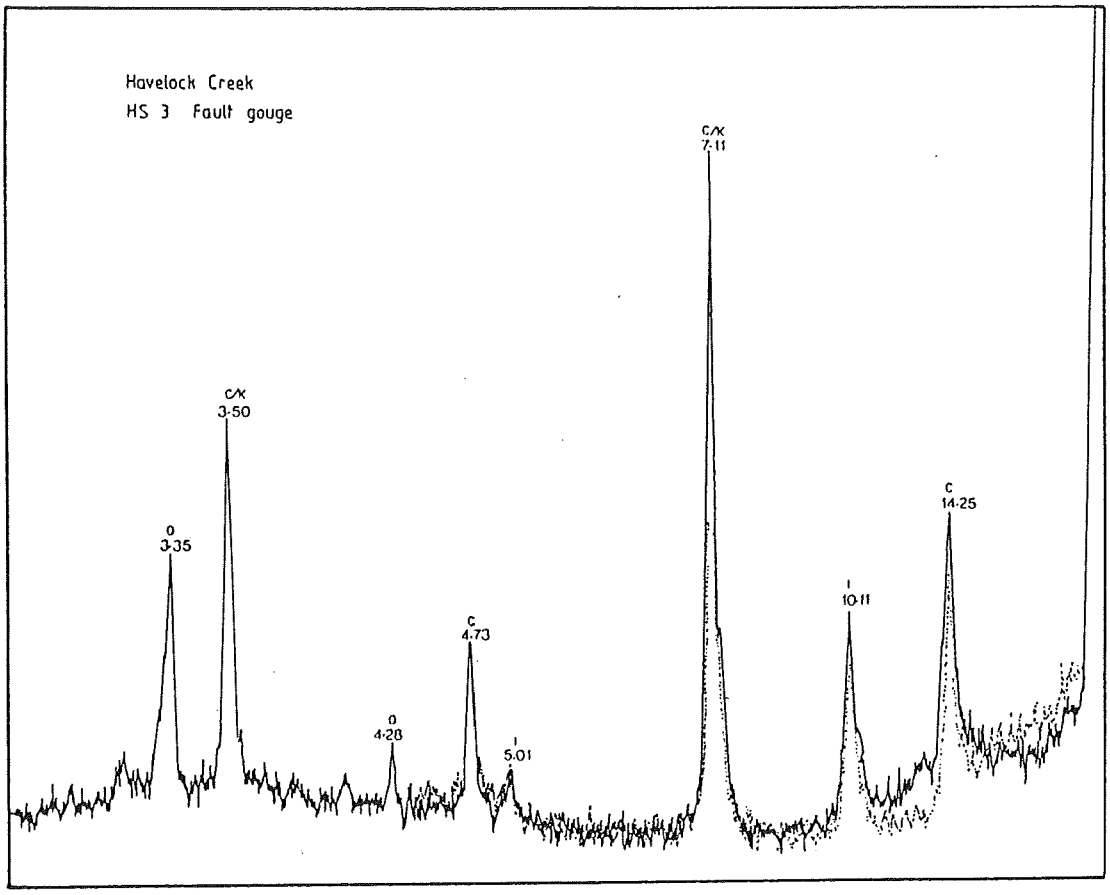

Fig. A5.1a Typical diffractograms of samples from Boulder and Havelock Creeks.

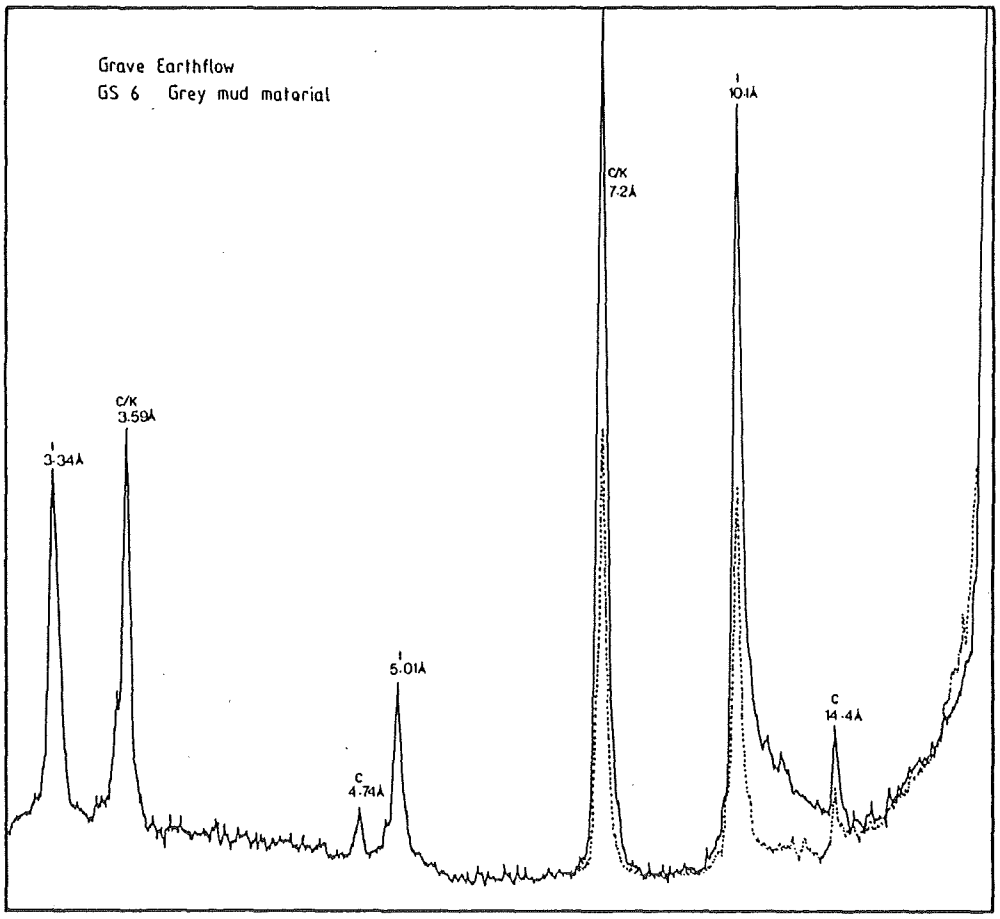

Fig. A5.1b Typical diffractogram of samples from from the Grave Earthflow.

A5.3 MISCELLANEOUS TESTS

A5.3.1 Determination of Moisture Content

New Zealand Standard 4402 Part 1 (1980) Test 1, pp. 15-17.

A5.3.2 Determination of Atterberg Limits

Liquid Limit: New Zealand Standard 4402 Part 1 (1980) Test 2, pp. 18-23.

Plastic Limit: New Zealand Standard 4402 Part 1 (1980) Test 3, pp. 24-26.

Plasticity Index: New Zealand Standard 4402 Part 1 (1980) Test 4, pp. 27.

APPENDIX SIX

STEREOGRAPHIC ASSESSMENT OF SLOPES IN INTACT HORNFELSED SANDSTONE AT BOULDER CREEK

A6.1 Scope

A6.2 Method

A6.3 Results

A6.4 Defect Survey Sheets

A6.1 SCOPE

Assessment of the instability of intact hornfelsed sandstone slopes at Boulder Creek is limited to ascertaining whether failure by sliding is kinematically possible and if so, whether planar or wedge shaped. Figure A6.1 (Hoek & Bray 1981) illustrates the main types of slope failure and presents stereoplots of structural conditions likely to give rise to these failures. Calculation of the factor of safety of these slopes was considered beyond the scope of this study due to the small relative importance of this slope setting to the overall slope instability of Boulder Creek and the lack of shear strength data.

A6.2 METHOD

Assessment of stability is made by stereographic analysis, with a rock defect survey being carried out utilising four traverse lines at varied orientations. Section A6.4 presents the rock defect survey sheets for each traverse line measured, and joint defect orientation data for all four traverses (313 defects) were plotted as poles to planes on the lower hemisphere of the Schmidt equal area projection (Fig. A6.2). Data recorded on shear zones, fault gouge zones, and cleavage from the whole map area are also included in this point diagram. Poles to joint defects were contoured by the Schmidt method (Fig. A6.2) defining three pole concentrations which have the following mean strike and dip values:-

SET	STRIKE	DIP
A	038°	52°SE
B	002°	37°W
C	112°	84°NE

The raw orientation data was not corrected for sampling bias since the four traverse lines were positioned at varying orientations, this compensating for any bias that may be present. Stauffer (1966) presents a method for finding if apparent pole concentrations are representative of the parent population, and he stated that concentrations with a 0.01 net probability may be significant and those with a 0.001 net probability are probably significant. For 313 points, a concentration must have a contour value of 4.2% for a net

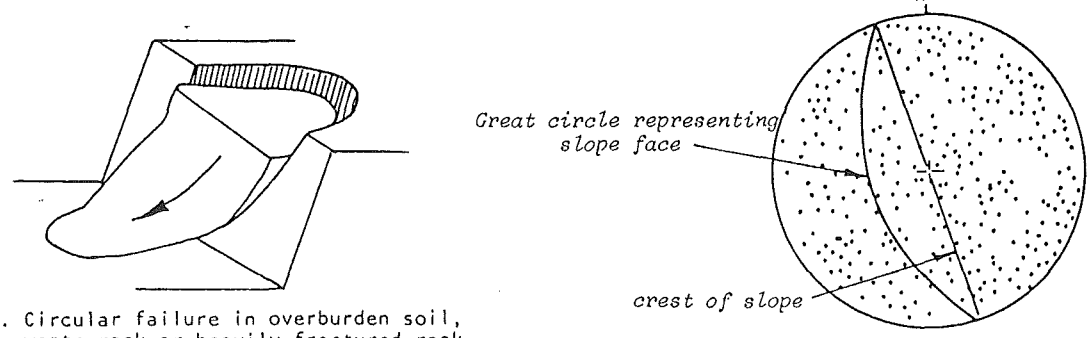

a. Circular failure in overburden soil, waste rock or heavily fractured rock with no identifiable structural pattern.

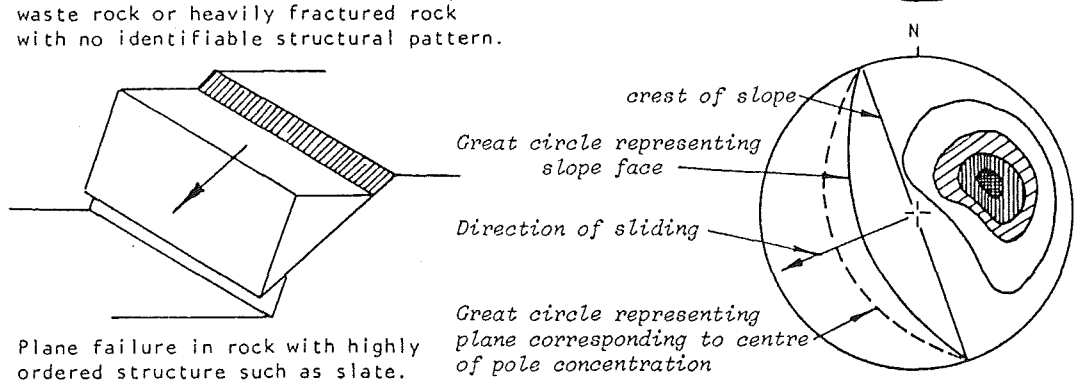

b. Plane failure in rock with highly ordered structure such as slate.

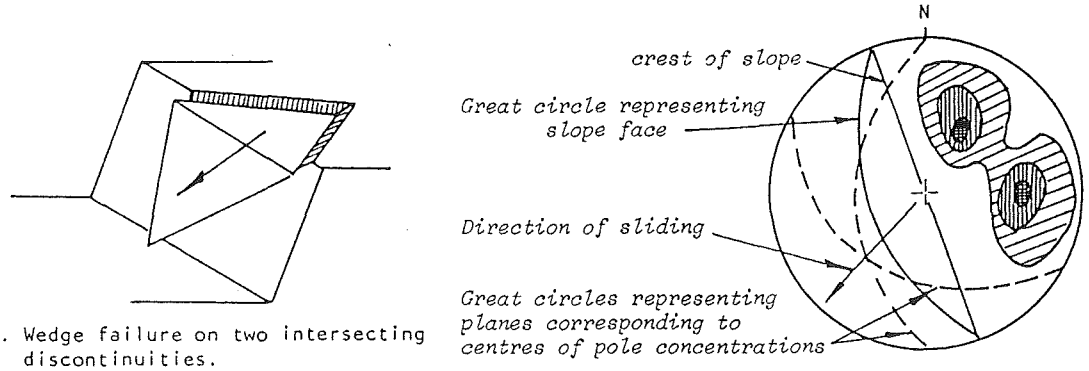

c. Wedge failure on two intersecting discontinuities.

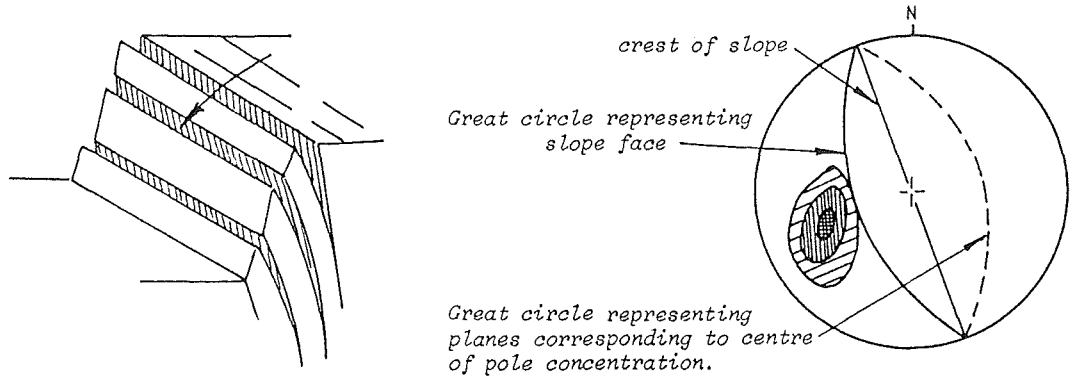

d. Toppling failure in hard rock which can form columnar structure separated by steeply dipping discontinuities.

Fig. A6.1 Main types of slope failure and stereo plots of structural conditions likely to give rise to these failures (from Hoek & Bray 1981).

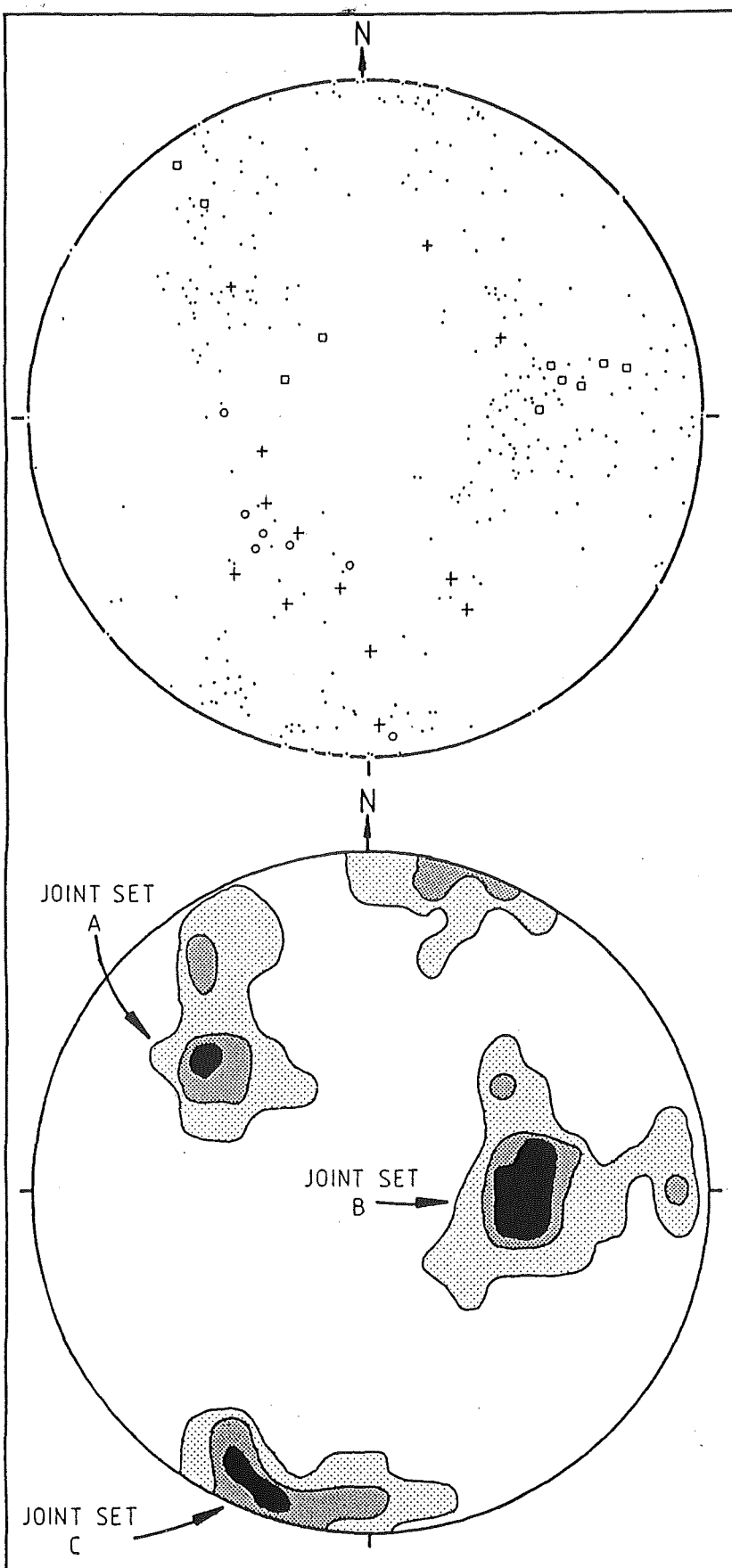

POINT DIAGRAM

LEGEND

Poles of rock defects

- Joint
- \+ Shear zone
- □ Fault gouge zone
- ○ Cleavage

NOTES:

1. Rock defects plotted on Schmidt equal area, lower hemisphere stereographic projection.
2. Joints shown as a contoured stereographic projection based on poles of 313 joints.
3. Contours based on the number (%) of poles within each 1% unit area of the projection.

CONTOUR DIAGRAM

LEGEND

Poles of joints

%	No.
0-2	0-4
2-3	5-8
3-4	9-12
>4	13-17

FIG. A6.2 Stereographic Plot of Rock Defects, Boulder Creek.

probability of 0.001. All 3 pole concentrations exceed this value, and so are regarded as being statistically significant concentrations.

The Markland test was used to establish the possibility of a wedge failure in which sliding takes place along the line of intersection of two planar defects. Plane failure is also covered by this test, since it is a special case of wedge failure. If contact is maintained on both planes, sliding can only occur along the line of intersection which must "daylight" in the slope face. This means that the plunge of the line of intersection must be less than the dip of the slope face, when measured in the direction of the line of intersection (Hoek & Bray 1981).

The factor of safety of a slope also depends on the shear strength of the defect surfaces and the geometry of the wedge. A first approximation of wedge stability is obtained by considering whether the plunge of the line of intersection exceeds the angle of friction for the rock surfaces, but is less than the dip of the slope face (Hoek & Bray 1981).

A6.3 RESULTS

Figure A6.3 shows the Markland test for the intact bedrock slope at locality BE 6 with an average slope angle of 46^{o} and average slope aspect of 138^{o} (SE). A friction angle of 30^{o} is estimated from typical values published by Hoek & Bray (1981). The test shows that the plunge of the lines of intersection do not fall in the zone of instability, however, the intersection between joint sets A and C plunges at 50^{o}, just 4^{o} steeper than the average slope angle.

The Hocking refinement to the Markland test shows that the dip direction of joint set A lies between the dip direction of the slope face and the trend of the line of intersection between joint sets A and C. Therefore if a portion of the rock buttress with a slope aspect not less than the dip direction of set A (128^{o}) has a slope angle greater than 50^{o}, failure is kinematically possible by plane sliding. If a section of the rock buttress with an aspect of less than 128^{o} has a slope angle greater than 50^{o}, then failure is possible

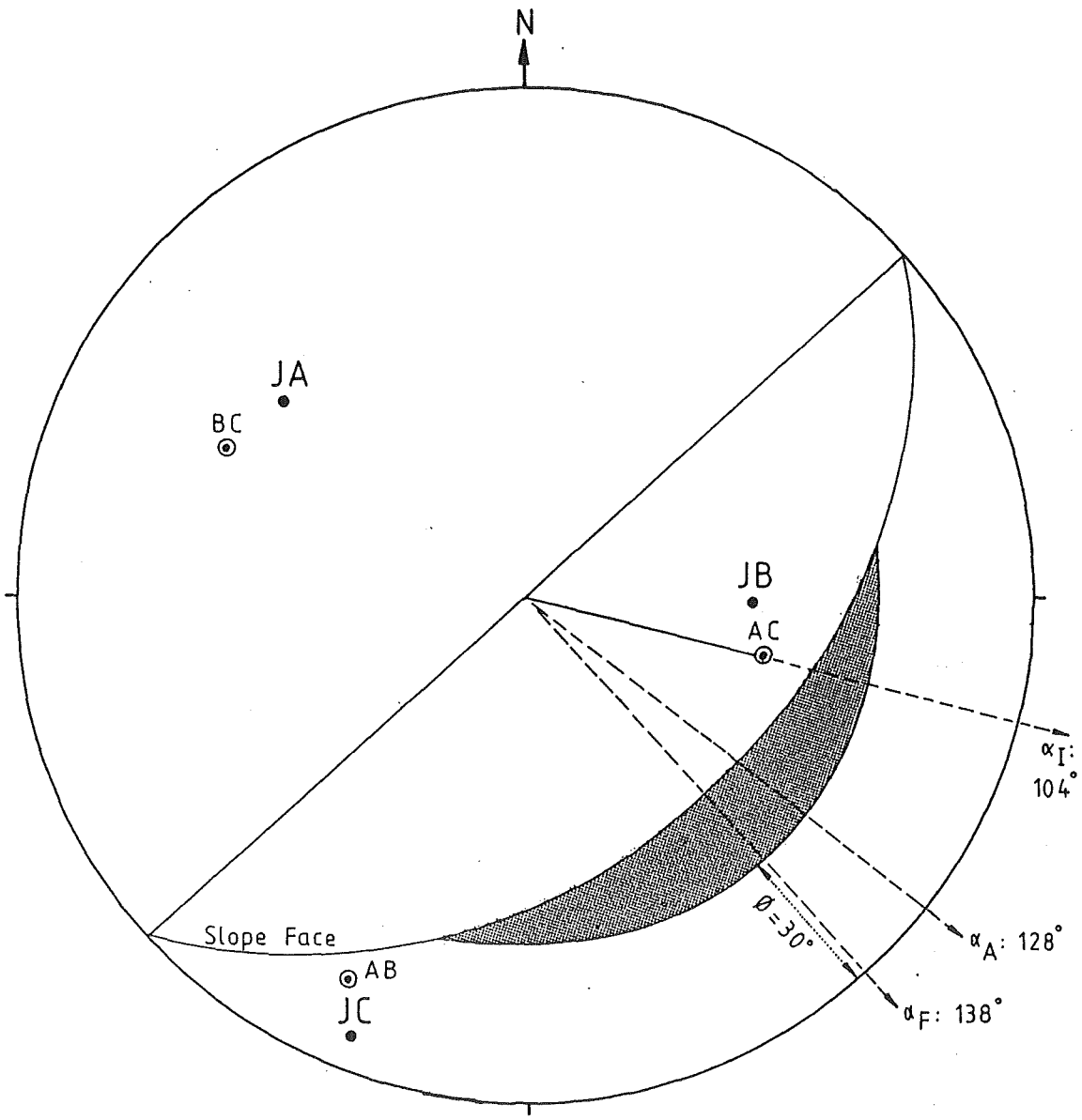

LEGEND

- • Pole to joint set
- ⊙ Plunge of intersection
- ϕ Estimated angle of friction
- α_I Line of intersection AC
- α_A Dip direction of joint set A
- α_F Dip direction of slope face
- ▒ Zone of potential instability

FIG. A6.3 Marklands test with Hocking refinement for intact bedrock slope at BE 6.

by wedge sliding along the line of intersection between joint sets A and C. Due to the dynamic nature of these slopes, either of these conditions could possibly exist and produce unstable conditions.

Figure A6.3 also shows that joint set C has the potential to produce a toppling failure, as illustrated in Figure A6.1. This situation was not observed in the field; however, toppling failure may initiate rock fall movements producing a complex rock topple-fall failure.

A6.4 DEFECT SURVEY SHEETS

Defect survey sheets for each of the four traverse lines are presented in the following pages.

DEFECT SURVEY SHEET

PROJECT: M Sc South Westland LOCATION: BE 1

DATE: 19 Feb. 1986 ROCK TYPE: Hornfelsed Sandstone

TREND: 055° INCLINATION: +9°

No.	Distance		Defect Type	Strike	Dip
	m	cm			
1	0	0	sz	142	32NE
2	0	45	jt	105	84NE
3	0	45	jt	032	60SE
4	0	72	jt	042	44SE
5	0	80	jt	104	85NE
6	1	05	jt	106	83NE
7	1	45	jt	103	83SW
8	2	15	jt	355	40W
9	2	90	cz	096	83N
10	3	30	jt	045	40SE
11	3	40	jt	118	81NE
12	3	50	jt	290	46N
13	5	45	jt	100	82NE
14	5	90	jt	095	75N
15	7	25	jt	057	50SE
16	7	95	jt	114	80NE
17	9	20	jt	102	84NE

DEFECT SURVEY SHEET

PROJECT: M Sc South Westland LOCATION: BE 1

DATE: 19 Feb. 1986 ROCK TYPE: Hornfelsed Sandstone

TREND: 049° INCLINATION: +11°

No.	Distance		Defect Type	Strike	Dip
	m	cm			
18	0	0	jt	086	56S
19	0	77	jt	115	82S
20	1	25	sz	114	50NE
21	1	70	jt	102	52N
22	2	35	jt	068	66SE
23	2	55	jt	099	74N
24	2	90	sz	164	27E
25	3	50	jt	136	40NE
26	5	65	jt	114	25NE
27	6	17	jt	085	87S
28	6	85	jt	085	74N
29	7	35	jt	064	73SE
30	8	12	jt	108	74S
31	8	65	jt	093	76N
32	9	40	jt	115	55NE
33	9	85	jt	112	85N
34	9	85	jt	058	53S

DEFECT SURVEY SHEET

PROJECT: M Sc South Westland LOCATION: BE 1

DATE: 19 Feb. 1986 ROCK TYPE: Hornfelsed Sandstone

TREND: 102° INCLINATION: +8°

No.	Distance		Defect Type	Strike	Dip
	m	cm			
35	0	35	jt	128	57SW
36	1	18	jt	051	66SE
37	1	52	jt	047	60SE
38	1	80	jt	172	80SW
39	1	85	jt	062	34NW
40	1	95	jt	141	44NE

DEFECT SURVEY SHEET

PROJECT: M Sc South Westland LOCATION: BE 1

DATE: 19 Feb. 1986 ROCK TYPE: Hornfelsed Sandstone

TREND: 050° INCLINATION: +13°

No.	Distance		Defect Type	Strike	Dip
	m	cm			
41	0	00	jt	060	77SE
42	1	00	jt	076	62NW
43	2	20	jt	111	86S
44	2	52	jt	115	78N
45	2	64	jt	086	78N
46	2	79	jt	103	82S
47	4	46	jt	093	85S
48	4	51	jt	102	86S
49	4	20	jt	094	84S
50	5	60	sz	090	58N
51	5	70	jt	036	30NW
52	5	80	jt	014	64W
53	6	15	jt	082	78N
54	5	67	jt	069	63SE
55	7	80	jt	102	85S
56	7	78	jt	043	29NW
57	8	75	jt	094	90
58	8	94	jt	097	90
59	8	92	jt	034	51SE
60	9	10	jt	039	30NW
61	9	29	jt	105	74S
62	10	60	jt	030	36NW

DEFECT SURVEY SHEET

PROJECT: M Sc South Westland LOCATION: BE 1

DATE: 19 Feb. 1986 ROCK TYPE: Hornfelsed Sandstone

TREND: 310° INCLINATION: +40°

No.	Distance		Defect Type	Strike	Dip
	m	cm			
63	0	0	jt	048	20NW
64	0	30	jt	051	19NW
65	0	54	jt	056	48NW
66	0	54	jt	164	44SW
67	1	02	jt	137	67NE
68	1	23	sz	090	90
69	1	58	jt	022	30NW
70	2	18	jt	037	32NW
71	2	74	jt	039	40NW
72	2	85	jt	056	51NW
73	2	96	jt	058	49NW
74	2	00	jt	044	54SW
75	5	38	jt	043	38NW
76	5	51	jt	127	39NE
77	6	12	jt	042	31NW
78	6	35	jt	064	63SW

DEFECT SURVEY SHEET

PROJECT: M Sc South Westland LOCATION: BE 9

DATE: 19 Feb. 1986 ROCK TYPE: Hornfelsed Sandstone

TREND: 169° INCLINATION: -20°

No.	Distance		Defect Type	Strike	Dip
	m	cm			
1	0	0	jt	005	26W
2	0	58	jt	034	63SE
3	1	22	jt	036	61SE
4	0	80	jt	152	37SW
5	0	64	jt	142	80SW
6	1	00	jt	103	59S
7	1	75	jt	100	84S
8	1	80	jt	173	46W
9	1	86	jt	150	32SW
10	2	69	jt	168	46W
11	2	50	sz	088	80N
12	3	60	cz	097	66N
13	4	45	jt	002	58W
14	4	75	jt	010	68W
15	4	10	jt	073	88S
16	4	22	jt	101	70SW
17	4	75	jt	147	47SW
18	5	83	jt	100	60N
19	5	30	jt	176	42W
20	5	95	jt	180	38W
21	6	70	sz	060	90
22	7	75	cz	008	44W

DEFECT SURVEY SHEET

PROJECT: M Sc South Westland LOCATION: BE 9

DATE: 19 Feb. 1986 ROCK TYPE: Hornfelsed Sandstone

TREND: 020° INCLINATION: -22°

No.	Distance		Defect Type	Strike	Dip
	m	cm			
23	0	68	jt	118	86N
24	0	80	jt	120	84N
25	0	80	jt	020	41W
26	1	05	jt	032	31W
27	1	75	jt	012	26W
28	2	00	jt	015	32W
29	1	65	jt	180	72W
30	2	37	jt	052	66SE
31	2	76	jt	052	66SE
32	3	21	jt	052	66SE
33	3	78	jt	052	66SE
34	4	20	jt	052	66SE
35	4	43	jt	052	66SE
36	2	11	jt	177	50W
37	2	70	jt	173	86W
38	2	82	jt	168	88W
39	3	00	jt	171	90
40	4	63	jt	124	68NE
41	4	78	jt	156	76SW
42	5	73	jt	175	49W
43	5	12	jt	065	56SE
44	5	95	jt	004	32W

No.	Distance		Defect Type	Strike	Dip
	m	cm			
45	4	80	jt	120	80NE
46	4	96	jt	120	80NE
47	5	14	jt	120	80NE
48	5	33	jt	120	80NE
49	5	54	jt	120	80NE
50	5	70	jt	120	80NE
51	6	13	jt	120	80NE
52	6	32	jt	120	80NE
53	6	71	jt	120	80NE
54	7	60	jt	104	90
55	8	20	jt	064	50NW
56	8	20	jt	104	90
57	8	65	jt	064	50NW
58	8	65	jt	101	90

DEFECT SURVEY SHEET

PROJECT: M Sc South Westland LOCATION: BE 4

DATE: 19 Feb. 1986 ROCK TYPE: Hornfelsed Sandstone

TREND: 022° INCLINATION: +36°

No.	Distance		Defect Type	Strike	Dip
	m	cm			
1	0	43	jt	126	88NE
2	0	84	jt	067	79SE
3	1	17	jt	077	70SE
4	1	18	jt	047	42SE
5	1	00	jt	132	78SW
6	2	05	jt	059	81SE
7	1	99	jt	041	47SE
8	1	87	jt	173	32W
9	2	96	jt	080	56N
10	3	33	jt	061	86SE
11	3	33	jt	360	39E
12	3	48	jt	164	37SW
13	3	40	jt	069	76SE
14	3	80	jt	020	34E
15	4	50	jt	164	86SW
16	4	70	jt	031	65NW

DEFECT SURVEY SHEET

PROJECT: M Sc South Westland LOCATION: BE 4

DATE: 19 Feb. 1986 ROCK TYPE: Hornfelsed Sandstone

TREND: 360° INCLINATION: +19°

No.	Distance		Defect Type	Strike	Dip
	m	cm			
17	8	84	jt	081	87S
18	9	20	jt	103	34N
19	9	60	jt	051	72SE
20	9	66	jt	071	87NW
21	9	93	jt	098	38N
22	11	30	jt	063	70SE
23	11	30	jt	048	41SE
24	11	30	jt	002	84W
25	11	50	jt	017	44W
26	12	30	jt	360	88W
27	12	46	jt	097	84S
28	12	81	jt	112	86SW
29	13	01	jt	037	42SE
30	12	12	sz	100	86S
31	12	72	jt	048	72SE
32	13	28	jt	167	77SW
33	13	43	jt	160	78SW
34	14	13	jt	008	51W
35	13	66	jt	144	82NE
36	14	00	jt	126	88SW
37	14	26	jt	122	87SW
38	14	38	jt	125	86SW

No.	Distance		Defect Type	Strike	Dip
	m	cm			
39	12	72	jt	003	58W
40	14	32	jt	166	53W
41	14	41	jt	003	54W
42	14	98	jt	139	52SW
43	14	55	jt	021	46SE
44	14	91	jt	131	33NE
45	15	37	jt	121	81SW
46	15	75	jt	172	48W
47	16	33	jt	156	44SW
48	15	91	jt	116	74N
49	16	30	jt	118	45N
50	16	02	sz	033	52SE
51	16	40	jt	148	53SW
52	18	87	cz	148	62SW
53	18	84	jt	167	42SW
54	19	20	jt	038	46SE
55	19	50	jt	170	39SW

DEFECT SURVEY SHEET

PROJECT: M Sc South Westland LOCATION: BE 4

DATE: 19 Feb. 1986 ROCK TYPE: Hornfelsed Sandstone

TREND: 018° INCLINATION: +10°

No.	Distance		Defect Type	Strike	Dip
	m	cm			
56	20	20	jt	059	88SE
57	20	25	jt	035	56SE
58	21	12	cz	161	45SW
59	23	10	jt	027	52SE
60	21	98	jt	166	40SW
61	23	40	jt	170	37SW
62	22	62	jt	078	84NW
63	23	01	cz	099	90
64	23	19	cz	095	90
65	24	23	jt	170	56W
66	25	20	jt	160	59W
67	26	30	jt	180	30W
68	25	22	jt	038	37SE
69	25	90	jt	033	40SE
70	25	92	jt	137	45SW
71	26	24	jt	137	45SW
72	26	46	jt	137	45SW
73	26	71	jt	134	40SW
74	26	89	jt	135	44SW

DEFECT SURVEY SHEET

PROJECT: M Sc South Westland LOCATION: BE 7

DATE: 19 Feb. 1986 ROCK TYPE: Hornfelsed Sandstone

TREND: 097° INCLINATION: +22°

No.	Distance		Defect Type	Strike	Dip
	m	cm			
1	0	0	jt	006	64W
2	0	48	jt	008	60W
3	0	59	jt	018	44E
4	0	66	jt	015	42E
5	1	12	jt	160	66NE
6	1	05	jt	017	38E
7	1	08	jt	158	36NE
8	2	23	jt	016	34W
9	2	50	jt	014	38W
10	2	62	jt	015	38W
11	1	35	jt	054	28SE
12	2	01	jt	024	43SE
13	2	20	jt	037	53SE
14	3	20	jt	001	37W
15	2	71	jt	175	63W
16	3	17	jt	122	68SW
17	3	80	jt	105	65S
18	2	63	jt	174	68W
19	2	92	jt	085	55S
20	4	24	jt	010	46W
21	4	73	jt	014	51W
22	4	78	jt	007	34W

No.	Distance		Defect Type	Strike	Dip
	m	cm			
23	5	65	jt	174	31W
24	4	10	jt	172	74W
25	3	25	jt	046	39SE
26	3	95	jt	100	62S
27	4	24	jt	038	56SE
28	4	86	jt	175	76W
29	4	75	jt	114	83N
30	5	90	jt	010	41W
31	4	58	jt	043	32SE
32	4	96	jt	038	49SE
33	5	18	jt	034	54SE
34	5	92	jt	022	58W
35	7	00	jt	078	79NW
36	6	55	jt	020	39W
37	7	40	jt	134	49NE

DEFECT SURVEY SHEET

PROJECT: M Sc South Westland LOCATION: BE 7

DATE: 19 Feb. 1986 ROCK TYPE: Hornfelsed Sandstone

TREND: 078° INCLINATION: +19°

No.	Distance		Defect Type	Strike	Dip
	m	cm			
38	0	51	jt	020	38W
39	0	77	jt	026	54W
40	1	15	jt	022	40W
41	1	24	jt	027	87W
42	1	54	jt	026	87W
43	1	89	jt	030	90
44	1	90	jt	124	50SW
45	2	18	jt	052	44SE
46	2	21	jt	118	65SW
47	2	39	jt	144	80NE
48	2	48	jt	057	72SE
49	2	12	jt	100	71N
50	2	69	jt	016	54W
51	3	12	jt	006	54W
52	2	83	jt	062	36SE
53	2	69	jt	124	65NE
54	3	12	jt	056	35SE
55	3	36	jt	034	41W
56	3	47	jt	019	79W
57	3	58	jt	005	36E
58	4	69	jt	092	77N
59	4	63	jt	165	45SW

DEFECT SURVEY SHEET

PROJECT: M Sc South Westland LOCATION: BE 7

DATE: 19 Feb. 1986 ROCK TYPE: Hornfelsed Sandstone

TREND: 041° INCLINATION: +7°

No.	Distance		Defect Type	Strike	Dip
	m	cm			
60	0	75	jt	133	44SW
61	1	59	jt	109	64S
62	1	20	jt	013	50W
63	1	47	jt	177	33W
64	1	82	jt	080	84N
65	2	12	jt	011	36W
66	2	48	jt	011	36W
67	2	88	jt	129	30SW
68	3	17	jt	128	21SW
69	3	52	jt	008	81W
70	4	07	jt	118	53S
71	3	74	jt	111	88S
72	3	62	jt	105	85S
73	3	90	jt	110	88S
74	4	20	jt	010	77W
75	4	32	jt	176	35W
76	5	24	jt	175	36E
77	5	58	jt	075	79NW
78	5	64	jt	015	88W
79	5	98	jt	064	87SE
80	5	97	jt	095	85S
81	6	32	jt	003	39W

DEFECT SURVEY SHEET

PROJECT: M Sc South Westland LOCATION: BE 7

DATE: 19 Feb. 1986 ROCK TYPE: Hornfelsed Sandstone

TREND: 033° INCLINATION: +7°

No.	Distance		Defect Type	Strike	Dip
	m	cm			
82	6	39	jt	100	90
83	6	68	jt	016	50W
84	6	40	jt	168	81W
85	6	32	jt	059	83SE
86	6	91	jt	103	83N
87	7	35	jt	003	75W
88	7	41	jt	018	84E
89	7	43	jt	100	86S
90	8	41	jt	080	64S
91	8	80	jt	171	35W
92	8	94	jt	090	90
93	9	52	jt	059	37SE

APPENDIX SEVEN

GEOTECHNICAL ASSESSMENT OF SLOPE INSTABILITY ON CRUSHED HORNFELSED SANDSTONE AND TECTONIC BRECCIA SLOPES AT BOULDER CREEK

A7.1 Stability Assessment

A7.2 Slopes in Crushed Hornfelsed Sandstone

A7.3 Slopes in Tectonic Breccia

A7.1 STABILITY ASSESSMENT

The main mechanism of failure in crushed bedrock and tectonic breccia slopes was described as a debris slump/slide -avalanche in Section 4.4. Failure begins by translational sliding, or rotational sliding on slopes generally less than 45^{o}, which commonly disintegrates into an avalanche-type movement. Analysis of this movement mechanism assumes that failure is initiated by circular sliding to allow the use of the circular failure charts produced by Hoek & Bray (1981). These charts allow an easy check on the factor of safety of a slope or upon the sensitivity of the factor of safety to changes in groundwater conditions or slope profile. To use these charts the following assumptions are made (Hoek & Bray 1981):-

1. The material forming the slope is assumed to be homogeneous; that is, its mechanical properties do not vary with direction of loading;
2. The shear strength of the material is characterised by a cohesion C and a friction angle 0 which are related by the Mohr-Coulomb equation;
3. Failure is assumed to occur on a circular failure surface which passes through the toe of the slope (toe failure gives the lowest factor of safety provided that $0 > 5\frac{1}{2}$);
4. A vertical tension crack is assumed to occur in the upper surface or in the face of the slope;
5. The locations of the tension crack and of the failure surface are such that the factor of safety of the slope is a minimum for the slope geometry and groundwater conditions considered.

Table A7.1 presents the results of the analysis for crushed bedrock slopes and Table A7.2 for puggy tectonic breccia slopes. Two groundwater conditions were analysed for each slope: fully drained (dry) and saturated, while slope height and slope angle data for each slope setting analysed was obtained from field measurements and from the contour photogrammetric base map. Values for unit weight, angle of friction, and cohesion properties were estimated from typical values published by Hoek & Bray (1981).

Slope Locality and Groundwater Conditions	Unit Weight (KN/m^3)	Angle of Friction	Cohesion (KPa)		Slope Height	Slope Angle	Factor of Safety		Critical Cohesion (KPa)
			Estimated	Calculated			Cohesionless	Cohesion	
A. BE 2									
(i) Fully drained	16	35°	0	20	45m	47°	0.6	1.1	16
(ii) Saturated	20	35°	0	20	45m	47°	<0.1	0.6	67
B. BE 6									
(i) Fully drained	16	35°	0	20	70m	43°	0.8	1.1	16
(ii) Saturated	20	35°	0	20	70m	43°	<0.1	0.6	81
C. BE 11									
(i) Fully drained	16	35°	0	20	40m	41°	0.8	1.3	6.3
(ii) Saturated	20	35°	0	20	40m	41°	0.1	≤0.7	44

Table A7.1 Results of stability assessment of crushed bedrock slopes using circular failure charts of Hoek & Bray (1981).

Slope Locality and Groundwater Conditions	Unit Weight (KN/m^3)	Angle of Friction	Cohesion (KPa)		Slope Height	Slope Angle	Factor of Safety		Critical Cohesion (KPa)
			Estimated	Calculated			Cohesionless	Cohesion	
A. BE 1									
(i) Fully drained	15	30°	0	60	35m	55°	0.4	1.4	38
(ii) Saturated	19	30°	0	60	35m	55°	<0.1	0.9	69
B. BE 9									
(i) Fully drained	15	30°	0	60	60m	58°	0.4	1.0	58
(ii) Saturated	19	30°	0	60	60m	58°	<0.1	0.6	128

Table A7.2 Results of stability assessment of puggy tectonic breccia slopes using circular failure charts of Hoek & Bray (1981).

A7.2 CRUSHED BEDROCK SLOPES

The unit weight and angle of friction values estimated for crushed hornfelsed sandstone material were based on typical values for broken sandstone and shale rock. However, since the bedrock has been metamorphosed to a hornfels, these values may be a little low since metamorphism may have imparted a greater shear strength and weight to the rock. Correction was not made for this since an increase in the unit weight, which would decrease stability, would probably be compensated by an increase in the friction angle, which would increase stability.

Crushed bedrock slopes were initially assumed to have no cohesion since the rock mass is very loose with open joints. However, under dry conditions, cohesionless slopes recorded a factor of safety of 0.6-0.8 (Table A7.1). Field observations suggest that these slopes are at least at limiting equilibrium under dry conditions. Using a factor of safety of 1.0, back calculations give critical cohesion values under dry conditions ranging from 4.4-16kPa (Table A7.1).

A plot of slope height versus slope angle using a cohesion of 20kPa is presented in Figure A7.1. This shows that all four slopes analysed are stable under dry conditions (F.S.=1.1-1.3), but unstable under saturated conditions (F.S.=0.7-0.6). This confirms field observations that failure occurs during rainstorm events when groundwater conditions approach the saturated state.

A7.3 TECTONIC BRECCIA SLOPES

Puggy tectonic breccia slopes were analysed both without cohesion and with an estimated cohesion. Similar results were obtained to those for crushed bedrock slopes: under dry conditions, cohesionless slopes recorded a factor of safety less than 1.0 and cohesive slopes greater than 1.0. This suggests that the puggy breccia material has some cohesion since these slopes are stable under dry conditions.

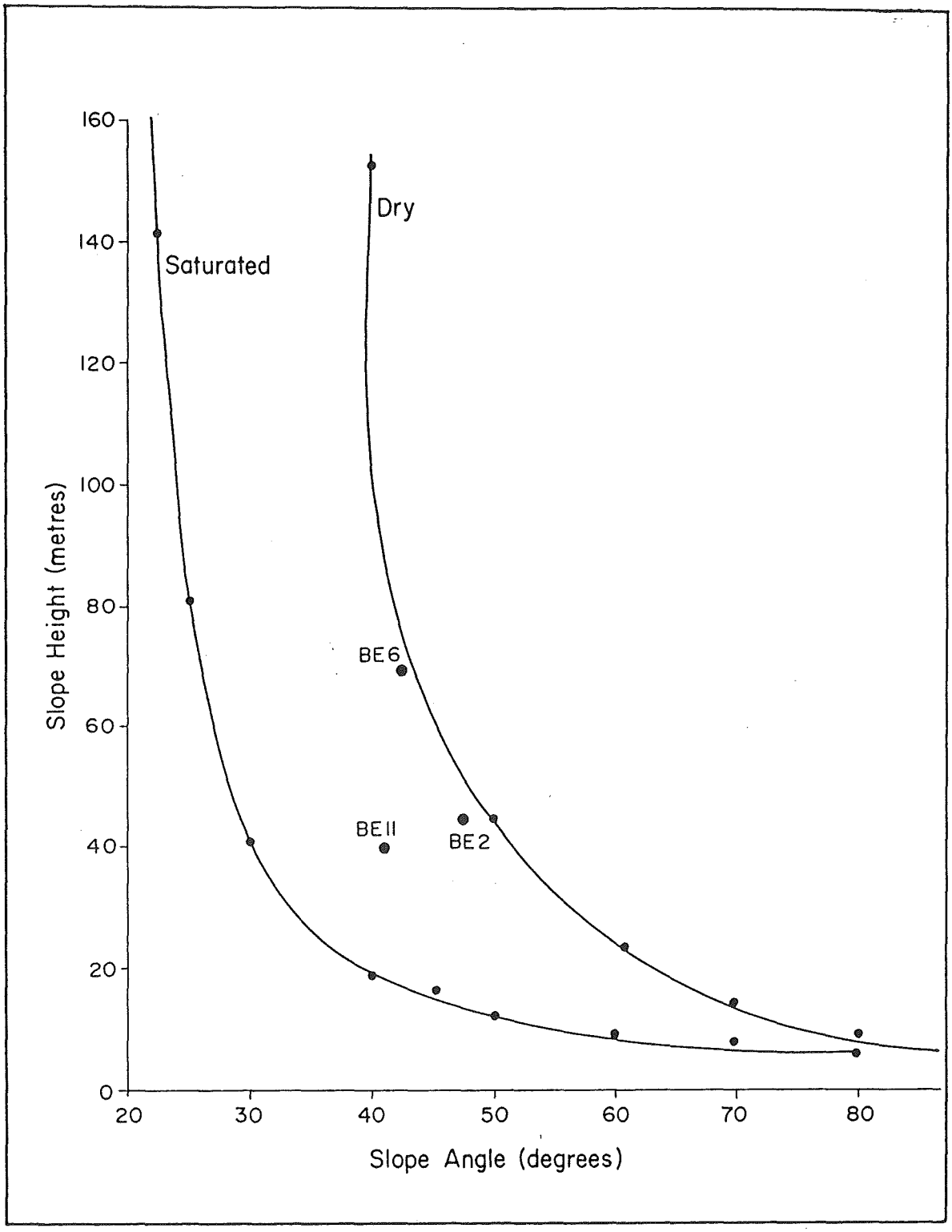

Fig. A7·1 Slope height versus slope angle graph for crushed hornfelsed sandstone at limiting equilibrium (F.S. = 1·0)

Figure A7.2 presents the slope height versus slope angle diagram using an estimated cohesion of 60kPa. Again the puggy breccia slopes react in a similar manner to crushed bedrock slopes. Under fully drained conditions, the slopes are stable with factors of safety ranging from 1.0 to 1.4, but once saturated the factor of safety drops to 0.9-0.6, indicating the importance of rainstorm events in causing failure.

Both puggy breccia slopes analysed have slope angles greater than 48^{o} (55 and 58^{o}), indicating that the initial failure is probably by translational sliding. This would limit the accuracy of these results since an assumption of using the charts is that failure is by circular sliding. However, assuming a direct relationship in the condition of limiting equilibrium between circular and planar sliding mechanisms, the results are considered to be applicable within the accuracy of this analysis where shear strength data have been estimated from published typical rock property values.

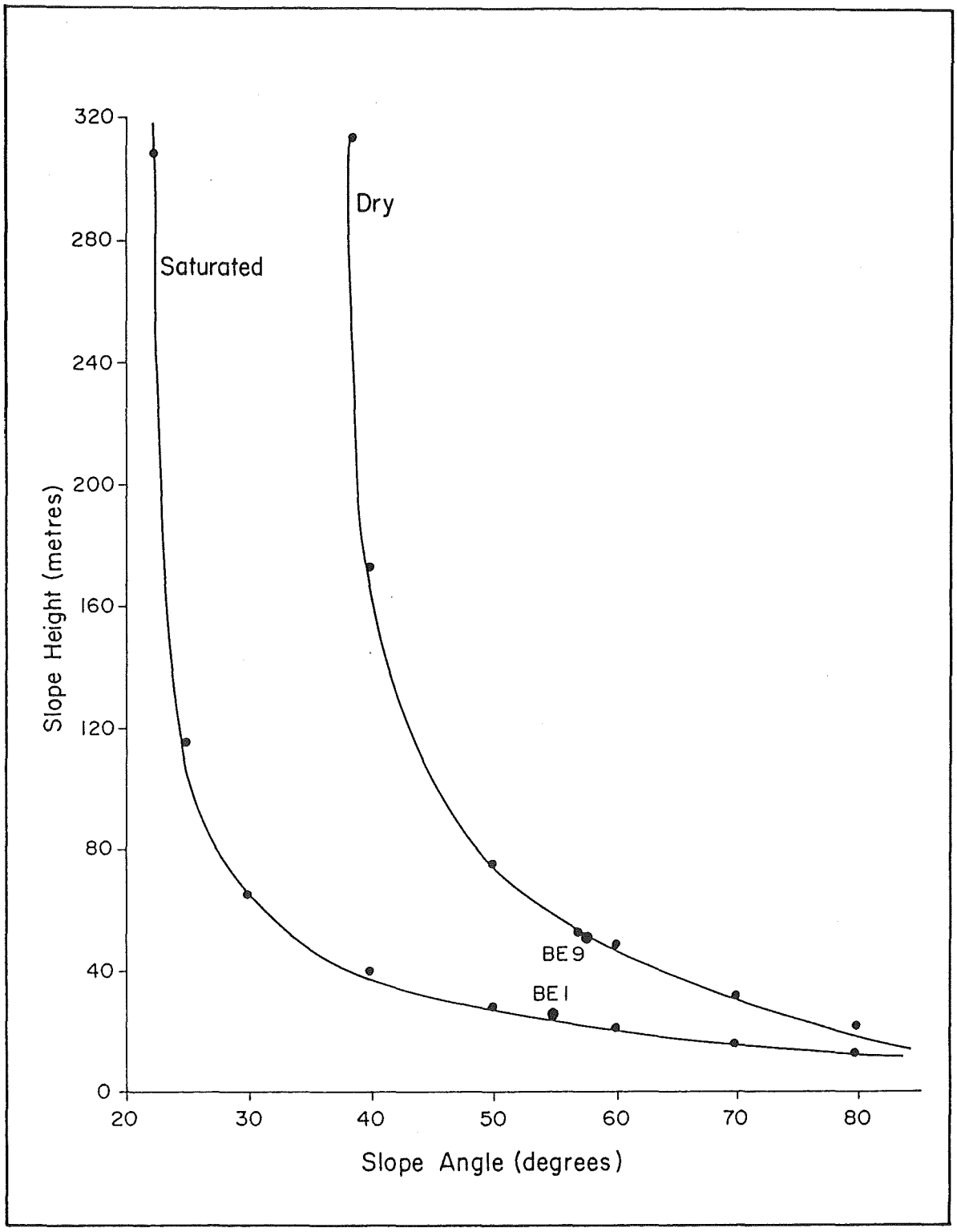

Fig. A7·2 Slope height versus slope angle graph for tectonic breccia slopes at limiting equilibrium (F.S. = 1·0)

APPENDIX EIGHT

GRAVE CREEK SURVEY NETWORK

A8.1 Methodology

A8.2 Accuracy

A8.3 Results and Future Monitoring

A8.1 METHODOLOGY

A survey network was established in the Grave Creek area during March 1985 to provide a local base grid for topographical mapping of the Grave Earthflow and to monitor ground surface movements of the earthflow. Monitoring was over a 15 month period from March 1985 to June 1986 and comprised seven individual surveys.

The Grave Creek survey network consists of five base stations (GE 1 to 5, see Fig. A8.1) installed around the Grave Creek gully to provide a closed traverse system for surveying of the monitoring points on the earthflow. A local grid system was established using base stations GE 1 - GE 2 as the local grid baseline and station GE 1 as the local origin for coordinates. Relative levels were obtained by a levelling traverse between station GE 5 and Lands and Survey benchmark SC 13 (Fig. A8.1). Difficulty was experienced in establishing the position of the base stations as the majority of the ground in the Grave Creek gully is potentially unstable and heavily vegetated limiting the field of view. Section 6.4.2 gives more details on the problems experienced in setting up the survey network. Base stations GE 1 and GE 2 were constructed of a 0.8m lengths of 25mm galvanised iron pipe set in concrete (Fig. A8.2) while stations GE 3,4, and 5 consisted of 50cm wooden pegs driven into the ground.

Positioning of the monitoring stations both parallel and perpendicular to the axis of the earthflow, to provide a regular system of monitoring, was hampered by the presence of vegetation cover within the earthflow which obscured the line of sight. Figure A8.3 gives the location of each monitoring point and the base station from which they were surveyed. Initially nine stations were installed in March 1985, but this system was extended to 16 stations in October 1985 to include the headscarp area of the earthflow. This required an open traverse line to be established from base station GE 1 to monitoring station GEM 12 as a closed traverse base station could not be established in this area due to the limited field of view through the forest vegetation on this part of the slope. The monitoring stations consist of 0.4m lengths of 25mm galvanised iron pipe driven into the ground to leave

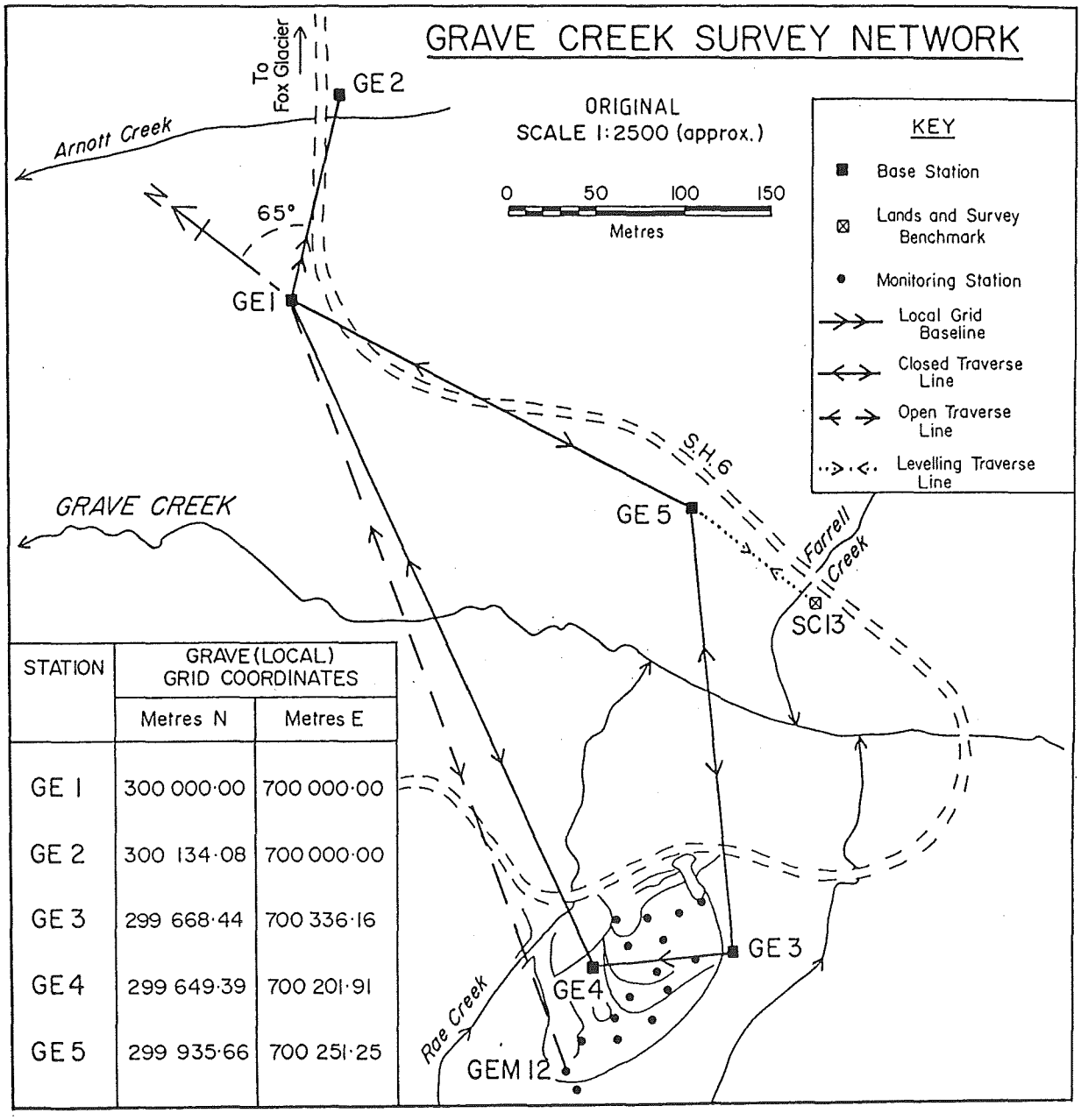

STATION	GRAVE (LOCAL) GRID COORDINATES	
	Metres N	Metres E
GE 1	300 000·00	700 000·00
GE 2	300 134·08	700 000·00
GE 3	299 668·44	700 336·16
GE 4	299 649·39	700 201·91
GE 5	299 935·66	700 251·25

Fig. A8.1 Grave Creek Survey Network

Fig. A8.2 Base station GE 2, constructed of a 0.8m length of 25mm galvanised iron pipe set in concrete.

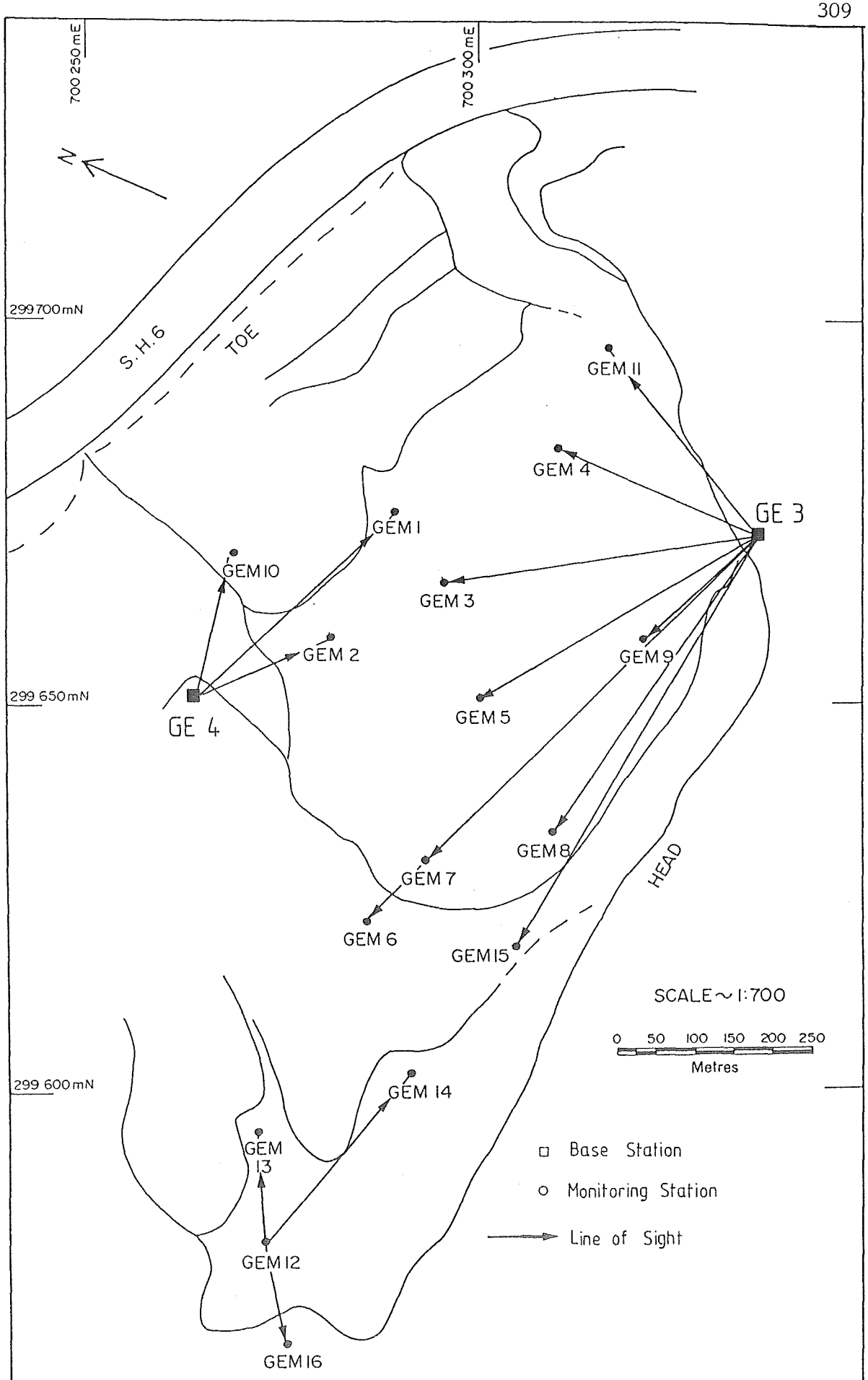

Fig. A8.3 Grave Earthflow Monitoring Network

about 50mm projecting above the ground which were sprayed with "dazzle" to facilitate identification through the undergrowth (Fig. A8.4).

A variety of survey instruments were used during the monitoring period as the author had no regular access to any one instrument, and these are listed below:-

26/3/85	Wild Citation CI-450 EDM & T16 theodolite;
4/6/85	Wild DI-3 EDM & T16 theodolite;
7/9/85	" " " " " "
3/12/85	" " " " " "
6/2/86	Nikon NTD-3 uniaxial theodolite-distancemeter;
9/4/86	Wild T1000 EDM & T1000 theodolite;
28/6/86	" " " " " "

A8.2 ACCURACY

The accuracy of survey results was affected by the number of different instruments used during monitoring investigations and by poor weather conditions during most survey days. An indication of the survey error of measurements to each monitoring station was obtained by considering the root mean square of the closing error for all seven surveys which was calculated to be 61mm. The error at each monitoring station is approximately 5/16 of the root mean square of the closing error which is 19mm. Therefore only those monitoring stations which showed more than 20mm of change were considered a reliable indication of movement.

A8.3 RESULTS AND FUTURE MONITORING

Movement data obtained from monitoring investigations are presented in tables given in Appendix 9. Table A8.1 list survey data of the closed traverse system and monitoring stations to be used for future monitoring investigations. Although the movement rate of the Grave Earthflow is relatively high, the bearings and distances to each monitoring station will aid locating these stations for future surveys.

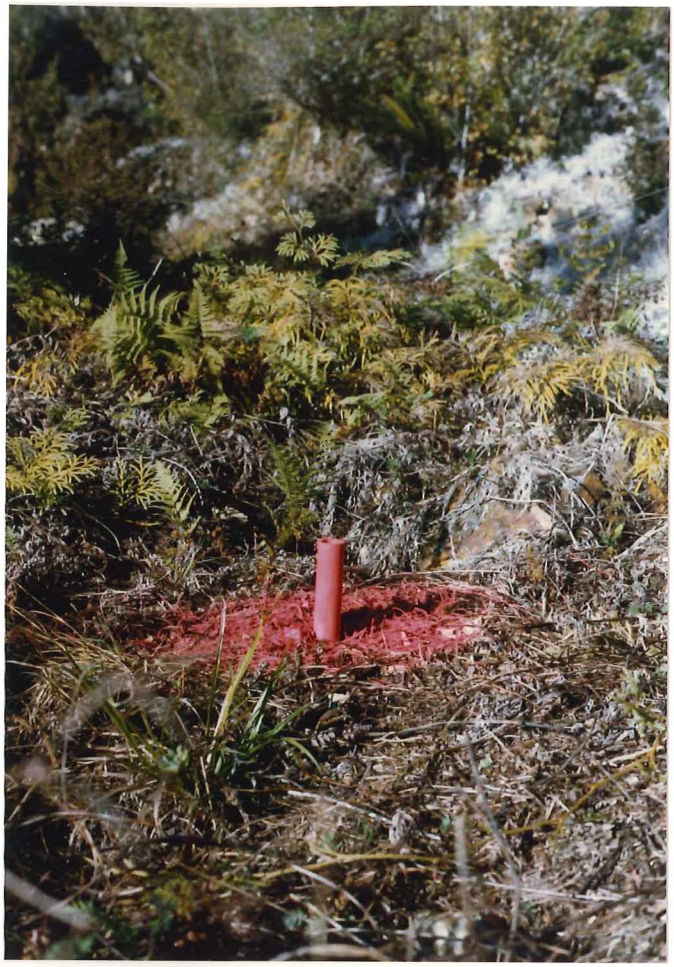

Fig. A8.4 Monitoring station GEM 3, constructed of a 0.4m length of 25mm galvanised iron pipe driven into the ground surface.

SURVEY LINE	BEARING O ' "	HORIZ. DISTANCE (metres)
GE 1 to GE 2	000 00 00	134.076
GE 1 to GE 5	104 21 55	259.355
GE 5 to GE 3	162 22 18	280.399
GE 3 to GE 4	255 36 35	76.652
GE 4 to GE 1	323 14 25	437.597
GE 1 to GEM 12	147 30 48	500.948
GE 3 to GEM 3	263 07 33	42.119
GE 3 to GEM 4	293 11 43	29.692
GE 3 to GEM 5	241 43 38	42.503
GE 3 to GEM 6	226 44 17	72.499
GE 3 to GEM 7	227 00 10	61.348
GE 3 to GEM 8	215 44 50	47.798
GE 3 to GEM 9	228 01 43	20.875
GE 3 to GEM 15	211 58 05	62.533
GE 4 to GEM 1	049 41 43	33.781
GE 4 to GEM 2	068 14 29	18.879
GE 4 to GEM 10	019 46 02	20.646
GEM 12 to GEM 13	358 38 33	14.301
GEM 12 to GEM 14	042 59 11	28.987
GEM 12 to GEM 16	168 28 08	13.668

Note: Bearings and distances are given as they were surveyed on 28/6/86.

Table A8.1 Survey data for the Grave Creek survey network and Grave Earthflow monitoring network.

APPENDIX NINE

GRAVE EARTHFLOW SURFACE MOVEMENT MONITORING RESULTS

A9.1 Surface Movement Data Tables

A9.1 SURFACE MOVEMENT DATA TABLES

Results of surface movement monitoring investigations are presented in two sets of tables which list the following information:-

Table A

1. coordinates;
2. reduced level;
3. components of displacement;
4. horizontal displacement;
5. total displacement.

Table B

1. rates of displacement;
2. direction of displacement.

These tables are presented in the following 32 pages.

GEM 1

Date	Coordinates		Reduced Level *	Components of Displacement						Horizontal Displacement (h) **			Total Displacement (t) **		
				Δx		Δy		Δz **							
	Metres N (x)	Metres E (y)	(z)	R	C	R	C	R	C	Recent	Cumul.	Average	Recent	Cumul.	Average
04/06/85	299 688.31	700 288.55	109.41												
07/09/85	299 669.57	700 288.15	109.02	126	126	- 40	- 40	- 39	- 39	132	132	132	138	138	138
03/12/85	299 670.18	700 287.96	108.59	61	187	- 19	- 59	- 43	- 82	64	196	196	77	215	212
06/02/86	299 670.58	700 287.93	108.35	40	227	- 24	- 83	- 24	-106	47	243	242	53	268	264
28/06/86	299 671.26	700 287.67	107.88	68	295	- 47	-130	- 47	-153	83	326	322	95	363	356

Notes - R - Recent; C - Cumulative

- * metres; ** centimetres

Table A9.1a Surface Movement Monitoring Results, Grave Earthflow.

GEM 1

Date	Rates of Displacement (V) *												Direction of Displacement	
	Vx		Vy		Vz		Vh			Vt			Recent	Average
	R	C	R	C	R	C	R	C	A	R	C	A	o ' "	o ' "
04/06/85	484	484	-154	-154	-149	-149	507	507	507	530	530	530	047 23 15	047 23 15
07/09/85	256	375	- 80	-118	-180	-164	268	393	393	323	431	425	047 41 58	047 29 21
03/12/85	225	335	-135	-123	-135	-157	264	359	358	298	396	390	060 42 39	049 43 25
28/06/86	175	277	-121	-122	-121	-393	213	306	302	244	341	334	044 04 32	048 23 24

Notes - R - Recent; C - Cumulative; A - Average

- * cm/yr

Table A9.1b Surface Movement Monitoring Results, Grave Earthflow.

GEM 2

Date	Coordinates		Reduced Level *	Components of Displacement						Horizontal Displacement (h) **			Total Displacement (t) **		
	Metres N (x)	Metres E (y)	(z)	Δx		Δy		Δz **							
				R	C	R	C	R	C	Recent	Cumul.	Average	Recent	Cumul.	Average
26/03/85	299 652.19	700 280.41	115.21												
07/09/85	299 654.62	700 279.99	113.55	243	243	- 42	- 42	-166	-166	247	247	247	297	297	297
03/12/85	299 655.34	700 279.68	113.00	72	315	- 31	- 73	- 55	-221	78	325	323	95	392	391
06/02/86	299 655.70	700 279.68	112.75	36	351	0	- 73	- 25	-246	36	361	358	44	436	434
28/06/86	299 656.41	700 279.44	112.24	71	422	- 24	- 97	- 51	-297	75	436	433	91	527	525

Notes - R - Recent; C - Cumulative

- * metres; ** centimetres

Table A9.2a Surface Movement Monitoring Results, Grave Earthflow.

Date	Rates of Displacement (V) *												Direction of Displacement	
	Vx		Vy		Vz		Vh			Vt			Recent	Average
	R	C	R	C	R	C	R	C	A	R	C	A	o ' "	o ' "
07/09/85	537	537	- 93	- 93	-367	-367	546	546	546	657	657	657	055 11 38	055 11 38
03/12/85	302	456	-130	-106	-231	-320	327	470	468	399	568	566	041 42 19	051 57 08
06/02/86	202	404	0	- 84	-140	-283	202	416	412	247	502	500	065 00 00	053 15 05
28/06/86	182	335	- 62	- 77	-131	-236	193	347	344	234	419	417	046 19 24	052 03 18

Notes - R - Recent; C - Cumulative; A - Average

- * cm/yr

Table A9.2b Surface Movement Monitoring Results, Grave Earthflow.

Date	Coordinates		Reduced Level *	Components of Displacement						Horizontal Displacement (h) **			Total Displacement (t) **		
				Δx		Δy		Δz **							
	Metres N (x)	Metres E (y)	(z)	R	C	R	C	R	C	Recent	Cumul.	Average	Recent	Cumul.	Average
26/03/85	299 659.49	700 295.86	113.84												
04/06/85	299 660.54	700 295.46	113.05	105	105	- 40	- 40	- 79	- 79	112	112	112	137	137	137
07/09/85	299 661.73	700 294.96	112.46	119	224	- 50	- 90	- 59	-138	129	241	241	142	279	278
03/12/85	299 662.35	700 294.80	112.20	62	286	- 16	-106	- 26	-164	64	305	305	69	348	346
06/02/86	299 662.67	700 294.56	112.00	32	318	- 24	-130	- 20	-184	40	345	343	45	393	389
09/04/86	299 662.97	700 294.49	111.99	30	348	- 7	-137	- 1	-185	31	376	374	31	424	417
28/06/86	299 663.41	700 294.34	111.65	44	392	- 15	-152	- 34	-219	46	422	420	57	481	474

Notes - R - Recent; C - Cumulative

- * metres; ** centimetres

Table A9.3a Surface Movement Monitoring Results, Grave Earthflow.

Date	Rates of Displacement (V) *												Direction of Displacement	
	Vx		Vy		Vz		Vh			Vt			Recent	Average
	R	C	R	C	R	C	R	C	A	R	C	A	o ' "	o ' "
04/06/85	547	547	-208	-208	-412	-412	584	584	584	714	714	714	044 08 44	044 08 44
07/09/85	457	495	-192	-199	-227	-305	496	533	533	546	617	615	042 12 34	043 06 38
03/12/85	260	414	- 67	-153	-109	-237	268	442	442	289	504	502	050 31 47	044 39 50
06/02/86	180	366	-135	-150	-112	-212	225	397	395	253	452	448	028 07 48	042 45 54
09/04/86	177	335	- 41	-132	- 6	-178	182	362	359	182	408	402	051 51 57	043 30 41
28/06/86	201	312	- 68	-121	-155	-174	210	336	334	260	382	377	046 10 31	043 48 21

Notes - R - Recent; C - Cumulative; A - Average

- * cm/yr

Table A9.3b Surface Movement Monitoring Results, Grave Earthflow.

Date	Coordinates		Reduced Level *	Components of Displacement						Horizontal Displacement (h) **			Total Displacement (t) **		
	Metres N (x)	Metres E (y)	(z)	Δx		Δy		Δz **							
				R	C	R	C	R	C	Recent	Cumul.	Average	Recent	Cumul.	Average
26/03/85	299 677.80	700 309.97	106.72												
04/06/85	299 678.43	700 309.69	106.29	63	63	- 28	- 28	- 43	- 43	69	69	69	81	81	81
07/09/85	299 679.01	700 309.51	105.94	58	121	- 18	- 46	- 35	- 78	61	130	129	70	151	151
03/12/85	299 679.38	700 309.29	105.90	37	158	- 22	- 68	- 4	- 82	43	173	172	43	194	190
06/02/86	299 679.63	700 309.10	105.68	25	183	- 19	- 87	- 22	-110	31	204	203	38	232	231
09/04/86	299 679.83	700 309.02	105.68	20	203	- 8	- 95	0	-110	21	225	224	21	253	249
28/06/86	299 680.14	700 308.87	105.46	31	234	- 15	-110	- 22	-132	34	259	259	40	293	291

Notes - R - Recent; C - Cumulative

- * metres; ** centimetres

Table A9.4a Surface Movement Monitoring Results, Grave Earthflow.

Date	Rates of Displacement (V) *												Direction of Displacement	
	Vx		Vy		Vz		Vh			Vt			Recent	Average
	R	C	R	C	R	C	R	C	A	R	C	A	o ' "	o ' "
04/06/86	328	328	-146	-146	-224	-224	360	360	360	422	422	422	041 02 15	041 02 15
07/09/85	223	268	- 69	-102	-134	-172	234	288	285	269	334	334	047 45 31	044 11 06
03/12/85	155	229	- 92	- 98	- 17	-119	180	251	249	180	281	275	034 15 52	041 42 50
06/02/86	146	211	-106	-100	-123	-127	174	234	232	213	267	265	027 45 55	039 34 23
09/04/86	117	195	- 47	- 91	0	-106	123	217	215	123	244	240	043 11 55	039 55 17
28/06/86	141	186	- 68	- 87	-100	-105	155	206	206	182	233	229	039 10 44	039 49 21

Notes - R - Recent; C - Cumulative; A - Average

- * cm/yr

Table A9.4b Surface Movement Monitoring Results, Grave Earthflow.

Date	Coordinates		Reduced Level *	Components of Displacement						Horizontal Displacement (h) **			Total Displacement (t) **		
				Δx		Δy		Δz **							
	Metres N (x)	Metres E (y)	(z)	R	C	R	C	R	C	Recent	Cumul.	Average	Recent	Cumul.	Average
26/03/85	299 645.85	700 299.18	120.37												
04/06/85	299 646.30	700 299.11	120.01	45	45	- 7	- 7	- 36	- 36	46	46	46	58	58	58
07/09/85	299 647.08	700 299.06	119.64	78	123	- 5	- 12	- 37	- 73	78	124	124	86	144	144
03/12/85	299 647.50	700 298.97	119.35	42	165	- 9	- 21	- 29	-102	43	167	166	52	196	196
06/02/86	299 647.69	700 298.77	119.27	19	184	- 20	- 41	- 8	-110	28	195	188	29	225	218
09/04/86	299 647.96	700 298.76	119.16	27	211	- 1	- 42	- 11	-121	27	222	215	29	254	247
28/06/86	299 648.32	700 298.73	118.85	36	247	- 3	- 45	- 31	-152	36	258	251	47	301	293

Notes - R - Recent; C - Cumulative

- * metres; ** centimetres

Table A9.5a Surface Movement Monitoring Results, Grave Earthflow.

Date	Rates of Displacement (V) *												Direction of Displacement	
	Vx		Vy		Vz		Vh			Vt			Recent	Average
	R	C	R	C	R	C	R	C	A	R	C	A	o ' "	o ' "
04/06/85	235	235	- 36	- 36	-188	-188	240	240	240	302	302	302	056 09 29	056 09 29
07/09/85	300	272	- 19	- 26	-142	-161	300	274	274	330	318	318	061 19 56	059 25 40
03/12/85	176	239	- 38	- 30	-122	-147	180	242	240	218	284	284	052 54 19	057 44 48
06/02/86	107	212	-112	- 47	- 45	-127	157	224	216	163	259	251	018 31 52	052 26 18
09/04/86	159	203	- 6	- 40	- 65	-116	160	214	207	171	245	238	062 52 44	053 44 32
28/06/86	164	196	- 14	- 36	-141	-121	164	205	200	214	239	233	060 14 11	054 40 29

Notes - R - Recent; C - Cumulative; A - Average

- * cm/yr

Table A9.5b Surface Movement Monitoring Results, Grave Earthflow.

Date	Coordinates		Reduced Level *	Components of Displacement						Horizontal Displacement (h) **			Total Displacement (t) **		
				Δx		Δy		Δz **							
	Metres N (x)	Metres E (y)	(z)	R	C	R	C	R	C	Recent	Cumul.	Average	Recent	Cumul.	Average
26/03/85	299 617.26	700 283.35	134.71												
07/09/85	299 617.98	700 283.36	134.41	72	72	1	1	- 30	- 30	72	72	72	78	78	78
03/12/85	299 618.22	700 283.39	134.22	24	96	3	4	- 19	- 49	24	96	96	31	109	108
06/02/86	299 618.33	700 283.39	134.21	11	107	0	4	- 1	- 50	11	107	107	11	120	118
09/04/86	299 618.50	700 283.36	134.17	17	124	- 3	1	- 4	- 54	17	124	124	17	137	135
28/06/86	299 618.76	700 283.36	133.92	26	150	0	1	- 25	- 79	26	154	150	36	173	169

Notes - R - Recent; C - Cumulative

- * metres; ** centimetres

Table A9.6a Surface Movement Monitoring Results, Grave Earthflow.

Date	Rates of Displacement (V) *												Direction of Displacement	
	Vx		Vy		Vz		Vh			Vt			Recent	Average
	R	C	R	C	R	C	R	C	A	R	C	A	o ' "	o ' "
07/09/85	159	159	2	2	- 66	- 66	159	259	259	172	172	172	065 47 45	065 47 45
03/12/85	101	139	13	6	- 80	- 71	101	139	139	130	158	156	072 07 30	067 23 09
06/02/86	62	123	0	5	- 6	- 58	62	123	123	62	138	134	065 00 00	067 08 27
09/04/86	100	119	- 18	1	- 23	- 52	100	119	119	100	132	128	054 59 31	065 27 43
28/06/86	119	119	0	1	-114	- 63	119	122	11 9	16 4	138	134	065 00 00	065 22 55

Notes - R - Recent; C - Cumulative; A - Average

- * cm/yr

Table A9.6b Surface Movement Monitoring Results, Grave Earthflow.

Date	Coordinates		Reduced Level *	Components of Displacement						Horizontal Displacement (h) **			Total Displacement (t) **		
				Δx		Δy		Δz **							
	Metres N (x)	Metres E (y)	(z)	R	C	R	C	R	C	Recent	Cumul.	Average	Recent	Cumul.	Average
26/03/85	299 623.89	700 291.50	131.18												
04/06/85	299 624.34	700 291.47	130.80	45	45	- 3	- 3	- 38	- 38	45	45	45	59	59	59
07/09/85	299 625.21	700 291.46	130.38	87	132	- 1	- 4	- 42	- 80	87	132	132	97	156	154
03/12/85	299 625.76	700 291.44	129.99	55	187	- 2	- 6	- 39	-119	55	187	187	67	223	222
06/02/86	299 625.97	700 291.32	129.87	21	208	- 12	- 18	- 12	-131	24	211	209	27	250	247
09/04/86	299 626.21	700 291.32	129.83	24	232	0	- 18	- 4	-135	24	235	233	24	274	269
28/06/86	299 626.61	700 291.29	129.48	40	272	- 3	- 21	- 35	-170	40	275	273	53	327	322

Notes - R - Recent; C - Cumulative

- * metres; ** centimetres

Table A9.7a Surface Movement Monitoring Results, Grave Earthflow.

Date	Rates of Displacement (V) *												Direction of Displacement	
	Vx		Vy		Vz		Vh			Vt			Recent	Average
	R	C	R	C	R	C	R	C	A	R	C	A	o ' "	o ' "
04/06/85	235	235	- 16	- 16	-198	-198	235	235	235	308	308	308	061 11 09	061 11 09
07/09/85	334	292	- 4	- 9	-161	-177	334	292	292	373	345	341	064 20 29	063 15 51
03/12/85	231	271	- 8	- 9	-164	-172	231	271	271	281	323	321	062 55 03	063 09 44
06/02/86	118	239	- 67	- 21	- 67	-151	235	247	239	152	288	284	035 15 18	060 03 14
09/04/86	141	223	0	- 17	- 23	-130	141	226	224	141	264	159	065 00 00	060 33 49
28/06/86	182	216	- 14	- 17	-160	-135	182	219	217	242	260	256	060 42 39	060 35 07

Notes - R - Recent; C - Cumulative; A - Average

- * cm/yr

Table A9.7b Surface Movement Monitoring Results, Grave Earthflow.

Date	Coordinates		Reduced Level *	Components of Displacement						Horizontal Displacement (h) **			Total Displacement (t) **		
				Δx		Δy		Δz **							
	Metres N (x)	Metres E (y)	(z)	R	C	R	C	R	C	Recent	Cumul.	Average	Recent	Cumul.	Average
26/03/85	299 628.50	700 308.26	129.17												
04/06/85	299 628.75	700 308.24	129.00	25	25	- 2	- 2	- 17	- 17	25	25	25	30	30	30
07/09/85	299 629.08	700 308.22	128.88	33	58	- 2	- 4	- 12	- 29	33	58	58	35	65	65
03/12/85	299 629.27	700 308.28	128.74	19	77	6	2	- 14	- 43	20	78	77	24	89	88
06/02/86	299 629.31	700 308.23	128.69	4	81	- 5	- 3	- 5	- 48	6	84	81	8	97	94
09/04/86	299 629.46	700 308.23	128.65	15	96	0	- 3	- 4	- 52	15	99	96	15	112	109
28/06/86	299 629.66	700 308.24	128.52	20	116	1	- 2	- 13	- 65	20	119	116	24	136	133

Notes - R - Recent; C - Cumulative

- * metres; ** centimetres

Table A9.8a Surface Movement Monitoring Results, Grave Earthflow.

Date	Rates of Displacement (V) *												Direction of Displacement	
	Vx		Vy		Vz		Vh			Vt			Recent	Average
	R	C	R	C	R	C	R	C	A	R	C	A	o ' "	o ' "
04/06/85	130	130	- 10	- 10	- 89	- 89	130	130	130	156	156	156	060 25 34	060 25 34
07/09/85	128	128	- 8	- 9	- 46	- 64	127	128	128	134	144	144	061 31 54	061 03 17
03/12/85	80	111	25	3	- 59	- 62	84	113	112	101	130	128	082 31 32	066 29 16
06/02/86	22	93	- 28	- 3	- 28	- 55	34	97	93	45	112	108	013 39 35	062 52 44
09/04/86	88	92	0	- 3	- 23	- 50	88	95	92	88	108	105	065 00 00	063 12 36
28/06/86	91	92	5	- 2	- 59	- 52	91	95	92	109	108	106	067 51 45	064 00 44

Notes - R - Recent; C - Cumulative; A - Average

- * cm/yr

Table A9.8b Surface Movement Monitoring Results, Grave Earthflow.

Date	Coordinates		Reduced Level *	Components of Displacement						Horizontal Displacement (h) **			Total Displacement (t) **		
				Δx		Δy		Δz **							
	Metres N (x)	Metres E (y)	(z)	R	C	R	C	R	C	Recent	Cumul.	Average	Recent	Cumul.	Average
26/03/85	299 653.30	700 320.94	119.41												
04/06/85	299 653.53	700 320.89	119.09	23	23	- 5	- 5	- 32	- 32	24	24	24	40	40	40
07/09/85	299 653.94	700 320.86	119.00	41	64	- 3	- 8	- 9	- 41	41	65	64	42	82	76
03/12/85	299 654.08	700 320.79	118.84	14	78	- 7	- 15	- 16	- 57	16	81	79	23	105	97
06/02/86	299 654.16	700 320.70	118.76	8	86	- 9	- 24	- 8	- 65	12	93	89	14	119	110
09/04/86	299 654.30	700 320.69	118.70	14	100	- 1	- 25	- 6	- 71	14	107	103	15	134	135
28/06/86	299 654.49	700 320.64	118.59	19	119	- 5	- 30	- 11	- 82	20	127	123	23	157	148

Notes - R - Recent; C - Cumulative

- * metres; ** centimetres

Table A9.9a Surface Movement Monitoring Results, Grave Earthflow.

Date	Rates of Displacement (V) *												Direction of Displacement	
	Vx		Vy		Vz		Vh			Vt			Recent	Average
	R	C	R	C	R	C	R	C	A	R	C	A	o ' "	o ' "
04/06/85	120	120	- 26	- 26	-167	-167	125	125	125	209	209	209	052 44 07	052 44 07
07/09/85	157	141	- 11	- 18	- 35	- 91	157	144	143	161	181	168	060 48 54	057 52 30
03/12/85	59	113	- 29	- 22	- 67	- 82	67	117	114	96	152	140	038 26 06	054 06 52
06/02/86	45	99	- 50	- 28	- 45	- 75	67	107	102	79	137	127	016 38 01	049 24 26
09/04/86	82	96	- 6	- 24	- 35	- 68	82	103	99	88	129	120	060 54 52	050 57 49
28/06/86	87	95	- 23	- 24	- 50	- 65	91	101	98	105	125	118	050 15 23	050 51 02

Notes - R - Recent; C - Cumulative; A - Average

- * cm/yr

Table A9.9b Surface Movement Monitoring Results, Grave Earthflow.

Date	Coordinates		Reduced Level *	Components of Displacement						Horizontal Displacement (h) **			Total Displacement (t) **		
	Metres N (x)	Metres E (y)	(z)	Δx		Δy		Δz **							
				R	C	R	C	R	C	Recent	Cumul.	Average	Recent	Cumul.	Average
02/10/85	299 666.92	700 269.92	105.03												
03/12/85	299 667.64	700 269.50	104.49	72	72	- 42	- 42	- 54	- 54	83	83	83	99	99	99
06/02/86	299 668.09	700 269.29	104.13	45	117	- 21	- 63	- 36	- 90	50	133	133	62	161	161
09/04/86	299 668.19	700 269.23	104.03	10	127	- 6	- 69	- 10	-100	12	145	144	16	177	175
28/06/86	299 668.84	700 268.89	103.56	65	192	- 34	-103	- 47	-147	73	218	218	87	264	263

Notes - R - Recent; C - Cumulative

- * metres; ** centimetres

Table A9.10a Surface Movement Monitoring Results, Grave Earthflow.

Date	Rates of Displacement (V) *												Direction of Displacement	
	Vx		Vy		Vz		Vh			Vt			Recent	Average
	R	C	R	C	R	C	R	C	A	R	C	A	o ' "	o ' "
03/12/85	424	424	-247	-247	-318	-318	489	489	489	583	583	583	034 44 37	034 44 37
06/02/86	253	336	-118	-181	-202	-259	281	382	382	348	463	463	029 58 59	036 41 57
09/04/86	59	245	- 35	-133	- 59	-193	71	280	278	94	342	338	034 02 11	036 29 04
28/06/86	296	260	-155	-140	-214	-199	333	296	296	397	358	357	037 23 13	036 47 18

Notes - R - Recent; C - Cumulative; A - Average

- * cm/yr

Table A9.10b Surface Movement Monitoring Results, Grave Earthflow

Date	Coordinates		Reduced Level * (z)	Components of Displacement						Horizontal Displacement (h) **			Total Displacement (t) **		
	Metres N (x)	Metres E (y)		Δx		Δy		Δz **							
				R	C	R	C	R	C	Recent	Cumul.	Average	Recent	Cumul.	Average
02/10/85	299 691.71	700 316.22	103.20												
03/12/85	299 692.00	700 316.03	103.15	29	29	- 19	- 19	- 5	- 5	35	35	35	35	35	35
06/02/86	299 692.31	700 315.81	102.95	31	60	- 22	- 41	- 20	- 25	38	73	73	43	78	77
09/04/86	299 692.50	700 315.70	102.88	19	79	- 11	- 52	- 7	- 32	22	95	95	23	101	100
28/06/86	299 692.87	700 315.45	102.77	37	116	- 25	- 77	- 11	- 43	45	140	139	46	147	145

Notes - R - Recent; C - Cumulative

- * metres; ** centimetres

Table A9.11a Surface Movement Monitoring Results, Grave Earthflow.

Date	Rates of Displacement (V) *												Direction of Displacement	
	Vx		Vy		Vz		Vh			Vt			Recent	Average
	R	C	R	C	R	C	R	C	A	R	C	A	o ' "	o ' "
03/12/85	171	171	-112	-112	- 29	- 29	206	206	206	206	206	206	031 46 06	031 46 06
06/02/86	174	172	-123	-118	-112	- 72	213	210	210	241	224	223	029 38 15	030 39 14
09/04/86	112	152	- 65	-100	- 41	- 62	129	183	183	135	195	194	034 55 53	031 38 45
28/06/86	169	157	-114	-104	- 50	- 58	205	190	189	210	199	197	030 57 15	031 25 27

Notes - R - Recent; C - Cumulative; A - Average

- * cm/yr

Table A9.11b Surface Movement Monitoring Results, Grave Earthflow.

Date	Coordinates		Reduced Level *	Components of Displacement						Horizontal Displacement (h) **			Total Displacement (t) **		
	Metres N (x)	Metres E (y)	(z)	Δx		Δy		Δz **							
				R	C	R	C	R	C	Recent	Cumul.	Average	Recent	Cumul.	Average
02/10/85	299 577.44	700 269.37	155.29												
06/02/86	299 577.34	700 269.01	155.01												
09/04/86	299 577.51	700 269.21	154.99												
28/06/86	299 577.44	700 269.06	155.00		0		- 31		- 29			31			42

Notes - R - Recent; C - Cumulative

- * metres; ** centimetres

Table A9.12a Surface Movement Monitoring Results, Grave Earthflow.

Date	Rates of Displacement (V) *												Direction of Displacement	
	Vx		Vy		Vz		Vh			Vt			Recent	Average
	R	C	R	C	R	C	R	C	A	R	C	A	o ' "	o ' "
28/06/86		0		- 42		- 39			42			57		335 00 00

Notes - R - Recent; C - Cumulative; A - Average

- * cm/yr

Table A9.12b Surface Movement Monitoring Results, Grave Earthflow.

Date	Coordinates		Reduced Level *	Components of Displacement						Horizontal Displacement (h) **			Total Displacement (t) **		
	Metres N (x)	Metres E (y)	(z)	Δx		Δy		Δz **							
				R	C	R	C	R	C	Recent	Cumul.	Average	Recent	Cumul.	Average
02/10/85	299 591.76	700 269.28	148.64												
06/02/86	299 591.67	700 268.68	148.44												
09/04/86	299 591.81	700 268.89	148.62												
28/06/86	299 591.74	700 268.72	148.45		- 2		- 56		- 19			56			59

Notes - R - Recent; C - Cumulative

- * metres; ** centimetres

Table A9.13a Surface Movement Monitoring Results, Grave Earthflow.

Date	Rates of Displacement (V) *												Direction of Displacement	
	Vx		Vy		Vz		Vh			Vt			Recent	Average
	R	C	R	C	R	C	R	C	A	R	C	A	o ' "	o ' "
28/06/86		-3		- 76		- 26			76			80		332 57 16

Notes - R - Recent; C - Cumulative; A - Average

- * cm/yr

Table A9.13b Surface Movement Monitoring Results, Grave Earthflow.

Date	Coordinates		Reduced Level *	Components of Displacement						Horizontal Displacement (h) **			Total Displacement (t) **		
				Δx		Δy		Δz **							
	Metres N (x)	Metres E (y)	(z)	R	C	R	C	R	C	Recent	Cumul.	Average	Recent	Cumul.	Average
02/10/85	299 598.29	700 289.12	146.28												
06/02/86	299 598.35	700 288.76	145.85												
09/04/86	299 598.52	700 288.94	145.87												
28/06/86	299 598.64	700 288.82	145.57		35		- 30		- 71			46			85

Notes - R - Recent; C - Cumulative

- * metres; ** centimetres

Table A9.14a Surface Movement Monitoring Results, Grave Earthflow.

Date	Rates of Displacement (V) *												Direction of Displacement	
	Vx		Vy		Vz		Vh			Vt			Recent	Average
	R	C	R	C	R	C	R	C	A	R	C	A	o ' "	o ' "
28/06/86		47		- 41		- 96			62			115		024 23 55

Notes - R - Recent; C - Cumulative; A - Average

- * cm/yr

Table A9.14b Surface Movement Monitoring Results, Grave Earthflow.

Date	Coordinates		Reduced Level *	Components of Displacement						Horizontal Displacement (h) **			Total Displacement (t) **		
				Δx		Δy		Δz **							
	Metres N (x)	Metres E (y)	(z)	R	C	R	C	R	C	Recent	Cumul.	Average	Recent	Cumul.	Average
02/10/85	299 614.74	700 303.06	136.98												
03/12/85	299 614.99	700 303.09	136.79	25	25	3	3	- 19	- 19	25	25	25	31	31	31
09/04/86	299 615.19	700 303.04	136.67	20	45	- 5	- 2	- 12	- 31	21	46	45	24	55	55
28/06/86	299 615.40	700 303.05	136.44	21	66	1	- 1	- 23	- 54	21	67	66	31	86	85

Notes - R - Recent; C - Cumulative

- * metres; ** centimetres

Table A9.15a Surface Movement Monitoring Results, Grave Earthflow.

GEM 15

Date	Rates of Displacement (V) *												Direction of Displacement	
	Vx		Vy		Vz		Vh			Vt			Recent	Average
	R	C	R	C	R	C	R	C	A	R	C	A	o ' "	o ' "
03/12/85	147	147	18	18	-112	-112	147	147	147	182	182	182	071 50 34	071 50 34
09/04/86	57	87	- 14	- 4	- 34	- 60	60	89	87	69	106	106	050 57 49	062 27 19
28/06/86	96	90	5	1	-105	- 73	96	91	89	141	117	115	067 43 35	064 07 55

Notes - R - Recent; C - Cumulative; A - Average

- * cm/yr

Table A9.15b Surface Movement Monitoring Results, Grave Earthflow.

Date	Coordinates		Reduced Level *	Components of Displacement						Horizontal Displacement (h) **			Total Displacement (t) **		
	Metres N (x)	Metres E (y)	(z)	Δx		Δy		Δz **							
				R	C	R	C	R	C	Recent	Cumul.	Average	Recent	Cumul.	Average
02/10/85	299 564.36	700 272.21	164.65												
06/02/86	299 563.95	700 271.76	164.58												
09/04/86	299 564.16	700 271.96	164.67												
28/06/86	299 564.05	700 271.79	164.58		- 31		- 42		- 7			52			52

Notes - R - Recent; C - Cumulative

- * metres; ** centimetres

Table A9.16a Surface Movement Monitoring Results, Grave Earthflow.

Date	Rates of Displacement (V) *												Direction of Displacement	
	Vx		Vy		Vz		Vh			Vt			Recent	Average
	R	C	R	C	R	C	R	C	A	R	C	A	o ' "	o ' "
28/06/86		- 42		- 57		- 9			71			71		298 34 09

Notes - R - Recent; C - Cumulative; A - Average

- * cm/yr

Table A9.16b Surface Movement Monitoring Results, Grave Earthflow.